1990

THE CHARACTERIZATION AND MODELLING/OF SOIL WATER PATHWAYS BENEATH A CONIFEROUS HILLSLOPE IN MID WALES

CHAPPELL, NICHOLAS ARTHUR

http://hdl.handle.net/10026.1/2037

http://dx.doi.org/10.24382/3593
University of Plymouth

THE CHARACTERIZATION AND MODELLING OF SOIL WATER PATHWAYS BENEATH A CONIFEROUS HILLSLOPE IN MID WALES

NICHOLAS ARTHUR CHAPPELL

A thesis submitted in partial fulfilment of the
requirements of the Council for National Academic Awards
for the degree of Doctor of Philosophy

September 1990

Polytechnic South West (Plymouth)
in collaboration with
Institute of Terrestrial Ecology (NERC)
Institute of Hydrology (NERC)

Abstract.

The Characterization and Modelling of Soil-Water-Pathways beneath a Coniferous hillslope in Mid-Wales.

Nicholas Arthur Chappell

Streams draining coniferous plantations contain higher loadings of hydrogen ion, aluminium, sulphate and nitrate, in comparison with streams in adjacent grasslands. Almost all of this ion-load is transported to streams via subsurface water-pathways. An incontrovertible, physical characterization of these pathways within a natural, layered hillslope, has yet to be presented. This research has sought to provide such a characterization for two hillslopes - one afforested with conifers, the other an improved grassland.

Much of the uncertainty associated with the identification of soil-water-pathways stems from an inadequate characterization of the errors imposed by the use of each measurement technique. This research has, therefore, compared the predictions of a number of quasi-independent field and analytical techniques, to attempt to lessen the impact of measurement error upon the observed response of the true hydrological system.

The impact of conifers upon the detailed water-pathways and lumped catchment response was monitored to educe any changes in the hydrological response which could account for the increased loading of *acidic solutes* within forest streams.

The results of the analysis, indicated that the pathways of water through hillslopes could be predicted from the response of hydrological properties averaged over control volumes of soil-pores. The accuracy of these solutions was proven by the concordance of the response of all of the properties contained within the Darcy-Richards equation.

The marked horizon development within the ferric podzol soil of the instrumented forest hillslope, in particular the presence of an indurated B horizon, deflects most percolation laterally within the O/A and A/E horizons. This pathway was indicted by the results of techniques which included numerical and approximative calculations, discontinuities between the state-dependent hydraulic conductivity of each soil horizon, and the generation of steep, vertical potential gradients in layered porous media. The instrumented grassland hillslope was ploughed 11 years prior to instrumentation. This greatly increased the conductivity of the controlling B horizon, allowing almost all flow to percolate to depth. During winter-storms, the forest hillslope generated flows smaller than those within the grassland hillslope, concomitant with the 29 percent difference in the rainfall-runoff behaviour of the catchment areas. This increased loss of runoff within the afforested areas, may result from the high losses of wetted-canopy-evaporation (39 percent of gross-precipitation) from the Sitka spruce (*Picea sitchensis*, Bong. Carr.) trees.

Individual conifer trees growing on the steep, ferric podzol hillslope appeared to enhance the lateral deflection of flow within the O/A and A/E horizons, probably as a result of their platy root systems, and the high rates of precipitation input to soil at the stem-base.

The enhancement of both lateral near-surface flow and below-canopy ion concentrations could, therefore, generate the chemical signatures characteristic of streams draining coniferous forests.

Contents.

CHAPTER 3.

Research Design and Methodology.

CHAPTER 4.

Instrumentation.

CHAPTER 5.

Hillslope and Catchment Rainfall-Runoff.

CHAPTER 9.

Synthesis and Conclusions.

Figures.

(1987).

30. Change of moisture content at individual neutral gauging sites, within the forest hillslope.
31. Average change of moisture content within the A/E,B and B/C horizons of the forest hillslope.
32. Change of moisture content within the regolith (C horizon) at a depth of 60 cm.
33. Two possible kinematic waves of moisture content change within the A/E horizons of the forest hillslope.
34. Average moisture content at the inflow and mid-point of the riparian zone, at the base of the forest hillslope.
35. Change of moisture content beneath a large tree (44 cm DBH) within the forest riparian zone, and that at 1m across-slope of the same tree.
36. Gravitational potential within the forest hillslope; included for comparison with the distribution of total capillary potential presented within Figures 42, 43, and 44.
37. Capillary potential monitored by the borehole (for a depth of 100 cm) within the forest riparian zone against that monitored by a tensiometer (100 cm deep: BT100) located 50 cm away.
38. The difference in measured capillary potential indicated by a tensiometer (100 cm deep: 0t100) and that indicated by a piezometer (100 cm deep). The instruments are located 60 cm appart within the forest riparian zone. Positive values reflect the larger values of capillary potential measured by the piezometer.
39. Variation in the capillary potential measured by a manometer tensiometer located above-ground in a container in which a constant head of water was maintained. Measurements were taken at temperatures ranging in between 3 and 15 degrees.
40. The dynamics of the deep phreatic zone within the riparian zone of the forest hillslope, during storm-periods 3-4.
41. Dynamics of the shallow phreatic surface at the A/E horizon of the forest hillslope, during storm-period 3-4.
42. The distribution of total potential within the forest hillslope, prior to storm 3-4.
43. The distribution of total potential within the forest hillslope, at the peak rainfall and streamflow within storm 3-4.
44. The distribution of total potential within the forest hillslope, during the 10 day, dry period in May 1988.
45. Capillary potential within the B/C horizon (45 cm depth) beneath a large conifer (47 cm DBH), beneath the butress root of a small conifer (29 cm DBH), and 1.5 m downslope of the same small conifer.
46. Capillary potential at a depth of 1 m beneath a small conifer (29 cm DBH), and at the same depth, but 1.5 m downslope of the same small conifer.
47. Vertical potential gradients between the A/E and B/C horizons of the forest hillslope

beneath two small conifers (29 and 30 cmDBH), and within the area in between the two conifers (1.5 m away from both conifers). Each line represents the average gradient between three pairs of tensiometers.

48. Periods in which the largest differences in vertical potential gradients beneath conifers with those within inter-tree areas (see Figure 46) were monitored.
49. Capillary potentials of the below-tree and inter-tree A/E horizon, during two storm events (storm 9 (part 2) and 10). Each line represents an average capillary potential monitored by three tensiometers.
50. Capillary potentials of the below-tree and inter-tree B/C horizon, during two storm events (storm 9 (part 2) and 10). Each line represents an average capillary potential monitored by three tensiometers.
51. Range in bulk density within each soil horizon of the podzolic slopes and riparian zones of the forest and grassland hillslopes.
52. Range in porosity within each soil horizon of the podzolic slopes and riparian zones of the forest and grassland hillslopes.
53. Moisture capacity within the A/E horizon of the forest hillslope determined by both *in situ* and laboratory based techniques.
54. Moisture capacity within the B/C horizon of the forest hillslope determined by both *in situ* and laboratory based techniques.
55. Moisture capacity within the A/E horizon of the grassland hillslope determined by both *in situ* and laboratory based techniques.
56. Moisture capacity within the B/C horizon of the grassland hillslope determined by both *in situ* and laboratory based techniques.
57. Variability of laboratory-determined moisture capacities within the A/E, B and B/C horizons of the forest and grassland hillslopes.
58. Mean moisture capacities within each horizon of the forest and grassland hillslopes, over a range of 0 to -100 cm capillary potential.
59. Mean moisture capacities within each horizon of the forest and grassland hillslopes, over a range of 0 to -15,000 cm capillary potential.
60. The relationship between water temperature and water viscosity correction factor.
61. Distribution of saturated hydraulic conductivity at 20 °C (cm hr^{-1} : top) and intrinsic permeability (cm^2 : bottom), within the forest hillsope.
62. Distribution of saturated hydraulic conductivity at 20 °C (cm hr^{-1} : top) and intrinsic permeability (cm^2 : bottom), within the grassland hillsope.
63. Distribution of saturated hydraulic conductivity (at 20 °C) within the forest riparian zone (top) and grassland riparian zone (bottom).
64. The relative hydraulic conductivity function at capillary potentials of between 0 and -10 cm, predicted by the techniques developed by Campbell (1974), Brooks and Cory (1964,

1966), Millington and Quirk (1959, 1960), and Van Genuchten (1980). The moisture capacity data for the forest B horizon is used for the comparisons.

65. The best fit or optimization of the parameters within Campbell's (1964) and Brookes and Cory's (1964, 1966) equations approximating the shape of the moisture capacity curve for the forest B horizon. The moisture capacity for this horizon has the least complex shape (Section 7.4.3).
66. Mean relative hydraulic conductivity function for each soil horizon within the forest and grassland hillslopes. The functions are predicted by the Millington-Quirk equations using moisture capacity data parameterized with a cubic spline.
67. Relative hydraulic conductivity against available water saturation for each soil horizon, predicted by the Millington-Quirk equation.
68. Relative hydraulic conductivity against available water saturation for each soil horizon, predicted by the Van Genuchten equation.
69. The KB/KE ratio predicted by the moisture capacity method (Millington-Quirk equation) against the KB/KE ratio predicted by a Tangent-Continuity method: Downward flow at the 2.5 m position on the forest hillslope.
70. The KB/KE ratio predicted by the moisture capacity method (Millington-Quirk equation) against the KB/KE ratio predicted by a Tangent-Continuity method: Upward flow at the 2.5 m position on the forest hillslope.
71. The KB/KE ratio predicted by the moisture capacity method (Millington-Quirk equation) against the KB/KE ratio predicted by a Tangent-Continuity method: Downward flow at the 5 m position on the forest hillslope.
72. The KB/KE ratio predicted by the moisture capacity method (Millington-Quirk equation) against the KB/KE ratio predicted by a Tangent-Continuity method: Upward flow at the 5 m position on the forest hillslope.
73. A mean relative hydraulic conductivity curve for the peaty O/A horizon of an ironpan stagnopodzol at Plynlimon, determined by steady-state permeametry (data from Knapp, 1970) and the mean relative hydraulic conductivity curves for the O/A and A/E horizons of the forest hillslope and that of the A/E horizon of the grassland hillsope. The curves for the forest and grassland hillslope were derived from moisture capacity data applied to the Millington-Quirk equation.
74. Mean state-dependent hydraulic conductivities of the A/E and B horizon within the forest hillslope, over time.
75. Mean state-dependent hydraulic conductivities of the A/E and B horizon within the grassland hillslope, over time.
76. Specific stream discharge (per unit hillslope area) against the capillary potential or head

monitored within the borehole at the base of the forest hillslope.

77. Calculation of the mean head within the riparian zone of the forest hillslope.
78. Streamflow predicted from the application of the free-surface method to the hydrological properties within the riparian zone at the base of the forest hillslope, together with the streamflow monitored by the upper-drain-weir at the slope base. Only storm-periods 7,8, and 9 are shown.
79. The calculation of inter-horizon conductivity using an arithmetic mean.
80. Specific flux through the B horizon of the forest hillslope, during storm-period 3-4.
81. Specific flux through the B horizon of the grassland hillslope, during storm-period 3-4.
82. Specific lateral flux within the un-saturated upper zone of the forest A/E horizon, during storm 3-4.
83. Specific lateral flux within the un-saturated upper zone of the grassland A/E horizon, during storm 3-4.
84. Specific lateral flux within the un-saturated upper zone of the forest A/E horizon, during storm 10.
85. Specific lateral flux within the un-saturated upper zone of the grassland A/E horizon, during storm 10.
86. Specific lateral flux within the un-saturated upper zone of the forest A/E horizon, during the 10 day, dry period 14-24/5/88.
87. Specific lateral flux within the un-saturated upper zone of the grassland A/E horizon, during 10 day, dry period 14-24/5/88.
88. Instantaneous lateral flux within the saturated basal zones of the A/E horizon of the forest hillslope.
89. Lateral flux within the saturated basal zone of the O/A horizon ofthe forest hillslope during storm-period 10. The flux is an average value calculated from 7 litter-layer piezometer located at the 0, 2.5, 5, 10, 20, 30 and 40 m slope locations.
90. Predicted Lateral flow within the saturated basal zone of the forest O/A horizon, based upon linear-scaling of the average storm-flux calculated from piezometer measurements against the outflow from the O/A horizon throughflow trough (non-linear convergence is not taken in to account). Data for storm-period 3-4.
91. Predicted Lateral flow within the saturated basal zone of the forest O/A horizon, based upon linear-scaling of the average storm-flux calculated from piezometer measurements against the outflow from the O/A horizon throughflow trough (non-linear convergence is not taken in to account). Data for storm-period 10.
92. Predicted lateral flow within the saturated basal zone of the forest O/A horizon, based upon scaling the outflow from the O/A horizon throughflow troughs against a non-linear function of the average storm-flux calculated from piezometer measurements. A non-

linear function is used to remove the non-linearity in the convergence towards the throughflow troughs. Data for storm-period 3-4.

93. Parallel and serial coupling within the forest and grassland hillslopes.
94. A segment of the equipotential net within the A/E horizon of the forest hillslope predicted by a boundary-constrained numerical simulation applied to internal and boundary conditions at the peak of storm 3-4.
95. The specific flux predicted at the centroid of each element at the interface between a podzolic slope with a marked hydraulic discontinuity (between the topsoil and subsoil) and the riparian zone.

Tables.

22. Evapo-transpiration losses plus catchmant storage changes during selected storm and inter-storm periods, for the Tir Gwyn grassland catchment.
23. Evapo-transpiration losses plus catchmant storage changes during selected storm and inter-storm periods, for the Tir Gwyn forest catchment.
24. The difference in storm-period streamflow duration between the forest and grassland catchments.
25. Runoff generated during storm and inter-storm periods within the forest and grassland catchments.
26. The antecedent and storm, peak discharges monitored at the forest flume and grassland flume, stream gauging sites.
27. Storm period duration at the gauging structures within the drainage channel and stream, downstream of the instrumented forest hillslope.
28. Time to peak storm discharge at all gauging stations within the Tir Gwyn catchments.
29. Runoff generated during storm and inter-storm periods by the forest hillsope, drain micro-catchment, and forest catchment.
30. Rainfall-runoff ratios for individual storm and inter-storm periods within the forest and grassland catchments.
31. Ratio of the forest catchment R-R ratio to the grassland catchment R-R ratio for storm and inter-storm periods during the field seasons 9-27/11/87 and 23/1/88 - 26/6/88.
32. Rainfall-runoff ratios for the forest hillslope, drain micro-catchment, and forest catchment, during individual storm and inter-storm periods.
33. Wallingford neutron-probe (with a mark II L ratescaler) : count-time experiment 14/7/87.
34. The application of the Topp equation to TDR readings within the Tir Gwyn ferric podzol soil.
35. TDR calibration : the application of the Stein equation to the O/A and E horizons, and Alharthi equation to the B, B/C and C horizons of the ferric podzol soil (Experiment 13:30 27/3/88).
36. Average volumetric wetness of the soil horizons within the forest and grassland hillslopes.
37. Mean absolute change in the volumetric moisture content of each soil horizon, during the 12 monitoring periods between 7/11/87 and 22/6/88.
38. deleted.
39. Soil moisture content close to the butress root of a large conifer (47 cm DBH) in relation to that 2 m downslope of the same tree.
40. Lateral total potential gradients within the A/E horizon and vertical total potential gradients from the A/E to B horizon within the forest hillslope, during 1987.
41. Lateral total potential gradients within the A/E horizon and vertical total potential gradients from the A/E to B horizon within the forest hillslope, during 1988.
42. Lateral total potential gradients within the A/E horizon and vertical total potential

gradients from the A/E to B horizon within the ploughed section of the hillslope, from 1987 to 1988.

43. Bulk densities and porosities of brown forest soil, beneath a spruce stand in the Begliki district of Bulgaria (Molchanov, 1960).
44. Secondary-porosity of 22 samples extracted from the Tir Gwyn research hillslopes.
45. Saturated hydraulic conductivities measured by 7069 cm^3 ring permeameter cores versus 192 cm^3 small-core permeameter cores.
46. The range in saturated hydraulic conductivities of primary-structures ranging from gravel to clay.
47. Saturated hydraulic conductivity and intrinsic permeability within the forest and grassland riparian soils, determined using the Kirkham and Ernst equations.
48. Saturated hydraulic conductivity values calculated by both well and ring permeametry.
49. Wettability of soils after being dried at 105 °C for 48 hours.
50. The calculation of hillslope hydraulic condictivity using an inverse solution based upon the discharge recorded at the upper drain weir.
51. Studies using approximative solutions to hillsope flux.
52. Hillslope hydrological studies using numerical solutions of the full Richards equation.
53. Selected studies using numerical solutions employing local coordinates.
54. Lateral flow within the O/A and A/E horizons, and vertical flow through the B horizons of the forest hillsope.
55. Lateral flow within the O/A and A/E horizons, and vertical flow through the B horizons of the grassland hillsope.
56. Water-flux based upon internal-state response against those based upon the external-state response.

Acknowledgments.

I am indebted to Drs. Les Ternan and Andrew Williams (Department of Geographical Sciences) for their exemplary supervision. The extraordinary assistance of Dr. John Dowd (University of Georgia) and Dr. Brian Reynolds (Institute of Terrestrial Ecology) is also gratefully acknowledged.

Faultless technical support provided by the Central Workshop and Mrs. Sheila Ternan, Mr. Kevin Solman, Mr. Richard Hartley, Mrs. Ann Kelly, and Mr. Adrian Holmes of the Department of Geographical Sciences, Polytechnic South West, is much appreciated. Mr. Kevin Gilman and his staff at the Institute of Hydrology, Plynlimon field-station are thanked for their generous provision of transport, accommodation, and research equipment. Thanks are also extended to the NERC Automatic-Weather-Station Pool for the loan of two Mussel dataloggers, the Institute of Terrestrial Ecology for the loan of the Technolog and Campbell dataloggers, and Dr. Ian Foster for the loan of a Scanivalve system. Local farmers, Messrs. Jarmon and Jones, and the Llandrindod Division of the Forestry Commission are acknowledged for allowing unrestricted access to the research sites. Mr. Brian Rogers (Polytechnic South West), Mr. Graham Bowden and Mr. Nick Searle (University of Manchester) are thanked for their cartographic and typographic assistance.

Financial support was provided by the Natural Environment Research Council (NERC) studentship grant GT4/AAPS/86/41. Further fieldwork and conference grants awarded by the NERC University Support Section are also gratefully acknowledged.

Lastly, I would like to thank my parents for their unreserved encouragement over the last four years.

Declaration.

No portion of the work refered to in this thesis has been submitted in support of an application for another degree or qualification of this or any other academic institution.

The instrumented forest hillslope within the Tir Gwyn experimental catchments.

CHAPTER 1.

Introduction.

1.1. Soil-Water-Pathways: A Critical Environmental Control.

The physical processes which govern the movement of water within hillslopes are difficult to characterize (Bear *et al* 1968; Nielsen *et al*, 1986), and yet *must* be, if we are to predict the impacts of environmental change upon any hydrological or water-dependent natural system. Hillslope hydrological processes govern both the response of our rivers and streams (Freeze, 1972), and the transport of potentially damaging contaminants within our surface-waters and ground-waters. These contaminants may be acidic solutes (Bache, 1984), pesticides (Neary *et al*, 1985), fertilizers, industrial solvents (Lawrence and Foster, 1987), or radionuclides (Luxmoore and Abner, 1987). In addition, such water pathways are major controls upon the solute and particulate fluxes associated with slope instability, soil erosion, and landform development (Bunting, 1961; Pierson, 1983; Williams *et al*, 1984).

Recent concern over the acidification of streams draining coniferous forests (Hornung, 1984; Hornung *et al*, 1987a,b) has prompted research into the explanation of the sources of the solutes found within such streams. Current theories *suggest* that the transport of solutes along particular *water-pathways* is a major determinant of the chemical signature of these forest streams (Bache, 1984; Bricker, 1987; Hornung *et al*, 1986a; Lawrence *et al*, 1986; Neal *et al*, 1989). No research has, however, provided an incontrovertible physical characterization of the *water-pathways* within a natural hillslope system. Eduction of an accurate characterization of the hydrological control of the transport of acidic solutes into forest streams, provided the main impetus for this research.

1.2. Research Aims and Preface.

This research seeks to quantify the magnitude and direction of water movement within two hillslope segments, one afforested with conifers, the other ploughed and re-seeded with grass. This internal behaviour of the two hillslopes will be compared with the external-expression of that behaviour at both the hillslope and catchment scales. Differences between both the internal and external behaviour of the two land-covers will be explained with reference to the impacts of forest stands, individual conifer trees, and ploughing during pasture improvement.

The main emphasis of the research was the production of an *accurate*, physical characterization of the water-pathways within the two hillslopes. Although many previous studies have attempted to characterize hillslope water pathways, analyses based upon different types of field-technique applied at the same hillslope, have predicted *very* different water-pathways (Beven, 1989; Dunne, 1983; Erichsen and Nordseth, 1984; Hammermeister *et al*, 1982ab; Pearce *et al*, 1986). As a corollary to this, no mathematical simulation has been presented, which can accurately predict the internal behaviour of a *natural* hillslope. To date, all models simulating water-flow within layered hillslopes, have required the alteration of at least one *measured* hydrological parameter, to predict the response of the hydrological variables (see Stephenson and Freeze, 1974).

The reason for the discrepancy between the results based on different field techniques stems partly from the inevitable errors which arise from the conceptualization of very complex processes, but also from an inadequate characterization of the *errors associated with the use of each technique.* All techniques used in the assessment of soil-water-movement impose their own set of totally artificial boundary conditions upon the *true* hydrological system (Anderson and Burt, 1978; Bear, 1972; Dunne, 1983; Beven and O'Connell, 1982).

This research seeks to over-come this problem of measurement error, by combining numerous independent and quasi-independent field and analytical techniques to characterize the water-pathways within each hillslope segment. The use of two hillslopes with very different land uses and hence different water-pathways (?), further tests the accuracy of the techniques employed. Although the errors associated with the use of each technique must be fully characterized, the research is directed towards an understanding of the *physical processes*, rather than towards an understanding of the techniques. The research is *process-driven* rather than *technique-driven* (Collins, 1987; Klemes, 1986).

Analysis of the hydrological behaviour of the two hillslope and catchment areas is divided into the four key areas of:

1. the external rainfall-runoff response of the hillslope and catchment areas, and its implications for the water-pathways (Chapter 5),
2. the response of the internal-state hydrological variables in relation to the water-pathways (Chapter 6),
3. the impact of the internal-state hydrological parameters upon and the water-pathways (Chapter 7), and
4. the predictions of the water-pathways using approximative and boundary-constrained numerical calculations (Chapter 8).

The results of the analysis of the chemistry of precipitation, soil-waters and stream waters within the Tir Gwyn forest hillslope system, are presented within Chappell *et al* (1990). The combinations of water-pathways that could produce the observed chemical signatures within the stream and riparian zone, are expounded within Chapter 9.

Implications of the predicted water-pathways for the movement of solutes to streams conclude Chapter 9.

A summary of the aims which are addressed within the thesis are:

1. To produce concordant predictions of the direction and magnitude of soil-water-movement within a coniferous hillslope and a grassland hillslope, using several independent and quasi-independent techniques of measurement and analysis.
2. To compare the internal-state behaviour of the forest hillslope with that of the ploughed, grassland hillslope, and educe the impact forest stands and ploughing upon water-pathways.
3. To investigate the local effect of individual trees, under a particular set of physical controls, upon hillslope water movement as a whole.
4. To examine the external-state response at the catchment and hillslope scale, to both elucidate characteristics of the internal response that are exhibited in the external behaviour, and to verify the predictions of internal response.
5. To examine the impacts of forest and grass covers upon the external-state, or rainfall-runoff behaviour of catchments and hillslopes.

Further release from the constraints imposed by the various techniques used to measure and analyze soil-water-movement was achieved by building upon the ideas developed within the fields of *hillslope hydrology* (Section 1.4), *forest hydrology* (Section 1.5) and the *physics of flow through porous media* (Section 1.4.3). Given that many of the principles developed within each these of fields have not been fully embraced by the other hydrological fields, three principles underlying the measurement and analysis used within this eclectic approach to soil water movement are outlined.

1.3. The Three Principles of Hillslope Hydrology.

The innate difficulties associated with characterizing physical, soil-water processes, are known as the *Identification or Inverse Problem* (Bear and Veruijtt, 1988; Yeh, 1986). They result from the complexities of the flow-regime, solution geometry, and spatial variability of the hydrological properties.

I. Flow Regime : The movement of water within soil pores can be non-Newtonian (molecular / slip / Knudsen), Darcian (laminar / viscous / conductive), Oseen (Forchheimer/partially turbulent), or turbulent (convective) depending upon the fluid velocity and viscosity, and upon the pore resistance (Bear, 1972; Chow *et al*, 1988; Hannoura and Barends, 1981). Under these different flow regimes the relationship between the energy gradient and the resultant flow alters, i.e.

Turbulent	*Oseen*	*Darcian*	*Non-Newtonian*
0.5	..hydro-dynamic region..	1	>>1 a

where: $q \alpha J^a$ [1]

Where q is water-flux and J is potential gradient. Under Darcian conditions, water movement within a completely saturated volume of soil is, therefore, directly proportional to the average energy or *potential* gradient (Darcy, 1856; Hubbert, 1940). This simple relationship is known as *Darcy's Law* (Section 1.3.3).

II. Solution Geometry : Flow within hillslope soils can be calculated from a characterization of the hydrological properties (i.e. variables and parameters) of either individual pores or volumes of pores.

Water movement within individual pores can be calculated using Knudsen's Equation for predominantly non-Newtonian flow (Knudsen, 1909), either Poiseuille's equation (Poiseuille, 1846), or Snow's equation (Snow, 1968) for Darcian flow, and Navier-Stokes equations (Lamb, 1932; Navier, 1822; Stokes, 1845) for Oseen or fully-turbulent flow. The hydrological properties required to solve *these* equations for hillslope flow problems are, however, extremely difficult to identify and measure (Bear *et al*, 1968; Bouma and Anderson, 1973; Cvetkovic, 1986; Marsily, 1986; Millington and Quirk, 1960; Muskat and Meres, 1936; Scheidegger, 1974).

Hillslope water movement is, therefore, usually analysed by the characterization and solution of equations relating to volumes of soil-pores, known as *control-volumes* or *CV's* (Euler, 1755; Section 3.5.1). The size of these volumes, therefore, determines the spatial resolution to which the pathways can be described. When the flow regime is Darcian, then Darcy's equation can be used (Section 1.3.3); if flow begins to lose inertia, then Forchheimer's equation (Forchheimer, 1901) is more applicable. In both cases, the average water flux at the centre of each control-volume is calculated by multiplying the respective potential gradients by a proportionality coefficient, known as the *hydraulic conductivity*. This coefficient or parameter is empirically determined for each control-volume of soil.

The division of the energy gradient by a resistance, rather than multiplication by a conductivity would be more intuitive and physically correct. Conductivity is, however, used within almost all representations of the macroscopic motion equation (Equations 3 to 19), and is, therefore, used within this thesis both to maintain consistency and prevent misconception.

III. Spatial Variability : While it is not usually feasible to measure all of the hydrological properties within all of the control-volumes of a hillslope soil, the sampled control-volumes must accurately *represent* the true distribution within the whole hillslope (Binley *et al*, 1989; Klute, 1973; Freeze, 1980; Marsily, 1986; Sharma *et al*, 1987; Warrick and Nielsen, 1980). A failure to represent zones of preferential flow (Section 1.3.2) for example, would result in very inaccurate solutions (Sharma and Luxmoore, 1979).

Despite the major problems associated with identifying and representing the processes governing the movement of water within hillslopes, our knowledge of hillslope hydrology has made considerable advances over the past 60 years (Warrick *et al*, 1986; Section 1.4).

1.4. Hillslope Hydrology : Synthesis of Pertinent Research.

Research into the movement of water at the hillslope scale can be divided into essentially three levels of analytical and measurement detail:

1. Hillslope Rainfall-Runoff (Section 1.4.1),
2. Hillslope Hydrological Mechanisms (Section 1.4.2), and
3. Hillslope Hydrological Processes (Section 1.4.3).

1.4.1. Hillslope Rainfall-Runoff.

Techniques aimed at predicting the volume of streamflow generated by particular hillslopes, from the historical streamflow response and current rainfall data, were initially developed by engineering hydrologists assessing the probability of flooding. These techniques are based upon the external manifestation of hillslope response, and, therefore, do not require the accurate characterization of hydrological properties within the hillslopes. The first of these *fitted* techniques were the ***unit hydrograph approach*** (e.g. Brater, 1939; NERC, 1975; Sherman, 1932; Snyder, 1938) and the ***rationale method*** (Mulvany, 1851).

More recently, techniques based upon conceptual models (e.g. ***Birkenes:*** Christophersen *et al*, 1982; ***Stanford-Watershed-Model:*** Crawford and Linsley, 1966), ***auto-regressive-moving-averages*** (Box-Jenkins, 1971), hydrograph separation (e.g. ***R-Index:*** Hewlett *et al*, 1977), and topographic indexes (e.g. ***Topmodel:*** Beven and Kirkby, 1979) have been *fitted* to both streamflow, and hydrochemical response. More complex, mathematical models such as the ***Institute of Hydrology Distributed Model*** (Beven *et al*, 1987) and the ***Systeme Hydrologique Europeen*** model (Abbott *et al*, 1986) could be described as rainfall-runoff models, as they have to date, only been *fitted* (or optimized) to historical streamflow response (Beven 1989; Klemes, 1986; Rogers *et al*, 1985).

1.4.2. Hillslope Hydrological Mechanisms.

Although streamflow response within particular catchments can be predicted using the simple rainfall-runoff approach, the effects of land-use changes upon that response cannot be predicted unless such changes were evident during the *calibration* period (Beven and O'Connell, 1982). To make predictions about the impact of future land-use changes within an existing experimental catchment, or to make predictions about the response of an uninstrumented catchment, requires an understanding of how changing environmental conditions affect the detailed processes which govern hillslope water movement. As there are numerous hydrological processes (Section 1.3.3) and possible interactions between such

processes, hillslope water movement and subsequent streamflow generation can be conceptualized and assessed at a slightly more empirical level. A *mechanism* is the result of the interaction between the physical processes (Section 1.4.3) and the distribution of the physical controls (Section1.4.4).

Streamflow generation mechanisms can be grouped into those mechanisms providing the large volumes of streamflow during *storm-periods* (Section 5.3.1), and those generating streamflow during periods of low-flow. Streamflow during periods of low flow is usually seen to be generated solely by various forms of subsurface flow (see Horton, 1933; Hewlett, 1961); while streamflow during storm periods has been shown to be generated generated by:

1. direct in-channel precipitation,
2. Hortonian infiltration-excess overland flow,
3. saturation-excess overland flow, and
4. dynamic subsurface stormflow.

Direct In-Channel Precipitation.

Precipitation which falls directly into the stream channel naturally generates part of the rapid runoff appearing during storm events. This component can dominate streamflow hydrographs during high intensity, low volume (i.e. <20 mm) rainfall events, and a during the initial stages of major storm events (Hursh and Brater, 1941). The direct in-channel input of small volumes of highly concentrated throughfall beneath forest canopies, can be critical in the calculation of ion fluxes during storm periods (Potter *et al*, 1988).

Hortonian Infiltration-Excess Overland Flow.

Horton (1933) considered subsurface flow to be too slow a mechanism to generate the large volumes streamflow seen during storm periods. He thought that all storm-period streamflow was generated by water movement across the land surface. This so called *overland flow* was produced by rainfall intensities greater than a soil's *infiltration capacity* (equivalent to the sorptivity in dry soils and saturated hydraulic conductivity in wet soils: Section 7.4).

This mechanism, once considered to be the dominant storm-flow mechanism in *all* catchments, is now seen to be restricted to arid zones (e.g. Dubreuil, 1985; Yair and Lavee, 1985) and small intra-catchment areas (e.g. Herwitz, 1986; Williams, *et al*, 1984) (Hewlett and Nutter, 1970; Dunne, 1978). Hortonian overland-flow predominates in arid zones, because desert soils often develop *surface crusts* (Valentin, 1981) and a hydrophobicity (or non-wettability: Section 7.4.5) when very dry (Krammes and Debano, 1965).

Saturation-Excess Overland Flow.

The second mechanism which generates storm-period streamflows by the flow of water across the land surface, is *saturation-excess overland flow*. This type of overland flow can be induced by two separate conditions: first, by precipitation falling directly on to saturated areas (Dunne and Black, 1970a,b) and second, by the exfiltration of subsurface stormflow (Cook, 1946; Whipkey and Kirkby, 1978). This exfiltration or *return flow* of soil water is produced when upslope additions of water exceed the combined drainage and storage capacity of a downslope zone.

As saturation-excess overland flow is produced on saturated soils, areas likely to develop such flow are zones with thin soils, contour convergence, slope concavity, or relatively impermeable subsoils (Betson and Marius, 1969; Bonell *et al*, 1983; Dunne, 1978; Kirkby and Chorley, 1967; Quinn *et al*, 1989). Saturated zones which produce saturation-excessoverland olow are known as *partial areas* (Betson, 1964).

Dynamic Subsurface Stormflow.

The generation of streamflows during storm-periods in catchments with infiltration and percolation rates too high to produce overland flow, indicates a rapid supply of water by below-ground or *subsurface* routes (Hursh, 1936; Hursh and Hoover, 1941). This *subsurface stormflow*, also known as *throughflow* (King, 1899), *shallow seepage* (Lowdermilk, 1934; Bunting, 1961), *quick subsurface runoff* (Cook, 1946) and *interflow* (Arnett, 1974; Betson and Marius, 1969), was largely ignored until the research of Hewlett in the early 1960's (e.g. Hewlett, 1961; Hewlett and Hibbert, 1963, 1967). Hewlett's *new* mechanism was similar to an earlier model envisaged by Hursh (*op. sit*), in which storm period streamflow was generated by *the recharge of stream-side areas by lateral flow from surface soil horizons, followed by a delayed input to the stream* (Hursh and Hoover, 1941). Hewlett demonstrated how streamflow appeared to respond to the build-up of water within stream-side areas, which he called *variable source areas* (Hewlett, 1969, 1974). As the size of these apparent *source areas* increased, so did the amount of streamflow. This new model was somewhat different from Hursh's original model, in that the stream-side (or riparian) areas were rapidly recharged by a displacement process termed *translatory flow*, within *all* of the partially-saturated upslope soils (Hewlett and Hibbert, 1967).

Although nearly all of the subsequent models include the riparian component of the Hursh/Hewlett model, three basic *source area models* can be defined:

1. the displacement model,
2. the macro-pore model, and
3. the near-surface flow model.

Each of the models are, however, not mutually exclusive (Dunne, 1978), and all involve the idea of the generation of streamflow from soil-zones of preferential flow.

1. Displacement Model : Numerous hydrological studies using stable isotopes (e.g. Abdul and Gillham, 1984; Brunsden, 1981; Herrmann and Stichler, 1980; Kennedy *et al*, 1986; Martinec, 1975; Rodhe, 1981; Sklash and Farvolden, 1979 Sklash *et al*, 1982; Turner *et al*, 1987) indicate that precipitation mixes with and displaces considerable volumes of *pre-event* water prior to reaching any water course. This *miscible displacement* mechanism (Nielsen and Biggar, 1961) may operate within both the groundwater zone (defined as water within the saturated or phreatic zone: Freeze and Cherry, 1979; Hewlett, 1982) or under-saturated zone (Kennedy *et al*, 1986) of any catchment. Elevated levels of displacement are induced by three possible mechanisms:

1. An increased gas-phase pressure in the partially-saturated zone, caused by air-entrapment during infiltration (Meyboom, 1966; Morel-Seytoux, 1983; Stauffer and Dracos, 1986).
2. A 'thickening of the water films surrounding soil particles' in the partially-saturated zone (Hewlett and Hibbert, 1963). The actual existence of this so called *translatory* mechanism has, however, been questioned by Bernier (1982), Bonell *et al* (1984), and Burt (1985).
3. The near-instantaneous saturation of the secondary-structure (or macro-porosity) within near-saturated soils (Beven, pers. comm. 1988; Gillham, 1984).

2. Macro-Pore Model : Macro-pores or *secondary-pores* (Section 7.3.6) are defined within this thesis as both:

1. *soil pores which conduct water at rates far greater than the mean pore velocity, i.e.*

$$\langle q_{pore} \rangle = \frac{\langle q_{macroscopic\ flux} \rangle}{\langle \eta \rangle - dps} \qquad [2]$$

where q is specific flux or velocity (dim. LT^{-1}), <> is mean, η is porosity of the control-volume ($cm^3\ cm^{-3}$), and dps is proportion of *dead* or inactive pore-space, where η - dps is η_e effective porosity (Dupuit, 1863: in Bear *et al*, 1968 p53).

2. *pores that conduct far more new rather than stored or old water through a control-volume.*

Macro-pore voids may be formed by a number of quite separate processes, including: internal erosion, root penetration, clay desiccation, freeze/thaw weathering, and animal burrowing (Bear, 1972; Beven and Germann, 1982; Dixon and Simanton, 1979).

The importance of macro-pore flow as a streamflow generation mechanism, has been shown by both direct gauging and tracer studies. The direct gauging of flow within large macro-pores, known as *pipes* within the upper parts of the Institute of Hydrology, Plynlimon Catchments (mid-Wales) provides perhaps the most compelling evidence (Gilman and Newson, 1980; Jones, 1981; Pond, 1971; Wilson and Smart, 1984; Section 2.6.2). Occasionally these large macro-pores have been seen to conduct water to the stream-bank (Jones and Crane, 1981; Section 2.5.2). The movement of relatively conservative tracers through hillslope soils, at velocities greater than those predicted by the Eulerian approach (Section 3.5.1), *may* provide a second source of evidence, assuming that the calculated control-volume-based flows were accurate (Smart and Wilson, 1984; Trudgill *et al*, 1984). Although streamflow generation by large macro-pores has been proven by direct gauging, the role of smaller macro-pores (e.g. 0.06 to 20 mm in diameter) remains less certain (Burt, 1985, 1987; Horton and Hawkins, 1965; Nielsen *et al*, 1986; Pearce *et al*, 1986).

The hydrological properties governing water-flow within individual pores are discussed within Sections 1.2 and 1.4.3.

3. Near-Surface Flow Model : The permeability of soils found within particular hillslopes often varies over several orders of magnitude (Bonell *et al*, 1983; Hoover, 1949; Knapp, 1970; Nielsen *et al*, 1973). Most of this variability results, however, from deterministic changes between different catenal positions and different profile positions (Sections 3.5.3., 3.5.4., 7.4.2. and 7.4.3)).

When near-surface soil horizons are more conductive than deeper horizons, the resultant *hillslope anisotropy* (Section 6.6; Bear, 1972) produces lateral soil water movement (Section 6.2.3. and 8.2.2). The greater the relative discontinuity between the conductivity of each horizon, the greater the lateral deflection (Burt and Butcher, 1985). The discontinuity in the properties must be relative not absolute, because continuity must be maintained between soil horizons possessing at least some hydraulic conductivity (Zaslavsky, 1964). When conductivity differences are marked, perched water tables in otherwise unsaturated soil can develop above the discontinuity (Betson and Marius, 1969; Bonell *et al*, 1981; Section 6.3.3).

Even when hillslopes have near-isotropic and homogenous *intrinsic permeabilities* (Equation 11; Section 7.4), but are only partially-saturated with water, the *state-dependent hydraulic conductivity* (Section 7.4) may be different at different positions within a profile, and so produce an anisotropy within the profile as a whole (McCord and Stevens, 1987; Price and Hendrie, 1983; Zaslavsky and Rogowski, 1969). The infiltration of rainfall into a relatively dry isotropic soil will, therefore, induce lateral flow within the surface soil.

If a partially saturated soil horizon with a fine texture overlies a coarse textured soil horizon which is also partially saturated, then the base of the fine soil horizon must approach saturation to allow water to flow into the lower horizon. This results from the greater importance of capillary-induced flows within the finer soil, when the soil is only partially saturated. When saturated with water, gravity-induced flows acting more equally within the two soil horizons, become more important. This retardation of flow at the horizon discontinuity can promote lateral flow (Miyazaki, 1988). In addition, as the saturated wetting front advances into the lower horizon, its movement will be controlled not by the saturated hydraulic conductivity of the lower horizon, but by the rate of loss from the upper horizon. This produces an instability, which leads to a vertical *fingering* of flow (Parlange, 1974).

Any change in vertical conductivity within hillslope soils (often within the near-surface horizons) will, therefore, inhibit vertical percolation and thus promote lateral flow. This model could be called the *percolation-excess lateral flow model.*

Hursh and Brater (1941) suggested how a temporal sequence of some of these *hillslope hydrological mechanisms* might generate the storm hydrograph within a temperate forest. A precis of this theoretical sequence begins with:

1. direct in-channel precipitation,
2. response of shallow water tables within the riparian zone (possibly producing saturation excess overland flow),
3. near-surface flow of sub-surface waters,
4. subsurface flow in localized or preferred zones within deep regolith, and
5. subsurface flow within deep regolith, fed by subsurface) flow from steap slopes.

Although all of these mechanisms can to some degree be monitored and quantified, the precise relationships between each of these mechanisms and streamflow response, requires a more detailed understanding of the physical processes governing water movement at some representative scale.

1.4.3. Hillslope Hydrological Processes.

Hillslope hydrological processes are defined as those interactions within the hydrolog ical system which can by described by elementary principles and laws and hence solvable over successive short-time steps. The scale usually chosen to examine hillslope hydrological processes is the *control-volume-scale* (CV-scale; Sections 1.3., and 3.5.1), although both larger (e.g. Beven, 1982) and smaller (e.g. Yeh, 1981; Section 1.3) scales have been used. The average movement of water through a control-volume of soil pores can then be described by various extensions of Darcy's original equation (Darcy, 1856), provided flow is relatively laminar (Section 1.2).

The General Motion Equation (For Darcian Flow).

Darcy's macroscopic flow equation was originally developed for the calculation of water-flow within completely water-saturated volumes of soil pores (Equation 3; Darcy, 1856; Section 1.2).

$$q = \frac{d}{dx}\left\{ K_s . \frac{d(\phi_g + \phi_c)}{dx} \right\} \qquad [3]$$

The actual form of the original equation is given within Childs (1969)

where q is specific water flux (or specific discharge) (dim. LT^{-1}), K_s is saturated hydraulic conductivity (dim. LT^{-1}), $d(\phi_g+\phi_c)/dx$ is potential (energy) gradient (dim. LL^{-1}), ϕ_g is gravitational (or elevational) potential (dim. L), and ϕ_c is capillary potential (i.e. the negative of a suction/tension) (dim. L).

The equation has, however, been extended to the calculation of flow within partially-saturated (or multi-phase air-water) soils by the use of a *relative hydraulic conductivity function* in place of the single value of saturated hydraulic conductivity (Equation 4; Richards, 1931). It has been assumed that Darcy's Law (Section 1.2) still applies (Richards, 1931; Nikolaevskii and Somov, 1978; Wyckoff and Botset, 1936).

$$\frac{d\theta}{dt} = \frac{d}{dx}\left\{ K . \frac{d(\phi_g + \phi_c)}{dx} \right\} \qquad [4]$$

where:

$$K = K_s . K_r \qquad [5]$$

where $d\theta/dt$ is change of moisture content with time (i.e. discharge) (dim. $L^3L^{-3}T^{-1}$), K is hydraulic conductivity function (dim. LT^{-1}), K_s is saturated hydraulic conductivity (dim. LT^{-1}), K_r is relative hydraulic conductivity of the wetting (i.e. water) phase (dimensionless) and $d(\phi_g+\phi_c)/dx$ is potential gradient (or change of total potential with distance) (dim. LL^{-1}).

The relationship between the moisture content (Section 6.2) and matric potential (Section 6.3) properties, is called the *specific moisture capacity* (Section 6.4). The incorporation of this function within Equation 4, which requires the solution of the *derivative of the rate of change* of both ϕ_c and θ, enables the Richards equation to be solved for only ϕ_c (Equation 6; Richards, 1931) or θ (Equation 7; Buckingham, 1907; Klute, 1952; Richards, 1931; Sposito, 1986).

$$\frac{d\theta}{d\phi_c} . \frac{d\phi_c}{dt} = \frac{d}{dx}\left\{ K . \frac{d(\phi_g+\phi_c)}{dx} \right\} \qquad [6]$$

where $d\phi_c / d\theta$ is inverse specific moisture capacity (dim. $LL^{-3}L^{-3}$), $d\phi_c / dt$ is change of capillary potential with time (dim. LT^{-1}), K is hydraulic conductivity function (dim. LT^{-1}), $d(\phi_g+\phi_c)/dx$ is potential gradient (dim. LL^{-1}).

$$\frac{d\theta}{dt} = \frac{d}{dz}\left\{ K . \frac{d\phi_c}{d\theta} . \frac{d\theta}{dz} - K \right\} \quad [7]$$

where:

$$K . \frac{d\phi_c}{d\theta} = \textit{hydraulic diffusivity} \quad (D_h) \quad [8]$$

where $d\theta / dt$ is change of (volumetric) moisture content with time (dim. $L^3L^{-3}T^{-1}$), K is hydraulic conductivity function (dim. LT^{-1}), $d\phi_c / d\theta$ is inverse specific moisture capacity (dim. $LL^{-3}L^{-3}$), $d\theta / dz$ is change of (volumetric) moisture content with vertical distance (dim. $L^3L^{-3}L^{-1}$) and D_h is hydraulic diffusivity (dim. $L^{-2}T^{-1}$).

The Richards Equation can be further extended to include both compression of the porous media (i.e. non-zero storativity: Equation 9; Cooper, 1966; Freeze, 1971; Jacob, 1940) and the effects of changing water density and viscosity (Equation 10; Hubbert, 1940; Nutting, 1930).

$$\frac{d\phi_c}{dt}\left\{ \rho_f \frac{d\theta_v \eta}{d\phi_c} + \theta_v \rho_f (a + \eta B) \right\} = \frac{d}{dx}\left\{ K . \frac{d\phi_c}{dx} \right\} \quad [9]$$

where $d\phi_c / dt$ is change of capillary potential with time (dim. LT^{-1}), ρ_f is fluid density (dim. ML^{-3}), θ_v is percent saturation (dim. $L^3L^{-3}L^3L^{-3}$), η is porosity (dim. L^3L^{-3}), $d\theta_v\eta / d\phi_c$ is specific moisture capacity (or C) (dim. $L^3L^{-3}L^{-1}$), $\theta_v (a+\eta B)$ is specific storativity, a is matrix compressibility, B is fluid compressibility, K is hydraulic conductivity function (dim. LT^{-1}) and $d\phi_c / dx$ is total potential gradient (dim. LL^{-1})

$$\frac{d\theta}{d\phi_c} . \frac{d\phi_c}{dt} = \frac{d}{dx}\left\{ \frac{k\rho_f g}{\nu} . K_r . \frac{d(\phi_g + \phi_c)}{dx} \right\} \quad [10]$$

where:

$$k\rho_f g / \nu = K_s \quad [11]$$

where $d\theta / d\phi_c$ is specific moisture capacity (or C) (dim. $L^3L^{-3}L^{-1}$), $d\phi_c / dt$ is change of capillary potential with time (dim. LT^{-1}), k is intrinsic permeability (dim. L^2), ρ_f is fluid density (dim. ML^{-3}), g is gravitational acceleration (dim. LT^{-2}), ν is dynamic fluid viscosity (dim. $ML^{-1}T^{-1}$, where ν/ρ_f = ν kinematic fluid viscosity dim. L^2T^{-1}), K_s is saturated hydraulic conductivity (dim. LT^{-1}), K_r is relative hydraulic conductivity of the wetting (i.e. water) phase (dimensionless) and $d(\phi_g+\phi_c)/dx$ is potential gradient (dim. LL^{-1}).

Mass Balance Equations (For Control-Volumes of Pores).

Implicit to the Darcy-Richards Equation (Equations 3 to 10) is the notion that the difference between the water lost and gained by a *control-volume* of soil, is equal to the change in volumetric water content (plus any changes in storativity: Equation 9). In other words, the change in water content minus the flux equals zero (Equation 12: *spatial-Eulerian-description of continuity*: Euler, 1755), i.e.

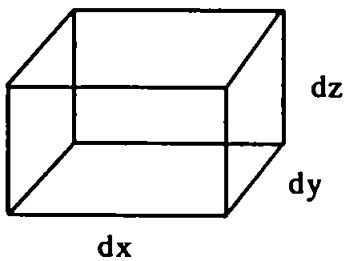

$V_y dxdz$
(mass inflow across dxdz)

$$\{ V_y + \frac{dV_y}{dy} dy \} dxdz$$

(mass outflow across dxdz at dy distance from inflow)

Thus: Net outflow in y direction
(for an incompressible fluid)

$$\{ V_y + \frac{dV_y}{dy} dy \} dxdz - V_y dxdz = \frac{dV_y}{dy} dxdydz$$

Thus: Total net outflow (in x, y, and z directions)

$$\{ \frac{dV_x}{dx} + \frac{dV_y}{dy} + \frac{dV_z}{dz} \} dxdydz$$

Mass of water in parallelepiped at any time = qdxdydz

$$\text{Temporal change of mass} = \frac{dq}{dt} dxdydz$$

$$\text{Thus: } \{ \frac{dV_x}{dx} + \frac{dV_y}{dy} + \frac{dV_z}{dz} \} dxdydz - \frac{dq}{dt} dxdydz = 0$$

Or:

$$\text{div } q - \frac{dq}{dt} = 0 \qquad [12]$$

Where:

$$\text{div} = \frac{d}{dx} + \frac{d}{dy} + \frac{d}{dz}$$

$$q = V_x + V_y + V_z$$

where $d\theta/dt$ is change of moisture content with time (dim. $L^3L^{-3}T^{-1}$), q is specific water flux (or specific discharge) (dim. LT^{-1}) and div is divergence operator.

The movement of water in and out of a static control-volume can be calculated at specific points in time, using *standard* (or Eulerian / global) coordinates. To track the movement of water through a hillslope where the moisture status is changing, then we need to move the control-volumes through the hillslope. To reduce dispersion we usually move a control-volume by reference to the position of a notional *fluid-particle* (Bear, 1972) located at the centre of the control-volume, using a *local* (or Lagrangian) coordinate system (Bear and Verruijt, 1987).

Flowline Continuity (For Control-Volumes of Pores).

The movement of water along a flowline must cross the boundaries between control-volumes of pores according to the *Tangent-Refraction Law* (Hubbert, 1940; Jacob, 1940). This continuity (or mass-balance) equation can be written as:

(a) Refraction of equipotential-lines:

$$\frac{J_{s1}}{J_{n1}} = \tan a_1 \quad [13] \qquad \frac{J_{s1}}{J_{n2}} = \tan a_2 \quad [14]$$

$$K_1 . J_{n1} = K_2 . J_{n2} \quad [15]$$

thus

$$\frac{K_1}{K_2} = \frac{\tan a_1}{\tan a_2} \quad [16]$$

(b) Refraction of streamlines:

$$q_1 \cos b_1 = q_2 \cos b_2 \quad [17]$$

thus

$$\frac{K_1}{K_2} = \frac{\tan b_1}{\tan b_2} \quad [18]$$

where q_1 is incidence (advective) mass flux (dim. LT^{-1}), q_2 is refraction (advective) mass flux (dim. LT^{-1}), a_1 is equipotential-line incidence angle (degrees), a_2 = equipotential-line refraction angle (degrees), b_1 is stream-line incidence angle (degrees), b_2 = stream-line refraction angle (degrees), K_1 is (isotropic) hydraulic conductivity: first CV (dim. LT^{-1}), K_2 is (isotropic) hydraulic conductivity: second CV (dim. LT^{-1}), J_{s1} is slope-ward hydraulic gradient: first CV (dim. LL^{-1}), J_{n1} is slope-normal hydraulic gradient: first CV (dim. LL^{-1}), J_{s2} is slope-ward hydraulic gradient: second CV (dim. LL^{-1}) and J_{n2} is slope-normal hydraulic gradient: second CV (dim. LL^{-1}). A *stream-line* is an isoline of instantaneous or steady-state, specific flux (Bear, 1972).

Hydrodynamic Dispersion.

(Microscopic Flow within the Control-Volume of Pores)

The *Eulerian control-volume approach* seeks to describe only the *average* flux across control-volumes of pores, and not the actual flow of water within individual pores. To approximate the impact of microscopic flow (or flow within individual pores), upon the average macroscopic flux, an extra term - **D** or *dispersion* can be introduced into the flow equation. This term is applied using local (or Lagrangian) coordinates. As the flow equation now includes both advective (or macroscopic) and dispersive terms, it is naturally called the *advection-dispersion* or *hydrodynamic dispersion equation* (Equation 19; Bear, 1961; Nikolaevskii, 1959; Scheidegger, 1961). When solute transport is being predicted, the dispersion term can include a component representing *molecular* or *Fickian diffusion*.

$$\frac{d\theta}{dt} = \frac{d}{dx}\left\{ \mathbf{D}\frac{d\theta}{dx} + \langle q_{pore}\rangle\theta \right\} \qquad [19]$$

where $d\theta / dt$ is change of volumetric moisture content (or water mass concentration: Bear *et al*, 1968) with time (dim. $L^{-3}L^{-3}T^{-1}$), **D** is coefficient of dispersion (dim. L) and $\langle q_{pore}\rangle$ is mean pore velocity (Equation 2)(dim. LT^{-1}).

If a significant proportion of the hillslope flow is concentrated into discrete pores, then such flow may be more realistically represented by the solution of flow equations for individual pores (Section 1.2; 1.3).

Macro-Pore Representation

(Equations of Flow within Individual Pores).

If the distribution of discrete and highly conductive pores within a hillslope soil is relatively simple, then this preferred flow can be included within the Eulerian CV-approach by the addition of a *fluid-sink* at the pore entrance and a *fluid-source* at the pore exit (Beven and Germann, 1981b). If, however, the distribution of such pores is both complex and widespread, then more complex *two-domain models*, or models based upon pore equations should be used (Section 1.3).

1.4.4. Physical Controls.

The principal environmental conditions controlling the movement of soil water, include: (1) climate, (2) topography and slope, (3) depth of porous media, (4) soil and water hydrological properties, and (5) vegetation. Although all of these *physical controls* can be identified within all hillslope hydrological studies, the relative importance of each varies from site to site (Dunne, 1978; Freeze, 1974).

Climate.

Precipitation input is by far the best single predictor of streamflow generation (Bren *et al*, 1979). The input of large volumes of precipitation results in the output of large volumes of streamflow (Section 5.3.). The absolute volume of precipitation available for streamflow is, however, dependent upon the evapo-transpiration losses. These losses can be as small as 16 percent (400 mm) per annum in a cool grassland catchment (Hudson, 1988) or as much as 70 per percent per annum (1468 mm) in tropical rain-forest catchments (Walsh, 1987; Section 1.5.1).

Topography and Slope.

The predominant energy gradient (Section 6.3) within soils found within cool temperate climates, is largely a function of the elevational gradient or slope (Anderson and Burt, 1978). As slopes steepen, the energy gradients steepen, and, therefore, soil water velocity increases (Hursh, 1944; Hewlett and Hibbert, 1963; Kirkby, 1971).

When lines of equal elevation (i.e. contours) converge, then subsurface flow will concentrate. This concentration of flow leads to the development of saturated zones in otherwise unsaturated hillslopes (Anderson and Kneale, 1980; Beven *et al*, 1987; Bren *et al*, 1979; Burt and Butcher, 1985; Kirkby and Chorley, 1967; Zaslavsky and Rogowski, 1969; Section 8.2.1).

Depth of the Porous Media.

When the depth of the porous media (i.e. soil and regolith) is shallow, then the storage capacity and length of the water pathways are both much smaller. This again produces more rapid streamflow generation (Betson and Marius, 1969; Cook, 1943; Pilgrim *et al*, 1978; Hewlett and Hibbert, 1967).

Soil and Water Hydrological Properties.

When steep, convergent hillslopes with thin soils are close to saturation (i.e. they have a high antecedent moisture status), even small precipitation inputs will produce rapid soil water and streamflow responses (Ragan, 1968).

Given the moisture status and dimensions of the hillslope flow-region, the pathways and rates of water movement within the hillslope are controlled by the spatial distribution of the soil pores within each CV and across the CV-distribution. Pore- size and connectivity distributions are often markedly different in different soil horizons and at different slope positions, which can confine most hillslope water movement to specific horizons or slope positions (Nielsen *et al*, 1973; Rogowski *et al*, 1974; Walsh and Voigt, 1977; Weyman, 1970; Sections 3.5.3., 3.5.4., 7.2., 7.4.2., 7.4.3., and 8.2.2).

Vegetation.

Vegetation is perhaps the process-control least understood and researched (Brenner, 1976; Lelong *et al* 1987). The few studies which do exist, include the hydrological effects of grass (e.g. Bouma and Dekker, 1978; Hino *et al* 1987), bracken (e.g. Arnett, 1974, 1976; Carter, 1983; Williams, *et al* 1987), heather (e.g. Calder *et al*, 1982), and trees (e.g. Hursh, 1944; Hoover, 1956; Law, 1956; Reynolds, 1966). Because of their greater biomass trees are likely to have the greatest impact and thus warrant the greatest emphasis. The hydrological relations of trees are commonly referred to as *Forest Hydrology.*

1.5. Forest Hydrology : Synthesis of Pertinent Research.

The impact of forests upon the hydrological cycle can be divided into the effects of:

1. canopy processes and water relations (Section 1.5.1),
2. forest soil hydrology (Section 1.5.2), and
3. UK forestry practices (Section 1.5.3).

1.5.1. Canopy Processes and Water Relations.

Surficial evaporative processes (i.e. direct evaporation) within tree canopies combined with biological transpiration, deplete the total amount of moisture available to generate streamflow. Precipitation which is not evaporated from canopy surfaces, is re-directed along stems and branches before reaching the forest floor. The relative importance of each of the three mechanisms of *wetted-canopy-evaporation*, *transpiration* and *re-distribution* is dependent upon the tree species, individual canopy characteristics, and the storm characteristics (Voigt, 1960).

Evaporation from Wet Canopies (Interception).

Trees have much larger canopy surface areas compared to other types of vegetation, and are, therefore, able to intercept and evaporate greater volumes of precipitation (Waring *et al*, 1981). Examples of interception losses from forest and other types of vegetation are shown within Table1. Interception loss from Sitka spruce (*Picea sitchensis* Bong. Carr.) stands, at sites throughout the UK are shown within Table 2. The estimates range from 254 to 876 mm, or 25 to 49 percent of gross precipitation.

Table 1. Interception losses from selected forest and non-forest canopies.

REFERENCE	COVER/SPECIES	ANNUAL INTERCEPTION (% gross-precipitation)
Non-Forest Canopies:		
McMillan and Burgy (1958)	Grassland	
Williams *et al* (1987)	Bracken (*Pteridium aquilinum*)	20
Forest Canopies:		
Bo *et al* (in press)	Rigid and Loblolly pine (*P. rigida* and *P. taeda*)	18
	Oak and Alder (*Q. mongolica* and *Alnus hirsuta*)	16
Calder (1976)	Norway spruce (*Picea abies*)	28
Crabtree and Trudgill (1985)	Beech (*Fagus sylvatica*)	20
Gash *et al* (1980)	Scots pine (*Pinus sylvestris*)	42
Helvey (1971) (review: US forests)	Red pine (*Pinus resinosa*)	13-24
	Loblolly pine (*Pinus taeda*)	6-27
	Shortleaf pine (*Pinus echinata*)	8-15
	Ponderosa pine (*Pinus ponderosa*)	8-18
	Eastern White Pine (*Pinus strobus*)	14-17
Hudson (1988)	Sitka spruce* (*Picea sitchensis*)	25
Kasran (in press)	mixed dipterocarp (*Dipterocarpus* and *Shorea* spp)	27
Kittredge *et al* (1941)	Canary Island Pine (*Pinus canariensis*)	20
Lai and Omar (in press)	Acacia (*Acacia mangium*)	39
Stalfelt (1961)	Spruce (*Pinus excelsa*)	46
Rutter (1963)	Scots pine (*Pinus sylvestris*)	35
Walsh (1987) (review: tropical rainforests)	Rainforest spp.	12-42

* predominant vegetation type

Table 2. Interception losses from Sitka spruce stands within the UK.

REFERENCE	SITE	ANNUAL-INTERCEPTION	
		mm	% ppt
Calder *et al* (1980)	Knapdale (Argyll)	710	39
Chappell (this study)	Plynlimon (Powys)	-	39*
Courtney (1978)	Trentbank (Stafford)	-	39
Ford and Deans (1978)	Greskine (Dumfries)	429	30
Gash and Stewart (1977)	Thetford (Suffolk)	-	31
Gash *et al* (1980)	Plynlimon (Powys)	479	27
"	Kielder (Northumber'd)	254	32
Hudson (1988)	Plynlimon (Powys)	521	25
King *et al* (1986)	Kielder (Northumber'd)	299	28
Law (1956)	Stocks (Lancs)	376	38
Leyton *et al* (1967)	Bagley (Salop)	-	49
Williams (1983)	Narrator (Devon)	876	46

* = 7.5 months interception measurements (9/11/87 to 24/6/88)

RANGE: 25-49 percent of gross precipitation

Precipitation Re-distribution.

Incoming precipitation which is re-directed along leaves, needles, branches and stems, eventually reaches the ground as drips of *throughfall* or streams of *stemflow*. The *throughfall* component is, however, often concentrated towards the stem (Ford and Deans, 1978; Kittredge *et al*, 1945; Rutter, 1963), because of irregularities at the branch-stem insertion points (Voigt, 1960) and because major branches are often angled downward towards the stem (Rutter, 1963). This partitioning of net-precipitation into stemflow and throughfall is determined by tree species, age, and individual canopy characteristics, and is, therefore, highly variable (Table 3).

Table 3. Throughfall and stemflow percentages of gross-precipitation within selected forest stands.

REFERENCE	TREE SPECIES	THROUGHFALL	STEMFLOW
Bo *et al*, (in press)	Rigida and Loblolly pine (*P. rigida* and *P. taeda*)	77	5
"	Oak and Alder (*Q. mongolica* and *Alnus hirsuta*)	82	2
Calder (1976)	Norway spruce (*Picea abies*)	51	22
Chappell (this study) *(Plynlimon)*	Sitka spruce (*Picea sitchensis*)	56	5
Crabtree and Trudgill (1985)	Beech (*Fagus sylvatica*)	67	12
Ford and Deans (1978)	Sitka spruce (*Picea sitchensis*)	43	27
Gash and Stewart (1977) (Thetford)	Scots pine (*Pinus sylvestris*)	67	1.6
Gash *et al* (1980) *(Plynlimon)*	Sitka spruce (*Picea sitchensis*)	45	28
Helvey (1971) (review: US forests)	Red pine (*Pinus resinosa*)	74-83	2-3
"	Loblolly pine (*Pinus taeda*)	71-92	8-20
"	Shortleaf pine (*Pinus echinata*)	80-90	2-10
"	Ponderosa pine (*Pinus ponderosa*)	76-89	2-6
"	Eastern White Pine (*Pinus strobus*)	78-81	5-9
Hoover (1953)	Loblolly pine (*Pinus taeda*)	71	16-18
Institute of Hydrology (1976) *(Plynlimon)*	Sitka spruce (*Picea sitchensis*)	55	23*
Kasran (in press)	mixed dipterocarp (*Dipterocarpus* and *Shorea* spp)	73	0.4
Lai and Omer (in press)	Acacia (*Acacia mangium*)	57	4
Law (1957)	Sitka spruce (*Picea sitchensis*)	60	7
Pathak *et al* (1985)	Sal (*Sorea robusta*)	82	0.9
"	*Pinus roxburghii* / *Quercus glauca*	92	0.4
"	Chir pine (*Pinus roxburghii*)	75	0.3
"	*Quercus leucotrichophora* / *Pinus roxburghii*	83	0.4
"	*Quercus floribunda* / *Quercus leucotrichophora*	85	0.4
"	*Quercus lanuginosa* / *Quercus floribunda*	81	0.9
Patric (1966)	*Tsuga heterophylla* / *Picea sitchensis*	68	1
Reynolds and Leyton (1961)	Norway spruce (*Picea abies*)	73	5
Rutter (1963)	Scots pine (*Pinus sylvestris*)	48	16
Voigt (1960)	Red pine (*Pinus resinosa*)	80	1*
"	Eastern hemlock (*Tsuga canadensis*)	61	13*
"	American beech (*Fagus grandifolia*)	66	37*

+ estimated from the catchment water balance

* percent gross precipitation falling upon crown area

Biological Transpiration.

Rates of biological transpiration from forest canopies are extremely difficult to estimate with any accuracy (Morton, 1984). For example, the annual transpirational losses from spruce trees at Plynlimon have been estimated from a lysimeter study to be 17 percent of gross precipitation (340 mm : Calder, 1976) , but only 5 percent from a catchment water-balance study (105 mm : Hudson, 1988). The ratio of the transpiration to wet-canopy-evaporation from the lysimeter and catchment studies are 1:1.7 and 1:5 respectively. This ratio has been previously estimated to be 1:1.5 (Law, 1956), 1:3.1 (Stewart, 1977), and 1:6 (Ebermayer: in Brown, 1877) for other spruce stands. Peak transpiration rates from the forest canopy at Plynlimon range from 1.5-1.8 mm d^{-1} (Hudson, 1988). The transpirational losses from a grassland catchment, adjacent to the forested catchment at Plynlimon, accounted for most of the 16 percent total evapo-transpiration losses calculated from a catchment water-balance(335 mm : Hudson, 1988; Stewart, 1977).

1.5.2. Forest Soil Hydrology.

The impacts of forests upon the movement of precipitation into and through hillslope soils are as poorly perceived as the canopy processes (Brenner, 1976; Pritchett, 1979). Present understanding is restricted to the semi-quantitative hydrology of the *forest floor*, tree roots, forest mineral-soil, and forestry management.

Forest Floor Hydrology.

Although the hydrological role of the *forest floor* (i.e. surficial organic horizons: McColl, 1972) has been recognized for at least 60 years (e.g. Lowdermillk, 1934), surprisingly little quantitative information has been produced (Chaney, 1981; Walsh and Voigt, 1977). The few studies which do exist show that the *active organic layer* markedly alters hillslope water pathways by both reducing the *observable* overland flow, and by altering the ratio of lateral to vertical flow.

Surficial Infiltration : Many forest soils exhibit enhanced (surface) infiltration rates when compared with adjacent grassland soils (Table 4). Increases of between one quarter of an order of magnitude to over two and a half orders of magnitude have been noted (Table 4). The forest floor, which comprises litterfall, roots, humus and peat, is able to enhance *surficial* infiltration, first by reducing lateral overland flow, through the increased surface roughness (Arnett, 1974; Bonell *et al*, 1984; Hoover, 1949) and cushioned raindrop impact (Plamondon *et al*, 1972). Second, infiltration is enhanced by the more open soil structure, evidenced in both decreased bulk densities (Bergund *et al*, 1980; Jackson, 1973) and increased porosities (Hoover, 1943, 1949; Mosley, 1979).

As the surface organics become humified, then they begin to exhibit *variable wettabilities* (Section 7.4.5). On desiccation, this produces a marked hydrophobicity (Grelewicz and Plickta, 1983, 1985; Nielsen *et al*, 1972), which may localize the initial infiltration to the secondary-structure (Burch *et al*, 1987; deVries and Chow, 1978; Plamondon *et al*, 1972; Reynolds 1966; see Section 7.4.5).

Lateral versus Vertical Flow : Deciduous trees may increase the vertical to lateral flow ratio within hillslope soils, through the incorporation of organic matter within the mineral soil, root growth, and favourable biological activity (Ternan *et al*, 1987).

Coniferous trees, however, often develop a marked relative hydraulic discontinuity (Sections 1.4.2., 7.2., 7.4.2., 7.4.3. and 7.4.9) between their organic and mineral soil layers, which can add a considerable lateral component to the path of percolating water (Bonell *et al*, 1983; Grieve, 1978; Molchanov, 1960; Tischendorf, 1969; Walsh and Voigt, 1977). Field evidence to support the presence of lateral flow, includes the *near-surface* lateral displacement of tracers (e.g. Reynolds, 1966) and soil-pit-face outflow (e.g. Mosley, 1979; Table 4-2).

Table 4. Infiltration capacities (or near-surface saturated hydraulic conductivities) of forest and adjacent grassland soils: cm hr-1.

REFERENCE	GRASSLAND	FOREST	
	cm hr^{-1}	cm hr^{-1}	(logF-logG)
Berglund *et al* (1981)[2]	6	22	(0.56)
Burch *et al* (1987)[1]	0.9-8	6-22	(0.44-0.82)
Burt *et al* (1983)	0.4-4	18	(0.65-1.65)
Costales (1979)[2]	0.94	4.5	(0.68)
Hoover (1949)[3]	5	110	(1.33)
Jackson (1973)[2]	3	60	(1.29)
Mathur *et al* (1982)[2]	26.8	46.8	(0.24)
Molchanov (1960)[2]	27	48	(0.25)
Ternan *et al* (1987)[3]	3	42	(1.15)
Wood (1977)[2]	0.3	39.7	(2.12)

(logF-logG) Order of magnitude increase in the forest soil infiltration rate compared with the grassland soil infiltration rate

1 Tension-infiltrometer technique
2 Ponded double-ring infiltrometer technique
3 Constant-head permeameter technique

Root Hydrology.

The distribution of tree roots within soil profiles governs the rate and pattern of localized additions and abstractions of water.

Tree-Root Distribution : The vertical and horizontal distribution of tree roots is dependent upon the tree species, phenology, and soil conditions. The vertical penetration of for example Sitka spruce (*Picea sitchensis,* Bong. Carr) roots has been shown by numerous studies (e.g. Armstrong *et al,* 1976; Boggie and Knight, 1980; Messenger, 1980; Strong and La Roi, 1985) to be severely restricted by anaerobic and indurated conditions. Equally, drainage channels (known as *grips*) and stand density, restrict the horizontal distribution of roots (Chaney, 1981; Ford and Deans, 1977; Henderson *et al,* 1983).

Tree-Root Absorption : Tree roots absorb soil water to supply nutrients and to replace moisture lost by transpiration (Pritchett, 1979). This water uptake is centred in those soil horizons with the greatest density of roots (Messenger, 1980; Petrov, 1980). Some water may be abstracted from soil at some distance from the root distribution (Section 6.3.6.; Figure 46) The rate of this so called *remote extraction* is debatable (Nnyamah and Black, 1977; Patric *et al,* 1965). Perhaps the most obvious expression of root abstraction is the depression of the water table (or phreatic surface), in the form of *local sinks* (Chaney, 1981; Reynolds and Leyton, 1961). Although individual roots behave like local sinks, they also act as local sources, aiding the flow of water into soils.

Tree-Root Flow : Water may preferentially move along tree roots, as a result of their longitudinal form and surrounding *rhizosphere soil* (Tinker, 1976). This rhizosphere soil consists of both a *pedotubule* - a void at the soil-root interface (Brewer and Sleeman, 1963) and *void wall.* The pedotubules are produced either by the growth of the root into a pre-existing void of animal or root origin (Aubertin, 1971; Messenger, 1980), or by the contraction of both soil and roots (Tinker, 1976; Holtan, 1971; Hoover, 1962). Roots can shrink by up to 25 percent when dried to 2-5 bar (Huck *et al,* 1970). Tree movement during windy conditions may be an additional void producing mechanism (Hornung, 1984; Romans, 1959; Savill, 1976). The formation of the *void wall* can result from three mechanisms:

1. Root penetration and subsequent soil compaction (Aubertin, 1971).
2. The deposition and orientation of clay cutans (Blevins *et al,* 1970; Brewer, 1960; Pilgrim *et al,* 1978; Sullivan and Koppi, 1987). The orientation of clay cutans is, however, not diagnostic of preferred water-flow, they can also be orienntented by wetting and drying cycles (Crampton, 1963) and matrix movement (Rudeforth, 1967).
3. The hydrophobicity of locally dried soil (Pierce, 1967).

Despite this knowledge of the soil-root interface, the actual pathway of water along individual roots remains uncertain, with both spiral (Aubertin, 1971) and underside (Reynolds, 1966) motions being suggested. When roots die, the preferential pathways may not be lost, as the bark may remain intact and infill material may be permeable (Gaiser, 1952a). Evidence to support the preferential flow of water along both live and old root channels includes:

1. Higher gravimetric moisture values near roots (Gaiser, 1952b).
2. Preferential movement of dye and tritium tracers (e.g. Aubertin, 1971; Boggie and Knight, 1980; Mosley, 1982).
3. Direct observation of flow from around root channels (given the artificial *sink* boundary condition created by a soil-pit-face: Section 8.2.2; e.g. Beasley, 1976; Gilmour *et al*, 1980; Whipkey, 1967, 1969).

The role of tree roots as preferential pathways for water-flow is not always a certainty. Graham (1960), for example, noted that dyes moved only short distances along tree roots and then stopped inexplicably.

Forest Mineral-Soil Hydrology.

The impact of trees upon the mineral-soil hydrology is a function of both the penetration of individual roots, and the interaction with the overlying forest floor.

Mineral-soils beneath deciduous forests and some coniferous forests, have greatly increased porosities and hydraulic conductivities, as a result of both localized root penetration and more general structural enhancement (Imeson and Jungerius, 1976; Ternan *et al*, 1987). Wood (1977) for example, demonstrated how the structural aggregation beneath a predominantly *Eucalyptus* spp. forest was significantly greater than that beneath adjacent pastureland. The *minimum-mean-weight-diameter* of aggregates within the forest soil was 1.84 cm and only 0.56 cm beneath the pasture-land.

Recently, a number of studies have shown that coniferous forests within moist temperate regions can actually promote the structural deterioration of soils, rather than structural enhancement (Bonneau *et al*, 1979; Grieve, 1978; Hornung *et al*, 1986b). The increased acidification and podzolization of soils beneath coniferous forests tends to *rot* the clay mineralogy (Crampton, 1963; Nys, 1981; Van Vliet-Lanoe, 1985) and reduce the micro-porosity of the eluvial, A_2 horizon (Nys and Ranger, 1985). As the structural deterioration increases then the eluvial horizon becomes progressively less permeable (Adams and Raza, 1978; Rudeforth, 1967).

1.5.3. Hydrological Effects of UK Forestry Practices.

Different types of forestry practice during the site preparation, stand management, and logging phases can have profound effects on the movement of water within the canopy, soil and stream.

Site Preparation (Drainage, and Road Construction).

As new forest plantations are established, the practices of road construction and site drainage can increase both subsurface and surface water movement. Extensive drainage of forest stands in upland Britain from the late 1950's to early 1980's has lead to more peaked responses from those areas (Robinson, 1980, 1985). Recent attempts at *contour ploughing* and terminating drains before they discharge into streams (Leeks and Roberts, 1987) may reduce this enhanced rapid runoff. The practice of cutting deep drains (10-20 m apart) at right angles to the shallow furrows and turfs on which the coniferous trees are planted has, however, had little effect on the water table within peaty-gleyed areas (Boggie and Knight, 1980; Pyatt *et al*, 1985; Robinson and Newson, 1986; Savill, 1976).

Very little quantitative evidence of the hydrological effects of forestry roads is available for upland Britain (Leeks and Roberts, 1987). Evidence from catchments within the USA and the tropics does, however, show that forest roads can induce overland flow and hence increase stream peakflows (W. Swank pers.comm. 1988; W. Sinun pers.comm, 1989).

To date very few areas of the UK have been fired prior to planting, a practice which can induce rapid overland flow (Berndt, 1971; Conway and Miller, 1960).

Management.

Forest stands within upland Britain are normally *thinned*, some 5 to 10 years prior to clearance (i.e. at an age of 40-45 years). This removal of selected trees reduces both interception and transpiration loss (Butcher, 1977; Hewlett, 1982).

In an attempt to ameliorate the effects of inputs of acidic groundwater into streams, coniferous trees have been cleared from a 10 m strip either side of selected Welsh streams, and then limed (B. Reynolds pers.comm. 1989). This will increase the effective (or net) precipitation additions to the soil adjacent to the stream, thereby producing a disproportionately large increase in rapid runoff (Douglass and Fletcher, 1947).

Logging.

When forests are clear-felled, the use of heavy machinery compacts soils which may then induce localized overland flow (Hornung *et al*, 1986b). Interception and transpirational losses are reduced, probably to levels even lower than from grasslands (Hibbert, 1969). Annual discharge (or yield) is increased by a concomitant amount (Harr, 1986; Hewlett *et al*, 1984; Hibbert, 1967; Pierce *et al*, 1970).

1.6. Research Needs.

Although many hydrological mechanisms *describing* the movement of water towards streams have been identified (Section 1.4.2), comparatively little research has been directed towards the *physical characterization* of those hydrological processes underpinning these mechanisms. This has resulted in conflicting results, misconceptions, and an inability to mathematically simulate water-pathways over successive short time increments (Section 1.2).

There is, therefore, a need to integrate the quasi-physical hillslope hydrological mechanisms with the physical theory developed within the fields of the physics of flow through porous media, groundwater hydrology, petroleum hydro-geology and soil-water physics. As a result, *this research seeks to develop a more precise characterization of the mechanisms of streamflow generation, using those field and mathematical techniques required to represent and validate the physical theory.*

An accurate characterization of those mechanisms and processes controlling the pathways of water to streams would enable biogeochemists to develop a greater understanding of the transport of solutes to streams. Given that such a characterization of water-pathways is achievable, the impact of any physical control upon these pathways could be examined. This physical control could be, for example, individual conifer trees.

Streams within coniferous forests have been shown to be undergoing enhanced acidification in comparison with neighbouring grasslands (Hornung *et al* 1986a, 1987b). An alteration of the water-pathways as a result of the growth of conifer trees may be one of the factors contributing to this enhanced acidification (Hornung and Newson, 1986; Newson, 1984). *The detailed impact of individual conifers upon water-pathways within a hillslope generating streamflows loaded with hydrogen ion, aluminium, sulphate and nitrate (Chappell* et al, *1990) will, therefore, be characterized.* This understanding would add to the understanding of water-pathways within the hillslope as a whole.

CHAPTER 2.

Research Site.

2.1. Introduction.

The reasons for selecting the Tir Gwyn massif within the Plynlimon region of mid-Wales, U.K. as the research site, are discussed within Sections 2.2 and 2.3.

The background characteristics of the instrumented areas, and the region as a whole, are then systematically addressed. These characteristics include: climate (Section 2.4), geology (Section 2.5), geomorphology and topography (Section 2.6), stream morphometry (Section 2.7), soils (Section 2.8), vegetation (Section 2.9), and land management (Section 2.10). The main similarities and differences between the instrumented grassland and forest sites, are summarized within Section 2.11.

The regional characteristics are based primarily upon those determined within the Institute of Hydrology's Plynlimon Catchments.

2.2. Regional Site Selection.

The principal reason for the choice of the Plynlimon (*Pumlumon*) massif as the area to instrument (Figure 1) arose from previous research (e.g. Calder and Newson, 1979; Hornung and Newson, 1986) which focused on the impacts of the local afforestation upon both hydrological and hydro-chemical regimes.

The chemistry of the stream-waters draining the afforested parts of the Plynlimon massif is characterized by high loadings of hydrogen ion, aluminium, sulphate, and nitrate (Chappell *et al*, 1990; Hornung *et al*, 1987; Neal *et al*, 1985). Elevated levels of acidity and aluminium have been implicated in the decline of freshwater fish and invertebrate populations (Stoner and Gee, 1985). The transport of these solutes to streams is governed by the pathways of the soil water (Bache, 1984). These pathways must, therefore, be quantified if we are to understand the movement of solutes into streams. Close co-operation with the Institute of Terrestrial Ecology *Acid Waters Project* team, at Plynlimon, has enabled synchronous hydrological and hydro-chemical monitoring, which should lead to an better understanding of the movement of ions within hillslope hydrological systems.

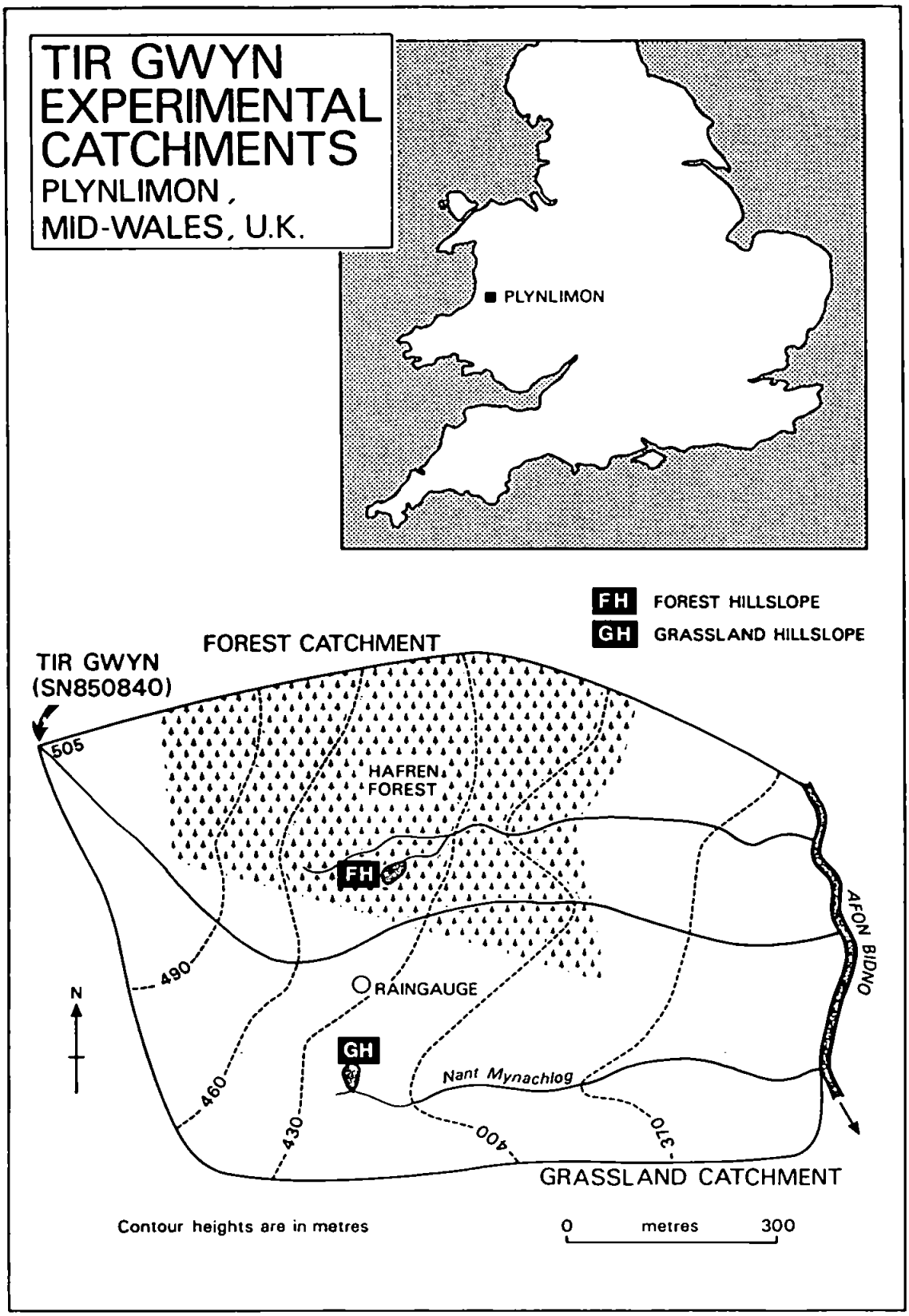

Figure 1. The Tir Gwyn Experimental Catchments.

Mid-Wales is an important region for the supply of water to the West-Midlands conurbation, and the source area of the rivers Severn and Wye. These two rivers periodically flood lowland parts of Shropshire, Hereford and Worcestershire, Gloucestershire, and Powys (NERC, 1975; Newson, 1978). Changes in the rates and pathways of water movement as a result of past or future afforestation (Centre for Agricultural Strategy, 1980) may, therefore, have a profound effect upon the supply of water and incidence of flooding.

The two further scientific considerations for choosing the Plynlimon as the research site, were: (1) the high annual precipitation, which produces more easily measurable hydrological responses (Anderson and Howes, 1986), and (2) the existence of a considerable body of background hydrological data, which has been monitored by the NERC Institute of Hydrology, following the instrumentation of the *Plynlimon Experimental Catchments* in 1967 (Institute of Hydrology, in press).

2.3. Local Site Selection.

Two adjacent catchments, draining the south-eastern slopes of the Tir Gwyn mountain (NGR: SN850840) were chosen, on account of their similarities in physical characteristics. The only significanr difference between the two catchments is that most of one catchment had been ploughed and re-seeded as improved pasture, while most of the other had been afforested with conifers (Figure5).

Both catchment streams are tributaries of the River Bidno (*Afon Bidno*), which itself is a tributary of the River Wye (*Afon Gwy*). Trapezoidal flumes delineate the instrumented catchment areas within both the grassland and forest catchments, of 0.12 and 0.11 km^2, respectively. The rainfall-runoff response of the forest and grassland areas presented within Chapter 5, are based upon these 0.1 km^2 catchments. Only the hydro-chemical response (e.g. Chappell *et al*, 1990) is examined at the larger (0.3 km^2) catchment scale. Catchment areas and percent cover are shown within Table 5.

Within each catchment a single hillslope system was selected and instrumented to monitor the internal-state hydrological properties (Section 3.5, Chapters 6 and 7). Both hillslope sections are approximately 50 m in length .

Table 5. Tir Gwyn catchment areas. (total area: 0.66 km²)

	GRASSLAND CATCHMENT (Nant Mynachlog)	FOREST CATCHMENT
Total catchment area	0.30 km²	0.36 km²
Area afforested	0.01 km² (4.3 %)	0.24 km² (66.5 %)
Area under grassland	0.29 km² (95.7 %)	0.12 km² (33.5 %)
Instrumented-catchment area above trapezoidal flumes	0.12 km²	0.11 km²
Instrumented-catchment afforestation	0 %	79.9 %
Instrumented-catchment under grassland	100 %	20.1 %
Area of bracketed section between weir and flume	0.045 km²	0.055 km²
Area above bracketed section (i.e. above weir)	0.053 km²	0.056 km²

2.4. Climate.

2.4.1. Regional Climate.

The Plynlimon area is described as having a *Western Marginal Upland Climate* (Newson, 1976a). Such climates are characterized by a cool temperate regime with a foreshortened growing season, low temperatures and high annual rainfall, with rain occurring with great frequency (Manley, 1952). The local climate is strongly influenced by *maritime* conditions (Reynolds, 1984).

Ninety-five percent of the 1585-2644 mm annual precipitation falling upon the Plynlimon catchments is in the form of rainfall (Calder and Newson, 1979; Hudson, 1988). Rainfall intensities are fairly low, with average storm intensities ranging from 2-4.4 mmhr^{-1}, and maximum intensities of 5.8-10.6 mm hr^{-1}. There are approximately 8 heavy (30-50 mm) rainfall events, and 4 very heavy (>50 mm) rainfall events each year (Newson, 1976a). The prevailing rain-bearing wind is south-westerly (Clarke *et al*, 1973). A strong correlation exists between rainfall and altitude (Newson, 1976a).

Annual evapo-transpirational (ET) losses from the acid grassland areas of the Plynlimon massif are approximately 16 percent of gross precipitation, and 30 percent from the areas afforested with conifers. An average of 83 percent of the ET loss (i.e. 25 percent of the gross precipitation) from the coniferous forests results from the interception and evaporation of rainfall from the wet canopies (Hudson, 1988).

The Plynlimon region receives an average 2.5 MJ $m^{-2}day^{-1}km^{-1}$ of solar radiation (Harding, 1979), has just over three hours of sunshine a day, and an mean annual temperature of 7.2 °C (Calder and Newson, 1979). Mean annual soil temperatures (at 0.3 m in peaty moorland soils) range from 6.7-8.0 °C (Gilman, 1980).

2.4.2. Grassland Site Climate.

During the period of study (8/6/87-8/6/88), the Tir Gwyn grassland catchment received an *annual* 2629mm of precipitation (Section 5.2.1). Only 127mm or 5.1 percent of that precipitation was in the form of snowfall. The maximum hourly rainfall intensity measured during the study period was 10 mm hr^{-1}. No marked seasonality in precipitation totals was apparent (Figure 25).

Evapo-transpiration loss from the grassland catchment is estimated from the Wye Catchment water balance, to be 15 percent of gross precipitation (Institute of Hydrology, 1989); which is equal to 400 mm a^{-1} for the period 8/6/87-8/6/88 (Section 5.2.2).

2.4.3. Forest Site Climate.

Gross precipitation falling upon the forest catchment was assumed to be the same as the grassland catchment (i.e. 2629 mm), as the altitudinal range, slope and aspect are similar (Figure 21).

Net precipitation inputs beneath the forest canopy were some 36 percent less than the gross precipitation inputs (Section 5.2.2). Moisture losses via biological transpiration and soil evaporation were not measured, but assumed to be within the range of 5 percent (=125 mm: mean 0.3 mm day^{-1}, Hudson, 1988) to 17 percent (=425 mm: mean 1.2 mm day^{-1}, Calder, 1976). Winter (December) transpiration rates can be as low as 0.03 mm day^{-1} (Calder, 1978), and peak summer rates can be as high as 1.5-1.8 mm day^{-1} (Hudson, 1988).

2.5. Geology.

2.5.1. Regional Geology.

Silurian shales dominate the geology of central Wales (Jenkins, 1967). The erosion of an anticlinal fold has, however, exposed the more resistant Ordovician or Van (local name) geology of the Plynlimon massif. The central and oldest part of the massif is characterized by massive grits, mudstones and conglomerates of the Lower Ordovician formation (Jones, 1929). Surrounding this formation are the soft blue shales of the Upper Ordovician formation. Progressively younger geologies are found as the distance from the massif increases.

Lower and Middle Valentian formations (Upper Ordovician-Lower Silurian transition) are characterized by shales and mudstones with some impure limestone bands. This formation is found within the lower sections of the Institute of Hydrology, experimental catchments (Newson, 1976b).

The surrounding Lower Silurian geology is characterized by shales and mudstones with some thin sandstone or siltstone bands.

The Ordovician and Silurian rocks both have chemical compositions dominated by SiO_2 (*c.* 60%) and Al_2O_3 (*c.* 21%), and mineralogical compositions dominated by illite (c. 33-41%), quartz (*c.* 26-37%), and chlorite (*c.* 20-36%) (Evans and Adams, 1975). The chlorite minerals weather readily to magnesium (B. Adams, pers. comm. 1988).

2.5.2. Geology of the Grassland and Forest Sites.

The south-eastern slopes of the Tir Gwyn mountain have a Lower Silurian geology, comprising shales and mudstones. Less resistant siltstone rocks are present within some of the valleys (D. Wenner, pers. comm. 1989). No calcareous beds were found.

2.6. Geomorphology and Topography.

2.6.1. Regional Geomorphology and Topography.

Three principal surficial deposits have developed upon the solid geologies at Plynlimon. These include: blue-grey *boulder clay*, soliflucted head, and colluvium (or scree) (Watson, 1967,1968).

The *boulder clay* is a highly impermeable glacial deposit, generally found within valley bottoms. It is occasionally found inter-bedded with the colluvial deposits (Newson, unpublished report).

The soliflucted head (Harris, 1987) is a periglacial deposit comprising predominantly gravel-sized fragments of shale. *Solifluction terraces* are very common feature in mid-Wales, and are often several metres deep on north facing slopes (Watson, 1967). Indurated *fragipan* layers (Fitzpatrick, 1956; Van Vliet-Lanoe, 1985) are present at several depths within these deposits .

Post-glacial scree or *colluvial* deposits are derived by the weathering of bare rock surfaces, and tend to occur on the south facing slopes where, presumably, the older periglacial deposits have been preferentially eroded due to a warmer micro-climate (Newson, unpublished report).

The Institute of Hydrology, Plynlimon catchments have an altitudinal range of 341-741m and a mean altitude of 450m. The modal altitude of the Wye Catchment (450-500m) is, however, significantly higher than the Severn Catchment (400-450m). Modal slope angles within both catchments are 5-15° (Newson, 1976b).

Slope failure is common during flood events (Newson, 1975). Features including: *rush flushes* (distinct peaty zones with pronounced continuous macro-pores), crescent-shaped *burrows* (slip features exacerbated by sheep), and *seepage steps* developed upslope in flights, are also common (Newson, 1976b).

2.6.2. Geomorphology and Topography of the Grassland and Forest Sites.

The grassland research hillslope is south-facing and is mantled by a relatively shallow colluvium, which is 5.7 m deep at the slope-base and only 0.8 m deep, 60 m upslope. These depths were calculated from a seismic survey of both the grassland and forest hillslope. Average slope angle of the grassland hillslope is 15.0° (Figure 2).

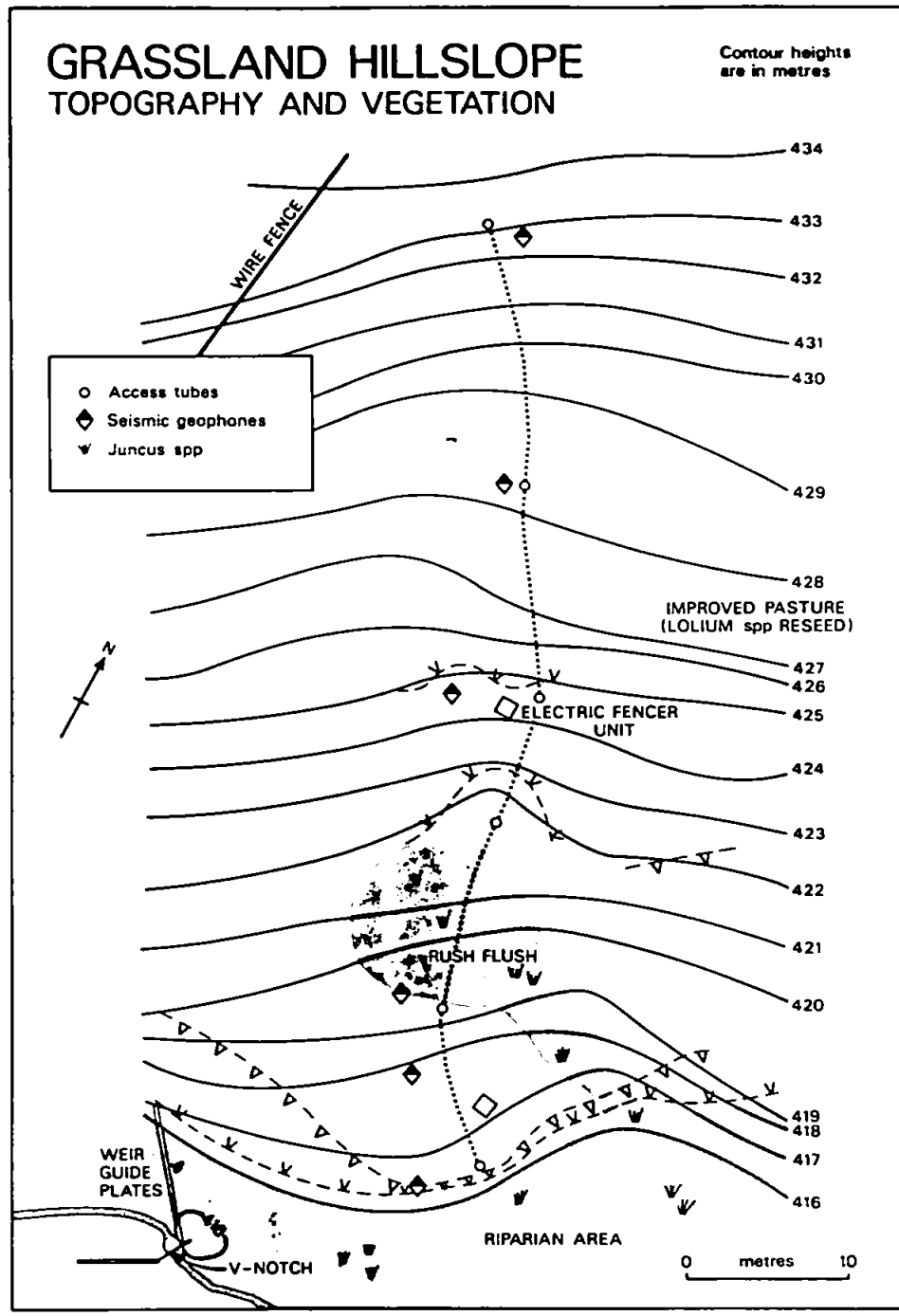

Figure 2. Topography of the grassland hillslope.

A *rush flush* (Section 2.6.1) is present at the slope-base (Figure 3). A 20 m high slope failure has developed on the thin soils of a *tor-like* feature, 25 m upstream of the grassland weir. Crescent-shaped slip features enlarged by the effects of sheep, are observed on the main hillslope (Figure 1). Above the instrumented grassland hillslope a *dry-channel* feature exhibits flow from a series of *seepage steps* during storm-events. A number of large *pipes* (20 cm i.d., 5 m length, Section 1.4.2) are observable within the peaty, riparian soils, downstream of the grassland flume.

The instrumented forest hillslope is slightly steeper than the grassland hillslope, with an average slope angle of 19.7°. The slope is north facing and has a much deeper regolith. The seismic refraction survey indicated that the deposit, a soliflucted shale is 3.86 m deep at the slope-base and 11.7 m deep 40 m upslope (Figures 3 and 4). Indurated *fragipan* layers are observed at depths of 0.65-0.75 m and 1.0-1.5 m. Exposures of this soliflucted head along road-cuts, exhibit further indurated layers at greater depth. The forest stand has obscured many of the geomorphological features observable within the grassland.

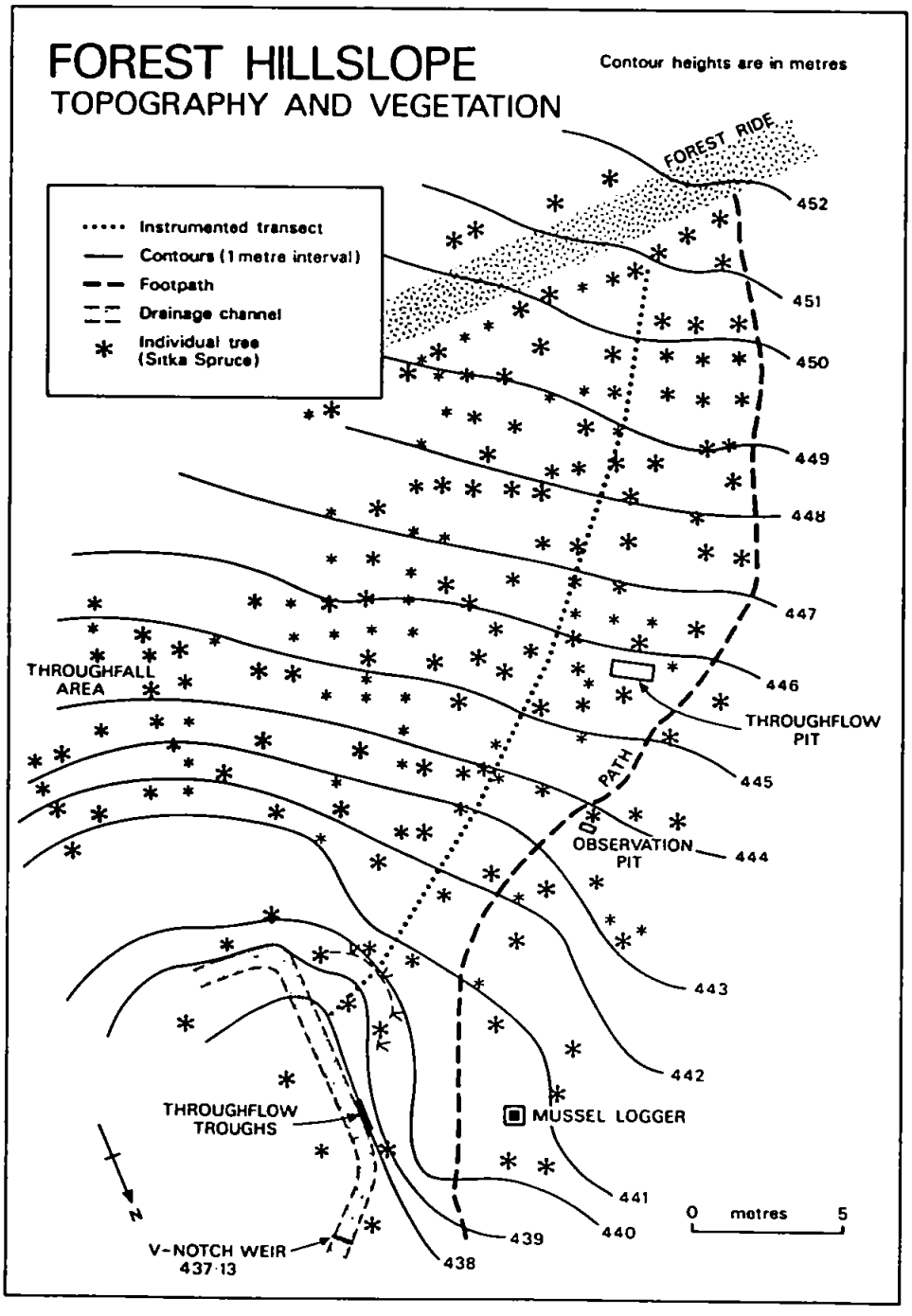

Figure 3. Topography of the forest hillslope.

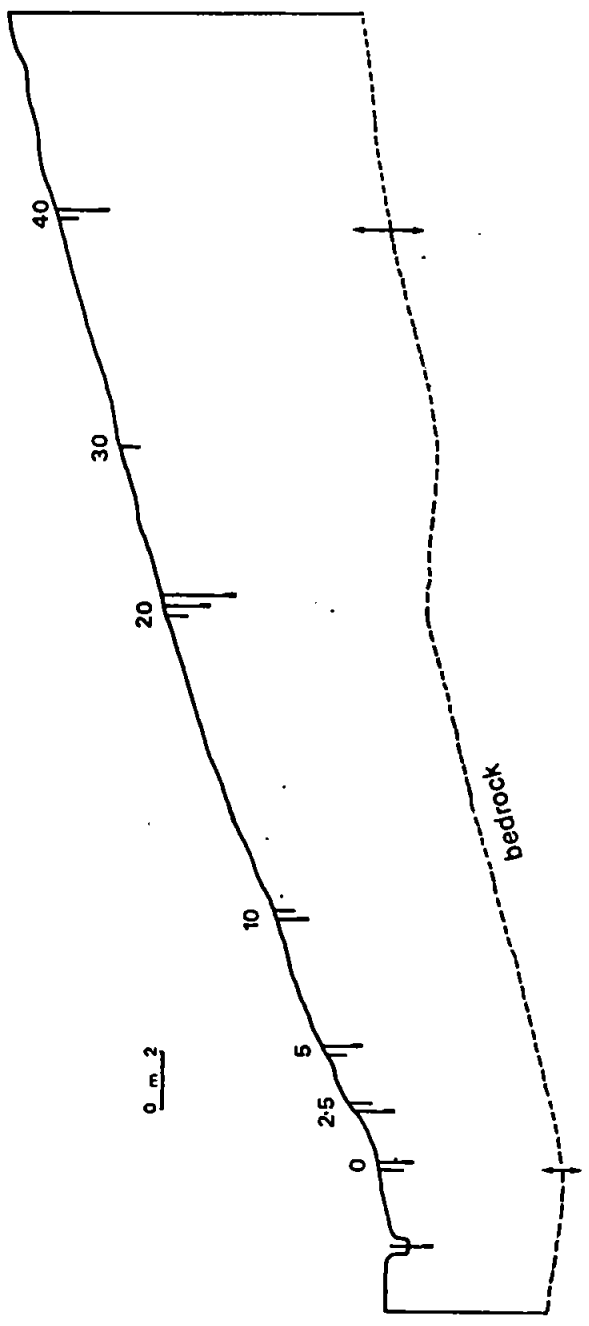

Figure 4. The slope profile of the instrumented forest hillslope.

2.7. Stream Morphometry.

2.7.1. Plynlimon Morphometry.

The morphometric characteristics of the Wye (grassland) and Severn (forest) catchments at Plynlimon are summarized in Table 6. Detailed reviews of the Plynlimon channel geometries and sediment dynamics are presented within Institute of Hydrology (1987), and Newson and Harrison (1978).

Table 6. The morphometric characteristics of the Institute of Hydrology, Plynlimon Catchments, mid-Wales, U.K. (after Newson, 1976b).

	WYE	SEVERN
Catchment area	10.55 km^2	8.7 km^2
Strahler basin order	4	4
Drainage density	2.04 km km^{-2}	2.40 km km^{-2}
Stream frequency	2.88	3.60
Outline shape (K)	1.36	1.37
Main channel slope	36.3 m km^{-1}	67.0 m km^{-1}
Main channel length	7.32 km	4.58 km
Bifurcation ratio	1.54	1.67

2.7.2. Morphometry of the Grassland and Forest Sites.

The morphometric characteristics of the two Tir Gwyn experimental catchments are summarized in Table 7.

Table 7. The morphometric characteristics of the Tir Gwyn experimental catchments at Plynlimon (mid-Wales, U.K.).

	GRASSLAND (Nant Mynachlog)	FOREST STREAM
Catchment area	0.72 km^2	0.66 km^2
Strahler basin order	1	1
Drainage density	1.0 km km^{-2}	1.2 km km^{-2}
Main channel slope	123.8 m km^{-1}	109.1 m km^{-1}
Main channel length	0.73 km	0.81 km

2.8. Soils.

2.8.1. Regional Hillslope Catena.

The Plynlimon region, with its the combination of high rainfall, cool climate and Silurian/ Ordovician deposits has given rise to characteristically wet soils (Oliver, 1967) of the Hafren Association. Figure 5 shows the idealized hillslope catena of the related soil types (or *series*), across the Plynlimon massif.

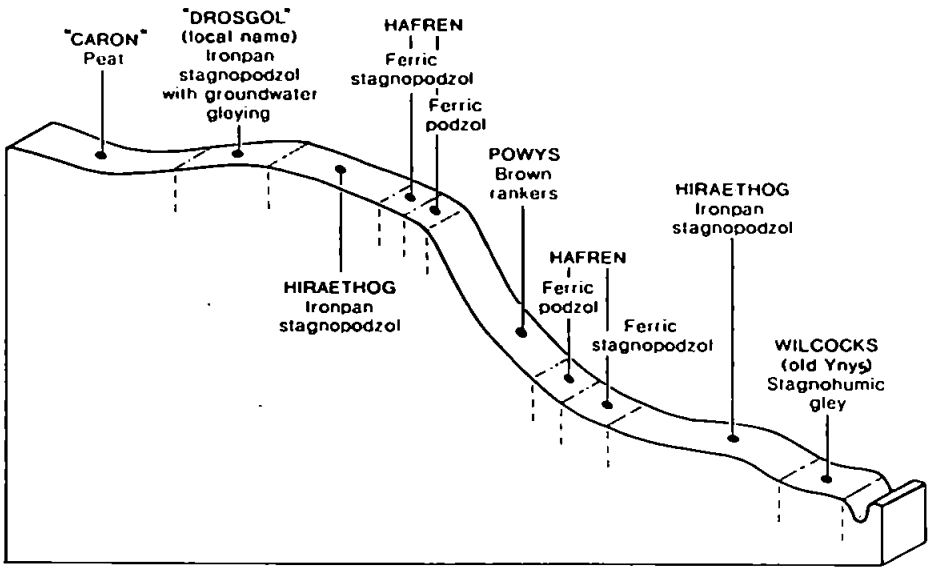

Figure 5. An idealized hillslope catena for the Plynlimon massif.

The high altitudes are covered with hill peat of the Crowdy (locally Caron) series and ironpan stagnopodzols with gleyed subsoils of the Hiraethog (locally Drosgol) series (Newson, 1976b). At slightly lower altitudes ironpan stagnopodzols of the Hiraethog (also locally Hiraethog) series grade into ferric stagnopodzols and then ferric podzols of the Hafren series (Crampton, 1967; Rudeforth *et al*, 1984). Brown podzolic soils of the Manod series may also be present (Knapp, 1970). These soils are distinguished from the *true* podzols, by the absence of an ashen eluvial (or A2) soil horizon (Avery, 1973). Very steep hillslope sections are only able to sustain thin brown rankers of the Powys series. Where slopes grade gradually into valley bottoms, then thin ferric podzols grade into ironpan stagnopodzols before grading to stagnohumic gleys of the Wilcocks (locally Ynys) series. When the transition is abrupt, hillslope rankers or ferric podzols grade first into stagnogley soils of the Cegin series, and then stagnohumic gleys (Pyatt, 1967; Rudeforth *et al*, 1984).

2.8.2. Hillslope Catenas of the Grassland and Forest Sites.

The soils which cover the eastern slopes of the Tir Gwyn mountain have a similar sequence to those which cover the region as a whole, except that the high altitute peaty soils are less developed. The idealized Tir Gwyn hillslope catena is shown within Figure 6. The distribution of each soil type within the Tir Gwyn catchments is shown within Figure 7. The possible impact of this sequence of soils upon hillslope water pathways is examined in Sections 7.4.2. and 7.4.3).

Some 36 percent of the grassland catchment (central area) and 27 percent of the forest catchment (lower grassland section) at Tir Gwyn has been recently ploughed and limed (Section 2.10.2). This *pasture improvement* may in time transform the ferric podzol found within these two catchment areas to brown podzolic soils of the Manod series (Lea, 1974).

Coniferous afforestation may have accelerated the podzolization processes within the soils of the *forest catchment* (Grieve, 1978; Hornung *et al*, 1987; Ternan and Williams, 1979). However, the improvement of the adjacent non-forested soils makes any comparison difficult.

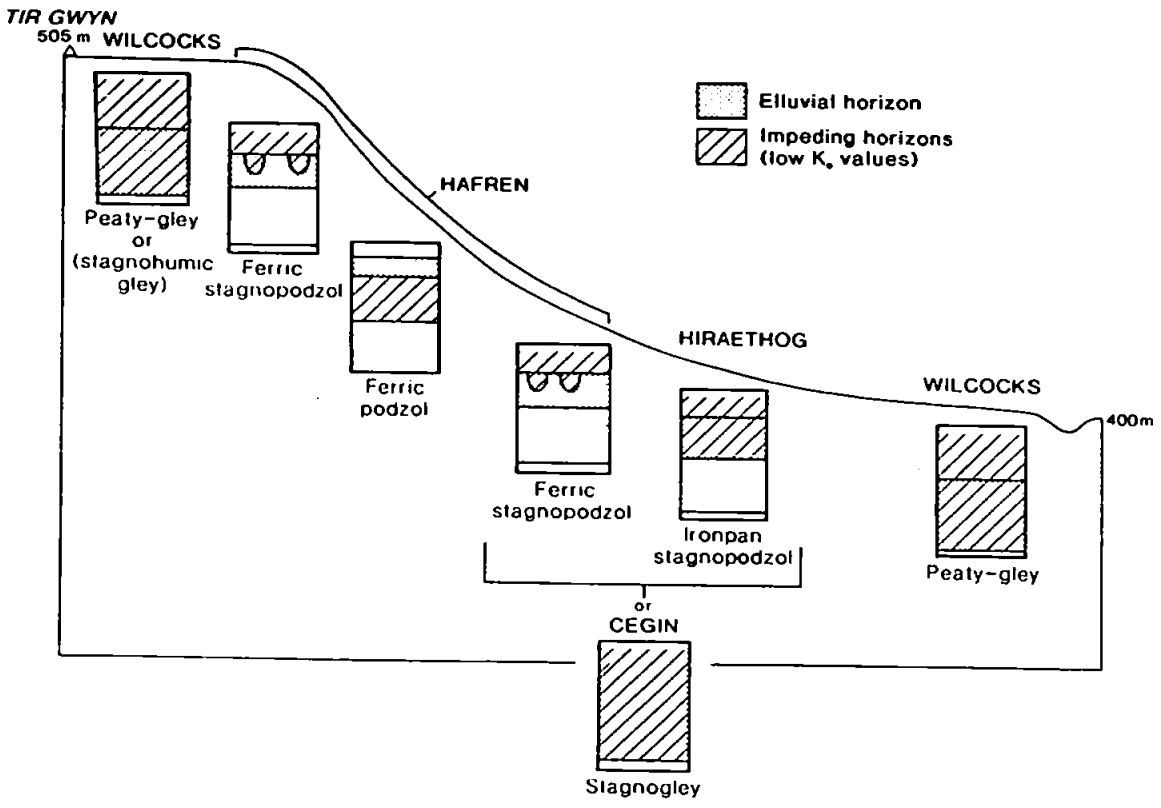

Figure 6. An idealized hillslope catena for Tir Gwyn

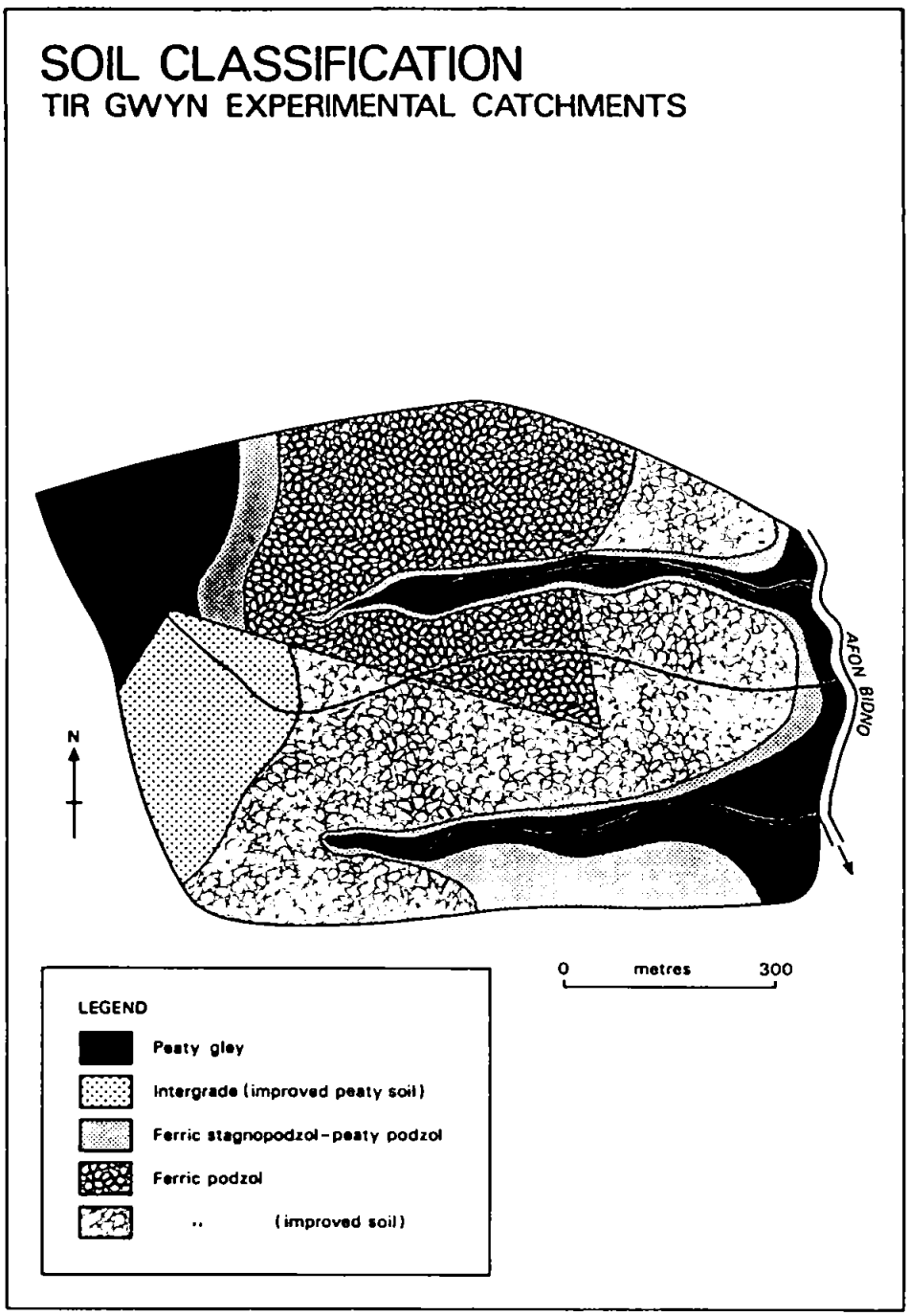

Figure 7. The distribution of soil types within the grassland and forest catchments.

The hillslope catenas specific to the two instrumented hillslopes are shown within Figures 8 and 9. The ferric podzol of the Hafren series is the dominant hillslope soil, and is described within Table 8.

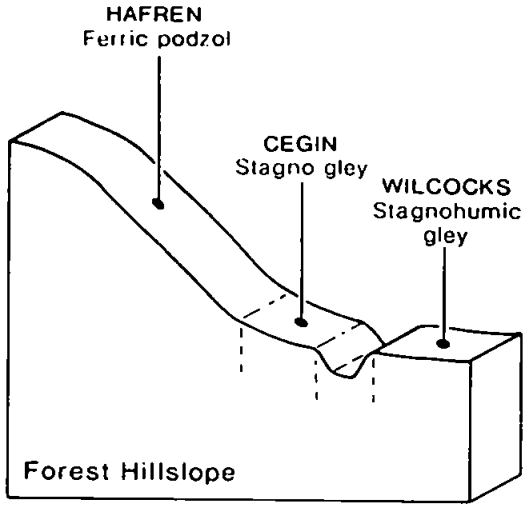

Figure 8. The forest hillslope catena.

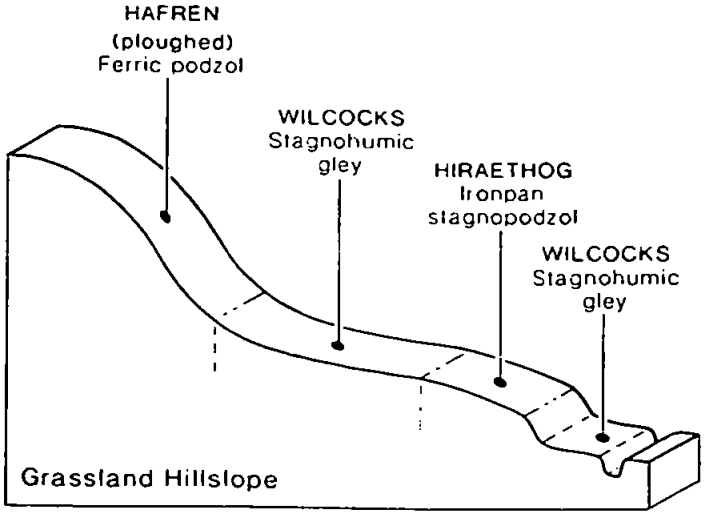

Figure 9. The grassland hillslope catena.

Table 8. The generalized soil profile description of the ferric podzol (Hafren series), at the instrumented forest hillslope, Tir Gwyn Experimental Catchments, mid-Wales, U.K.

Location: SN856838 **Altitude:** 450m O.D. **Slope:** 19.7° straight

Aspect: NNE **Drainage:** slow-moderate (K_s 0.1 cm hr^{-1}) Bs1 horizon.

Land use and vegetation: mature (48 year old) *Picea sitchensis* coniferous plantation.

Parent material: soliflucted Lower Silurian shale

Horizon	Depth (cm)	
L	0-3	Sitka spruce (*Picea sitchensis* , Bong. Carr) litter.
O/Ah	3-10	Very dark greyish brown (10YR 2/2) stoneless humose sandy silt loam; moist; weakly developed fine granular; many fine fibrous roots; sharp boundary.
Eag	10-20	Dark grey (10YR 5/1) silty clay loam; stoneless; medium subangular blocky; common fine fibrous roots; moist; moderately sticky; moderately plastic; abrupt boundary.
Bs1	20-40	Strong brown (7.5YR 5/6) moderately stoney silty clay loam; few small angular platy, shale stones; moist; weakly developed fine subangular blocky; few fine roots; gradual boundary.
Bs2 (B/C)	40-55	Yellowish brown (10YR 5/4) stoney silty clay loam; many small angular, shale stones; moist; weakly developed fine and medium angular blocky; few fine roots; gradual boundary.
C1	55-70	Greyish brown (10YR 4/2) laminated silty shale; roots absent.
C2u	70-75	Greyish brown (10YR 4/2) laminated silty shale; roots absent; continuous fragipan.

(standard SSEW terminology: Hodgson, 1976)

2.9. Vegetation.

2.9.1. Regional Vegetation Sequence.

Each of the soil types described in Section 2.8.1 are associated with particular hydrological and geomorphological regimes. It might, therefore, be expected that vegetation types may also follow similar associations. The *natural* vegetation succession across the Plynlimon massif comprises 3 major groups: *mire*, *heath* and *acid grassland* communities (Newson, 1976b):

1. The very wet, *mire* areas of Plynlimon with their stagnohumic gley soils, tend to be associated with *Eriophorum* spp. (cotton grass) and *Juncus* spp. (rush). The *Eriophorum* may be particularly dominant within areas of very acidic, stagnant water (Jeffries, 1917), and *Juncus* may dominate within *flush zones* (Section 2.5.1; Gilman and Newson, 1980).

2. Wet ironpan stagnopodzols often support *heath* communities of *Molinia* spp. (purple moor grass) with some *Vaccinium* spp. (bilberry) and *Calluna vulgaris* (heather) (Newson, 1976b). The *Vaccinium* spp. are often found in the channelized depressions produced by perennial pipes (i.e. large continuous macropores: seeSection 1.3.2) (Jones, 1981).

3. Natural *acid grassland* communities are dominated by *Festuca/Nardis* or*Nardis/Festuca* spp. (matgrass/fescue), and are developed on the slightly drier ferric stagnopodzol and ferric podzol soils. Very dry, brown podzolic and brown rankers may have *Pteridium* spp. (bracken), in addition to the *acid grassland* species (Pyatt, 1967).

Although this *natural* vegetation sequence is easily observable across the whole Plynlimon region, human impact has significantly altered the *natural* communities, by pasture improvement and afforestation. The pastureland within the Institute of Hydrology, Wye catchment was initially improved by annual burning to allow sheep easy access to the new growth of *Molinia* and *Calluna* spp.; and more recently by the addition of fertilizer (Newson, 1976b). Heavy grazing, may be causing some decline within *Calluna* spp. (Newson, 1976b).

Within the Institute of Hydrology, Severn catchment, the widespread planting of conifers between 1937 and 1964 has left only 32.5 percent of the natural vegetation remaining (Newson, 1976b). Most of this remaining vegetation comprises the *peat hags* and *mire* communities around the source of the river Severn. The earliest planting of conifers took place in the downstream/south-east corner of the catchment. Sitka spruce (*Picea sitchensis,* Bongard Carriere) and Norway spruce (*Picea abies*) were the preferred species. During the period 1948-50, the central part of the catchment was planted with predominantly Sitka spruce. In 1963 and 1964, the upstream parts of the catchment were planted with a mixture of Sitka spruce and Lodgepole pine (*Pinus contorta*).

2.9.2. Vegetation Sequence of the Grassland and Forest Sites.

The *natural* vegetation sequence of mire (*Eriophorum/Juncus* spp.), heath (*Molinia* spp.) and *acid grassland* (*Nardis/Festuca* spp.) seen within the Plynlimon region as a whole (Section 2.9.1), is observed within the Tir Gwyn grassland catchment. The name *Tir Gwyn* meaning *white mountain,* was probably given to this massif because of the characteristic pale *Nardis/ Festuca* spp. grassland (A.A. Rowan, Forestry Commission, pers. comm. 1989). Much of the central part of the grassland catchment was, however, ploughed and re-seeded with *Lolium* spp. (rye-grass), over the period 1976-1980 (T. Jones, pers. comm. 1987).

In 1943 approximately 67 percent of the Tir Gwyn *forest catchment* was afforested with Sitka spruce (*Picea sitchensis* Bong. Carr). Sitka spruce (a native of western North America) is the most extensively planted exotic in upland Wales and Britain as a whole .

Exposure of the root systems of Sitka spruce trees effected by *windthrow,* indicates that most of the roots are located close to the surface (i.e. 0-40cm) of the podzolic soils (Section 2.7.2) at Tir Gwyn (Section 1.5.1).

Of the remaining 33 percent of the forest catchment, 6 percent remains as ridgetop *heath-mire* (*Molinia/Juncus/Eriophorum* spp.), and 27 percent as improved pasture.

2.10. Land management.

2.10.1. Regional Land Management.

The Plynlimon massif is predominantly managed for sheep grazing and forestry. Although most of the grazing land can only be described as *rough pasture*, certain areas such as the Institute of Hydrology, Wye catchment have been improved by fertilizer additions. Re-seeding with lime additions and a light surface preparation is also common (Newson, 1976b). Some valley mires were drained during the 1950's, but have not been maintained since. Other past practices within the Wye catchment include: the annual burning of valley *Juncus* and hillslope *Molinia*, peat digging at Lyn y Fawnog, Nant Iago and Esgair y Maesnant, and lead/zinc/silver mining at the Nant Iago mine (Newson, 1976b).

The afforested area of the Plynlimon massif, known as the *Hafren Forest* was planted by the UK Forestry Commission, between 1937-1964 (Section 2.8.1). The earliest plantations were hand dug for *turf planting* and sparsely drained, again by hand. During the 1948-1950 planting of the central Severn catchment, extensive drainage channels were dug by machinery (Newson, 1976b). In 1974 potash (200 kg ha^{-1}) and phosphate (375 kg ha^{-1}) were aerially applied to the Hafren Forest (Newson, 1976b). The first thinnings took place in the early 1970's and continue to date. A large area (1.57 km^2) of the 1948-1950 plantation was clearfelled between 1985 and 1990, as part of a study to examine the impact of large scale forest removal upon hydro-chemical and sediment dynamics (Leeks and Roberts, 1987).

2.10.2. Land Management of Grassland and Forest Sites.

Only 39 percent of the Tir Gwyn massif remains as *semi-natural moorland*, used as rough pasture for the grazing of sheep. However, 64 percent of the grassland catchment, and 65 of the total unforested area remains within this relatively unmanaged state. Some 21 percent of Tir Gwyn (36% and 23% of the grassland and forest catchments respectively) has been ploughed, limed and re-seeded with predominantly *Lolium* spp. (rye-grass). The recent pasture improvement history is shown within Figure 10. These improved grassland areas are also grazed by sheep.

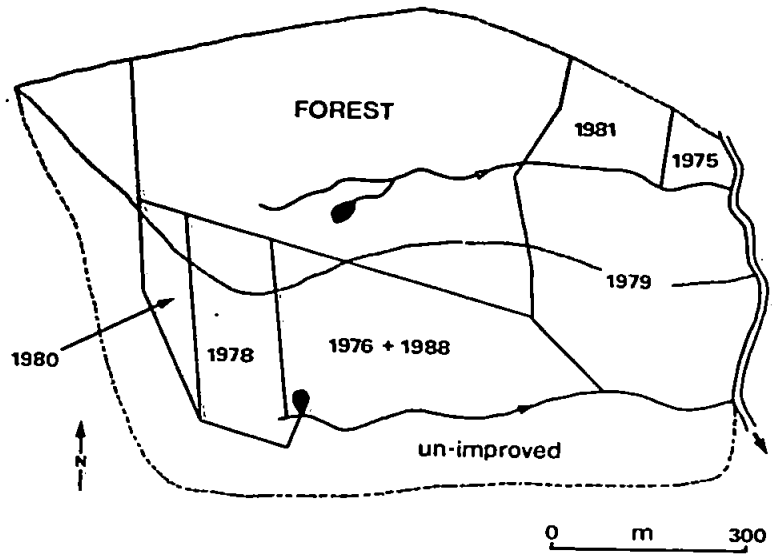

Figure 10. Years when the grasslands were improved by ploughing and liming

The Hafren Forest covers 40 percent of the Tir Gwyn massif, and 66.5 percent of the forest catchment. The local *Mynachlog* stand was planted in 1943 and thinned in 1978(?) and 1989. This exposed south-eastern area of the Hafren Forest has not been clearfelled (clearfelling normally takes place after 40-45 years), to afford the interior stands some protection from *windthrow* (Forestry Commission pers. comm, 1987). Three *forest roads* were laid during the planting phase of the Mynachlog stand.

2.11. Summary of Main Site Charcteristics.

PHYSICAL CHARACTERISTIC	GRASSLAND CATCHMENT (Nant Mynachlog)	FOREST CATCHMENT
climate	cold temperate maritime gross-precipitation: 2629mm ET (Wye): 16%	ET (Severn): 30% ET (Tir Gwyn): 47%
geology	Lower Silurian shales and mudstones	
geomorphology and topography	15.0° straight* 5.7-0.8 m regolith*	19.7° straight* 3.86-11.7 m regolith*
instrumented catchment area	0.12km^2	0.11km^2
stream morphometry (channel slope)	123.8m km^{-2}	109.1m km^{-2}
soils	ferric podzol (Hafren series)* also ferric stagnopodzols, ironpan stagnopodzols, brown rankers, stagnogleys and stagnohumic gleys	
vegetation	*Lolium spp.** (dominant) (improv. pasture) *Festuca/Nardis spp.* (moorland)	*Picea sitchensis* (coniferous afforestation)
land management	ploughed 1976* re-seeding 1976* liming 1976,1988*	planting 1943 thinning c.1978, 1989 (liming 1975-1981+)

* hillslope specific + improved pasture in the lower forest catchment

In summary, the grassland and forest sites have very similar site characteristics, with the exception of the vegetation cover and land management.

CHAPTER 3.

Research Design and Methodology.

3.1. Introduction.

The main aim of the research, is to quantify physically the major pathways of soil water movement beneath a coniferous hillslope. Six broad methodological approaches are used to realize this aim. In summary these include:

1. *Paired Site Approach:* Comparison of the hydrological response of grassland and forest areas at two scales - the 0.1 km^2 catchment scale and 1,480 m^2 hillslope scale (Section 3.2).
2. *Bounded Scale Approach:* Evaluation of the links between hydrological response at the scale of the hillslope catena and that of the bounding scales of the larger catchment and smaller individual tree (Section 3.4).
3. *External-State or Black Box Approach:* Examination of the external, rainfall- runoff response at the catchment and hillslope-catena scales (Section 3.5).
4. *Internal-State or White Box Approach:* Analysis of the internal behaviour of the hillslope in order to understand the external response (Section 3.6.). The internal-state approach is complex, and is, therefore, further sub-divided into approaches based upon the characterization of Eulerian control-volumes (Section 3.5.1), flow-strips (Section 3.5.2), hillslope catenary zones (Section 3.5.3), and soil horizons (Section 3.5.4). Approaches based upon simulation modelling (Section 3.5.5), and the validation of the calculated responses of the internal-state variables and parameters (Sections 1.6. and 3.5.6) werealso employed.
5. *Event-based Approach:* Hydrological variables were most intensively monitored during storm events, when the external behaviour of the catchments and hillslopes were at their most dynamic (Section 3.6).
6. *Natural-Tracer Approach:* Water samples were collected from each component of the hydrological system. Analysis of the ionic concentrations (Chappell *et al*, 1990) were compared with the results of hydrometric techniques (Section 3.7).

3.2. Paired Site Approach.

The impacts of conifers upon hydrological response of the afforested research site is examined by comparison with a similar site under improved pasture. The influences of the two contrasting vegetation covers are compared at both the catchment scale and hillslope scale.

3.2.1. Paired Catchment.

The rainfall-runoff behaviour of a forested watershed are compared with those of an adjacent grassland, *control catchment*. The use of a *control catchment*, enables the impacts of afforestation upon hydrological response to be examined at an easily measurable and realistic scale (Hewlett, 1982; Reynolds and Leyton, 1961; Weyman, 1975). Other paired-catchment studies comparing forest with grassland cover, are listed within Table 9.

Table 9. Studies comparing either the hydrological properties or response of forest catchments withthose of grassland catchments.

PUBLICATION	Topic	CATCHMENT
Berglund *et al* (1981)	hydrological properties	Tleta, Morocco
Burch *et al* (1987)	rainfall-runoff response	Costerfield, Major Creek Victoria, Australia
Costales (1979)	hydrological properties	Benguet Pine, Philippines
Institute of Hydrology (1973)	catchment hydrology	Severn and Wye, Powys U.K.
Jackson (1973)	catchment hydrology	Purukohukohu, N.Z.
King *et al* (1986)	soil hydrology	Kielder, Northumb. U.K.
Mathur *et al* (1982)	hydrological properties	Simla Forest, India
Molchanov (1960)	catchment hydrology/ hydrological properties	various, U.S.S.R.
Oxley (1974)	catchment hydrology	Llyn Ebyr, Powys, U.K.
Wood (1977)	hydrological properties	Hawaii, Mani and Kami, Hawaii, U.S.A.

3.2.2. Paired Hillslope.

Within each of the catchments one hillslope catena was monitored both to compare the hillslope hydrological properties of an unforested area with those of a forested area, and to provide a second research site by which to test the flow calculations (Beven *et al*, 1986; Ternan and Williams, 1979). Other paired-hillslope studies comparing forest with grassland cover, are shown within Figure 10.

Figure 10. Studies comparing either the hydrological properties or response of forest hillslopes with those of grassland hillslopes.

PUBLICATION	TOPIC	CATCHMENT
Burt *et al* (1983)	hillslope hydrology	Slapton Wood, U.K.
Mosley (1982)	hillslope hydrology	Mawheraiti, Donald Creek Camp Stream, N.Z.
Ternan and Williams (1979)	hillslope hydrology	Narrator Brook, U.K.

3.3. Bounded Scale Approach.

The *primary* hillslope scale (Section 3.5.3) is *bounded* by the smaller tree or plot scale (Hillman, 1972; Hoover *et al*, 1953; Zahner, 1958; Ziemer, 1968), and the larger scale of catchment streamflow generation. This *multi-scale* approach was adopted because of the difficulties associated with both representing the hydrological properties at particular scales, and a desire to understand the relationships between hydrological properties and responses determined at different scales (Beven, 1977, 1989; Dooge, 1986; Kirkby, 1985; Klemes, 1983; Yeh, 1986). The smaller plot-scale was used to examine the sensitivity of hillslope flux to the impact of individual trees (Section 6.2.5., 6.3.6., 7.4.4). The catchment scale was used to assess the sensitivity of the research hillslopes upon the hydrological response at the more realistic catchment scale (Section 3.3., 5.3.4.4., 5.3.5.2., 5.3.5.4).

3.4. External-State or Black-Box Approach.

The balance between the gross-precipitation input and the streamflow and evapo-transpirational outputs, is known as the *rainfall-runoff ratio* or *water balance*. This ratio was determined on both a 'long-term' basis (Section 5.2) and 'short-term' or storm basis (Section 5.3)

for both the hillslope and catchment scales (Section 3.2.). This relatively simple approach is used in addition to the internal-state or white-box approach, to:

1. Indicate the maximum and minimum soil water flux within the hillslope over specific time periods, as simple verification (Section 3.7) of solutions of the internal-state flow calculations (Freeze, 1978; Sections 8.2.1.; 8.2.3.; and 8.3).
2. Place the hydrological response of the research hillslopes within the more realistic context of catchment response (Klemes, 1978; Loague and Freeze, 1985; Chapter 5).
3. To aid the understanding of hillslope hydrological processes, through an examination of the *lumped* behaviour of two hillslope and catchment areas (Bren *et al*, 1979; Burch *et al*, 1987; Chapter 5).

3.5. Internal-State or White-Box Approach.

The relationship between the hillslope hydrological response and the streamflow produced, is generally non-linear (e.g. Equation 33), and non-stationary (Sections 1.2., 1.6., 7.4.5., and 7.4.9; Beven, 1977, 1987; Burt and Butcher, 1985; Weyman, 1973; Yeh, 1983). Simple black-box or rainfall-runoff relationships (Section 3.4; Chapter 5) are, therefore, poor predictors of hillslope hydrological processes (Hewlett and Hibbert, 1967). The *internal-state* of the hillslope must be characterized, to fully understand those processes governing streamflow generation (Beven, 1988; Dunne, 1983; Freeze, 1978). As the internal behaviour of individual hillslopes is very complex (Bear *et al*, 1968; Nielsen *et al*, 1986), our understanding of this internal behaviour could be facilitated by identifying a further six sub-ordinate conceptualizations.

3.5.1. Control-Volume or Eulerian Approach.

The movement of water within hillslopes could theoretically be examined over a *continuum of scale*, ranging from a molecule, through to the fluid particle, pore, control-volume, soil horizon, soil profile, hillslope-catena, and catchment. All of the scales coarser than the molecular structure, are averages of the hydrological processes (Bear, 1972). Many physical-mathematical approaches (e.g. Table 52) and field-based approaches (e.g. Harr, 1977; Tsukamoto and Ohta, 1988; Weyman, 1973) to the calculation of water-flow within hillslopes are based upon the characterization of hydrological properties within control-volumes of soil (Bear, 1972; Chow *et al*, 1988; Euler, 1755; Chapters 6 and 7). Within this study, the size of the control-volume is defined as *the largest volume of soil, at which the stationary hydrologi-*

cal properties (or hydrological parameters : Chapter 7) can be considered the most isotropic. This definition is similar to that defined for a representative-elementary-volume (REV's) of soil (Bear, 1972; Hubbert, 1956). The size of the control-volumes within the instrumented hillslopes is presented within Section 4.2.

3.5.2. Flow-Strip Approach.

To attempt to monitor every control-volume within a whole hillslope segment, would be impracticable for most studies. Representative hillslope sections, known as *flow-strips* (Kirkby, 1988) or two-dimensional transects are, therefore, used to characterize steep, straight hillslopes where across-slope soil water movement is insignificant (Anderson, 1982; Beven, 1977; Sharma *et al*, 1987). Each hillslope section must, however, include the complete sequence of soil types associated with the local hillslope catena (Section 2.8.2., 3.5.2), to enable the spatial relationships between the individual control-volumes to be characterized (Sharma *et al*, 1987).

3.5.3. Hillslope Catena Approach.

The research has focused upon the physical characterization of water-pathways within a natural hillslope catena (Milne, 1936), because previous research (e.g. Dixon, 1986; Hammermeister *et al*, 1982a,b; Krug and Frink, 1983; Rogowski *et al*, 1974; Tsukamoto and Ohta, 1988; Zaslavsky and Sinai, 1981c) has shown that most precipitation has to move through a particular sequence of soil types, known as a *hillslope catena*, before reaching a stream.

Typical hillslope catenas include a crest segment, a steep slope, and a riparian zone. A combination of hydrological, geomorphological and geochemical processes leads to the development of soil type characteristic to each of these segments. The riparian segment is often very distinct from the rest of the catena, as a result of:

1. A translocation of fines, downslope to the riparian zone (Dixon, 1986; Douglas, 1977; Williams *et al*, 1986),
2. different weathering rates within the riparian zone due to the dynamics of the zone of saturation (Section 6.3.3; Eden and Green, 1971), and
3. different resultant flow directions within the two zones (Sections 8.2.1. and 8.2.2.; Zaslavsky and Rogowski, 1969).

An idealized hillslope catena for the whole Plynlimon massif is presented within Figure 5. Those hillslope catenas specific to the two instrumented hillslopes are presented within Figures 8 and 9.

The primary scale of the research was the hillslope-catena, this scale was, however, *bounded* by an examination of the effect of individual trees upon hillslope water movement, and the effect of the individual hillslopes upon the streamflow generated within the sub-catchment as a whole (Section 3.3).

3.5.4. Soil Horizon Approach.

Numerous studies (e.g. Adams and Raza, 1978; Beasley, 1976; Bonell *et al*, 1984; Crampton, 1967; Hammermeister *et al*, 1982a,b; Hoover, 1949; Hursh and Hoover, 1941; Nielsen *et al*, 1973; Whipkey, 1965) have shown that the classification of a soil profile into different *soil horizons* is often associated with the layering or laminations within the hydrological properties. Crampton (1963) and Zaslavsky and Rogowski (1969) have suggested that the development of soil horizons can be dominated by the pathways of water within soil profiles of hillslopes.

Where soil horizons can be considered internally-homogenous in comparison with neighboring horizons, then a characterization of all of the control-volumes within a hillslope (Section 3.5.1) could be greatly simplified to a characterization of an average property for each soil horizon within each catenary zone (Section 3.5.3.; Figures 61 and 62).

3.5.5. Simulation Modelling Approach.

Numerical solutions (i.e. algebraic approximations) of the partial differential equations describing flow within porous media (Equations 3 to 19) are generally considered to be the most accurate method of *simulating* such flows within layered hillslopes. The other mathematical techniques which have been used include the analytical solutions based upon the tangent-continuity equation (Chappell *et al*, 1990; Zaslavsky and Sinai, 1981a,c,d,e), or the kinematic wave equation (Beven, 1982; Hurley and Pantelis, 1985; Smith and Hebbert, 1983; Tani and Abe, 1987).

The physical complexity of 2 dimensional flows within transiently saturated and layered hillslopes, has eluded all attempts at accurate simulation. The simulation modelling studies presented within Tables 51 and 52 , notably Ahuja and Ross (1982, 1983), Beven *et al* (1984) and Sharma *et al* (1987)have, however, added greatly to the understanding of water-pathways.

Numerical solutions developed within this thesis are applied to validate the field observations and approximative solutions. The two principal objectives are the prediction of:

1. the refraction of the equipotential-net within the A/E soil horizon (Section 8.3.2), and
2. the most important *source* horizon for the inflows into the riparian zone (Section8.3.3).

3.5.6. Internal-State Validation Approach.

Most empirical equations, physical laws, parameter estimates, measurement techniques, and numerical techniques are subject to simplifying assumptions, artificial boundary conditions, and approximations. Most techniques, therefore, require *validation* or testing.

Mathematical modelling has shown that very similar streamflow responses can be produced by very different combinations of hydrological properties and hence water-pathways. Predictions of water pathways *must*, therefore, be validated *internally* within the hillslope(Anderson and Rogers, 1987; Beven, 1989; Dunne, 1983; Klemes, 1983; Pickens and Lennox, 1976; Sorooshian, 1988). The possible sources of error within the prediction of water-pathways arise from:

1. the continuum approach,
2. the Darcian assumption,
3. simplification of multiphase flow,
4. the identification of the representative distribution of hydrological parameters,
5. measurement errors, and
6. mathematical approximation.

An explanation of each of these sources of error are outlined:

1. The Continuum Assumption: Application of the general-motion-equation to the calculation of moisture flux within soils, assumes that the governing hydrological properties can be averaged at some representative scale (e.g. the control-volume: Section 3.5.1), prior to any calculation of flow (Bear, 1972; Brachmat and Bear, 1986; Hubbert, 1956). This has been questioned (Dagan, 1979; Klute, 1973; Sposito, 1986).

2. The Darcian Assumption: The motion equation based upon Darcian flow (Section 1.3) becomes highly inaccurate when the flow regime becomes either partially-turbulent, or non-Newtonian (Englund, 1953; Gray and O'Neil, 1976; Hannoura and Barends, 1981; Nielsen *et al*, 1972; Raats, 1971).

3. Simplification of Multi-Phase Flow: The Darcy equation was originally developed for flow within completely saturated soils, and was extended for use within partially saturated soils by incorporating two functions: the moisture capacity and relative hydraulic conductivity (Buckingham, 1907; Muskat and Meres, 1936; Richards, 1931; Wyckoff and Botset, 1936). This simplification of the multi-phase air and water system, may not be valid (Muskat and Meres, 1936; Nikolaevskii and Somov, 1978). Moreover, the general omission of effects of air-flow upon water-flow within most flow-solutions, may also not be justified (Morel-Seytoux, 1983).

4. Identification of the Representative Distribution of Hydrological Parameters: Accurate flow prediction assumes that the hydrological parameters are accurately defined within *measured* control-volumes of soil, and within those un-measured control-volumes of soil which comprise the remainder of the flow region (Anderson and Burt, 1985). This is very difficult to achieve in complex field situations (Beven, 1987; Stephenson and Freeze, 1974).

5. Measurement Errors: All measurement introduces artificial (boundary) conditions in the form of sensor or sampling errors (Anderson and Burt, 1985; Bear, 1972; Dunne, 1983; Beven and O'Connell, 1982). An understanding of these errors is particularly important to calculations of flow based upon internal-state data. While water falling upon and flowing out of a catchment can be *measured directly* without the imposition of too many artificial conditions, the flow of water with subsurface strata cannot. These errors must be identified and removed from parameter values (Section 1.2).

6. Mathematical Approximation: Water-flow problems are usually too complex for the direct solution of the underlying partial differential equations. Approximative, analytical or numerical solutions are, therefore, required. The errors associated with the use of each of these techniques must be assessed, and tolerances applied to the calculated results.

The 6 possible sources of error within the predictions are evaluated by 7 field and mathematical techniques. These include:

1. The use of several techniques to measure the same hillslope hydrological property (Section 4.8). For example, moisture potential was measured by both tensiometry and piezometry (Section 6.3.2), and saturated hydraulic conductivity was measured by permeametry, recovery-tests and hillslope outflow (Section 7.3).
2. Comparison of the response and distribution of each of the hillslope hydrological variables and properties with the predicted water-pathways.
3. Validation of approximative mathematical solutions using boundary-constrained numerical predictions (Sections 8.3.2. and 8.3.3)
4. Calculation of water-flows within two hillslopes receiving similar temporal-distributions of precipitation input, using the same field and mathematical techniques (Section 8.2).
5. Comparison of the predicted inflow to a relatively homogenous riparian area, with the predicted outflows (Section 8.2.3).
6. Comparison of the calculated water-pathways predicted by the hydrometric analysis with observed changes in ionic concentration within the stream and riparian area
7. Validation of the predictions produced by the SUTRA model, which is based on a finite element/finite difference numerical solution, with the predictions produced by a boundary-integral-equation-method (BIEM) solution (Dowd, 1979). While the detailed results are not presented, steady-state simulations under varied internal and boundary conditions (see Section 8.3.1), produced very similar predictions.

3.6. Event-Based Approach.

Most of the field monitoring was conducted during the initial 3 to 10 days of each storm-period (defined in Section 5.3.1). This approach was adopted to allow accurate derivatives of the rate of change of the hydrological properties to be calculated (Beven and O'Connell, 1982; Sloan and Moore, 1984; Yeh, 1981; Zaslavsky and Sinai, 1981a,c,d,e). Furthermore, this period coincides with the period when the greatest loadings of *acidic solutes* are observed with forest streams (Neal *et al*, 1986; Reynolds *et al*, 1983).

3.7. Natural-Tracer Approach.

Although the details are presented elsewhere (e.g. Chappell *et al*, 1990), samples of precipitation, soil-water and stream-water were collected and analysed to compare the dynamics of the ionic concentrations. These data are used to verify the water-pathways predicted by the hydrometric techniques (Bricker, 1987; Dixon, 1986; Duysings *et al*, 1983; Heald and Rogowski, 1977; Pilgrim *et al*, 1978; Sklash *et al*, 1986).

CHAPTER 4.

Instrumentation.

4.1. Introduction.

This research aims to integrate hydrological properties and responses monitored over a range of scales (Section 3.3). A precise definition of the dimensions of each measured scale (Section 4.2) is, therefore, presented prior to the detailed discussion of the instrumentation. The temporal measurement *scale* or strategy is presented within Section 4.7.

A detailed discussion of the instrumentation used to assess the black-box (Section 3.4) or rainfall-runoff response (Chapter 5) of the hillslopes and catchments is presented within Section 4.3. The instrumentation used to assess the white-box (Section 3.5) or internal-state response of the hydrological variables and parameters (Chapters 6 and 7) is presented within Section 4.4. A summary of all of the hydrometric properties monitored for both the black- and white-box approaches is given within Section 4.5.

The sampling and analysis of the hydro-chemical properties monitored during field-season, are presented within Section 4.6. A review of the procedures used to control the quality of both the hydro-metric and hydro-chemical measurements, is given within Section 4.8.

4.2. Spatial Measurement Scale.

To integrate the tree-scale with other internal-state hillslope data (Beven, 1988a; Sections 6.3.6. and 7.4.4), and the internal-state data with the external-state rainfall and streamflow data (Section 8.2.3), required a precise definition of each spatial element being characterized (Klemes, 1983; Towner and Youngs, 1986). Five spatial elements are defined:

1. Catchment Areas: The effective precipitation inputs, and evapo-transpirational and streamflow outputs from both the forested and grassland catchments, were calculated for 0.1 km^2 catchment areas (Sections 5.2., and 5.3.).

2. Hillslope-Catenal Areas: The precipitation inputs to the forest hillslope and the evapo-transpirational plus streamflow outputs from the hillslope, were calculated for an area of approximately 30 by 50 m (Sections 5.2.2., 5.2.3.1., 5.2.3.3., and 5.3.). This area was delineated an the basis of both surface contours and the estimated catchment area of the 10 m slope-base section of the forest drainage channel.

3. Catenal Zone Lengths: The hillslopes beneath both the forest and grassland covers have two catenary elements: (1) a podzolic slope section, and (2) a riparian section (Figures \8 and 9). The riparian zone is separated from the podzolic zone on the basis of the marked difference in soil type (Figures 8 and 9). Within the forest hillslope, the riparian zone extends 2.5 m upslope of the drainage channel, and the podzolic slope extends from 2.5 m to 40 m upslope. There is an abrupt change in slope-angle between the two catenal zones (Figure 4). Within the grassland hillslope, the riparian zone extends some 5 to 10 m upslope from the stream (Nant Mynachlog), and the podzolic slope extends from riparian zone up to 40 to 60 m upslope. The junction between the podzolic slope and riparian area within the grassland is much less distinct (Figure 3), in comparison with the forest hillslope .

4. Soil Horizon Depths: The soil horizons within the podzolic section of the forest hillslope are well defined (Table 8). These ferric podzol soils (Section 2.8) have average soil horizon depths of 10 cm for both the O/A (including L) and Eag horizons, 20 cm for the Bs1 horizon, 15 cm for both the Bs2 (B/C) and C1 horizons (Table 8). The soil horizons within the grassland hillslope are not as clearly defined as the forest hillslope, probably as a result of the single ploughing operation in 1976. The depths of the soil horizons are, however, similar to the equivalent horizons within the forest.

5. Control-Volumes of Soil Pores: The size of the control-volume of soil within the research hillslopes was defined by the relatively *stationary* hydrological property of *intrinsic permeability* (Section 7.4). As each soil horizon within the relatively undisturbed forest hillslope has a very different intrinsic permeability to the neighboring horizons (Section 7.4.2), the minimum depth of these soil horizons is the major determinant of the size of the control-volume (Section 3.4.1). This minimum depth is 10 cm (see above).

Small-diameter cores (i.e. 7 cm) used to measure intrinsic permeability were subject to considerable measurement error (Section 7.4.1). Large diameter cores (i.e. 30 cm) were, therefore, used to measure the intrinsic permeability and define the size of the control-volume. This control-volume contains 7000 cm^3 of soil (i.e. Π x 15 cm^2 x 10 cm). The actual volume of soil sampled in the characterization of the other hydrological properties is defined within Table 11.

Table 11. The size of the defined control-volume versus that of the measured soil volumes

Hydrological Properties	Defined CV (cm^3)	Measured Volume (cm^3)
moisture content	7000	400 or 5000
capillary potential	7000	100-1000
bulk density and porosity	7000	50 or 400
specific moisture capacity	7000	400-5000 (*in situ*) 50 (lab.)
hydraulic conductivity and intrinsic permeability	7000	200-7000

NOTE: A hillslope segment only 10 m long, 70 cm deep, and 10cm wide has a volume of 700,000 cm^3, and would contain 100 control-volumes.

4.3. Measurement of Hillslope and Catchment Rainfall-Runoff.

The hillslope and catchment water balance was assessed by the measurement of the gross-precipitation and net-precipitation inputs, and the outputs of wetted-canopy-evaporation and streamflow.

4.3.1 Gross-Precipitation Input.

Gross precipitation input (or the precipitation received by the vegetation canopy) to both the forest and grassland sub-catchments was monitored by three raingauges located in the grassland (Figures 1 and 24). Two of these gauges were fitted with tipping-bucket devices to enable near-continuous datalogging (Section 4.7.3). Following the research of Rodda and his co-workers (e.g. Robinson and Rodda, 1969; Rodda, 1971; Harrison and Newson, 1977), one of the gauges was installed in a raingauge pit and covered by an *anti-splash grid* (Bucknell *et al*, 1977). This gauge was heated to prevent freezing, and melt snowfall. The orifice of the second tipping-bucket or *Rimco®* raingauge, was positioned at the British Meteorological Office standard height of 12 inches (30 cm) above ground-level. Both of the logged gauges were continuously calibrated against a standard storage-gauge (Plinston and Hill, 1974).

Canopy-level gauges (Bucknell *et al*, 1977) were not installed above the forest, because of the aero-dynamic problems associated with canopy-level gauges at the windward edge of forest stands (I. Wright, pers. comm. 1988). The gauges sited within the grassland were, however, only 150 m away from the forest hillslope. The gross precipitation records were extended beyond the monitoring period by scaling against the records monitored by a gauge at the Institute of Hydrology (NERC) Cefn Brwyn automatic-weather-station, sited in the adjacent Wye catchment (Strangeways, 1985; Templeman, 1978).

4.3.2. Net-Precipitation Input beneath the Forest Canopy.

Net precipitation onto the forest floor was assessed by a combination of stemflow-counters and throughfall collectors.

Stemflow: Stemflow collars were attached to 10 trees. Following Rutter (1963) who found a good correlation between stemflow volume and tree girth within a 16 year old Scots pine (*Pinus sylvestris*) stand, 7of the collars were attached to trees with girths (i.e. Diameter-Breast-Height: DBH) ranging from 14 to 44 cm (i.e. 14, 19, 24, 29, 34, 39, and 44 cm). These tree girths were representative of the range of girths measured over the whole forest hillslope (Calder, 1976; Rutter, 1963). The collars were made from un-vulcanized rubber. They directed stemflow into 100 ml tipping-buckets, which then advanced mechanical counters (Figures 11 and 12). Spiral collars, made from chemically-inert materials (Reynolds and Stevens, 1987), were attached to a further three trees so that they could be used to collect stemflow samples for the analysis of the water-chemistry (Figure 11).

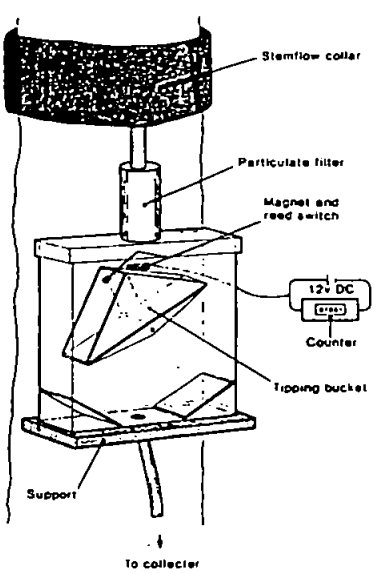

Figure 11. The stemflow collar and and tipping-bucket assembly.

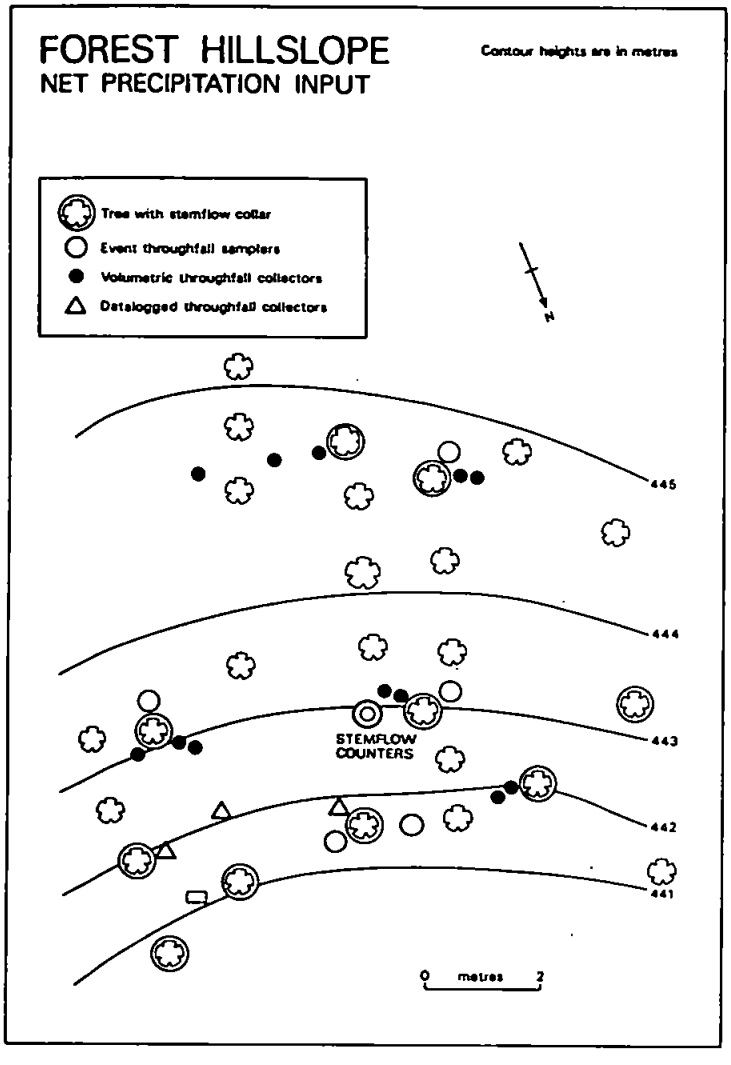

Figure 12. The distribution of the stemflow and throughfall collectors.

Throughfall: Seventeen volumetric throughfall collectors were installed around the same sample of trees fitted with stemflow collars (Figure 11). The throughfall volumes from 12 of these collectors were measured before and after major storm events, for a period of 10 months. Twelve collectors with an orifice diameter of 15 cm, have been shown by Gash *et al*, (1980) working in a nearby sitka spruce (*Picea sitchensis* , Bong. Carr.) stand, to be a sufficient number of collectors by which to average throughfall input (I. Wright pers. comm. 1988). The other five throughfall collectors installed, were used to sample throughfall chemistry, sequentially through selected storm events. To collect samples large enough for chemical analysis, these collectors were required to be 60 cm in diameter.

4.3.3. Evapo-transpirational Output.

The rate of evaporation from wetted forest canopies (i.e. canopy interception) was calculated by subtracting stemflow and throughfall volumes from gross precipitation (Calder *et al*, 1982; Milne *et al*, 1983). The total evapo-transpiration outputs were estimated from (1) catchment water balance calculations (Section 5.2.2), and (2) the empirical Thornthwaite method applied to monthly mean temperature data (based upon the daily mean of maximum and minimum air temperatures) monitored at the Moel Cynnedd meteorological site within the Institute of Hydrology Severn catchment (Section 5.2.2.1; Strangeways, 1985; Templeman, 1978).

4.3.4 Streamflow Output.

The generation of streamflow within the forest and grassland sub-catchments was monitored with a network of four weirs and two flumes (Figure 13).

Upper Drain Weir (Forest): The streamflow generated by the outflow from the 30 by 50 m forest hillslope was gauged by a 90 degree V-notch weir (British Standards Institution, 1965a), located at the head of an ephemeral drain. The height of water within this structure was measured with a float-operated water- level-recorder linked to a datalogger (Section 4.7.3), and with an *Institute of Hydrology Vertical Chart* water-level-recorder (Truesdale and Howe, 1977).

Lower Drain Weir (Forest): The effect of the streamflow generated by the instrumented forest hillslope upon the streamflow response some 20 m further along the forest drain, was measured with a 53 degree V-notch weir. A *Munro ®IH89* water level recorder was used to record the weir *stage* (or head).

Stream Weirs and Flumes: The artificial drain at the base of the instrumented forest hillslope, routed water into a first-order stream. A 130 m length of this stream, was, therefore, gauged to compare the hillslope response with the sub-catchment streamflow response. A compound 90 degree V-notch/rectangular weir equipped with an *Institute of Hydrology Vertical Chart* water-level- recorder, was installed at the top of the stream reach. The outflow from the gauged reach was monitored with a trapezoidal flume (Figure 13), because of the greatly increased sediment load. The stage within the flume was both datalogged with a float-operated water-level- recorder (Section 4.7.3) and chart-recorded with a *Negretti* ®pressure-bulb recorder (Section 4.7.2).

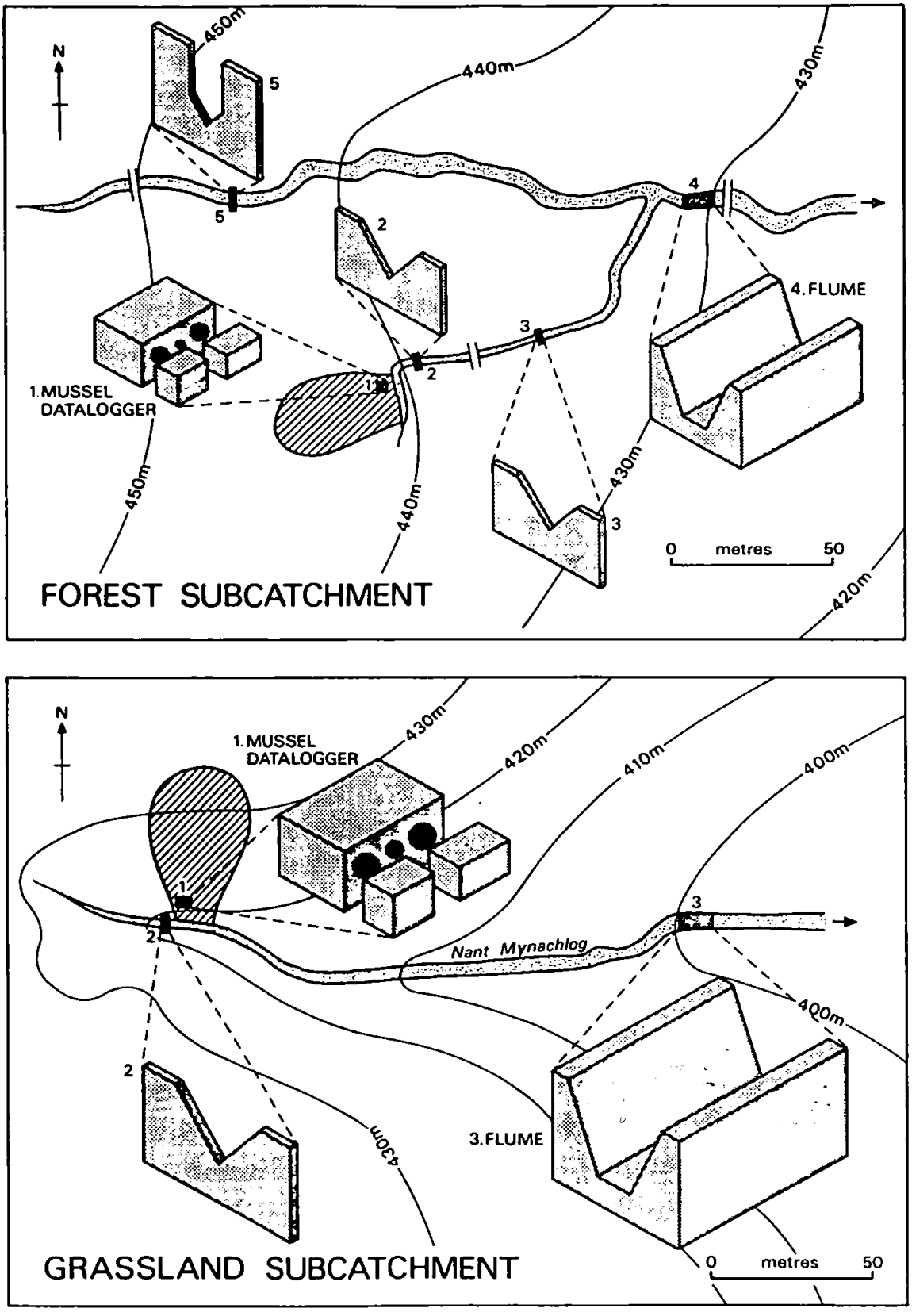

Figure 13. The stream gauging network within the Tir Gwyn Experimental Catchments.

In addition to the comparison of streamflow generation at the forest hillslope and forest sub-catchment scales, the streamflow generated along the forest stream was compared with an adjacent stream within the grassland sub-catchment. Both streams emerged from the same source area, close to the summit of the Tir Gwyn massif (Figure 1). The grassland reach was again gauged with an upstream weir and a downstream flume (Figure 13).

All of the weirs within the sub-catchments were installed into an impermeable mix of *local* peat and gleyed soil (M.D. Newson, pers. comm. 1987), and then calibrated by the volumetric measurement of the weir outfall. The two fibre-glass flumes had to be both installed within concrete, and calibrated by constant-rate dilution gauging (Section 5.2.3).

4.4. Measurement of Hillslope Hydrological Properties.

The internal-state properties of soil bulk density, porosity, soil moisture content, capillary moisture potential, specific moisture capacity, hydraulic conductivity, intrinsic permeability, and fluid viscosity are required to both characterize and model the major pathways of water movement, beneath specific hillslopes. On steep, straight hillslopes where across-slope soil water movement is insignificant (Anderson, 1982; Beven, 1977), a two-dimensional transect or *flow-strip* (Kirkby, 1988; Section 3.5.2) can be instrumented to represent the whole hillslope catena. A single flow-strip beneath the forested hillslope (Figures 4 and 17) and a duplicate beneath the grassland hillslope (Figures 3 and 18) was, therefore, instrumented to monitor the critical internal-state properties. Instrument plots, were located at a maximum distance of 10 m apart on both sites (Atkinson, 1978), and a minimum distance of 2.5 m at the base of the forest hillslope (Figure 17).

4.4.1. Soil Bulk Density and Porosity (ρ_b; η).

The two matrix properties of bulk density and porosity must be characterized prior to any calculation of volumetric moisture content (Section 6.2) or percent saturation (Section 7.4.6).

The soil bulk density (ρ_b) is the ratio of the mass of dry solids to the bulk volume (or volume of solids and pore space) of the soil (Blake and Hartage, 1986). Fifty-six soil samples were extracted from the forest and grassland hillslopes using a double-cylinder, hammer-driven core sampler. The samples were weighed, dried at 105 °C for 24 hours, and then weighed. The resultant weights were then divided by the volume of the core.

The porosity (η) of a soil is the ratio of the volume of pore space to the bulk volume of soil. Twenty-six soil samples were removed from the research hillslopes, and then gradually saturated from the base, over a 36 hour period. The samples were then weighed, dried at 105° C, and re-weighed. The total porosity was then calculated from:

$$\text{Porosity } (\eta) = \frac{\text{weight of water within a saturated soil}}{\text{weight of dry soil}} \times \text{bulk density } (\rho_b) \qquad [20]$$

4.4.2 Soil Moisture Content (θ_w; θ_v; θ_s).

Soil moisture content (SMC) is expressed as the fraction of a soil's dry-mass (θ_w), volume (θ_v) or pore-space (θ_s) occupied by water (Hillel, 1982). *Actual* soil moisture content can only be directly measured, by calculating the mass of water lost, after drying a soil sample at 105 °C, for 24 hours (British Standards Institute, 1975). This technique is known as *gravimetric sampling.*

Gravimetric Sampling: The determination of soil moisture content by the gravimetric technique requires the removal of a large number of samples from a research site. The technique is, therefore, not suitable for the continuous monitoring soil water movement, in medium- to long-term experiments (Curtis and Trudgill, 1974; Leuning and Talsma, 1979). Gravimetric sampling is, however, essential for the calibration of *analog-techniques* for estimating soil moisture, such as neutron moderation (Section 6.2) or time-domain reflectrometry (Section 6.2.1).

Neutron Moderation: Neutron moderation or neutron attenuation/ thermalization is a *de facto* measurement of hydrogen (H^+) ions. In non-organic soils where most of the hydrogen present is in the form of liquid water, the technique can be used to monitor changes in soil water content (Gardner, 1986; Gardner and Kirkham, 1952; Ting and Chang, 1985). The technique involves lowering both a neutron source and detector, into an aluminium *access-tube* installed within the soil. High-energy neutrons released from a source of radioactive Americium and Beryllium collide with the predominant hydrogen ions, to produce a *cloud* of low-energy neutrons. The density of this cloud is then measured over a specified period using a boron trifluoride detector (Bell, 1973). The neutron-instrument used during this research, was the *Wallingford Neutron Probe: Mark II* (Institute of Hydrology, 1981). Neutron probe readings were taken at depths of 15, 30, 45, and 60 cm from 12 access-tubes along the forest flow-strip and 6 access-tubes along the grassland flow-strip (Figure 14 and 15). A further 5 access-tubes

were installed immediately downslope of a tree (Figure 14; Section 6.2.5). The access-tubes were installed using a guide-tube and auger (Eeles, 1969) and allowed to *settle* for a period of 10 weeks (Ting and Chang, 1985). Calibration curves relating neutron probe readings to soil-moisture-content from gravimetric samples, were determined for *each soil horizon* within both forest and grassland hillslopes (Jayawardine *et al*, 1983; Haverkamp *et al*, 1984; Lawless *et al*, 1963; Section 6.2.1).

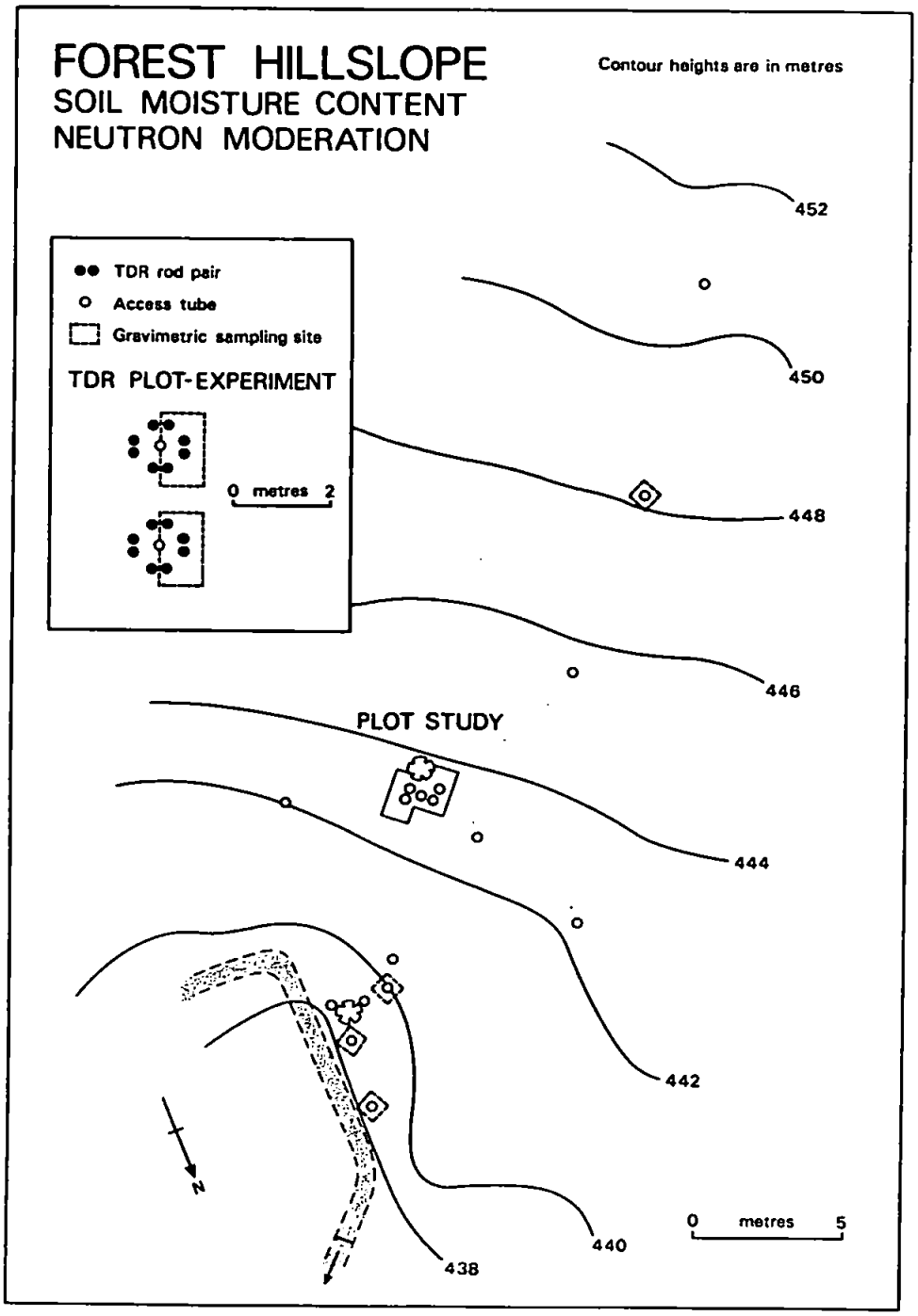

Figure 14. Locations on the forest hillslope, for the measurement of soil moisture content.

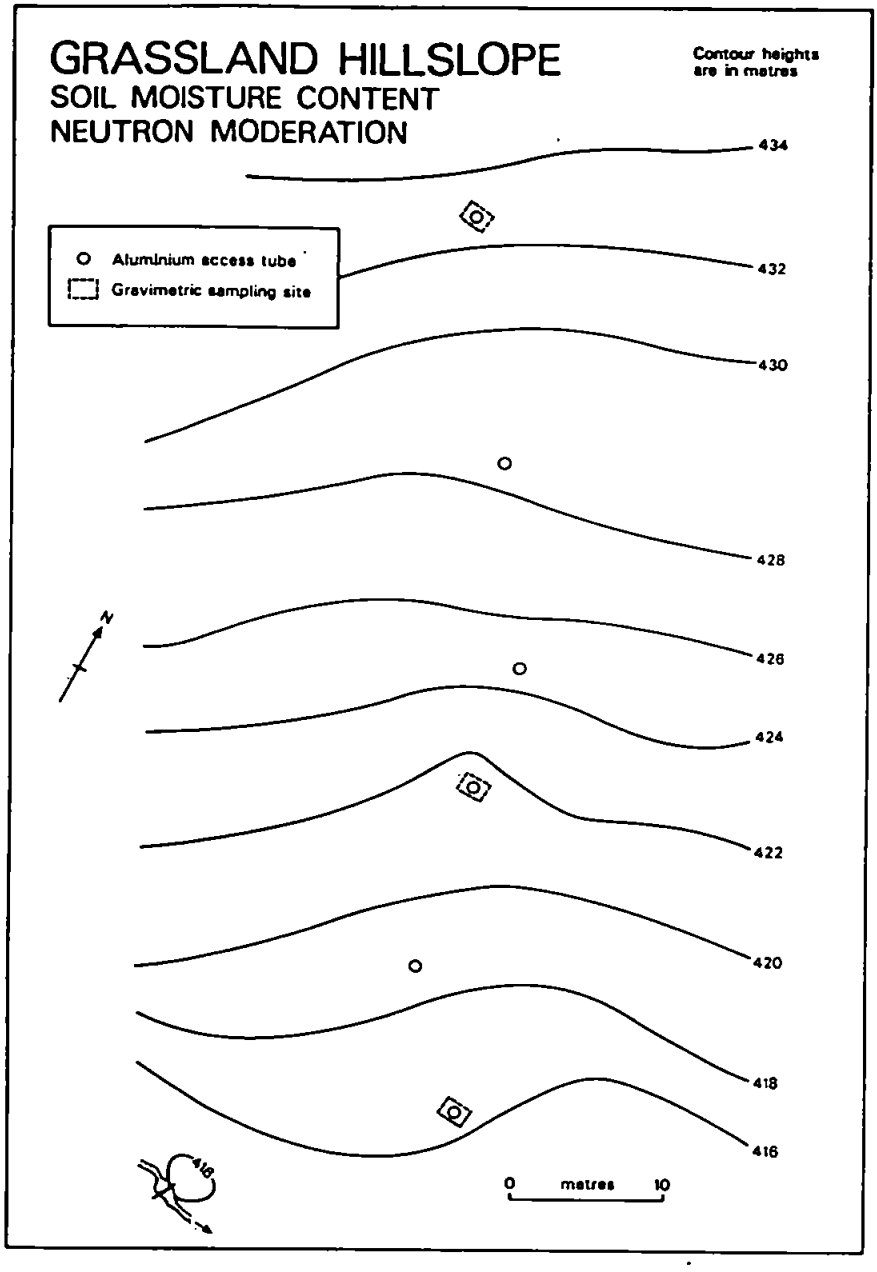

Figure 15. Locations on the grassland hillslope for the measurement of soil moisture content.

Time-Domain Reflectrometry (Plot Experiment): Time-domain reflectrometry or TDR, is a further technique for the indirect or analogue measurement of soil moisture content. TDR is based upon the transmission and reflection of electro-magnetic signals along parallel transmission lines. The point of reflection, depends upon the dielectric properties of the lines and the materials surrounding the lines (Fellner-Feldegg, 1969). For signals of between 1 MHz and 1 GHz, the dielectric *constant* of transmission lines inserted within soils only varies with changes in moisture content (Davis and Annan, 1977; Topp *et al*, 1980).

A small plot experiment was installed on the edge of the main forest hillslope, to compare the measurements of soil moisture calculated from time-domain reflectrometry with those calculated from neutron moderation (Figure 14; Section 6.2.1). Within the plot, neutron counts were taken from two access-tubes at depths of 15, 30, 45 and 60 cm, and *dielectric constants* were measured from transmission lines installed to the same depths. A standard Tectronix 1502B reflectrometer was used, in conjunction with 3 mm (diameter) stainless steel transmission lines (J. F. Dowd, pers. comm. 1988). The lines were not impedance-balanced (Stein and Kane, 1983; Zegelin *et al*, 1989). In addition to these two indirect methods, actual soil moisture content was determined within the plot, by the gravimetric analysis of four samples collected from each of the four depths.

4.4.3. Capillary Potential (ϕ_c).

The difference in capillary potential (or soil moisture potential) between two points within a soil, provides an *energy gradient* for the movement of soil water (Buckingham, 1907; Darcy, 1856; Hubbert, 1940). Capillary potential can be expressed in terms of energy, following the analogy with the Bernoulli Equation (Hubbert, 1940), but is more commonly expressed, simply in terms of pressure (Bear, 1972). This pressure can be measured with a range of different instruments (Burt, 1978; Curtis and Trudgill, 1974; Richards, 1949; Towner, 1986), the most widely used of which, are tensiometers and piezometers.

A *tensiometer* (Kornev, 1921; Gardner *et al*,1922) is a water-filled tube with one sealed end, and one end attached to a porous ceramic cup. The cup is buried within the soil at a specified depth. Water is constantly interchanged between the unit and the soil, so that the pressure within the unit is always the same as within the soil. The pressure within the tensiometer unit is then measured with either a manometer, or an electronic transducer (Figure 16).

In comparison to the tensiometer, a *piezometer* is usually much simpler in design: constructed of a narrow tube (0.3 to 3 cm internal-diameter), which is open to atmospheric pressure at the top, and capillary pressure at the base. The depth of water within a piezometer, represents the *head* or positive pressure within the soil, near to the piezometer's tip or *tapping-point*. The depth of water can be measured by (1) installing an electronic transducer, (2) autographic or digital recording (Section 4.7) of the depth of a float, or (3) lowering a probe attached to a graduated-tape.

In addition to these small diameter devices, larger piezometers or boreholes, can be used. Moreover, when such devices have entry points along their full length, they become *unconfined-boreholes* or wells (Archer and Marks, 1977).

In total, 93 tensiometers, 26 piezometers, and two wells were installed within both of the research sites.

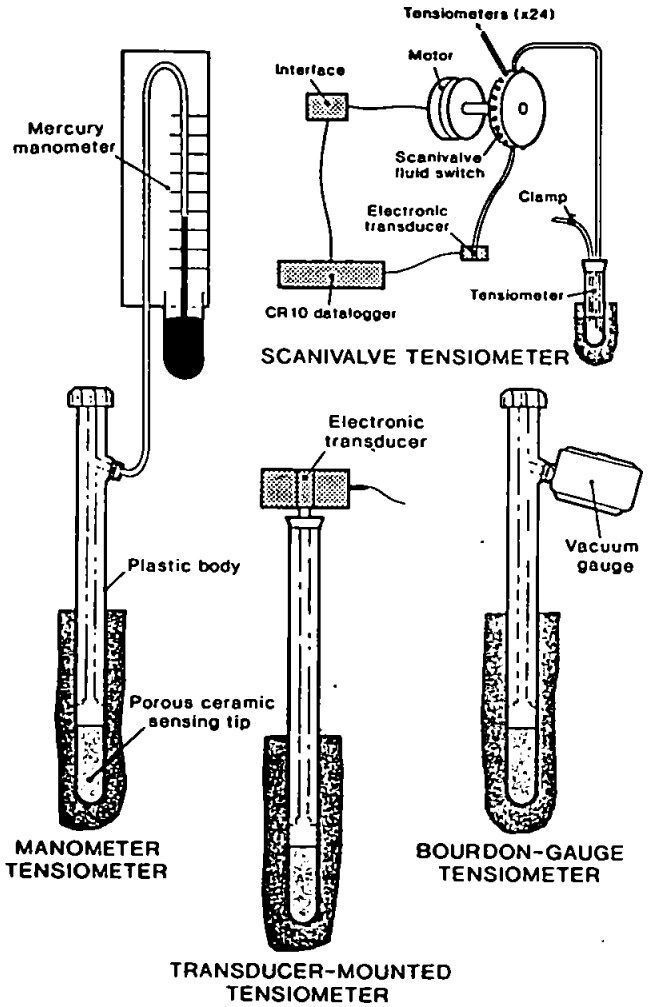

Figure 16. The types of tensiometer installed within the research hillslopes.

Mercury-Manometer Tensiometers: Mercury-manometer tensiometers (Figure 16) were installed along both the forest and grassland flow-strips at depths of 15, 30, 45, and 100 cm, corresponding to the E, B, B/C, and C soil horizons, respectively (Figures 17 and 18). The tensiometer (porous) pots were buried within 63 vm (fine) sand (A. Armstrong, pers. comm. 1987), to ensure a good contact between the pot and the soil. A 50/50 mixture of silt and coarse sand was also tested, and found to have no detrimental effects on the measurement of potential. A ring of bentonite clay prevented the percolation of water down the sides of the tensiometer tube.

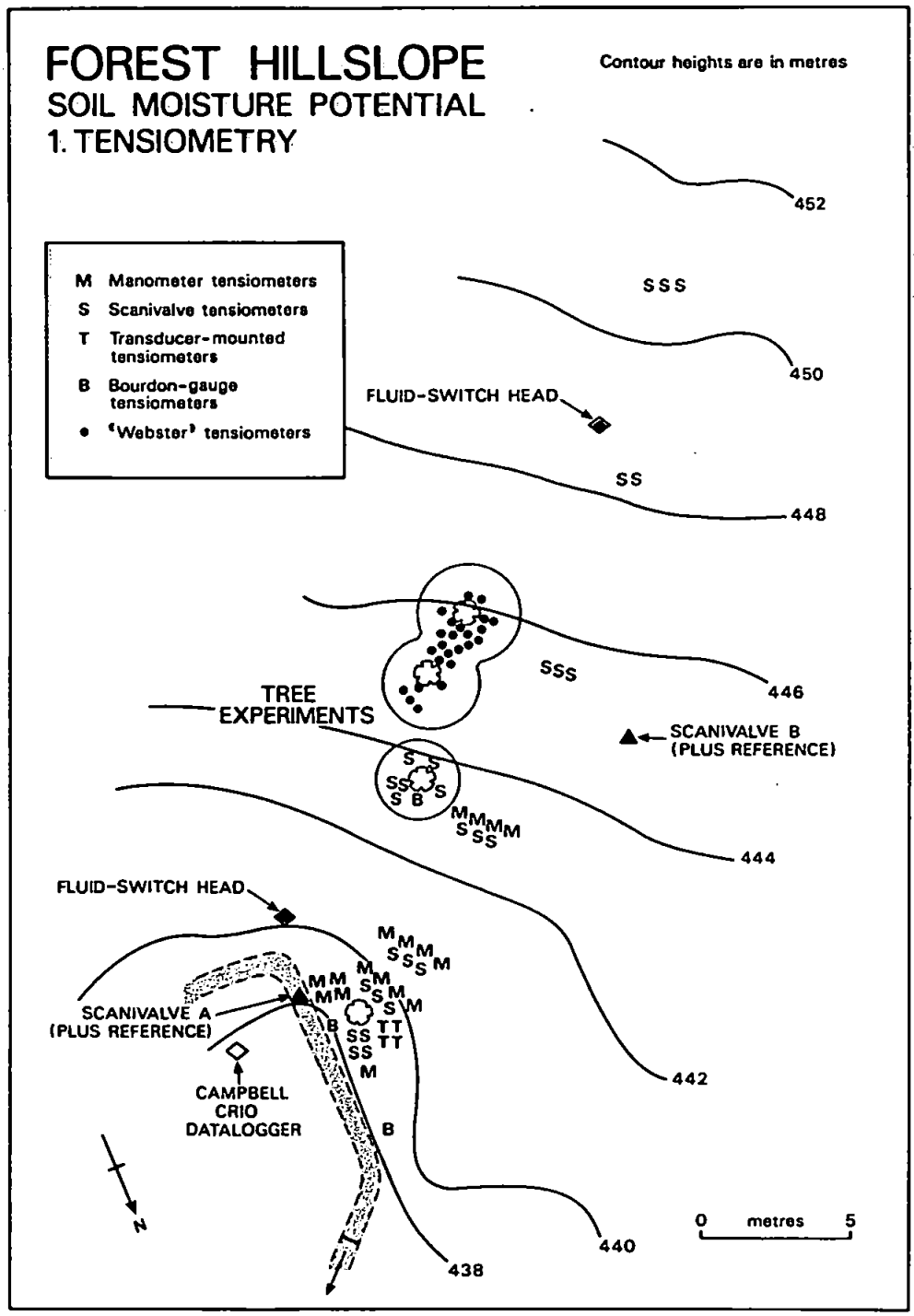

Figure 17. The tensiometer network within the forest hillslope.

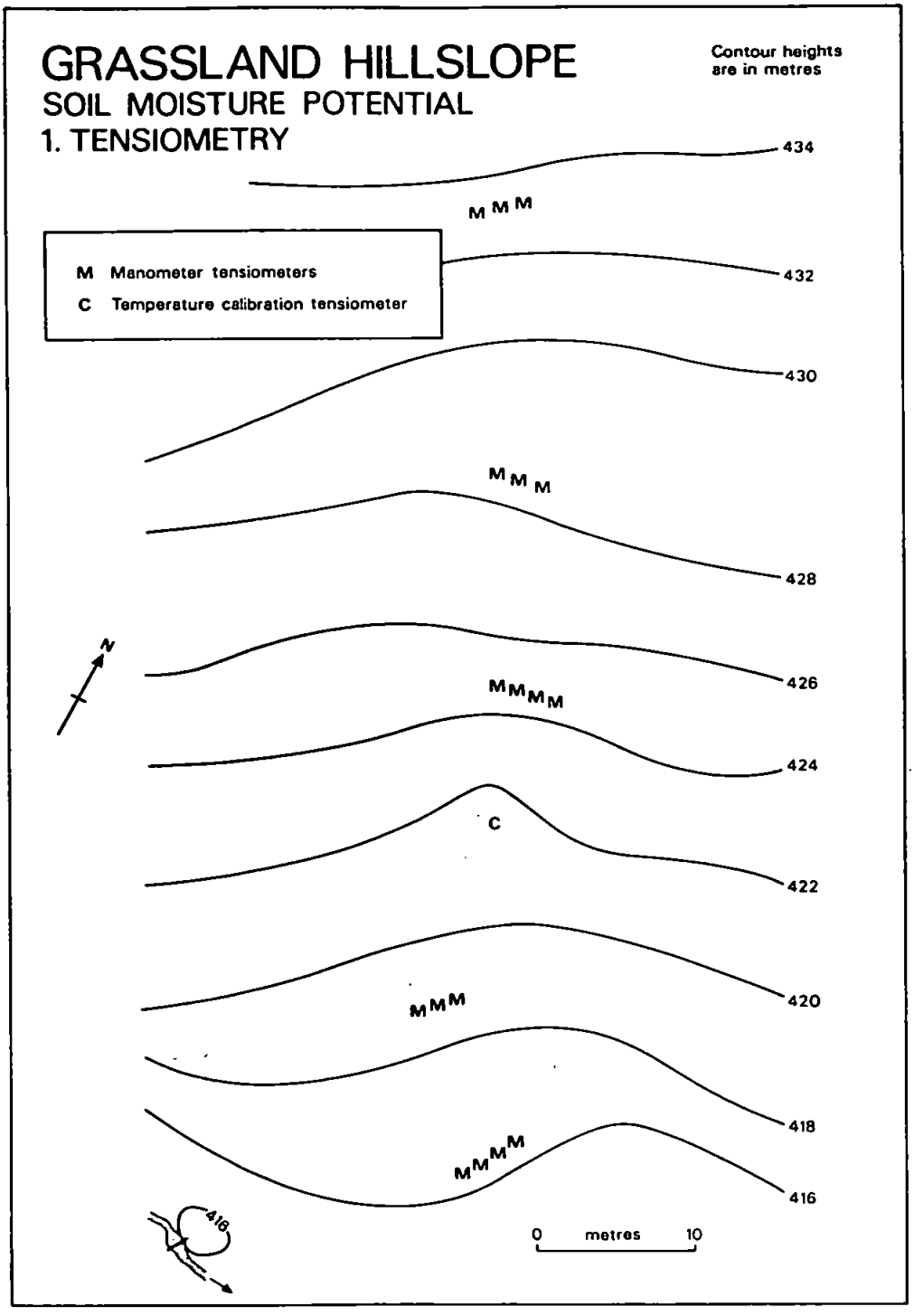

Figure 18. The tensiometer network within the grassland hillslope.

The scales on all of the manometer tensiometers were able to indicate maximum positive potential values of between 20 and 120 cm H_2O (2 to 12 KPa), and maximum negative potential values of between -680 to -800 cm H_2O(-68 to -80 KPa). Each tensiometer unit was individually calibrated to determine the *manomeric-depression* (MEXE, 1963) produced by *dirty* capillary-tubes or *impure* mercury. The manometer columns were frequently de-aired, during those periods when the soil became *dry* (i.e. greater than -200 cm negative potential). An additional manometer-tensiometer was sited above-ground within the grassland (Figure 18), to assess the effect of diurnal fluctuations in temperature on the manometer readings (Watson and Jackson, 1967; Section 6.3.2).

All of the 17 tensiometers along the forest transect and the 16 tensiometers along the grassland transect were independent, 1975-Pattern, *Soil Moisture Equipment Corporation*® units.

In addition to the manometer-tensiometers along the flow-strips, a network of 24 similar tensiometers were installed around and between two neighboring trees (Figure 17). The manometers for these tensiometers were attached to two separate boards (Webster, 1966).

Bourdon-Gauge Tensiometers: Two bourdon-gauge tensiometers were installed at the base of 2 trees within the forested hillslope (Figure 17; Section 6.3.6), as a comparison with the manometer-tensiometers. The gauges were accurate to 20 cm, when offset to 200 cm.

Scanivalve Automatic Tensiometers: A network of 30 tensiometers linked to two pressure transducers, were located next to the manometer-tensiometers within the forest flow-strip (Figure 17). A *Scanivalve* ®fluid-switch connected one of the tensiometers to a transducer every hour (Figure 16). The voltage output from the transducers, was then datalogged using a *Campbell* ® *CR10* datalogger (Section 4.7.3). The transducers, both *SenSym* ®*SCX15ANC*, were individually calibrated for linearity and repeatability using a *constant-head* device at the Whitehall Hydrology Laboratory, University of Georgia, U. S. A. (Dowd and Williams, 1989).

Transducer-Mounted Tensiometers: Three of the tensiometers installed at the base of the forest hillslope (Figure 17), were independently connected to three *SenSym* ®transducers (see above). These transducers were datalogged every 2.5 minutes, because previous studies (e.g. Gillham, 1984; Hursh and Brater, 1941; Sklash and Farvolden, 1979) have observed rapid hydrological responses within streamside and slope base areas.

Nested-Piezometers: Piezometers were installed along the flow-strips, both to increase the number of measurement points of (positive) capillary potential, and to improve the precision with which the surface of any unconfined-saturated zones could be located. Seven piezometer *nests*, comprising piezometers 10, 30, and 100+ cm in length were installed within the forest hillslope (Figure 19), and two within the grassland hillslope (Figure 20).

The shallow piezometers were installed at the O-E (10 cm) and E-B (30 cm) soil horizon boundaries, to monitor the possible development of perched water tables (or shallow saturated zones) observed at other research sites (Betson and Marius, 1969; Bonell *et al*, 1981; Rogowski *et al*, 1974; Walsh and Voigt, 1977). *Deep* piezometers (100-270 cm) were installed primarily to monitor the extent to which the riparian saturated zone, was able to expand up the main hillslope. The 30 cm and 100+ cm piezometers were manufactured by *Soil Moisture Instruments Ltd*, ® and had 30 cm long screened tapping-points and an internal diameter of 2.5 cm. A ring of bentonite clay at 5-10 cm above the screened tapping points, prevented the percolation of water down the piezometer pipes. The 10 cm piezometers were designed specifically for use in the humic-horizon of the ferro-podzolic soils at Tir Gwyn, and had much smaller (1 cm) screened tapping-points.

The depths of water within all of the piezometers (which corresponds to the capillary potential at the tapping-points), were measured by lowering an *dip-tone* acoustic sensor attached to a graduated tape.

Logged Wells (Unconfined Boreholes): Two wells equipped with float-operated water-level-recorders were drilled into the riparian areas at the base of both the forest and grassland hillslopes (Figures 19 and 20; Rogowski *et al*, 1974; Betson and Marius; 1969; Taylor, 1982; King *et al*, 1986). The use of unconfined devices (i.e. with tapping-points along the whole instrument length) for measuring capillary potential, was justified by the relative uniformity of the soil within the riparian areas. Marked horizon development leading to perched water tables, would produce inaccurate water table elevations within such devices (Archer and Marks, 1977). The counter-balanced floats within the wells turned electronic potentiometers, which regulated a voltage supply to a *Mussel* ® datalogger (Section 4.7.3). A simple calibration line was then used to relate the recorded logger-steps, to the actual capillary potential at the base of the well.

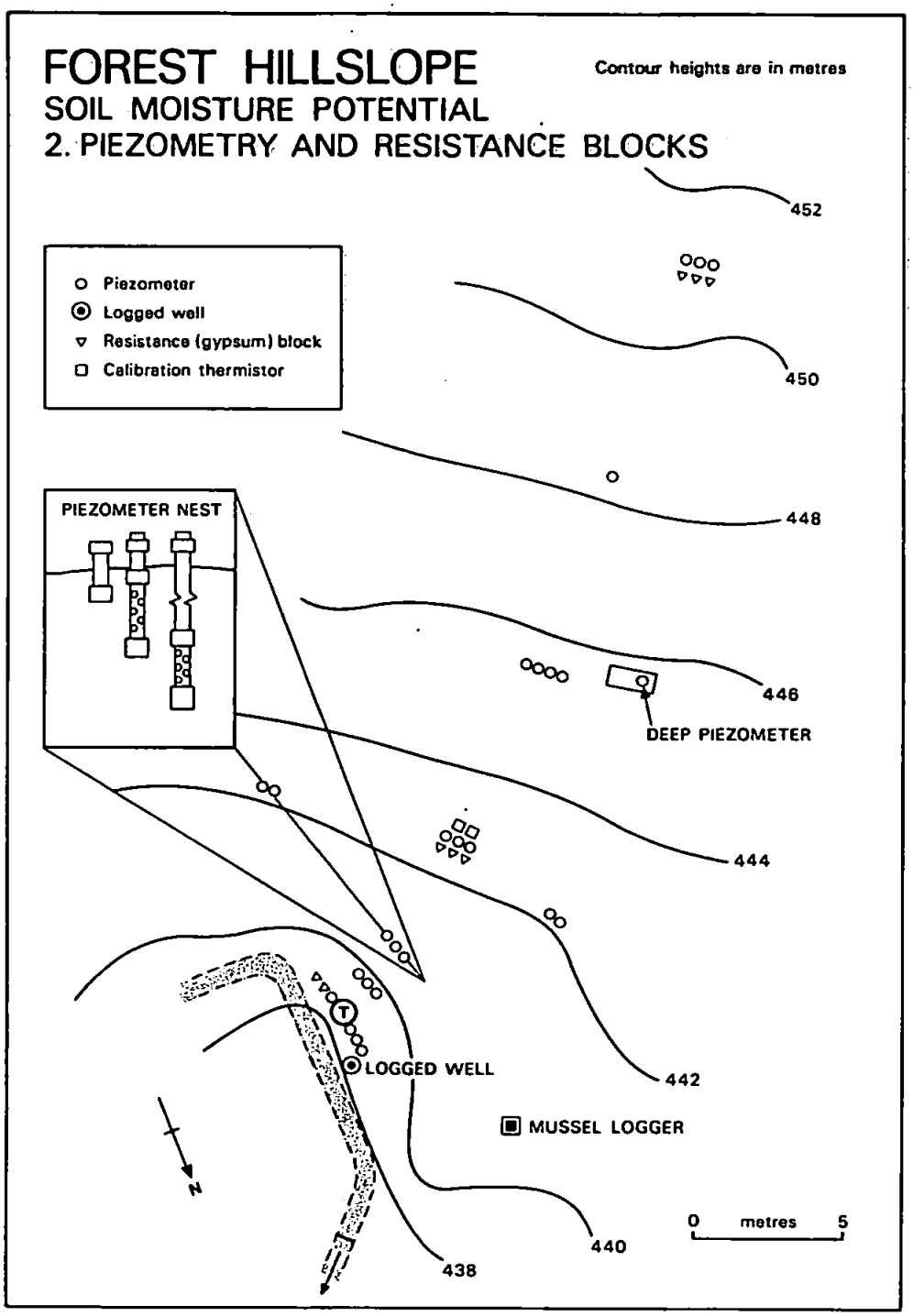

Figure 19. The piezometer network within the forest hillslope.

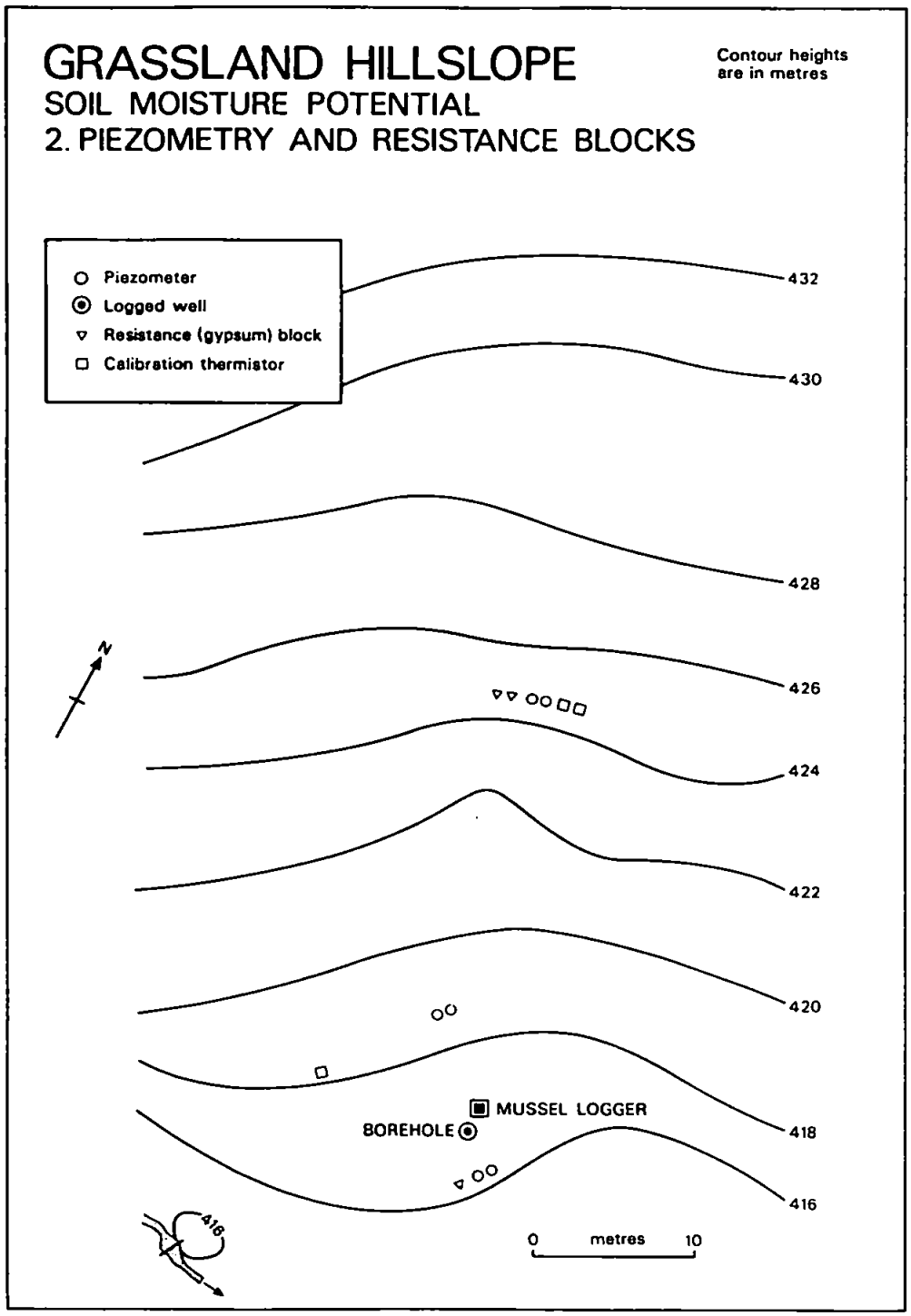

Figure 20. The piezometer network within the grassland hillslope.

Gypsum-Resistance Blocks: Eight gypsum blocks were installed at depths of 15, 50, and 100 cm within the forest flow-strip, and a further three blocks within the grassland (Figure 19 and 20). *Gypsum-resistance blocks* (Bouyoucous, 1972) can be buried within the soil to measure very high negative capillary potentials (i.e. -1000 to -15,000 cm). Although the blocks equilibrate with the surrounding capillary potentials, the actual measured changes of electrical resistance within the blocks, is largely dependent upon the block's water content and temperature (Wellings, 1985; Weyman, 1970). The gypsum blocks were installed within the research hillslopes, in case negative capillary potentials rose above the range of the tensiometers.

4.4.4. Specific Moisture Capacity (θ/ϕ_c).

The specific moisture capacity is the unit change in soil moisture content per unit change in capillary potential (i.e. θ/ϕ_c). Specific moisture capacity is equivalent to the *moisture retention and moisture release*, and the inverse of the *moisture characteristic*.

Wetting and drying of some soils can produce hysteresis in the θ/ϕ_c relationship (Liakopoulos, 1965; Mualem, 1974; Topp, 1969) and, therefore, require the description of two relationships or curves. Hysteresis is, however, rarely observed when the moisture capacity is determined by field methods alone (Carlson *et al*, 1956; Croney and Colman, 1954; Nielsen *et al*, 1973; Rics, 1959; Rogowski *et al*, 1974; Section 7.3.3).

Most *process-based* hydrological models simulate soil water movement by maintaining mass balance over specified volumes of soil (i.e. CV's) using values of moisture potential and not moisture content (Table 52; Section 8.3). Changes in capillary potential must, therefore, be related to changes in actual water content, using the soil moisture capacity (Bear and Verrujit, 1987).

The specific moisture capacities of the soil horizons within the Tir Gwyn research hillslopes were determined by both field (or *in situ*) and laboratory techniques.

***In situ* Determination:** The soil moisture capacity of each soil horizon within the forest and grassland hillslopes was determined directly from field-measurements of capillary potential and soil moisture content (Bruce and Luxmoore, 1986; Rogowski *et al*, 1974). Only low moisture capacities could, however, be determined, because the podzolic soils remained relatively wet throughout the monitoring period.

Laboratory Determination: Twenty-six soil cores (5 cm in diameter and 3 cm in height) were removed from the two flow-strips, to determine the moisture capacity by laboratory techniques. All of the samples were initially, equilibrated and weighed at 0, -5, -10, -15, -20, -30, -40, -60, and -80 cm capillary potential (or 0-80 cm suction) using a sand-tension table (Figure

21). The values of moisture capacity values determined using this technique were then compared with the field-monitored values (Section 7.3.9). The samples were then equilibrated and weighed at capillary potentials of -1000, -2500, -5000, -10,000 and -15,000 cm, using a *Soil Moisture Equipment Corp.*® pressure plate (Figure 21). Such high-suction moisture capacities were unable to be measured by the *in situ* technique, during the study period. Standard *Soil Survey of England and Wales* procedures (Hall *et al*, 1977) were used to both construct and operate the tension table and pressure plate apparatus. A standard temperature of 20°C was maintained during the 5 months monitoring of the tension table and pressure plate apparatus (2/8/88 to 30/6/88).

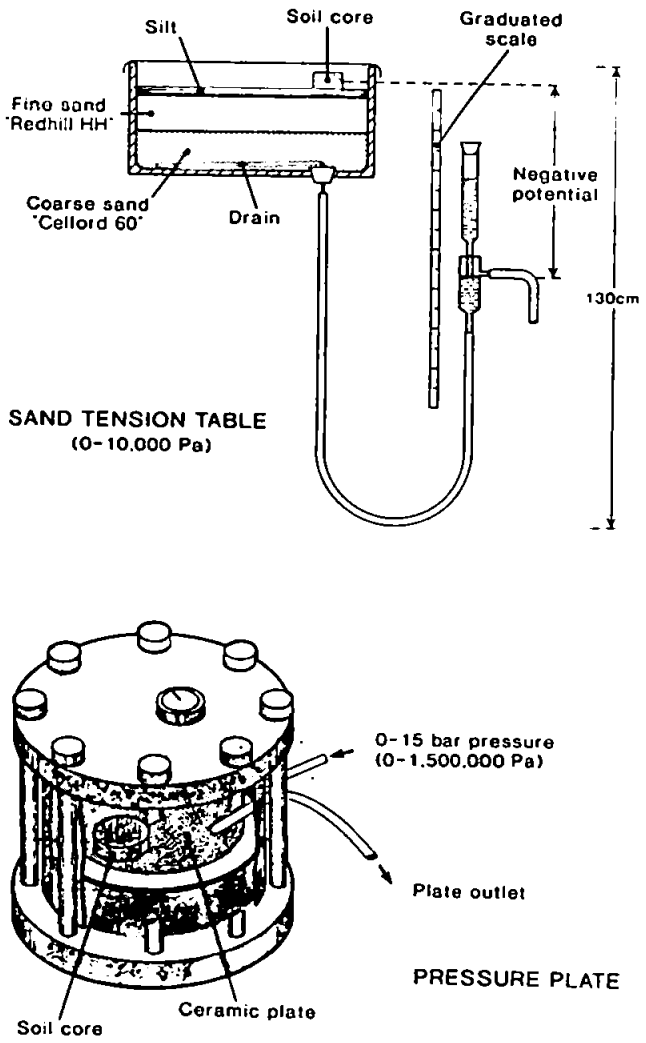

Figure 21. Tension table and pressure-plate apparatus.

4.4.5. Saturated Hydraulic Conductivity (K_s), Intrinsic Permeability (k) and Fluid Viscosity (ν).

Saturated hydraulic conductivity is the *coefficient of proportionality* by which the potential gradient is adjusted to fit measured soil moisture flux within control-volumes of soil (Darcy, 1856). A number of different techniques can be used to measure the hydraulic conductivity of saturated soils, though all are based upon transformations of Darcy's original equation (Section 1.4.3).

The saturated hydraulic conductivity is a function of both the soil's intrinsic permeability and the fluid's density and viscosity (Hubbert, 1940; Nutting, 1930), i.e.

$$K_s = \frac{k\ \rho_f}{\nu} \qquad [11]$$

where K_s is saturated hydraulic conductivity (dim. LT^{-1}), k is intrinsic permeability (dim. L^2), ν is dynamic fluid viscosity (dim. PTL^{-2} or $ML^{-1}T$), and ν/ρ_f is ν or kinematic fluid viscosity (dim. L^2T^{-1}).

Changes in water density are generally insignificant in most field situations (the boundary between saline and fresh waters is a notable exception) and can, therefore, be considered to be a constant. The viscosity of water does, however, change by some 40 percent as water temperature changes from 25° C to 5° C (Marsily, 1986). The temperature of the water from which the viscosity can be established was, therefore, measured during all saturated hydraulic conductivity tests and the values standardized at 20° C (Bonell *et al*, 1981; Section 7.4.1).

The saturated hydraulic conductivity tests carried out on both the forest and grassland soils at Tir Gwyn included: ring, small-core, and well permeametry, and piezometer recovery tests.

Ring permeametry: Ring permeametry involves the insertion and excavation of a large metal ring: 30 cm in diameter and 15 cm deep. The 10 cm deep, soil core within the ring is saturated, and a constant 4 cm head of water is supplied to the top surface. The hydraulic conductivity of the soil core is measured by noting the volume of water required to maintain the constant head (Figure 22). This field-technique has the advantage over similar laboratory techniques (Klute, 1965), because it allows the measurements to be made with large cores, which are less likely to be disturbed during excavation (Berryman, 1974; Gilmour *et al*, 1980; Talsma, 1969; Section 7.4.1). Some 38 soil cores were excavated from the research hillslopes, for ring permeametry measurements (Table 13; Sections 7.4.2. and 7.4.3).

Small-Core Permeametry: An attempt was made to examine the spatial variability of saturated hydraulic conductivity at a scale smaller than the ring permeametry measurements (Section 7.4.1). A field-permeameter, similar in design and operation to the ring permeameter was built to hold a soil core of only 7 cm in diameter and 5 cm depth (Figure 22). The disturbance to the soil core during sampling (Hill and King, 1982; Rogers and Carter, 1987), was minimized by the use of a *Pitman ®corer*. A total of 18 small cores were sampled from inside the larger ring-permeameter-cores (Table 13).

Well Permeametry: A relatively simple and quick technique was used to compare the hydraulic conductivity values of soil beneath trees, with the values for soil at some distance from trees (Section 7.4.4). The technique, known as *well permeametry* (Talsma and Hallam, 1980) or *shallow-well pump-in method* (Bouwer, 1962) involves measuring the volume of water required to maintain a constant head of water within an auger-hole (Figure 22).

Piezometer Recovery Tests: The recovery of piezometer water level, following an instantaneous draw-down, can be used to measure the hydraulic conductivity of soils beneath a water table. Recovery tests carried out using four piezometers, during a period when the local water tables were relatively constant. The analytical equations developed by Kirkham (Luthin and Kirkham, 1949; Reeve and Kirkham, 1951) and Ernst (1950) were applied to the results (Section 7.4.3).

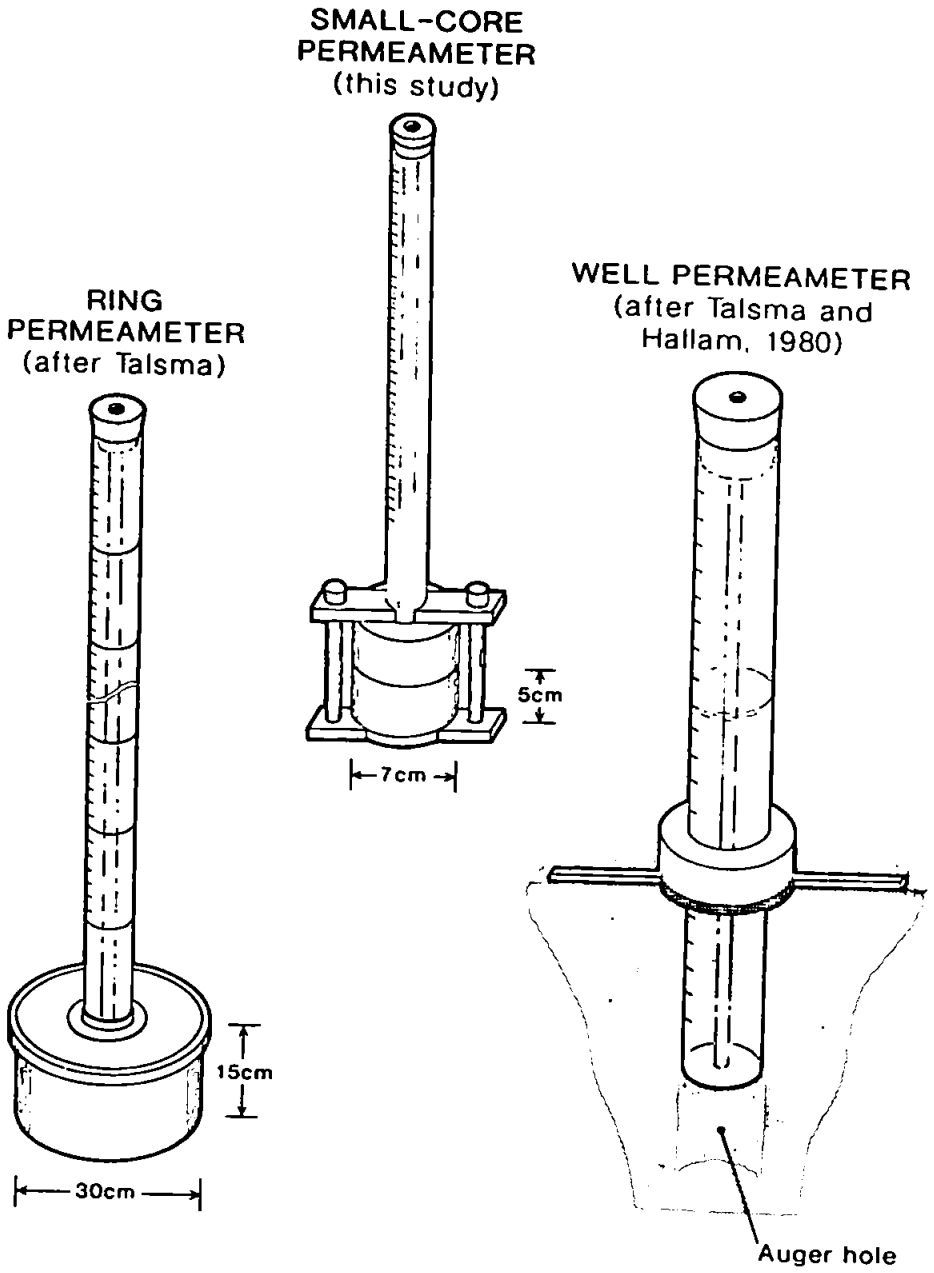

Figure 22. Three field permeameters.

4.4.6 Throughflow Trough Response.

Four troughs were inserted into the wall of a soil pit, located 20 m upslope of the forest drainage channel, and a further two troughs were installed within the drain channel itself (Figure 3). The water that flowed from each soil horizon, into these troughs was monitored to gain an estimate of lateral soil water movement within perched, saturated zones.

The measured discharges, were calibrated against piezometer-based fluxes, to account for the *artificial boundary-conditions* (Sections 3.5.3. and 8.3.1) created by digging a soil pit. (Ahuja and Ross, 1983; Knapp, 1973; Molchanov, 1960). An attempt was made to reduce the effect of these boundary conditions, by first, covering the exposed soil-face with a galvanized-steel wall, to reduce evaporation losses. Second, by using sloped fibre-glass troughs, to speed the movement of the water into the measuring devices; and third, by measuring the discharges with micro-tipping bucket devices (i.e. 6 ml per tip), to increase the precision of the timing. All of the tipping-buckets were datalogged with a *Mussel*® data-logger (Section 4.7.3). Other hillslope hydrological studies using throughflow troughs are shown within Table 12.

Table 12. Hydrological studies using throughflow troughs.

REFERENCE	NUMBER OF TROUGHS	TROUGH LENGTH (m)	RESEARCH SITE
Arnett (1974)	30	0.6	Caydale, Yorks, U.K.
Baloutsos (1985)	12	0.9	Lammermuir, Loth, U.K.
Beasley (1976)	41	2.2	Mississippi, U.S.A.
Chappell (this study)	5	1	Plynlimon, Powys, U.K.
Dunne and Black (1970a,b)	15	7.6-38.1	Sleepers River, VT, U.S.A.
Gilmour and Bonell (1979)	12	2	South Creek, QL, Aust.
Harr (1977)	1	nk	W10, H.J.Andrews Exp. Forest, OG, U.S.A.
Hursh and Hoover (1941)	2	2.4	Bent Creek, U.S.A.
Knapp (1970)	12	nk	Plynlimon, Powys, U.K.
Molchanov (1960)	various		various, U.S.S.R.
Mosley (1979, 1982)	52	1	Mawheraiti, Donald Creek, Camp Stream, New Zealand
Pilgrim *et al* (1978)	6	1.83	Stanford, CAL, U.S.A.
Selby (1973)	6	2	Otutira, New Zealand.
Stephens (unpubl.)	18	nk	Beddgelert Forest, Gwynedd, UK.
Ternan and Williams (1979)	36	1	Narrator Brook, Devon, U.K.
Trudgill *et al* (1984)	4	nk	Whitwell Wood, U.K.
Walsh (1980)	27	0.9	Palmas, Dominica
Wheater *et al* (1987)	9	0.5	Loch Chon, Dumfries and Galloway, U.K.
Weyman (1970, 1973)	6	1	East Twin Brook, Somerset, U.K.
Whipkey (1965)	5	2.4	Central States Forest, Ohio, U.S.A.

nk = not known

4.5. Summary of the Hydrometric Properties Measured.

A summary table showing all of the sampling sites for each hydrometric property within om the Tir Gwyn Experimental Catchments, is shown in Table 13.

Table 13. A Summary Table of all of the samples or sampling stations for each hydrometric property within the Tir Gwyn Experimental Catchments, UK.

PROPERTY	FOREST SITE	GRASSLAND SITE
PRECIPITATION-INPUT:		
Pg gross precipitation	-	3
Ps stemflow	10	-
Pt throughfall	17	-
SOIL MATRIX PROPERTIES:		
ρb bulk density	35	21
η porosity	12	14
SOIL MOISTURE CONTENT:		
θw gravimetric samples	23	7
θvn neutron moderation	17	6
θvr time-domain-reflectrometry	8	-
SOIL MOISTURE POTENTIAL:		
ϕ_cm manometer-tensiometer	41	16
ϕ_cb bourdon-gauge-tensiometer	2	2
ϕ_cs scanivalve-tensiometer	30	-
ϕ_ct transducer-mounted-tensiometer	3	-
ϕ_cp nested-piezometer	20	6
ϕ_cw logged-well	1	1
$\phi_c$gb gypsum-block	5	3
SPECIFIC MOISTURE CAPACITY:		
Cf field determination	18	14
Cl laboratory determination	12	14
SATURATED HYDRAULIC CONDUCTIVITY:		
K_sr ring permeameter	18	20
K_sc small-core permeameter	5	13
K_sw well permeameter	10	-
K_sp piezometer recovery test	3	2
DISCHARGE:		
Qt throughflow trough	5	-
Qw stream weir	3	1
Qf stream flume	1	1

4.6. Hydro-chemical Properties.

Hydro-chemical data werecollected and analysed both to *test* the predicted moisture fluxes, and be used within the predictions of the major solute pathways governing stream acidification. The results of the comparisons of ionic concentrations with the hydrometric analysis (Chappell *et al*, 1990) are summarized within Chapter 9.

Sampling: Water samples were collected from all of the components of the hydrological system, from precipitation input to streamflow output. All of the samples were collected over an 8 month period (11/11/1987 to 3/6/1988), throughout periods of very wet and relatively dry antecedent conditions. Emphasis was, however, given to sequential sampling throughout 2 *winter storms* and 3 *summer storms*.

Gross precipitation input was sampled using a large diameter (i.e. 60 cm) funnel located within the grassland. Throughfall beneath the forest canopy was sampled using a further 5 large diameter funnels (Section 4.3.2). Stemflow was collected from 3 trees, using spiral stemflow collars made from chemically inert materials (Reynolds and Stevens, 1987). Soil water samples were extracted from 9 *porous-cup-water-samplers* (Talsma *et al*, 1979; Stevens, 1981) augered into the A/E, B and B/C horizons of the forest hillslope (Figure 23). High-flow, 0.5 bar porous cups (*Soil Moisture Equipment Corporation* ®) were used to allow samples to be extracted every 2-3 hours during particular storm events (M. Hornung, pers.comm. 1987). All of the samplers were initially flushed out during 2 major storm events prior to the extraction of samples for chemical analysis.

Further soil water samples were removed from an unconfined borehole at the base of the forest hillslope (Figure 23). Stream-water was sampled at 12 locations downstream of the *upper drain weir* at the base of the forest hillslope (Figure23). A total of 288 samples were collected for analysis.

Analysis: Chemical analysis at the Institute of Terrestrial Ecology(NERC) Bangor Laboratories is summarized in Table 14.

Table 14. Techniques of chemical analysis used to determine the hydro-chemical properties at the Tir Gwyn Catchments.

PROPERTY	NUMBER OF SAMPLES	TECHNIQUE	REFERENCE
pH	288	potentiometerically	Neal and Thomas (1985)
Cl^-, SO_4^{2-}, NO_3^-, PO_4^- D.O.C	120	auto-analysis	Reynolds (1981, 1984)
K^+, Na^+, Mg^{2+}, Ca^{2+}, total Al^{3+}	275	atomic absorption spectrometry	Reynolds (1981)
monomeric Al non-labile monomeric Al	20	ion exchange fractionation	Driscoll (1984)
^{18}O	10	carbon dioxide gas* equilibration	Darling and Bath (1979)

* at the Riverside Laboratories, University of Georgia, GA, USA

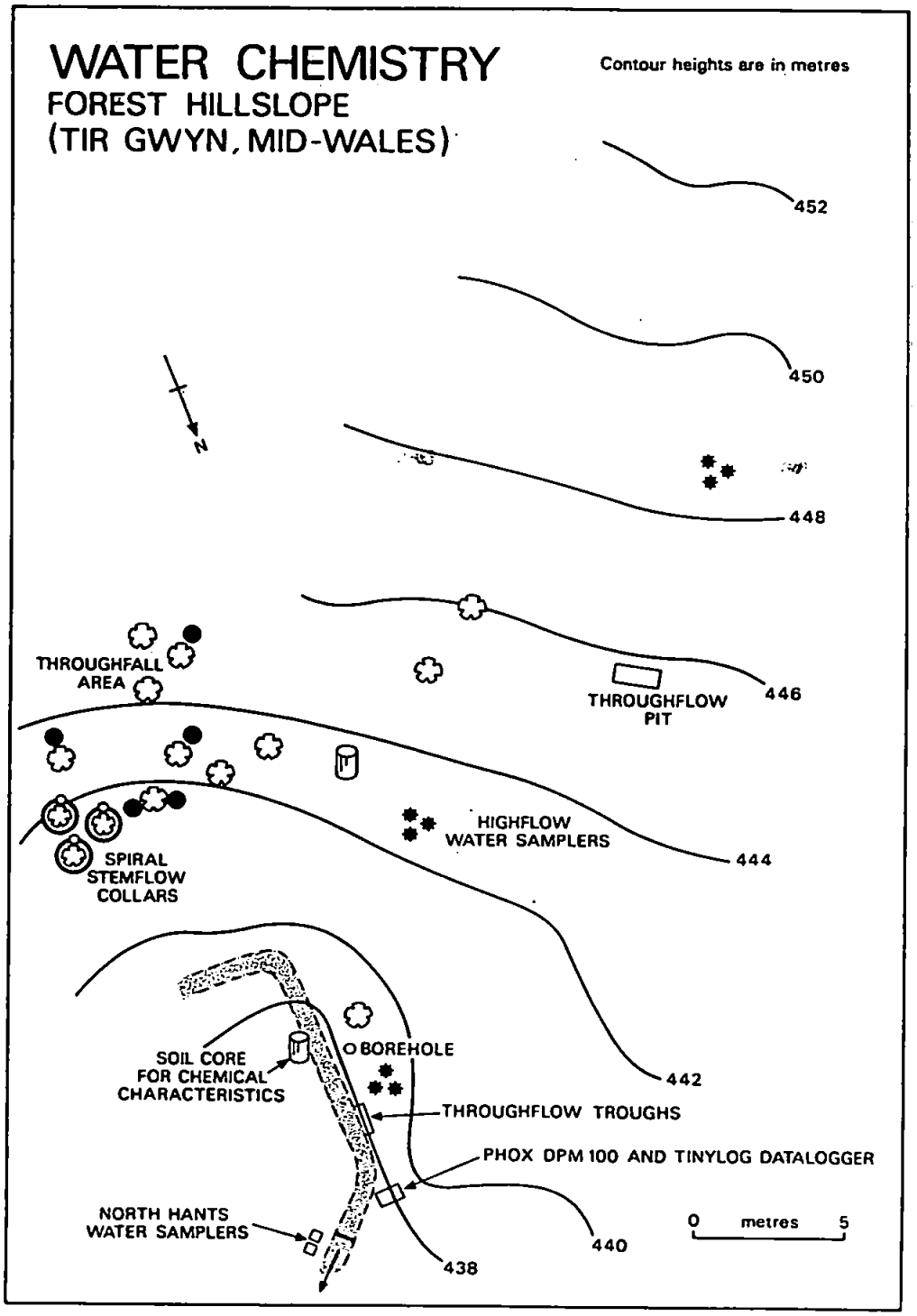

Figure 23. Locations within the forest hillslope system, where water samples were collected for chemical analysis.

4.7. Temporal Measurement Strategy.

A combination of manual-monitoring (Section 4.7.1), autographic or chart recording (Section 4.7.2), and datalogging (Section 4.7.3) was used to monitor the hydrological response of the forest and grassland catchments.

4.7.1. Manual Monitoring.

Readings from manometer-tensiometers, neutron probe ratescalers, and piezometers, were taken every 2-3 hours during major storm events. Antecedent conditions were monitored at least weekly.

4.7.2. Autographic Recording.

Three vertical chart-recorders, and three circular chart-recorders provided continuous records of streamflow at the six gauging structures (Figures 13 and 24). The *upper drain weir* and *upper stream weir* were equipped with *Institute of Hydrology Vertical Chart* recorders (Truesdale and Howe, 1977). The *lower drain weir* had a *Munro ®IH89* recorder, and the two trapezoidal flumes and *grassland weir* used *Negretti ®* pressure-bulb recorders. All of the charts were changed weekly. The chart recorders were installed primarily as a *back-up* for the electronic water-level-recorders, when the dataloggers failed.

4.7.3. Digital Logging.

A total of five dataloggers were used to continuously monitor precipitation input, capillary potential, throughflow tipping-buckets, and streamflow (Figure 24).

Golden River : Traffic Counter: A *Golden River ®Traffic Counter* was used to record the tips of a *Rimco ®* raingauge, prior to the use of a *Newlog ®*datalogger. The data was recorded on cassette tapes, which were then decoded at the research station.

Technolog : Newlog Programmable: A *Newlog* datalogger was programmed to record the time at which a 0.5 mm raingauge-bucket tipped. The precipitation data stored by the datalogger was transferred each month, onto an *Epson ®HX20* field-computer. At the research station, the data was transferred from the field-computer to an *IBM-PC ®compatible.*

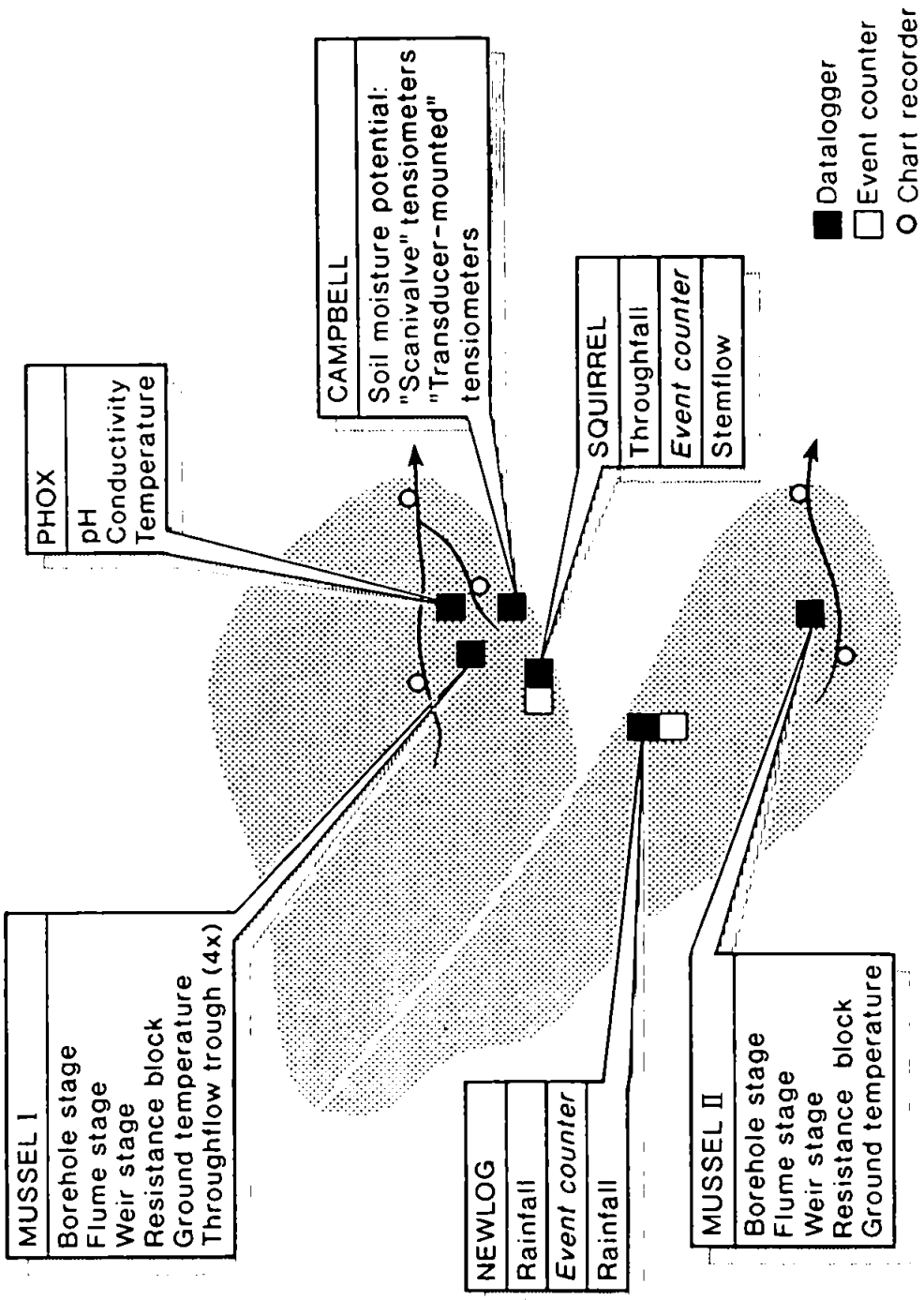

Figure 24. Autographic and digital recorders within the Tir Gwyn Experimental Catchments.

Campbell Instruments : CR10: The voltage output from the *SenSym* ®transducers connected to the tensiometer systems (Section 4.4.3), were excited (or *powered by*) and datalogged by a *Campbell* ®*CR10* logger. Three channels on the datalogger were used to record the output from the transducer-mounted tensiometers, every 2.5 minutes, and a fourth channel was used to monitor the output from the transducer connected to the *Scanivalve* ®tensiometer system. Each *Scanivalve* tensiometer was exited and logged every hour. The voltage measurements from the transducers were stored on *storage-modules*, which could be exchanged, and then taken to be *down-loaded* onto the *IBM-PC* ®*compatible*..

Computing Techniques : Mussel loggers: Two *Mussel* loggers were loaned to the research project, by the *NERC Automatic-Weather-Station-Pool.* The logger sited within the forest monitored the water-level within the well, the resistance across two gypsum blocks, the temperature of a ground-level thermistor (Section 6.3.2), the stage within the weir and flume, and the tipping-buckets attached to four throughflow troughs. These same inputs were logged by the logger within the grassland site, except that there were no throughflow tipping-buckets (Figure 24). Both loggers monitored the inputs every 10 minutes, and recorded the values on separate *stores*. These stores were then decoded using both a *IBM-PC* ®*compatible* and a *Digital PDP-11.* ®

4.8. Quality Control.

All of the field-monitored data were stored in a standardized format, within a *PC-based data-base-management-system* (DBMS). Descriptive statistics and graphics were applied to the raw-data immediately after collection to remove incorrect encoding, and to check for instrument failure.

The accuracy of all measured data, was verified by comparison with established data from other studies (Sections 5.2.1., 5.2.2., 5.2.3., 6.2.1., 6.2.2., 7.2., 7.4.1., 7.4.8., 8.2.1., 8.2.2. and 8.3.2), and by a number of experiments designed to test the performance of the instruments and techniques used (Sections 5.2.1., 6.2.1., 6.3.2., 7.3.1., 7.4.1., 7.4.3., 7.4.4., 7.4.6., 7.4.7., 8.2.1., 8.2.2., 8.2.3., 8.3.2. and 8.3.3).

CHAPTER 5.

Hillslope and Catchment Rainfall-Runoff.

5.1 Introduction.

The *rainfall-runoff response* of a hillslope or catchment is simply the streamflow response resulting from a precipitation input; the internal-state of the hillslope or catchment is not required in the calculation, and is usually not considered (Section 1.4.1). The principal reasons for examining this relatively simple external or black-box response in addition to the more complex internal response of the instrumented hillslopes, can be summarized as:

1. to enable the rates of stemflow, throughfall, wetted-canopy-evaporation and transpiration to be calculated and compared with published values (Sections 2.2.1., 2.2.2., 2.2.4., 5.3.2., 5.3.3. and 5.3.5),
2. to compare the timing and volume of streamflow generation within a forest and a grassland catchment (Sections 5.2.3, and 5.3.4),
3. to place the detailed internal and external response of the forest hillslope within the context of *catchment hydrology* (Sections 5.3.4. and 5.3.5), and
4. to provide the *actual* streamflows generated by the forest hillslope and the whole forest and grassland catchments, to verify the fluxes *predicted* by the internal-state calculations (Section 5.3.4).

Those hydrological properties external to the primary hillslope-scale are the precipitation *input*, and the evapo-transpirational and streamflow *outputs*. The response of these properties at the scale of the grassland catchment, forest catchment, forest drain-catchment and forest hillslope (Section 4.2) is examined over two temporal scales: *long-term* 6 to 12 month periods (Section 5.2) and short-term *storm-periods* (defined in Section 5.3.1) ranging from 3 to 41 days (Section 5.3).

5.2. Long-Term Rainfall-Runoff.

The long-term rainfall-runoff response of the research sites was developed from 12 months of gross-precipitation data (Section 5.2.1.2), 7.5 months of net-precipitation data (Section 5.2.1.3), and 6-11.5 months of streamflow data (Section 5.2.3). In detail, this longer-term rainfall-runoff was calculated in addition to the storm-period rainfall-runoff to:

1. allow the errors in the measurement of precipitation to be calculated (Section 5.2.1),
2. allow the precipitation records to be calibrated against longer Institute of Hydrology records, to enable the Tir Gwyn records to be extended (Section 5.2.1),
3. compare the total volume and spatial variability of the gross-precipitation within the grassland, with that of the throughfall and stemflow beneath the forest canopy (Section 5.2.1),
4. compare the volumes of throughfall and stemflow beneath the Tir Gwyn forest canopy, with values cited for other Sitka spruce (*Picea sitchensis* , Bong. Carr) canopies within the UK (Section 5.2.1),
5. reduce the considerable errors within the calculation of the evapo-transpiration rate from catchment water balances (Section 5.2.2),
6. allow evapo-transpiration rates developed within the forest and grassland catchments (0.11 and 0.12 km^2, respectively) to be compared with the annual rates calculated for the much larger Institute of Hydrology, Wye (10.55 km^2) and Severn (8.70 km^2) catchments (Section 5.2.2),
7. place the hydrological response of the Tir Gwyn catchments within the context of other small catchment studies, by a comparison of the streamflow regimes (Section 5.2.3)
8. compare the evapo-transpiration rate calculated for the forest catchment with that of the grassland catchment (Section 5.2.4).

5.2.1. Long-Term Precipitation Input.

Measurement Errors and Calibration.

Three raingauges were sited within the grassland catchment (Section 4.2.1.1.). The tipping-bucket *Rimco* ®gauge installed within a grid-covered pit, continuously monitored the precipitation input. A second *Rimco* ®gauge and a storage gauge both sited at the *British Standard* 12" height, were used to identify the measurement errors implicit to the primary gauge.

During the 4 month period 12 February to 10 June 1988, the *pit-Rimco* received 492.5 mm, the *above-ground-Rimco* received 499.0 mm, and the above-ground-storage gauge received 532.25 mm.

The difference between the two *Rimco*® gauges, one with its orifice at ground-level, the other with it at a height of 12", was insignificant (1.2 percent). A systematic error within measurements of the above-ground gauge, resulting from its exposure to wind (Rodda, 1971; Section 4.3.1)was, therefore, not observed.

In contrast, the two *Rimco* ®gauges caught approximately 7 percent less precipitation than the storage gauge. This is attributed to errors with the tipping-bucket technique for rainfall measurement (Plinston and Hill, 1974). The precipitation records monitored by the datalogged *Rimco* ®gauge were, therefore, multiplied by 1.075 percent.

In order to extend the rainfall records monitored within the Tir Gwyn grassland catchment, the precipitation totals for the period 31/1/88 to 24/5/88 monitored by the Tir Gwyn storage gauge were compared with those monitored by the storage gauge at the Institute of Hydrology, Cefn Brwyn automatic-weather-station.

During this period the Tir Gwyn storage gauge (alt. 430 m) received 782.75 mm of precipitation and storage-gauge at the Cefn Brwyn automatic-weather-station (alt. 320 m) received 651.5 mm of precipitation. The Tir Gwyn grassland, therefore, received 17 percent more rainfall than that recorded by the Cefn Brwyn gauge. The difference can be attributed to the 100 mm difference in precipitation associated with a 100 m difference in altitude (Clarke *et al*, 1973; J. Hudson, pers. comm. 1987; Newson, 1976a). As the temporal distribution of rainfall is generally similar for all gauges within the Plynlimon catchments (E. O'Connell, pers. comm. 1988), the precipitation record for the Tir Gwyn grassland catchment could be extended back to 10 June 1987, the beginning of the hydrological monitoring, by scaling against the Cefn Brwyn records.

Long-term Gross-Precipitation Input.

The total precipitation input to the research sites for the 12 month period 10 June 1987 to 10 June 1988 was *2629 mm.* Only 4.8 percent (127 mm) of the precipitation was in the form of snowfall.

No marked seasonality in the precipitation monitored at the Cefn Brwyn automatic-weather-station was observed (Figure 25). The maximum precipitation intensities recorded are shown within Table 15.

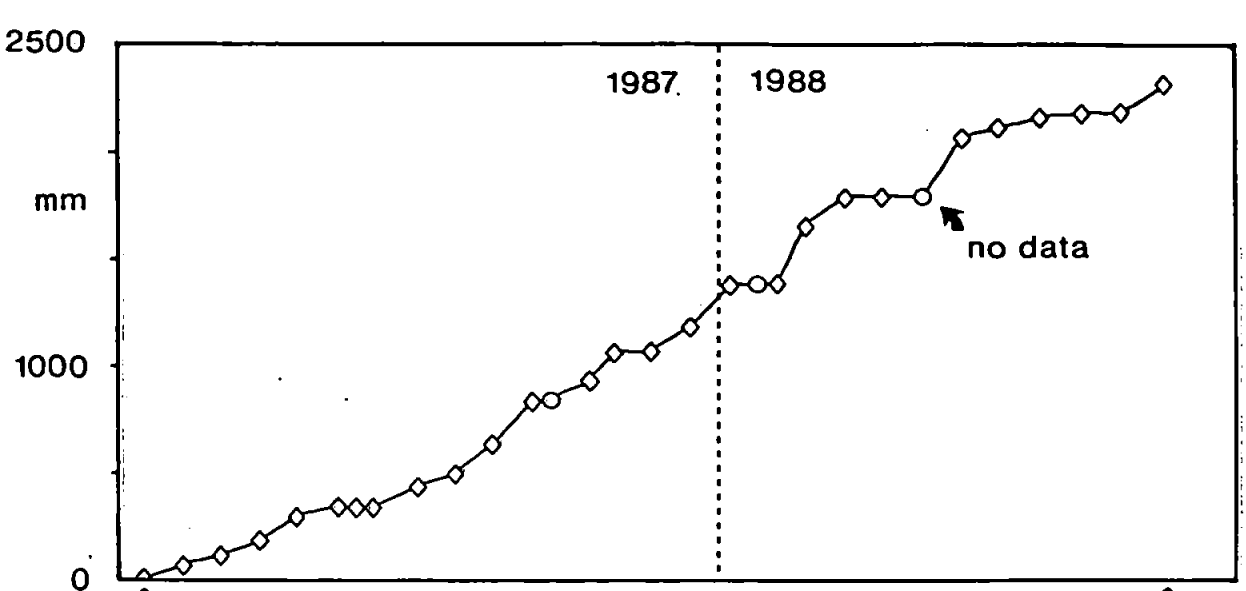

Figure 25. Cumulative precipitation between 8 June 1987 and 8 June 1988.

Table 15. Maximum precipitation intensities monitored at the Tir Gwyn and Cefn Brwyn raingauge sites, between 10 June 1987 and 10 June 1988.

Integration Period	Intensity
MONTH	320 mm $month^{-1}$
DAY	127 mm day^{-1} (snow)
HOUR	10 mm hr^{-1}
5 MINS	3 mm 5 $mins^{-1}$

Long-Term Net-Precipitation Beneath the Forest Canopy.

The total volume of throughfall monitored over a 7.5 month period between 9 November 1987 and 24 June 1988, was 883.6 mm. This is equal to 56 percent of the gross-precipitation (i.e. 883.6/1585 x 100) monitored within the grassland.

The total volume of stemflow monitored over the same period, was calculated for a 10 x10 m plot containing a distribution of 25 Sitka spruce (*Picea sitchensis*, Bong. Carr.) trees (Section 4.3.2). Stemflow accounted for 5 percent (78 mm) of the 1585 mm gross-precipitation, i.e.

Total volume of stemflow down 7 representative trees, during the period 9/11/87-24/6/88 = 2,176,800 cm^3

Total number of trees within the 10 x10 m plot = 25

Total area of the 10 x 10 m plot in cm^2 = 1,000,000 cm^2

Mean depth of stemflow

$$= \frac{2{,}176{,}800\ cm^3 \cdot (25/7)}{1{,}000{,}000\ cm^2}$$

$$= 7.8\ cm = 78\ mm$$

The total net-precipitation is, therefore, equal to 61 percent (i.e. 883.6 mm + 78mm) of the 1585 mm gross-precipitation, with throughfall accounting for 92 percent of its volume.

The 56 percent throughfall and 5 percent stemflow totals monitored at the Tir Gwyn hillslope are, therefore, comparable with the volumes monitored by Gash and Stewart (1977) and Law (1957) within similar thinned plantations (Table 16). Thinning would appear to reduce the relative volume of stemflow by some 67-90 percent (Table 16).

Table 16. Throughfall and stemflow percent of gross-precipitation within the thinned Tir Gwyn plantation, and other pine plantations within the U.K.

STUDY	Species	Stand Age	Thinning	Throughfall	Stemflow
Chappell (this study)	1	45	*thinned*	56	5
Gash and Stewart (1977)	2	45	*thinned*	67	1.6
Law (1956)	1	-	*thinned*	60	7
Ford and Deans (1978)	1	14	*un-thinned*	43	27
Gash *et al* (1980)	1	43	*un-thinned*	56	28
Rutter (1963)	2	18	*un-thinned*	48	16

1 SITKA SPRUCE (*Picea sitchensis*) 2 SCOTS PINE (*Pinus sylvestris*)

Comparative Spatial Variability of Rainfall, Throughfall and Stemflow.

As precipitation falls upon a forest canopy it is either evaporated back to the atmosphere or re-directed down needles, branches and stems. Differences in the structure of individual tree canopies will, therefore, affect the distribution and rate of movement of the intercepted precipitation. The spatial variability of the precipitation input to the soil increases as the vegetation concentrates water movement along particular branches and stems (Table 17).

Table17. The spatial variability of precipitation in the open and beneath the coniferous forest at Tir Gwyn.

PATHWAY	RANGE (mm)	DIFFERENCE ABSOLUTE (mm)	DIFFERENCE PERCENT (%)
OPEN	1575-1595	21	1.2*
THROUGHFALL	732-1127	395	35
STEMFLOW	20.5-183	162	88

* approximated from the difference between the 2 Rimco gauges within a 10x10m plot.
RANGE = Range of total volume monitored 9/11/87 to24/6/88 *for an equivalent 10x10m plot*.
ABSOLUTE DIFFERENCE = Absolute difference of maximum and minimum recorded volumes (max-min).
PERCENT DIFFERENCE = Percentage difference of maximum and minimum recorded volumes (((max-min)/max)x100).

Although the stemflow down a distribution of trees has the largest relative range in value (i.e. 88 percent difference), the variability in the throughfall is volumetrically the greatest (i.e. 395 mm absolute difference). This implies that the *average* hydrological response of a *whole hillslope* is more sensitive to throughfall variability rather than stemflow variability.

If the stemflow volume is integrated over the basal area of an individual tree (a circle of approx. 50 cm dia.), then the flux of stemflow into the soil at the base of an individual tree-stem, is almost 2 times that of the throughfall into the soil away from the tree bole, i.e.

Total volume of stemflow down 7 representative trees, during the period 9/11/87-24/6/88	= 2,176,800 cm^3
Mean Volume per tree	= 310,971 cm^3
Basal area of an individual tree	= 1,964 cm^2
Stemflow per unit basal area	$= \frac{310{,}971\ cm^3}{1{,}964\ cm^2}$
	= 158 cm = 1580 mm
Stemflow : throughfall ratio	= 1580 mm / 883.6 mm
	= 1.8

Although stemflow accounts for a relatively small percent of the total inflow into a hillslope, and hence its spatial variability has little impact upon the *average hillslope input*, high rates of inflow close to individual trees (i.e. 1.8 x throughfall rates) might significantly alter soil-water-pathways if sub-surface flow were to increase in a positive, non-linear manner with rate of inflow. Sub-surface flow is generally dominated by the dynamics of hydraulic conductivity rather than potential gradient (Sections 7.4 and 7.5). As there is a positive, non-linear increase in the relative hydraulic conductivity with increasing soil moisture content (Figure 67; Section 7.4.9), localized stemflow inputs may have a disproportionately large impact upon sub-surface flow (Sections 6.3.6 and 6.4).

A comparison of the total throughfall collected by each of the 12 gauges, with the canopy-cover above each gauge failed to show any trend (Figure 26a). It is, therefore, suggested that the variability in the throughfall, is dominated by the spatial distribution of *drip points* (Voigt, 1960) at which needle and branch flow concentrate.

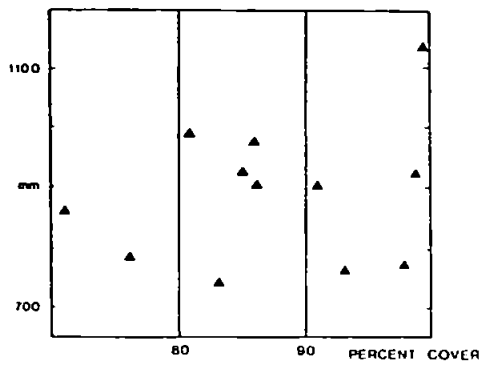

Figure 26a. Canopy cover, plotted against the total throughfall collected.

5.2.2. Long-Term Evapo-transpiration and Catchment Storage Change.

The *actual* evapo-transpirational (ET_a) losses from both upland grasslands and coniferous forests at Plynlimon are most accurately predicted by either lysimeter or catchment water-balances (i.e. mass budgets: Brutsaert, 1982; Calder, 1976; Hudson, 1988; Institute of Hydrology, 1988). Other quasi-physical techniques such as the Penman-Monteith method must be *fitted* to known evapo-transpiration rates (Morton, 1984; Freeze and Harlan, 1969). Cost precluded the use of natural lysimeters at Tir Gwyn. A water-balance technique:

$$\underset{\substack{\textit{evapo-}\\\textit{transpiration}}}{ET_a} = \underset{\textit{precipitation}}{P} - \underset{\textit{runoff}}{R} - \underset{\substack{\textit{change of}\\\textit{storage}}}{dS_t}$$

was, therefore, used to estimate the the evapo-transpiration losses from the grassland and forest catchments. Unfortunately, the water-balance technique is also very approximate within this study, because of:

1. the relatively short monitoring period of less than12 months, which means that changes in catchment storage could be large (Gregory and Walling, 1973; Hudson and Leeks, 1989).
2. the possibility that some of the catchment-outflow may pass beneath the gauging structures as *shallow under-flow* or *deep seepage* (Linsley *et al*, 1988).

Within the forest catchment, the dominant wetted-canopy-evaporation component of the ET-loss can, however, be calculated quite accurately by subtracting the throughfall plus stemflow from the gross-precipitation (see below).

Long-Term Evapo-transpiration from the Grassland.

The *potential* evapo-transpirational (ET_p) loss from the grassland estimated using the empirical Thornthwaite method (Section 4.3.3), was 592 mm for the period 1 July 1987 to 30 June 1988. This is equivalent to 22.5 percent of the 2629 mm gross precipitation. Seventy-seven percent of the annual ET_p losses occurred during the summer months (455 mm: April to September) compared with the winter months (136 mm: October to March).

During the periods 9-27 November 1987, and 23 January - 26 June 1988 the grassland catchment generated 25 percent less streamflow output (935 mm) compared to precipitation input (1243 mm). Allowing for anomalies arising from the shorter time period

and the possibility of some loss to deep seepage, such an actual evapo-transpirational (ET_a) loss of 25 percent is not too dissimilar from a 15 percent ET_a loss for the period 1 July 1987 to 30 June 1988 calculated for the neighboring Institute of Hydrology, Wye catchment (data from Institute of Hydrology, 1989). A mean annual ET_a loss from the Wye catchment of 16 percent was calculated from an 8 year water balance (Hudson, 1988). Interestingly, the *actual* evapo-transpiration rate (ET_a) from the Tir Gwyn water-balance is very similar to the potential evapo-transpiration rate (ET_p) calculated by the Thornthwaite method.

The individual wetted-canopy-evaporation and transpiration components of the ET_a loss have not been calculated for either the Tir Gwyn or Wye grassland catchments.

Long-Term Evapo-transpiration from the Forest.

The average evapo-transpiration loss (and possibly catchment storage change) during the periods 9-27 November 1987 and 23 January - 26 June 1988 was 47 percent (582 mm) of the 1243 mm gross-precipitation. This value of 47 percent is considerably higher than the 30 percent evapo-transpiration loss calculated for the Institute of Hydrology, Severn catchment over an 8 year period, from 1974 to 1981 (Hudson, 1988). This value is weighted to take account of the 34 percent of grassland cover within the upper reaches of the *afforested* Severn catchment (Institute of Hydrology, 1976).

The high ET_a value for the Tir Gwyn forest catchment relative to the average value for the Severn catchment, could have resulted from: (1) elevated levels of ET_a at the windward edge of a forest plantation (I. Wright, pers. comm. 1987), (2) the use of anomalous periods (only 175 days in total), (3) an error in the ET_a calculation caused by a large increase in catchment storage or losses to deep seepage (see below).

Total evapo-transpiration loss from forest stands can be divided into (i) the evaporational losses from wetted canopies during precipitation events, and (ii) *continuous* biological transpiration and soil evaporation.

Evaporation from Wetted Conifer Canopies : During the 7.5 month period 9 November 1987 to 24 June 1988, the forest canopy intercepted and subsequently evaporated 39 percent (623 mm) of the incident precipitation (i.e. 1585 mm - 883.6 mm - 78 mm, Section 5.2.1).

Conifer Transpiration, Forest Soil Evaporation and Catchment Storage : The biological transpiration rate (plus soil evaporation and changes in catchment storage) within the forest catchment can be *crudely estimated* by subtracting the interception loss from the total evapo-transpiration losses and storage changes.

During the periods 9-27 November 1987 and 23 January - 26 June 1988, the percentage of rainfall (1243 mm) not generating runoff was 47 percent (582 mm), and the percentage of evaporated rainfall was 39 percent ({39x1243}/100 = 485 mm). The biological transpiration rate (plus soil evaporation and changes in catchment storage) was, therefore, 8 percent (i.e. 47 - 39 percent) of the gross-precipitation. This transpirational rate lies in between the figure of 5 percent (of gross-precipitation), calculated from an 8 year water balance for the neighbouring, afforested Severn catchment (Hudson, 1988), and the figure of 17 percent (of gross-precipitation), calculated from a 84 m^2 lysimeter within the same catchment (Calder, 1976). A large amount of uncertainty must inevitably surround the value of 8 percent, as all of the errors within the water balance calculation are compounded within this term.

A biological transpiration rate of 8 percent of gross-precipitation if accurate, is equal to 13 percent of the net-precipitation beneath the Tir Gwyn forest canopy (i.e. {8/61}x 100, Section 5.2.1).

5.2.3. Long-Term Streamflow Output.

Stream-Gauge Calibration.

The four V-notch weirs within the Tir Gwyn catchments (Figure 13; Section 4.2.3) were calibrated by volumetric gauging (British Standards Institution, 1965b), and the two trapezoidal flumes were calibrated by salt-dilution gauging (Littlewood, 1986). The field-calibrations for the weirs were indistinguishable from the *British Standard* ratings (British Standards Institution, 1965a):

Upper Drain Weir (sharp 90° V-notch)	=	$1.38H^{2.5}$
Lower Drain Weir, Grassland Weir (sharp 1/2 90° V-notch)	=	$0.69H^{2.5}$
Forest Stream Weir (compound sharp 90° V-notch and rectangular)	=	$1.38H^{2.5}$ (V-notch) $1.86BH^{1.5}$ (rectangular)

Q = discharge (dim. cumecs); H = head (dim. m)

B = throat width (dim. m)

The field-calibrations for the two flumes varied slightly from the *standard* calibration developed by the *Forth River Purification Board* (FRPB) and *North of Scotland Hydro-Electric Board* (HEB; unpublished report):

Standard FRPB/HEB calibration (for FRPB small 88 l s^{-1} flume)	=	$1.10028H^{2.12}$
Grassland Flume (field-adjusted calibration)	=	$1.10028H^{1.93}$
Forest Flume (field-adjusted calibration)	=	$1.10028H^{1.88}$

Q = discharge (dim. cumecs); H = head (dim. m)

Long-Term Catchment Streamflow Regime.

The forest catchment generated a lower mean annual discharge and lower peak storm-discharges in comparison with the grassland catchment.

During the period 7 July 1987 to 26 June 1988, the forest catchment generated an average 0.007 cumecs (7 l s^{-1}) of streamflow, while the grassland catchment generated and average 0.012 cumecs (12 l s^{-1}).

The snow event (storm No.7) produced a peak discharge of 0.042 cumecs (42 l s^{-1}) within the forest, and 0.102 cumecs (102 l s^{-1}) within the grassland. Rainfall events Nos. 3,4,8,9 and 10 produced peak discharges ranging from 0.005 to 0.045 cumecs (5-45 l s^{-1}) within the forest and 0.018 to 0.050 cumecs (18-50 l s^{-1}) within the grassland. The streamflow regimes observed within the Tir Gwyn catchments are similar to those recorded during a number of other hillslope hydrological studies (Table 18).

For the calculation of the rainfall-runoff ratio, the streamflow (runoff) is standardized to that of the UK Surface Water Archive (e.g. Institute of Hydrology, 1989), i.e. the equivalent depth of water in millimetres over the catchment area.

During a 6 month period (9-27 November 1987 and 23 January - 26 June 1988), the two Tir Gwyn catchments received approximately 1243 mm gross-precipitation, and yet 29 percent more runoff per unit area, was generated by the grassland basin (935 mm), compared with the forest basin (661 mm).

Table 18. Cited ranges of stream discharge recorded during comparable hillslope hydrological studies.

REFERENCE	CATCHMENT	CITED RANGE OF STREAM DISCHARGE ($l\ s^{-1}$)
Anderson and Burt (1978)	Bicknoller Coombe, UK.	2-45
Anderson and Kneale (1980)	Winford, UK.	0.2-20
Finlayson (1977)	East Twin, UK.	5-50
Taylor (1982)	Telford, Canada	20-140
Weyman (1974)	East Twin, UK.	2-35

5.2.4. Long-Term Catchment Rainfall-Runoff Ratios.

The volume of precipitation which ultimately generates streamflow or *runoff* is known as the *rainfall-runoff ratio* (Hino *et al*, 1987), *runoff coefficient* or *yield*. The average rainfall-runoff ratio for the periods 9-27 November 1987 and 23 January - 26 June 1988 is **0.75** (i.e. 935 mm / 1243 mm) within the grassland catchment, and **0.53** (i.e. 661 mm / 1243 mm) within the forest catchment.

5.3. Storm-Period Rainfall-Runoff.

The rainfall-runoff or external-state behaviour of the forest catchment is compared with that of the grassland catchment for individual *storm hydrographs* to examine:

1. the impact of different precipitation volumes upon streamflow generation within the two catchments (Section 5.3.5),
2. the timing or rates of the stream response to differing precipitation inputs (Sections 5.3.4., and 5.3.5),
3. the impact of different antecedent conditions upon streamflow volumes (Sections 5.3.4 and 5.4.5).

The external-state behaviour of the forest hillslope is also determined for particular storm-periods to:

1. provide the streamflow outputs (Section 5.3.4) to compare with the response of each internal-state, hydrological variable (Section 6.3.3. and 6.3.4) and parameter (Section 7.4.9), and with the streamflows predicted by the internal- state calculations (Sections 8.2.1. and 8.2.2)
2. provide the net-precipitation inputs (Section 5.3.2. and 5.3.3) for the numerical simulations (Sections 8.3.2. and 8.3.3),
3. add to the understanding of the internal-state response of the forest hillslope (Chapters 6, 7, and 8) by the examination of the external-state response of the hillslope (1,480 m^2) , drain micro-catchment (2,680 m^2) and 110,000 m^2 (0.11 km^2) forest catchment (Sections 5.3.4., 5.3.5. and 5.4; Bren, 1978), and
4. enable the detailed, internal-state response of the forest hillslope to be related to responses observed at the larger catchment scales to allow generalizations to be made. (Sections 5.3.4., 5.3.5., and 5.4.).

5.3.1. Storm-Period Definition.

A *storm-period* is defined a period beginning with 1 to 2 days of heavy rainfall (i.e. > 20 mm) within an *inter-storm period*, and ending with the streamflow returning to that prior to the storm-period (Tables 19 and 20; Linsley *et al*, 1988). The start of rise in the storm hydrographs within each stream is always synchronous with this initial rainfall response.

Storm-period No. 7 begins before storm No. 6 streamflows recedes to the initial condition, and ends before the complete recession of storm No.7 streamflows. This was done to separate the streamflow response to a single, 127 mm snow-event from the responses to rainfall events.

Table 19. Storm and inter-storm periods for grassland catchment, during the field-season 6 September 1987 to 26 June 1988.

storm period	1	6-8 September 1987
	2	7-22 October 1987
	3-4	9-27 November 1987
	5-6	15 December 1987-22 January 1988
	7	23-27 January 1988
	8	31 January-7 February 1988
	9	10 March-19 April 1988
	10	28 May -26 June 1988
inter-storm period	1-2	7 September-6 October 1987
	2-3	23 October-8 November 1987
	8-9	8 February-9 March 1988
	9-10	20 April-27 May 1988

Table 20. Duration of storm periods monitored at each stream gauging structure (days).

Storm	forest flume	grassland flume	grassland weir	upper-drain-weir
3-4	21	19	19	22
7	5.2	4.2	4.2	10
8	6	6.5	6.5	>10
9	43.5	40.5	31.5	44
10	26	28	23.5	>>30

5.3.2. Storm-Period Precipitation Input.

Storm-Period Gross-Precipitation Input.

The precipitation totals monitored during individual *storm periods*, are presented within Table 21. The end of the storm period for rainfall was standardized to the return to the antecedent streamflow within the grassland flume. Although the return to the antecedent condition within the other gauging structures was up to a maximum of 9 days different from that within the grassland flume (Table 20), very little precipitation was monitored within those times when some gauging structures had stream discharges greater than those prior to the storm, and others had less.

Table 21. Storm event gross-precipitation : Tir Gwyn experimental catchments, mid-Wales, U.K.

STORM No.	PERIOD	PRECIPITATION TYPE	VOLUME (mm)	mean° (mm day^{-1})
1	6-8 Sept. 1987	*rainfall*	26*	9
2	7-22 Oct. 1987	*rainfall*	352*	22
3-4	9-27 Nov. 1987	*rainfall*	262	14
5-6	15 Dec. 1987-22 Jan. 1988	*rainfall*	383*+	10
7	23-27 Jan. 1988	*snow*	127	25
8	31 Jan.-7 Feb. 1988	*rainfall*	117	15
9	10 Mar.-19 Apr. 1988	*rainfall*	384	9
10	28 May -26 Jun. 1988	*rainfall*	109	4
8-9 (inter-storm-period between storms 8 and 9)			146	5
9-10 (inter-storm-period between storms 9 and 10)			98	3

mean° mean precipitation per day over the storm period
* calibrated from Cefn Brwyn AWS raingauge
+ incomplete hydrograph recession

5.3.3. Storm-Period Evapo-transpiration and Catchment Storage.

Storm-Period Evapo-transpiration and Catchment Storage within the Grassland Catchment.

The evapo-transpiration (ET_e) and catchment storage budget within the grassland catchment ranged from a *catchment loss* equivalent to 42 percent of the gross-precipitation during the period in late-spring between storm events 9 and 10, to a *catchment addition* equivalent to 132 percent of the gross-precipitation during the winter period between events 8 and 9 (Table 22).

Table 22. Evapo-transpiration losses plus catchment storage changes during selected storm and 'inter-storm' periods, for the Tir Gwyn grassland catchment.

STORM EVENT No.	3-4	7(snow)	8	9	10
ET_e (+dS)	**16%**	**22%**	**27%**	**3%**	**8%**
INTER-EVENT No.	8-9	9-10	NOTE: a negative number equals an increase in catchment storage		
ET_e (+dS)	**-32%**	**42%**			

Storm-Period Evapo-transpiration from the Forest.

The evapo-transpirational (ET_e) and storage losses from potential streamflow within the forest catchment were as small as 24 percent during storm event 3-4, and as large as 76 percent during the dry period in late-spring between storm events 9 and 10 (Table 23). Similarly large intra-annual fluctuations in the evapo-transpirational and storage losses have been observed within the Institute of Hydrology, Severn and Wye catchments (Hudson, 1988). As there is a good correlation between the the rainfall and runoff volume for each storm-period (R^2 86-91 percent) these fluctuations in the difference between the rainfall and runoff would appear relatively accurate.

Table 23. Evapo-transpiration losses plus catchment storage changes during selected storm and 'inter-storm' periods, for the Tir Gwyn forest catchment.

STORM EVENT No.	3-4	7(snow)	8	9	10
ET (+dS)	**24%**	**40%**	**51%**	**50%**	**58%**
INTER-EVENT No.	8-9	9-10			
ET (+dS)	**55%**	**76%**			

Forest Interception : The interception losses during 11-42 day integration periods within 1988, varied between 9 and 85 percent (Figure 27). The two storm periods No 8 (28 January - 11 February 1988) and No 9 part 2 (29 March - 19 April 1988) have very high interception losses (Figure26b), which are probably related to the very windy conditions which prevailed during those periods.

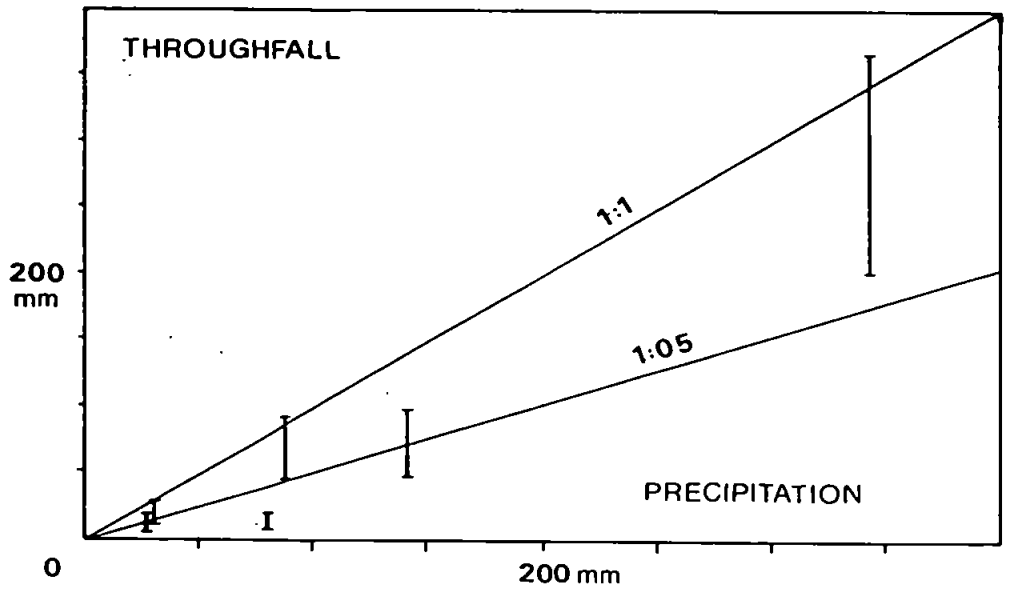

Figure 26b. Interception losses from the Sitka spruce (*Picea sitchensis*, Bong Carr.) stand at Tir Gwyn, during 6 integration periods between 9 November 1987 to 24 June 1988.

5.3.4. Storm-Period Streamflow.

Forest versus Grassland Catchment Storm-Period Durations.

During the winter-spring the duration of the storm-period streamflow was 7-10 percent greater within the forest catchment compared with that in the grassland catchment (Tables 20 and 24). During the dry summer period, however, the situation is reversed, with the grassland maintaining storm-period streamflows for 8 percent longer (Tables 20and 24). The single snowfall event resulted in a 19 percent greater storm period within the forest catchment (Table 24).

Table 24. The difference in storm-period streamflow duration between the forest and grassland catchments.

STORM EVENT		DAYS	PERCENT OF STORM PERIOD
3-4	*early winter*	+ 2	10
7	*winter snowfall*	+ 1	19
8	*late winter*	+ 0.5	8
9	*spring*	+ 3	7
10	*summer (dry period)*	- 2	8

+ = forest > grassland - = grassland > forest

Storm-Period Catchment Streamflow Volumes.

The grassland catchment generates more runoff than the forest catchment during both storm-periods and inter-storm periods (Table 25). The difference in runoff volumes is, however, very variable ranging from 19-180 mm or 9-66 percent.

Table 25. Runoff generated during storm and inter-storm periods within the forest and grassland catchments.

PERIOD	Forest Flume (mm)	Grassland Flume (mm)	Difference absolute (mm)	Difference percent (%)
storm 3-4	200	219	19	**9%**
storm 7	76	99	23	**23%**
storm 8	57	85	28	**33%**
inter 8-9	66	19	3127	**66%**
storm 9	192	372	180	**48%**
inter 9-10	24	41	17	**42%**
storm 10	46	>100	>54	**>54%**

Antecedent and Peak Catchment Storm-Period Discharges.

Based upon the data from storm events Nos. 3,4,7,8,9 and 10, the forest stream had on average a 32 percent lower antecedent storm discharge and a 41 percent lower storm peak discharge, when compared with the grassland stream (Table 26).

Table 26. The antecedent and peak storm discharges monitored at the forest flume and grassland flume stream gauging sites.

	DISCHARGE (mm)			
STORM No.	FOREST STREAM *(forest flume site)*		GRASSLAND STREAM *(grassland flume site)*	
	Antecedent	Peak	Antecedent	Peak
3	0.17	0.80	0.15	1.15
4	0.24	0.92	0.34	1.24
7	0.19	1.39	0.31	3.00
8	0.20	0.56	0.28	1.06
9	0.03	1.10	0.11	1.42
10	0.01	0.22	0.04	0.52

Forest Hillslope versus Catchment Storm-Period Streamflow.

The artificial drainage channel which drains the instrumented forest hillslope (Figures 3 and 13) has an ephemeral streamflow regime. The channel was completely dry during the summer months of both 1987 and 1988. Between storm event No. 1 (6-8 September 1987) and storm event No. 10 (26 May-28 June 1988) the drain was dry for only one day (23/5/88).

The average streamflow generated by the instrumented hillslope was 0.00012 cumecs (0.12 l s^{-1} or 7 l min^{-1}), although the snow event (storm No.7) produced a peak discharge of 0.0012 cumecs (1.17 l s^{-1} or 70 l min^{-1}) and rainfall events No. 4 and 9 produced peak discharges of 0.0006 cumecs (0.50 l s^{-1} or 30 l min^{-1}).

Storm-Period Streamflow Duration and Time To Peak Discharge : The storm-period streamflow duration at the base of the instrumented podzolic hillslope was sustained for some 10-20 percent longer than the stream response within the peaty valley-bottom area some 40 metres downstream (Figure 13 and Table 27). Observation of the time to peak of the stream discharge during individual storm events, shows that the response of the forest *catchment stream* particularly in its upper reaches (*forest weir* in Table 28) is occasionally quicker than the response of the grassland stream (Table 28).

Table 27. Storm period duration at the gauging structures within thedrainage channel and stream downstream of the instrumented forest hillslope .

STORM EVENT No.	PERIOD (days) *forest upper drain weir* PODZOLIC SLOPE	*forest lower drain weir* PEATY AREA	*forest flume*
3-4	22	-	21
7 (snow)	10	-	5.2
8	13	12	6
9	44	38	43.5
10	>30	26	25

Table 28. Time to peak storm discharge at all gauging stations within the Tir Gwyn catchments.

STORM No.	TIME TO PEAK DISCHARGE (Hours from start of grassland weir response) *forest u.drain*	*forest l.drain*	*forest weir*	*forest flume*	*grassland flume*	*grassland weir*
1	12	-	-	-	-	-
2	59	-	-	-	-	-
3	39	-	-	-	40	40
4	27	-	-	21	20	22
7	20.5	-	20	20.5	20.5	20
8	41.5	-	-	s29	36.5	37.5
9	-	66	56	67	66.5	68
10	61	67	42	s48	61	60

s = sustained/flattened/platykurtic peak

It is suggested that this rapid response is largely a function of the forestry road which crosses the stream just above the *forest weir* (Figure 13). In general, however, the peak discharge at all of the gauging structures within the forest and grassland catchments are relatively synchronous.

Dry Period (Lowflow) Discharge : The instrumented forest hillslope failed to generate as much runoff (per unit area) as the forest catchment or even the drain micro-catchment during dry *inter-storm* periods (Table 29). This presumably relates to the fact that larger catchments / aquifers have larger depth to length ratios and shallower gradients (Gregory and Walling, 1973; Horton, 1945), and thereby allow at least part of the incoming precipitation to move along a much longer and slower pathway.

Table 29. Runoff generated during storm and inter-storm periods by the forest hillslope, drain micro-catchment and forest catchment

PERIOD	DISCHARGE (mm)		
	FOREST HILLSLOPE (upper drain weir)	DRAIN CATCHMENT (lower drain weir)	FOREST CATCHMENT (forest flume)
storm 3-4	173	-	200
storm 7	98	-	76
storm 8	87	-	57
inter 8-9	55	44	66
storm 9	230	216	192
inter 9-10	**3**	**14**	**24 ***
storm 10	**16**	**31**	**46 ***

*** = dry period**

5.3.5. Storm-Period Rainfall-Runoff Ratios.

Catchment Storm-Period Rainfall-Runoff Ratios.

The rainfall-runoff (R-R) ratio ranged from 0.42 to 1.32 within the grassland catchment and from 0.25 to 0.76 within the forest catchment (Table 30). Moreover, the ratio of the forest catchment R-R Ratio to the grassland R-R Ratio varied throughout the year (Table 31). The forest catchment may have either *stored* or evapo-transpired much more of the incident precipitation relative to grassland catchment during the summer storm event, when compared with the early winter event (Table 31).

Table 30. Rainfall-runoff ratios for individual storm and inter-storm periods within the forest and grassland catchments

PERIOD	RAINFALL-RUNOFF RATIO	
	Forest Catchment	Grassland Catchment
storm No. 3-4	0.76	0.84
storm No. 7	0.60	0.78
storm No. 8	0.49	0.73
inter-storm Nos. 8-9	0.45	1.32
storm No. 9	0.52	1.00
inter-storm Nos. 9-10	0.25	0.42
storm No. 10	0.43	0.93

Table 31. Ratio of the forest catchment R-R Ratio to the grasslandcatchment R-R Ratio for storm and inter-storm periods during the field seasons 9-27/11/87 and 23/1/88-26/6/88.

PERIOD	FOREST R-R RATIO / GRASSLAND R-R RATIO	
	(ratio)	(% ratio)
storm No. 3-4 (early winter)	**0.90**	90%
storm No. 7 (snow event)	0.77	77%
storm No. 8 (late winter)	0.67	67%
inter-storm Nos. 8-9	0.34	34%
storm No. 9 (spring)	0.52	52%
inter-storm Nos. 9-10	0.60	60%
storm No. 10 (summer)	**0.46**	46%

Forest Hillslope versus Catchment Storm-Period Rainfall-Runoff Ratios.

Relative to the catchment rainfall-runoff ratios, the forest hillslope runoff-runoff ratios are generally larger during storms occurring in wet periods (Storm Nos. 7,8 and 9) and smaller during both inter-storm periods (Inter-Storm Nos. 8-9 and 9-10) and storms during dry periods (Storm No. 10: Table 32). This might imply that when the short (50 m), steep (19.7°) and shallow podzolic hillslope sections are wet, they will conuct water far more rapidly in comparison with the catchment area as a whole. As the catchment areas have longer slopes (170 m), are deeper and are more gently sloping, they will maintain more water-flow during dry periods in comparison with the hillslope sections.

Table 32. Rainfall-runoff ratios for the forest hillslope, drain micro-catchment and forest catchment, during individual storm and inter-storm periods.

PERIOD	RAINFALL-RUNOFF RATIOS		
	Forest Hillslope (upper drain weir)	Drain Catchment (lower drain weir)	Forest Catchment (forest flume)
storm 3-4	0.66	-	0.76
storm 7	0.77	-	0.60
storm 8	0.74	-	0.49
inter 8-9	0.38	0.30	0.45
storm 9	0.61	0.58	0.52
inter 9-10	0.03	0.14	0.25
storm 10	0.15	0.29	0.43

Catchment Rainfall-Runoff Functions.

Although the difference between the rainfall-runoff ratios for the forest catchment and those for the grassland catchment vary throughout the year (Table 32), an approximate linear rainfall-runoff relationship or function can be established for each area:

Forest Catchment Storm Runoff = -18.9 + 0.645P (R^2 = 86 % SE = 5.3 %)

Grassland Catchment Storm Runoff = -25.5 + 1.046P (R^2 = 91 % SE = 3.4 %)

where the storm-period runoff is between 100-400 mm and P is gross-precipitation input (mm)

Forest Hillslope versus Catchment Rainfall-Runoff Functions.

The forest hillslope would appear to generate a similar rainfall-runoff relationship on a storm period basis, to the forest catchment:

$$\text{Forest Hillslope Storm Runoff} = -36.2 + 0.744P \quad (R^2 = 87\ \%\quad SE = 4.9\ \%)$$

where the storm-period runoff is between 100-400 mm and P is gross-precipitation input (mm)

Intra Storm-Period Rainfall-Runoff.

A typical rainfall-runoff response during a storm-period is given in Figure ~~28~~ 27.

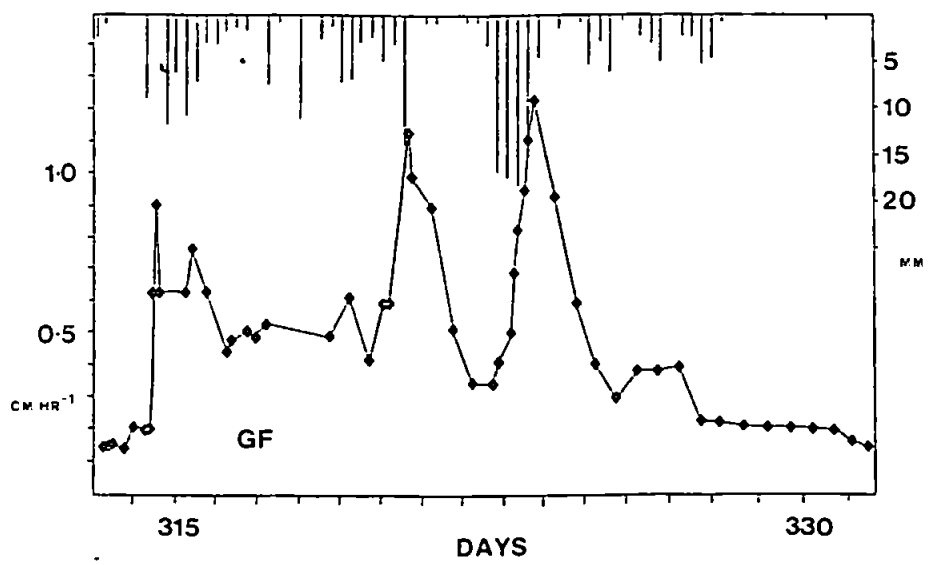

27

Figure ~~28~~ Intra-storm-period rainfall-runoffresponse during storm 3-4, monitored at the flume within the forest catchment.

CHAPTER 6.

Hillslope Hydrological Variables.

6.1. Introduction.

Those physical properties within hillslopes, shown to have an effect upon the movement of water (Sections 1.4.2., 1.4.3., 1.4.4. and 1.5.2) include soil bulk density, porosity, soil moisture content, potential gradient, specific moisture capacity, hydraulic conductivity, fluid viscosity, and intrinsic permeability.

Prediction of the hillslope water flux is possible as long as only one hydrological property is variable, while the others are constant values or functions (i.e. parameters) of the varying property (Crawford and Linsley, 1966). Within Richards' solution for water flux within variably-saturated pore systems, the hillslope hydrological variable is either soil moisture content or capillary potential (Section 1.4.3; Equations 6 and 7). The impact of the spatial and temporal response of these two variables upon water movement will, therefore, be discussed within the following sections (6.2 and 6.3). The impact on hydrological response of those hydrological parameters dependent upon the two variables, is discussed within Chapter 7.

6.2. Soil Moisture Content (θ_w, θ_v, θ_s).

The flux of water within a soil volume is equal to the change of moisture content with time (Euler, 1755; Equation 12). A total of 699 neutron moderation readings were recorded during the period 4 September 1987 to 23 June 1988, 440 of which were taken within the forest hillslope and 259 within the grassland hillslope. Volumetric moisture contents were calculated from these measurements by *in situ* verification of the standard calibrations for a *Wallingford neutron probe* with a mark II ratescaler (Institute of Hydrology, 1981).

6.2.1. Neutron Moderation Calibration.

The neutron moderation technique was calibrated and the errors in volumetric moisture content determined by:

1. examining the impact of neutron-counting over different integration times, and
2. comparing the standard calibrations with 30 measurements of bulk density and gravimetrically-determined moisture contents (Sections 4.2.2; 6.2.1; 7.2).

Topp *et al* (1980) suggested that an alternative technique for the non-destructive measurement of soil moisture, called *time-domain-reflectrometry* (TDR) was much simpler to use in comparison with the neutron moderation technique, as all readings could be calibrated by a single function. An experiment was conducted to compare the calibrated moisture contents derived by neutron moderation with those derived by TDR to verify this claim.

1. Neutron Count-Time: A field-count-time of 64 seconds (s) was chosen following an experiment to compare the errors associated with 16 s and 64 s count-times against the count determined over a 16 min period. A maximum difference of 6 counts was recorded between the integration times of 16 min and 64 s, and 12 counts between the 16 min and 16 s integration times (Table 33). For the particular soil (O/A) and profile-position (10 cm depth) that these measurements were taken, this equates with an error in volumetric moisture content of 0.8 and 1.5 percent respectively. The variability within these counts for each count-period are similar to those observed by Bell (1973).

Table 33. Wallingford neutron-probe (with a mark II L ratescaler) : count-time experiment 14/7/87

POSITION	READINGS (R)				
	16 min	64 s	Dmax	16 s	Dmax
GS N10	386	384 384 387 386	2	377 388 385 384	9
GS N40	-	369 369 366 370	-	360 371 366 367	-
GNN10	276	280 277 279 272	4	276 273 271 270	6
GNN40	277	277 277 276 274	3	275 280 282 273	5
G0 N10	632	629 637 626 635	6	638 620 629 631	12
G0 N40	-	602 596 602 603	-	599 597 606 606	-

Dmax = maximum deviation from the count at 16 mins

2. Calibration Equation for each Soil Horizon: The A/E and B soil horizons of both research hillslopes had a silty-clay-loam texture, and were, therefore, fitted to a *standard calibration* for loam soils (Institute of Hydrology, 1981 p16):

$$\theta_v = -0.016 + (0.867 * (R/Rw))$$

where θ_v is the volumetric moisture content (dim. $cm^3\ cm^{-3}$), R is the neutron probe reading within the soil (64 s count-time), and Rw is the neutron probe reading within a water-filled bin (16 min count-time).

The B/C and C horizons of both hillslopes contained a much greater percent of gravel and cobble-sized material and were therefore fitted to a standard calibration for coarse soil/regolith (Institute of Hydrology, 1981 p16):

$$\theta_v = -0.024 + (0.790 * (R/Rw))$$

Application of these calibrations to neutron probe measurements taken within the B horizon (20 to 40 cm depth) of the research hillslopes, yielded moisture contents almost identical to those determined from gravimetric sampling (Figure 28). The moisture contents determined by the gravimetric technique and neutron moderation technique were, however, very different within the A/E soil horizons (10 to 20 cm depth). The difference can be attributed to the loss of fast-neutrons from the soil surface (Bell, 1973; Jayawardane *et al*, 1983; Lawless *et al*, 1963; Zeimer *et al*, 1967). A *correction factor* of 1.6 to account for the surface-effect was, therefore, applied to the neutron probe calibration for the A/E horizon (Grant, 1975).

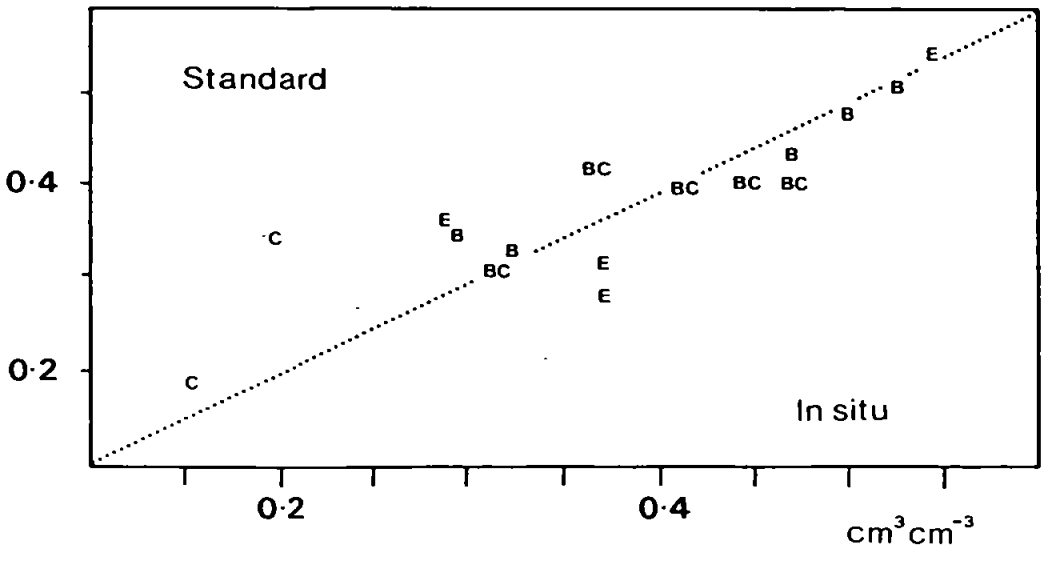

Figure 28. ***In situ*** **calibration of the neutron probe against a standard calibration.**

The difference between the moisture content derived by the neutron probe calibration and gravimetric techniques for the C horizon (Figure 28) was probably caused by disturbance of this coarse, laminated material during gravimetric sampling (Section 7.4.4; Bell, 1973).

Neutron Moderation versus Time-Domain-Reflectrometry Calibration: Application of Topp's equation: $\theta_v = -0.053 + 0.0292Ka - 0.00055Ka^2 + 0.00000Ka^3$ (Topp *et al*, 1980) to the TDR readings from the experiment at Tir Gwyn predicts moisture contents very different to those determined by both gravimetric and neutron moderation techniques (Table 43).

Table 34. The application of the Topp equation to TDR readings within the Tir Gwyn ferric podzol soil.

Location	sampling depth (cm) (horizon)	Mean Volumetric Moisture Content ($cm^3\ cm^{-3}$) (actual sampling depth, cm) gravimetric sampling	neutron moderation*	TDR (Topp Eq.)*
TGa5	5 (O)	0.604 (3-7)	-	
				0.418 (0-22)
TGa15	15 (E)	0.606 (12-17)	0.594 (10-20)	
TGa30	30 (B)	0.526 (27-32)	0.479 (25-35)	**0.856** (22-32)
TGa45	45 (B/C)	0.447 (42-47)	0.427 (40-50)	**0.176** (32-58)
TGa60	60 (C)	0.489 (57-62)	0.207 (55-65)	**0.000** (58-72)
TGb5	5 (O)	0.489 (3-7)	-	
				0.371 (0-22)
TGb15	15 (E)	0.500 (12-17)	0.415 (10-20)	
TGb30	30 (B)	0.500 (27-32)	0.449 (25-35)	**0.966** (22-32)
TGb45	45 (B/C)	0.367 (42-47)	0.443 (40-50)	**0.051** (32-58)
TGb60	60 (C)	0.198 (57-62)	0.365 (55-65)	**0.160** (58-72)

* using the mean calibration developed for the Tir Gwyn forest hillslope soils (Section 6.2.1).

* Topp's Equation : $\theta_v = -0.053 + 0.0292Ka - 0.00055Ka^2 + 0.00000Ka^3$
(where Ka = dialectic constant) used to determine the average moisture content along vertical TDR rods. Horizon-specific moisturecontents were then determined from the equation for weighted means :

$$\theta_1 = (\theta_{(1+2)/2} \cdot (L_1 + L_2) - \theta_2 \cdot L_2) / L_1 \qquad L = \text{rod length}$$

The second approach attempted involved the application of the Stein equation (Stein and Kane, 1983) for organic soils, to those dielectic constants monitored by the TDR rods penetrating only the forest O/A and E horizons. The dielectic constants monitored by TDR rods which extended through these near-surface horizons into the B, B/C and C horizons were applied to a further equation developed by Alharthi and Lange (1987) for for wet (i.e. greater than 80 percent saturated) loams (Table 35).

Table 35. TDR calibration: the application of the Stein equation to the O/A and E horizon and Alharthi equation to the B, B/C and C horizons of the Tir Gwyn ferric podzol soil (Experiment 13:30 27/3/88).

Location	sampling depth (cm) (horizon)	Mean Volumetric Moisture Content ($cm^3\ cm^{-3}$) (actual sampling depth, cm) gravimetric sampling	neutron moderation*	TDR (Stein/Alharthi)*
TGa5	5 (O)	0.604 (3-7)	-	
				0.477 (0-22)
TGa15	15 (E)	0.606 (12-17)	0.594 (10-20)	
TGa30	30 (B)	0.526 (27-32)	0.479 (25-35)	**0.542** (22-32)
TGa45	45 (B/C)	0.447 (42-47)	0.427 (40-50)	**0.473** (32-58)
TGa60	60 (C)	0.489 (57-62)	0.207 (55-65)	**0.300** (58-72)
TGb5	5 (O)	0.489 (3-7)	-	
				0.427 (0-22)
TGb15	15 (E)	0.500 (12-17)	0.415 (10-20)	
TGb30	30 (B)	0.500 (27-32)	0.449 (25-35)	**0.518** (22-32)
TGb45	45 (B/C)	0.367 (42-47)	0.443 (40-50)	**0.449** (32-58)
TGb60	60 (C)	0.198 (57-62)	0.365 (55-65)	**0.275** (58-72)

* using the mean calibration developed for the Tir Gwyn forest hillslopesoils(Section 6.2.1).

* Stein Equation : $\theta_v = -0.0252 + 0.0415Ka - 0.00144Ka^2 + 0.0000022Ka^3$
applied to the vertical TDR rods solely within the E horizon, and the Alharthi Equation : $\theta_v = 0.011Ka + (0.32 / (1.58^3))$ appliedto the vertical TDR rods entering the B, B/C and C horizons.Horizon-specific moisture contents were then determined from the the equation for weighted means :

$$\theta_1 = (\theta_{(1+2)/2} \cdot (L_1 + L_2) - \theta_2 \cdot L_2) / L_1 \quad L = \text{rod length}$$

NOTE: The application of either the Stein or Alharthi Equations to the whole soil profile failed to produce accurate moisture contents.

This combined approach produced moisture contents relatively similar to those recorded by gravimetric sampling, and neutron moderation (Table 35). Further measurements would, however, be required to prove the accuracy of such a calibration for ferric-podzol soils. The moisture content of the regolith (at a depth of 60 cm) seems to be the most uncertain (Table 35). This may result from the regolith's increased sensitivity to disturbance during the sampling of cores for the gravimetric technique (Section 7.4.4, see below).

Figure 29 corroborates the uncertainties in the use of a *standard equation* for the TDR measurments at Tir Gwyn. It shows that the three empirical equations produce very different moisture contents, particularly as soils approach saturation (i.e. 0.4 to 0.7 $cm^3 cm^{-3}$). The use of a *standard equation* for TDR measurements is, therefore, generally not justified. The perceived advantage of using the TDR technique without soil-texture-specific calibration as required with the neutron moderation technique is, therefore, equally untenable. Subsequent analysis of soil moisture content will be based upon neutron moderation measurements.

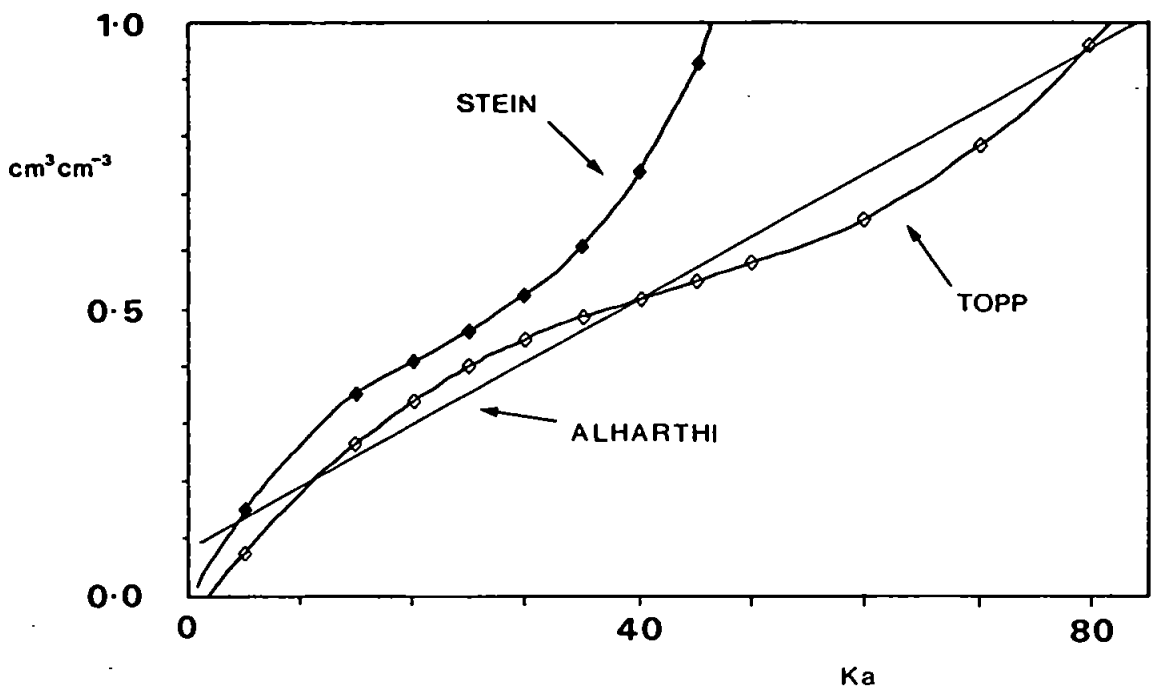

Figure 29. Relationship between the dielectic constant and the soil moisture content, using the equations given by Topp et al (1980), Stein and Kane (1983), and Alharthi and Lange (1987).

6.2.2. Hillslope Moisture Content (θ_v).

To calculate an average moisture content for each soil horizon within the forest and grassland hillslopes (Table 36), the moisture contents monitored during each measurement-run were *spatially-averaged* by the integration the moisture contents at the 0, 10, 20, 30, and 40 m slope locations. These moisture contents were then *temporally-averaged* over the 17 measurement-runs recorded over a period of 7 months (7/11/87-22/6/88). An arithmetic mean was used to both spatially and temporally average the *normally distributed* data-sets.

Table 36. Average volumetric wetness of the soil horizons within the forest and grassland hillslopes.

Soil Horizon	-------- Volumetric Moisture Content -------- θ_v $cm^3\ cm^{-3}$ (No. of measurements)		
	forest hillslope	*grassland hillslope*	*difference*
A/E	0.50 (72)	0.56 (67)	0.06
B	0.48 (72)	0.53 (71)	0.05
B/C	0.27 (72)	0.40 (65)	0.13

The difference between the spatial-averaging of moisture contents from the 0, 10,20, 30 and 40 m slope positions and those from 0, 2.5, 5, 10, 20, 30 and 40 m positions within the forest hillslope and 0, 10, 15, 20, 30 and 40 m postions within the grassland hillslope, was only 0.01 to 0.02 $cm^3\ cm^{-3}$).

The A/E and B soil horizons of the grassland hillslope were only 5 to 6 percent wetter than those within the forest hillslope. Given that the grassland has between 22 (Section 5.2.4) and 50 percent (Hudson, 1988) more *effective precipitation* (i.e. gross precipitation minus evapo-transpiration) this would imply that the grassland solum (A/E and B) is able to conduct water more rapidly than the forest solum, and hence have a similar mean moisture content.

The very marked discontinuity in the moisture content between that of the A/E plus B horizon and that of the B/C horizon of both hillslopes, implies that either:

1. the B/C horizons of both hillslopes are more conductive than the overlying horizons (Section 7.4.2), or
2. the B horizons are restricting the vertical flow of water into the B/C horizons (Sections 1.4.2; 8.2.2)

6.2.3. Change of Moisture Content within A/E and B Soil Horizons.

The changes of moisture content within the A/E horizon of both the forest and grassland hillslopes were consistently larger than the changes within the B and B/C horizons. This response was exhibited at individual neutron gauging sites (e.g. Figures 30and 34) and after averaging the moisture content measured at all of the slope positions (i.e. at 0, 2.5, 5, 10, 20, 30, and 40 m) (Table 37; Figure31). An arithmetic mean was again used (Section 6.2.2).

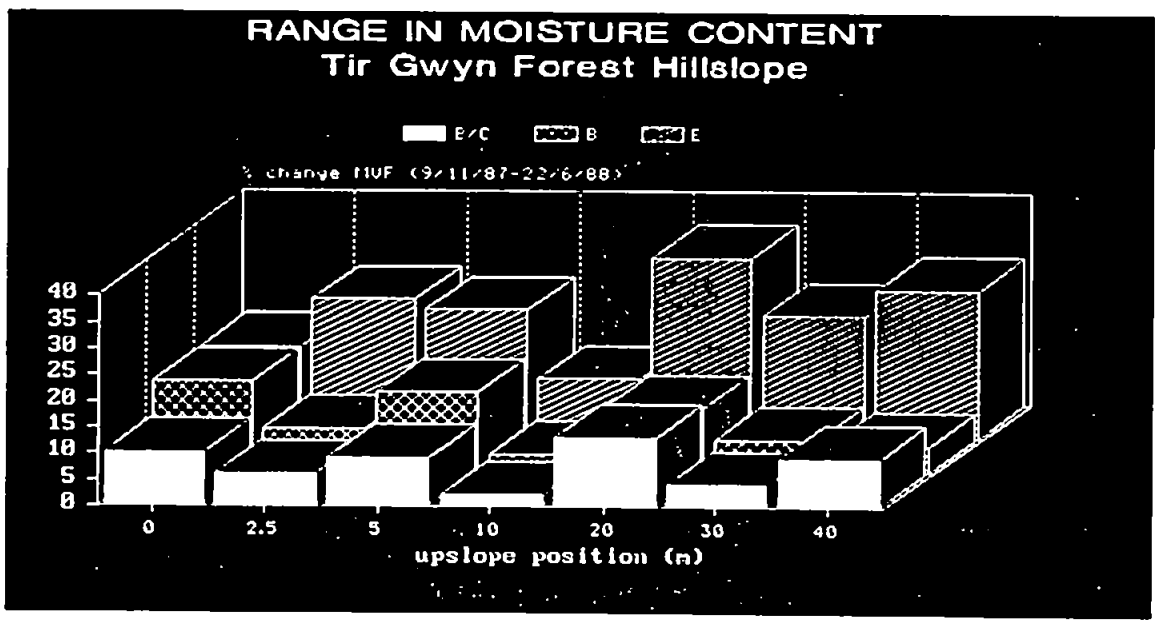

Figure 30. Change of moisture content at individual neutron gauging sites, within the forest hillslope.

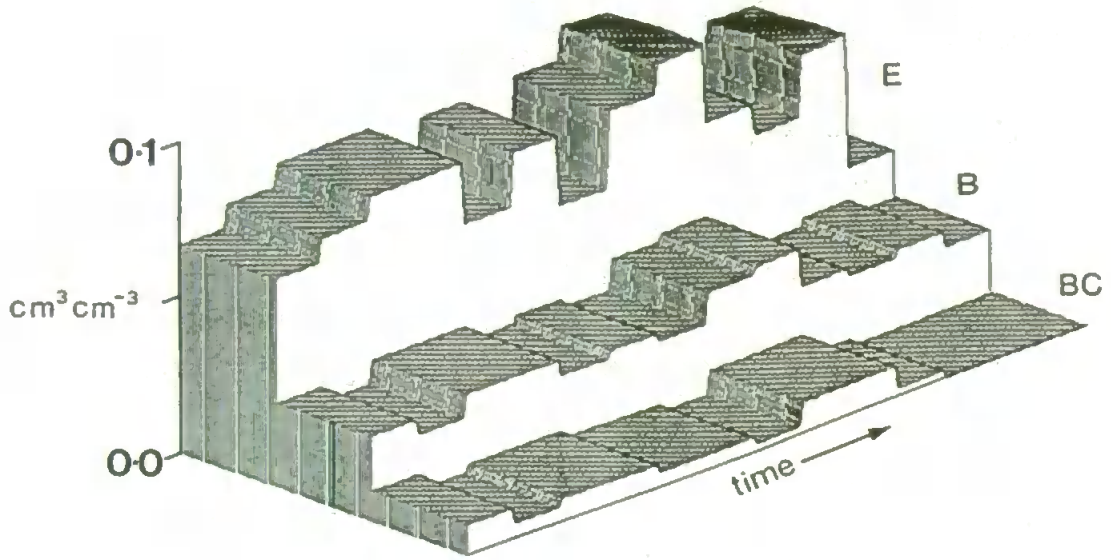

Figure 31. Average change of moisture content within the A/E, B, and B/C horizons of the forest hillslope (9/11/87 - 22/6/88).

Part of the large fluctuations of moisture content within the A/E horizons relative to the B and B/C horizons can be attributed to the localization of evapo-transpirational losses from the surface of the grassland and near-surface soils within the forest. A 65 percent difference between the moisture fluctuations of the A/E and B horizons in the forest (Table 37) cannot, however, be solely attributed to a 5 to 8 percent loss of soil water due to transpiration (Hudson, 1988; Section 5.2.2). Equally, an 86 percent difference in moisture fluctuation between the same two horizons in the grassland (Table 37), cannot be attributed solely to an evapo-transpiration rate of 15 to 25 percent (Section 5.2.2; Hudson, 1988).

Given that the B horizon maintains a similar volumetric wetness to that of the A/E horizon, the difference in the dynamics of the moisture content implies that either:

1. vertical flow through the A/E horizon is impeded as it moves into the B horizon, and hence lateral flow within the A/E horizon is induced (Sections 7.4.9., 8.2.2., 8.3.2. and 8.3.3), or
2. flow within the B horizon is more localized in the secondary-structure in comparison with the A/E horizon (Sections 7.3.1., 7.3.6. and 7.4.1), or
3. the gap between the neutron probe access-tube and the soil is allowing saturated parts of the overlying O/A horizon to artifically wet the A/E horizon around the access-tube (Hart and Lomas, 1979; McGowan, 1974).

Table 37. Mean absolute change in the volumetric moisture content (θ_v) of each soil horizon during the 12 monitoring periods between 7/11/87 and 22/6/88.

Integration period (Julian day plus decimal time)	Moisture Content Change (θ_v, $cm^3\ cm^{-3}$) FOREST A/E	FOREST B	FOREST B/C	GRASSLAND A/E	GRASSLAND B	GRASSLAND B/C
313.5833-314.3507	0.02	-0.02	-0.03	0.00	0.00	-0.01
314.3507-315.4681	0.04	0.03	0.00	-0.01	0.00	0.01
315.4681-315.5910	0.00	0.00	0.01	0.05	0.02	0.00
315.5910-331.6347	0.08	-0.02	-0.01	-0.12	-0.01	0.01
331.6347-397.4300	0.07	0.02	0.00	0.10	0.00	0.00
397.4306-417.5639	- 0.09	-0.02	0.00	-0.11	-0.02	0.02
417.5639-439.4382	0.09	0.04	0.01	0.16	0.02	0.02
439.4382-440.4611	0.03	0.00	0.00	0.01	0.00	-0.01
440.4611-473.5833	-0.09	-0.03	-0.02	-0.09	-0.02	-0.01
473.5833-485.4840	-0.02	-0.01	-0.01	-0.10	-0.01	-0.01
485.4840-490.3778	0.06	0.00	0.00	0.12	0.02	0.01
490.3778-539.3194	-0.15	-0.01	0.00	0.21	-0.04	-0.02
mean, absolute change in θ_v	**0.049**	**0.017**	**0.008**	**0.094**	**0.013**	**0.009**

6.2.4. Change of Moisture Content along the Forest Slope Catena.

The moisture content of the regolith just above the fragipan layer (50-70 cm depth) is much more variable over time at downslope locations (i.e. 0-5 m) when compared with those upslope (i.e. 5-40 m, Figure 38). Given the straight slope, this implies that there is a much greater *specific flux* of water within the regolith downslope. This implies, either that a considerable proportion of the water-flow within upslope areas is moving laterally, rather than to depth (50-70 cm), or that flow within the regolith is being forced to concentrate in the vertical-dimension as it moves towards the riparian zone.

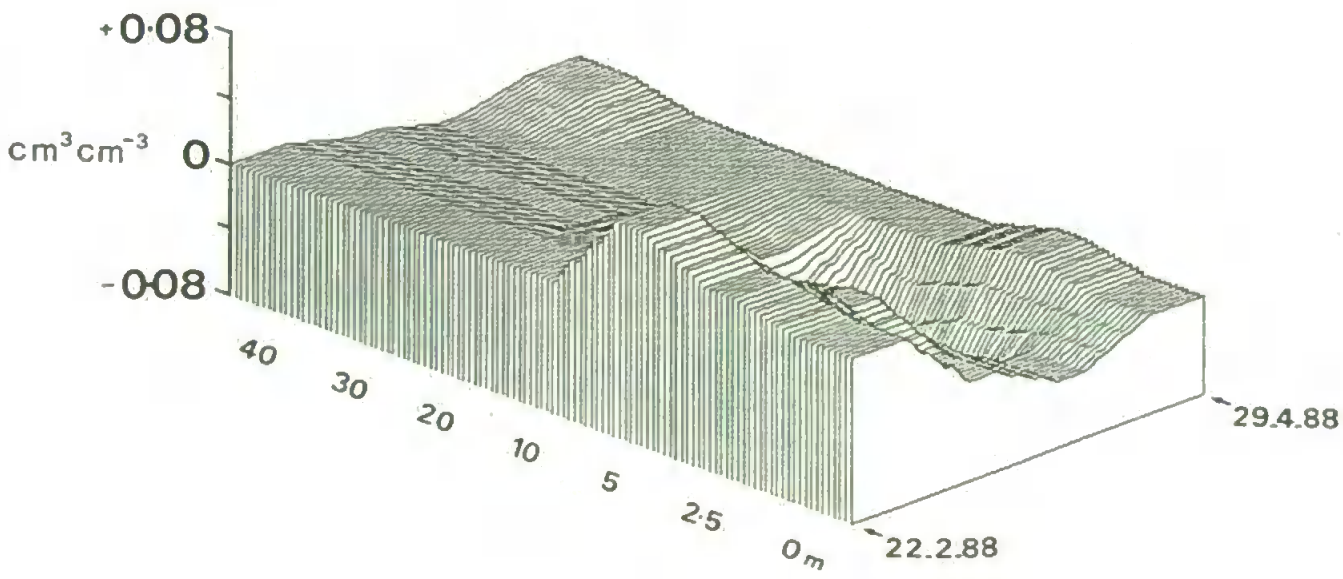

Figure 32 Change of moisture content within the regolith (C horizon) at a depth of 60 cm.

Although the spatial distribution of moisture content is very variable across the monitored flow-strips (Figure 30), the downslope movement of dynamic or kinematic waves (Chow *et al*, 1988) through time are easily observable. The movement of one and possibly a second such waves downslope within the forest A/E horizon is shown within Figure 33.

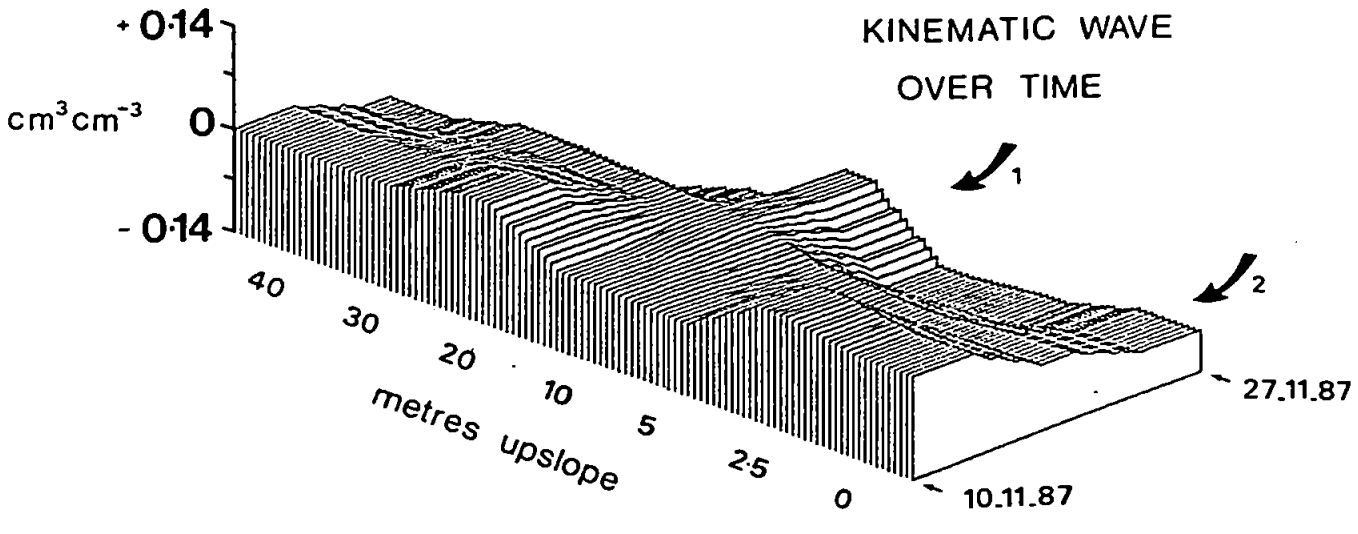

Figure 33. Two possible kinematic waves of moisture content change within the A/E horizon of the forest hillslope.

6.2.5. Moisture Content at the Inflow and Mid-Point of the Forest Riparian Zone.

The soil at a depth of 25 to 35 cm deep within the profile at the junction of the steep, podzolic slope with the gently sloping riparian slope is much wetter than that at the same depth a further 1.5m into the riparian zone (Figure 34). The soil at this junction is drier in all other horizons in comparison with that at the mid-point of the riparian zone (i.e. 1.5 m downslope of the junction and 1.5 m upslope of the stream channel). This might imply that water-flow moves from the podzolic slope into the riparian zone at a depth of 25 to 30 cm (equivalent to the B horizon on the podzolic slope).

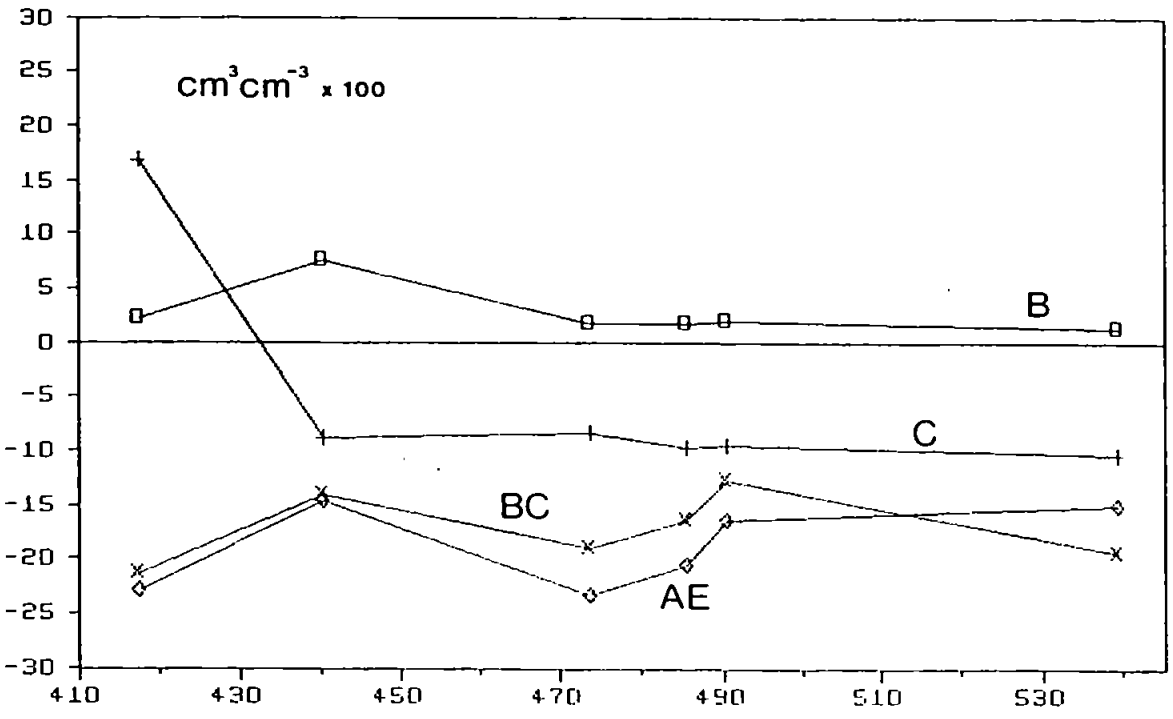

Figure 34. Moisture content at the inflow to the riparian zone minus that at the mid-point of the riparian zone (Julian days from 1987)

6.2.6. The Impact of Individual Trees upon the Moisture Regime of the Forest Hillslope.

The moisture content of soil close to the buttress root of a large conifer (47 cm DBH) was drier within the A/E and B horizons (approx. 10-35 cm depth) and slightly wetter in the B/C and C horizons (approx. 40-65 cm depth), in comparison with the same soil horizons 2 m downslope of the same tree (Table 39; Figure 15).

Table 39. Soil moisture content close to the buttress of a large conifer (47 cm DBH) relation to that 2 m downslope of the same tree.

		Soil Horizon Moisture Content (cm^3 cm^{-3})				
Location		A/E	B	B/C	Cu	No.
1	Transect	0.52	0.38	0.18	0.11	(12)
2	2 m downslope	0.52	0.38	0.24	0.12	(12)
3	Intermediate	0.39	0.35	0.24	0.12	(12)
4	Near tree root	0.33-0.42	0.31-0.33	0.25-0.28	0.14-0.16	(48)
	Percent difference (2 - 4)	**10-19 %**	**5-7 %**	**1-4 %**	**2-4 %**	
		drier	**drier**	**slightly wetter**		

Neutron gauging sites:
Transect = 10 m slope position on the forest hillslope, 3 m across-slope from the instrumented tree (10N); *2 m downslope* = 2 m downslope of the instrumented tree (P1N); *Intermediate* = 1.5 m downslope of the instrumented tree and 0.8 m away from a buttress root (P2N); *Near tree root* = 3 gauging sites within 1 m of the bole and 0.3 cm of a butress root (P3N, P4N, P5N).

Neutron gauging depth (per soil horizon):
E = 15 cm; B = 30 cm; B/C = 45 cm; Cu = 60 cm

Measurement Integration:
moisture contents are averages of 4 temporal measurements during the summer period 17 April to 22 June 1988.

The lower moisture contents of the A/E horizon close to thebuttress root, probably relate to a greater abstraction by *fine roots* to supply transpirational losses. Ford and Deans (1977) have shown that the fine roots of Sitka spruce (*Picea sitchensis*, Bong . Carr.) are concentrated within the near-surface soil horizons, close to individual trees.

The slightly wetter soil at a depth of 40 to 65 cm beneath the individual tree, relative to that at the same depth but 2 m downslope of the tree, *may* be caused by a slight increase in vertical flow beneath individual trees. This increase in moisture content at a depth of 40-65 cm beneath the buttress root is in sharp contrast with tensiometer measurements at the same depth, but immediately below the bole of the same tree (Figure 45 : a lower moisture content below the bole can be inferred from the large negative capillary potentials). A preferential movement of stemflow into the soil beneath the butress root rather than at the base of the tree might be inferred. During the installation of the neutron probe access-tubes, the regolith at a depth of 40-65 cm beneath this tree was visibly the driest of *all* of that augered within the forest hillslope, and as a result proved very difficult to auger. If a large gap was created between the access-tube and regolith whileaugering into the dry soil, water-flow within fully-saturated soil-pores would preferentially move down the outside of the access-tube and artificially wet the deeper soils (Section 6.2.3). Equally, if this gap were to infill with fines from overlying horizons, the moisture retention (Section 7.3) of the regolith close to the access-tubes would increase, and possibly lead to increased moisture contents.

The differences in soil moisture content between below-tree and inter-tree areas would not appear to be related to the spatial variablity of soils between the gauging sites, as the soil moisture contents monitored at the gauging site 2 m downslope of the tree are very similar to those monitored 3 m across-slope, at the 10 m slope position of the main instrumented transect (Table 39; Figure 15).

The moisture regime within the relatively homogenous, gleyed soil of the riparian zone was monitored for the period 21 January to 22 June 1988, both beneath an individual tree and at a distance 1 m from the same tree (Figure 15). The average change in moisture content during 6 integration periods was less at a depth of 15 cm and more at depths of 30, 45 and 60 cm beneath the tree, in comparison with that away from the tree (Figure 35). Given that a combination of stemflow inputs and transpirational outputs should increase the moisture change within near-surface soil beneath trees, this would imply that there is a much smaller lateral flux of water at a depth of 15 cm beneath the individual tree, in comparison with that within the inter-tree soil.

The larger change in moisture content at depth beneath the tree may be the result of either increased transpirational losses or increased vertical flow. It should be noted, however, that most of the moisture change whether beneath or at 1 m away from individual trees, occurs within the surface soils (see Section 6.2.3).

The impact of individual trees upon the capillary potential (ϕ_c) and potential gradient ($d\phi/dL$) of the forest hillslope as a whole is examined in Section 6.4.6., and the impact upon the saturated hydraulic conductivity (K_s) and intrinsic permeability (k) is examined in Section 7.4.4.

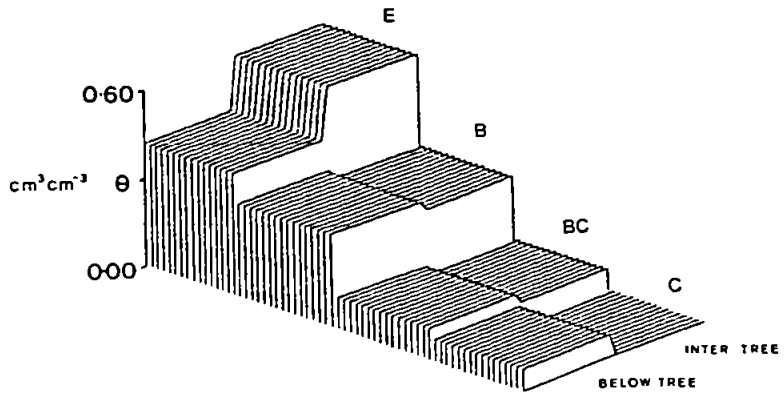

Figure 35. Change of moisture content beneath a large tree (44 cm DBH) within theforest riparian zone and that at 1 m across-slope from the same tree (Total change over 6 integration periods between 21/2/88 and 22/6/88).

6.3. Potentials (ϕ, ϕ_g, ϕ_c) and Potential Gradient ($d\phi/dL$).

The flow of water within a soil is equal to the gradient of the total potential (or energy) multiplied by the hydraulic conductivity (Darcy, 1856; Dupuit, 1863; Hubbert, 1940). The total potential (ϕ) within a control volume of a soil includes components generated by gravitational (ϕ_g), capillary (ϕ_c: Buckingham, 1907), inertial loss (ϕ_i: Hubbert, 1940), temperature (ϕ_t: Nielsen *et al*, 1972), osmotic (ϕ_o), and electro-kinetic (ϕ_e: Klute 1973) effects.

Within wet, conductive soils (Sections 6.2 and 7.4) under temperate climates, temperature gradients (i.e. multiphase heat-water flow), osmotic gradients (i.e. coupled flow) and electro-kinetic gradients are likely to be insignificant in comparison with the gravitational and capillary effects (Klute, 1973). Inertial losses (or partial-turbulence) are assumed to be insignificant within Darcian flow regimes (Section 1.2.). The total potential (or simply *potential*) within the two research hillslopes was, therefore, determined by the combination of gravitational potential (i.e. elevational positions measured during a site survey: Figures 3 and 4; Section 6.3.1) and, capillary potential measurements monitored by tensiometers, piezometers, and boreholes (Section 4.2.2.3).

6.3.1. Gravitational Potential (ϕ_g).

The stationary (or unchanging) property of gravitational potential within the forest flow-strip is shown within Figure 36.

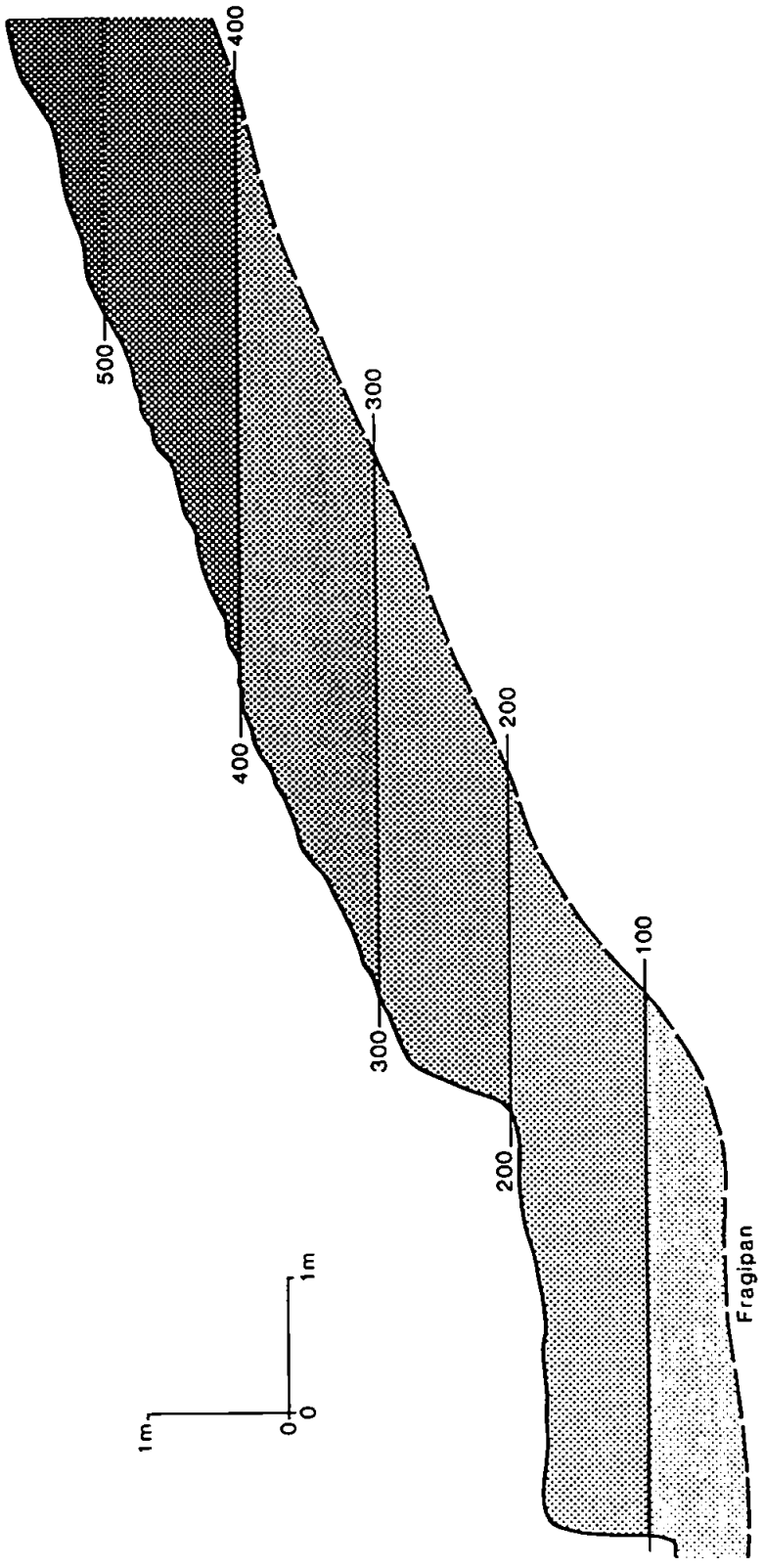

Figure 36. Gravitational potential within the forest hillslope; included for comparison with the distribution of total capillary potential presented within Figures 42, 43, and 44.

6.3.2. Capillary Potential (ϕ_c) : Measurement Errors.

The values of capillary potential recorded by the tensiometers, piezometers and borehole located at a depth of 1 m within the riparian zone of the forest hillslope, are very similar (given the slightly different locations) when the local phreatic surface approaches a depth of 1 m (e.g. Figures 37).

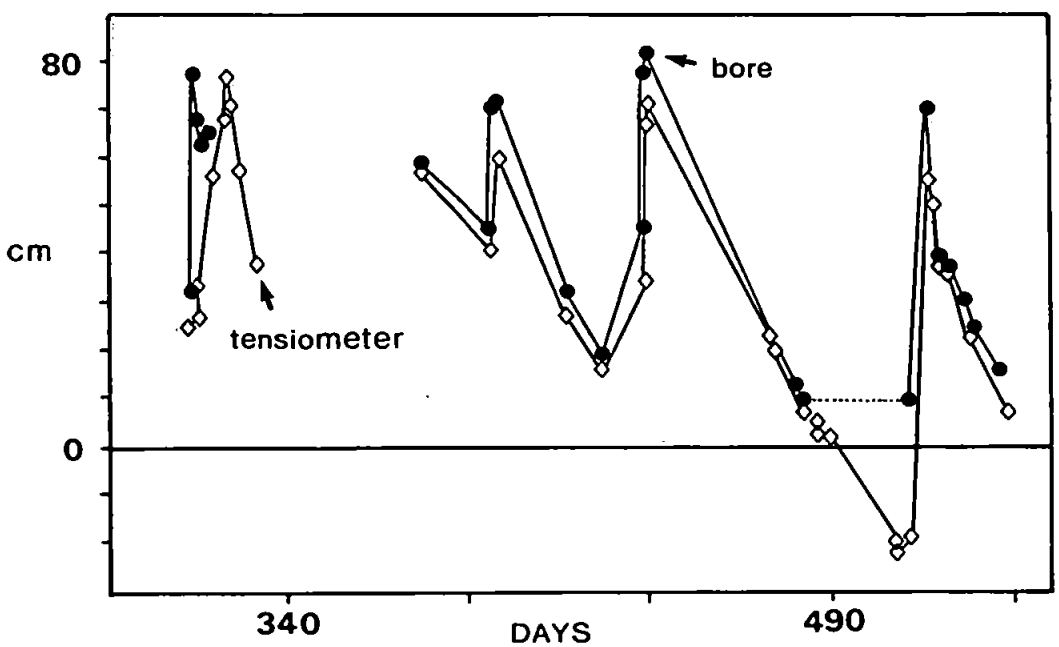

Figure 37. Capillary potential monitored by the borehole (for a depth of 100 cm) within the forest riparian zone against that monitored by a tensiometer (100 cm deep: BT100) located 50 cm away.

As the phreatic surface approaches the ground surface, and the instruments experience capillary potentials (or heads) of about 1 m H_2O, then the tensiometers record 10 percent less potential compared with that recorded by either the piezometers or borehole (Figures 37 and 38). This difference may result from a greater *manomeric depression* within the tensiometer (MEXE, 1963), than was observed at the time of the calibration (Section 4.4.3).

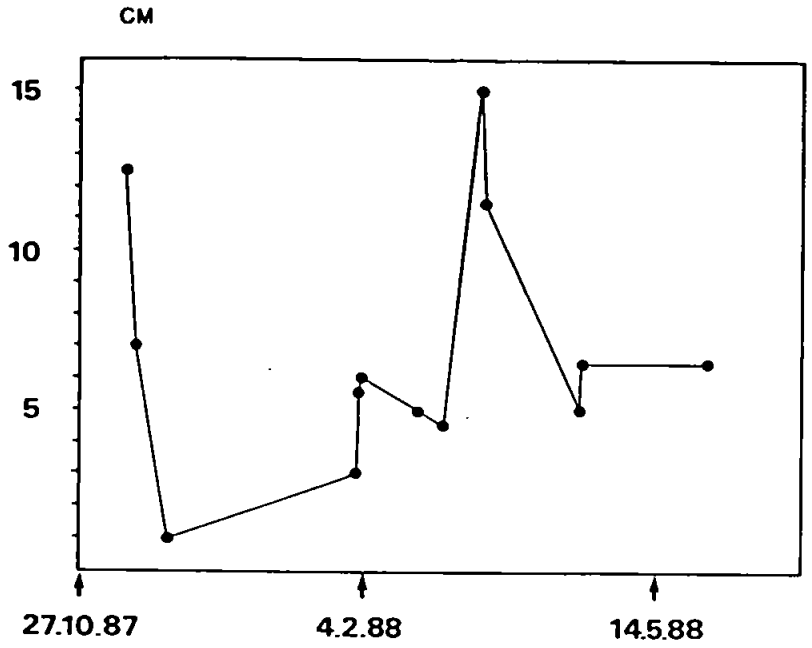

Figure 38. Difference between the *measured* capillary potential indicated by a tensiometer (100 cm deep: 0T100) and that indicated by a piezometer (100 cm deep). The instruments are located 60 cm apart within the forest riparian zone. Positive values reflect the larger values of capillary potential measured by the piezometer.

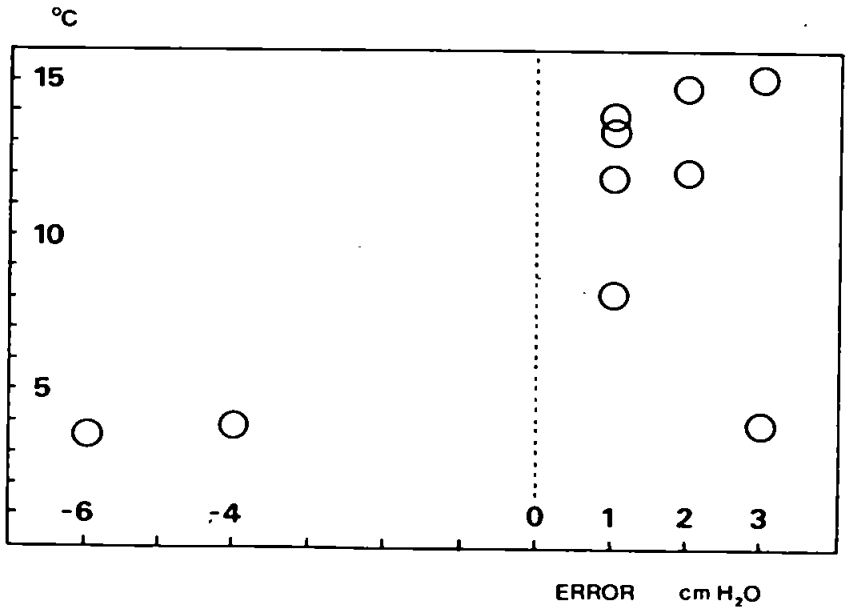

Figure 39. Variation in the capillary potential measued by a manometer tensiometer located above-ground in a container in which a constant head of water was maintained. Measurements were taken at temperatures ranging between 3 and 15 degrees.

The effect of temperature upon tensiometer readings via changes in a tensiometer's water and air density (Berryman *et al*, 1976; Dowd and Williams, 1989; Watson and Jackson, 1967) would appear to be relatively insignificant. From a sample of 11 random measurements taken over the period 31/1/88 to 4/5/88, covering a temperature range of 3-16°C, the capillary potential recorded by the *calibration tensiometer* (Section 4.4.3) drifted over a range of only 9 cm (Figure 39). On the 24 May 1988, during the driest few days of the monitoring period (Section 6.3.4), a diurnal range in *apparent* capillary potential recorded by the 50 cm deep transducer-tensiometer (Section 4.4.3) within the riparian zone of 3.7 cm (i.e. 11.3 to 15.0 cm) followed a diurnal ground-surface-temperature range of 4.2 °C (i.e. 3.3 to 7.5 °C). Similar diurnal fluctuations in apparent capillary potential have been recorded by Langan *et al* (1987) and Richards *et al*, (1937).

6.3.3. Dynamics of Phreatic Surfaces ($\phi_c = 0$).

During the monitoring period (8 September 1987 to 22 June 1988) *saturated wedges* (Section 1.3.2) developed within both the grassland and forest hillslopes. The maximum upslope extension of these *deep phreatic zones* (upto 60-70 cm in thickness) was 25 m within the grassland hillslope and 10 m within the forest hillslope, and was reached in both hillslopes on 15 March 1988 (Julian day 75 in storm-period No.9: Section 5.3; e.g. Figure 40). The dynamics of the size of these zones appeared to be synchronous with the streamflow outflow. For example, during storm period No. 3-4 (9/11/87-27/11/87) the growth and decline of the saturated wedge within the forest hillslope is paralleled by an increase and reduction in the stream discharge (Figure 40). Ragan (1968) noticed a similar association between the response of a stream and its adjacent riparian saturated zone.

In addition to the development of the deep phreatic zones, small saturated zones developed within the afforested hillslope, just above the boundary between:

1. the A/E and B soil horizon, and
2. the A/E and O/A soil horizon.

The tendency towards full-saturation at horizon breaks indicates that there is a marked discontinuity between the moisture flux of the two horizons, the upper horizon having a much larger flux (Zaslavsky, 1964). These *shallow saturated zones*, like the deeper zones are very dynamic during individual storm periods (Figure 41). In contrast, perched water-tables did not develop within the near-surface horizons of the ploughed section of the grassland hillslope. This may be the result of ploughing, which could have removed the marked discontinuity between the hydrological properties within the A/E and B horizons (Sections 2.10.2., 7.2., 7.4.1., 7.4.2., 8.2.2).

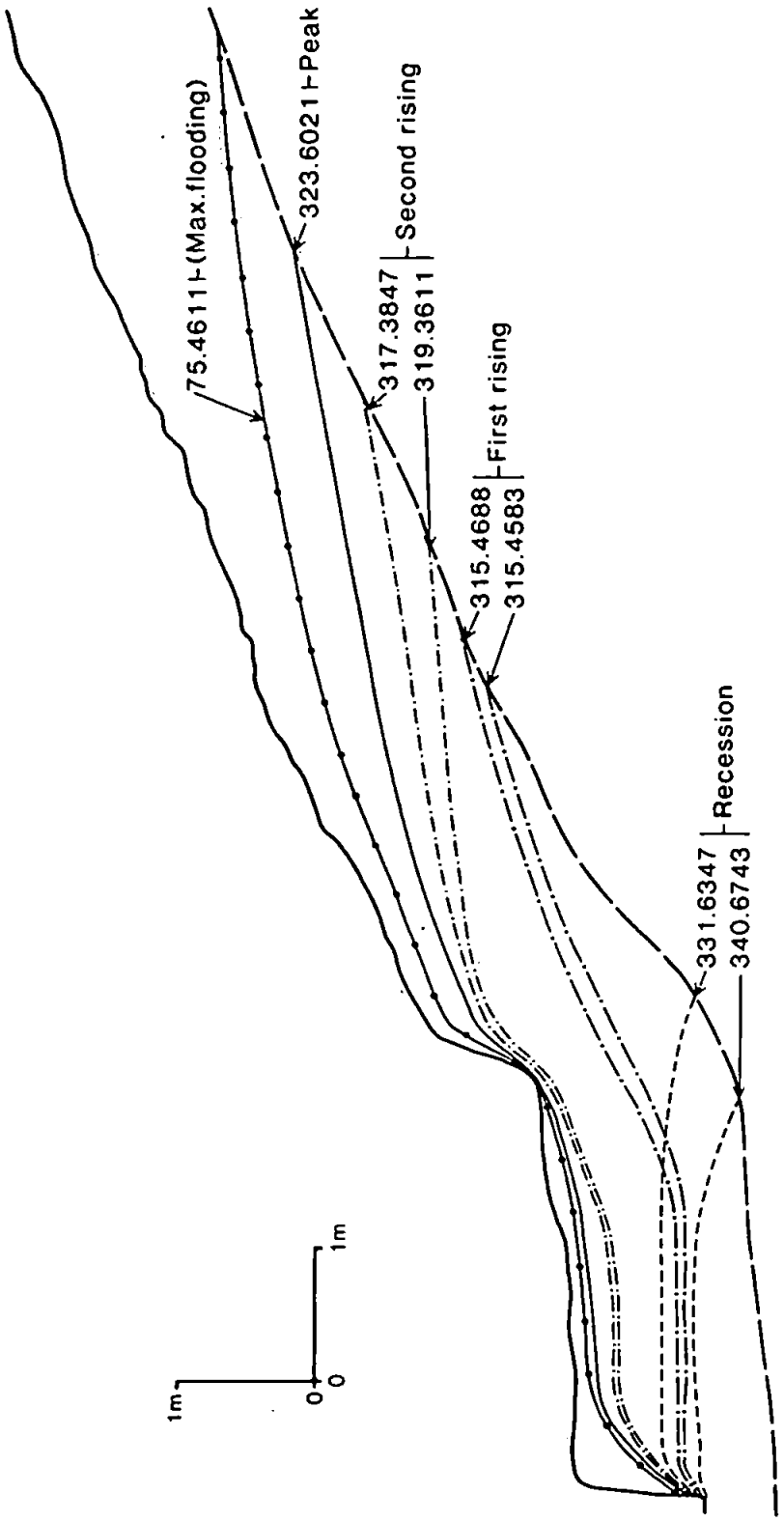

Figure 40. The dynamics of the deep phreatic zone within the riparian zone of the forest hillslope, during storm-period 3-4.

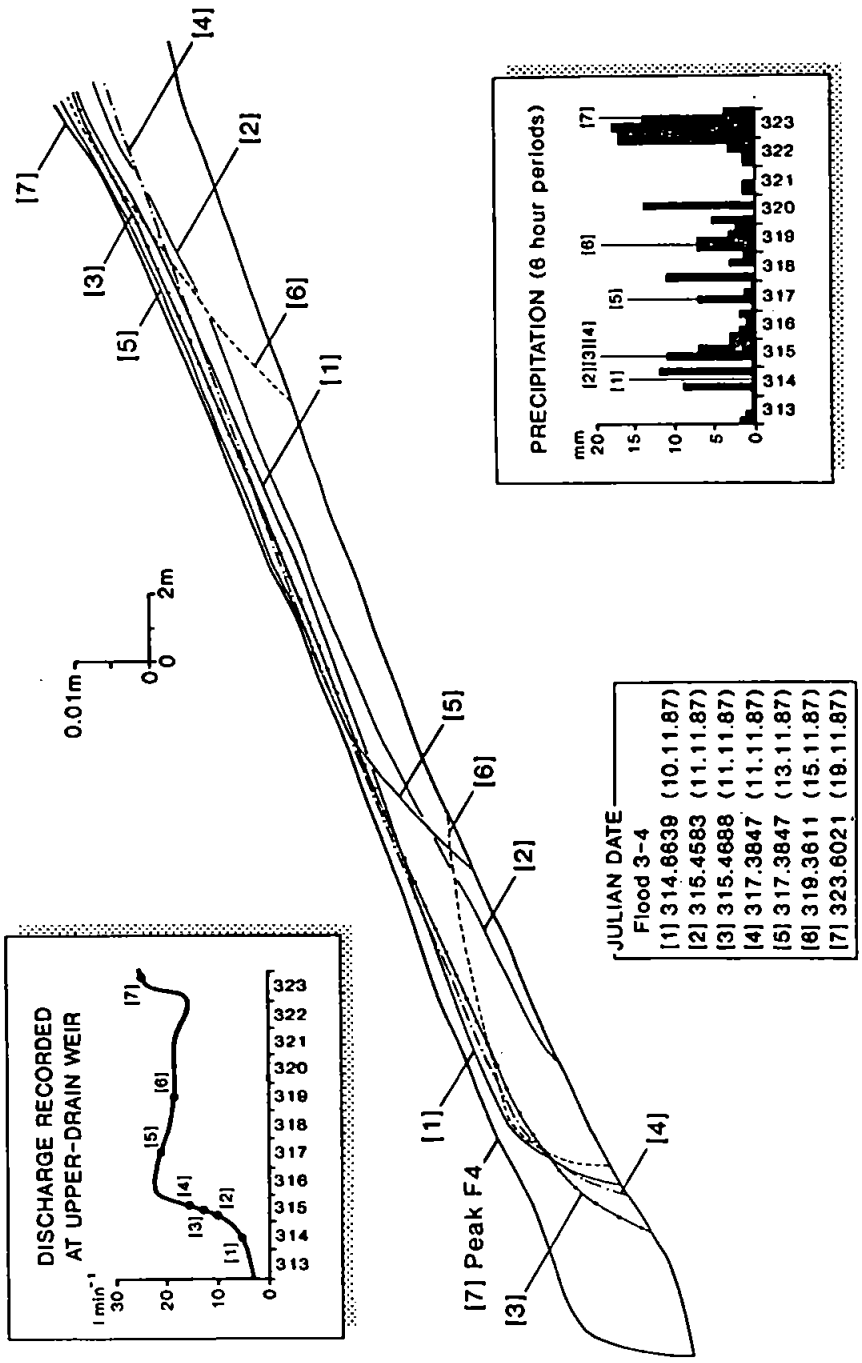

Figure 41. The dynamics of the shallow phreatic surface at the A/E horizon of the forest hillslope, during storm-period 3-4.

6.3.4. Total Potential (ϕ) within the Forest Hillslope.

Gravitational potential (ϕ_g: Figure 35) dominated the equipotential-net within the forest hillslope during all of the monitoring period (8 September 1987 to 22 June 1988)(e.g. Figures 42 and 43), except during the dry, 10 day period within May (14-24/5/88) when parts of the hillslope developed very large negative capillary potentials (or suctions) (e.g. Figure 44).

The dominance of stationary property of gravitational potential across the equipotential-net, meant that during most storm periods the total potential gradients ($d\phi/dL$) did not increase as much as the streamflow generation. For example, streamflow monitored at the upper-drain weir increased by 5.4 times (Table 26) during the 11 days between the relatively similar two equipotential-nets shown within Figures42 and 43. As the potential gradients do not increase greatly during storm-periods, then large changes in the *state-dependent hydraulic conductivity* (Section 7.4.6) are required to generate streamflow.

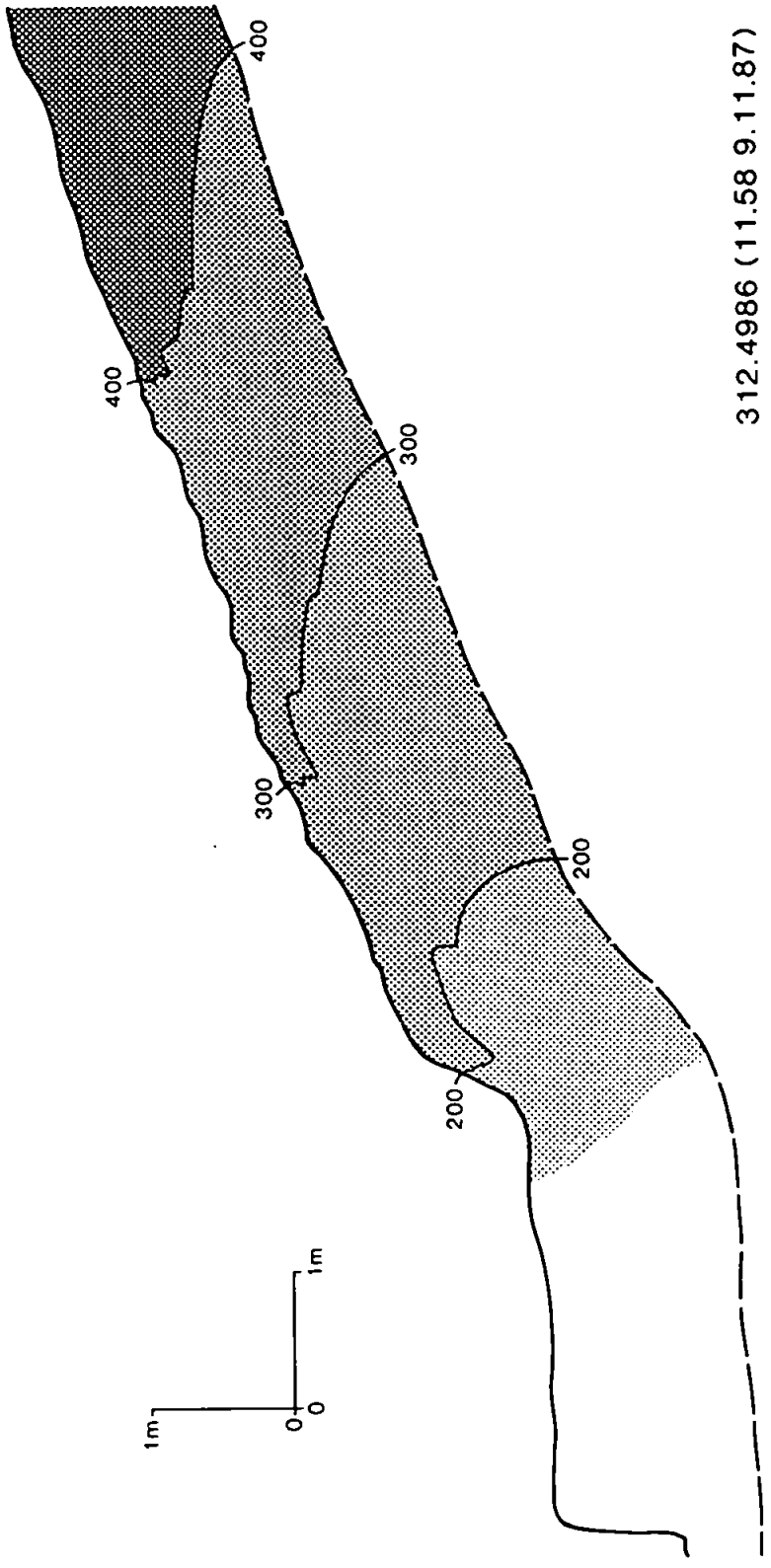

Figure 42. The distribution of total potential within the the forest hillslope, prior to storm 3-4.

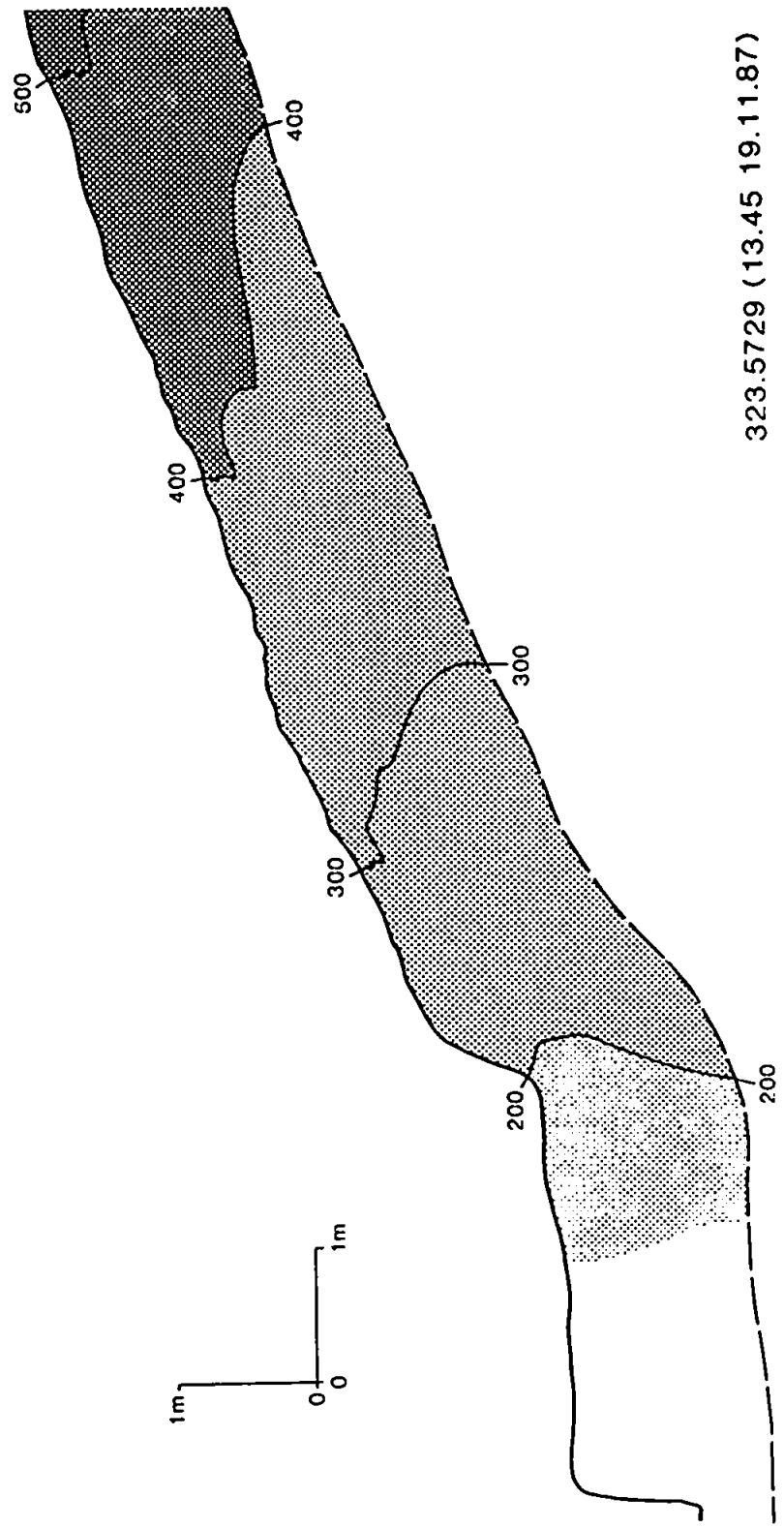

Figure 43. The distribution of total potential within the forest hillslope, at the peak rainfall and streamflow within storm 3-4.

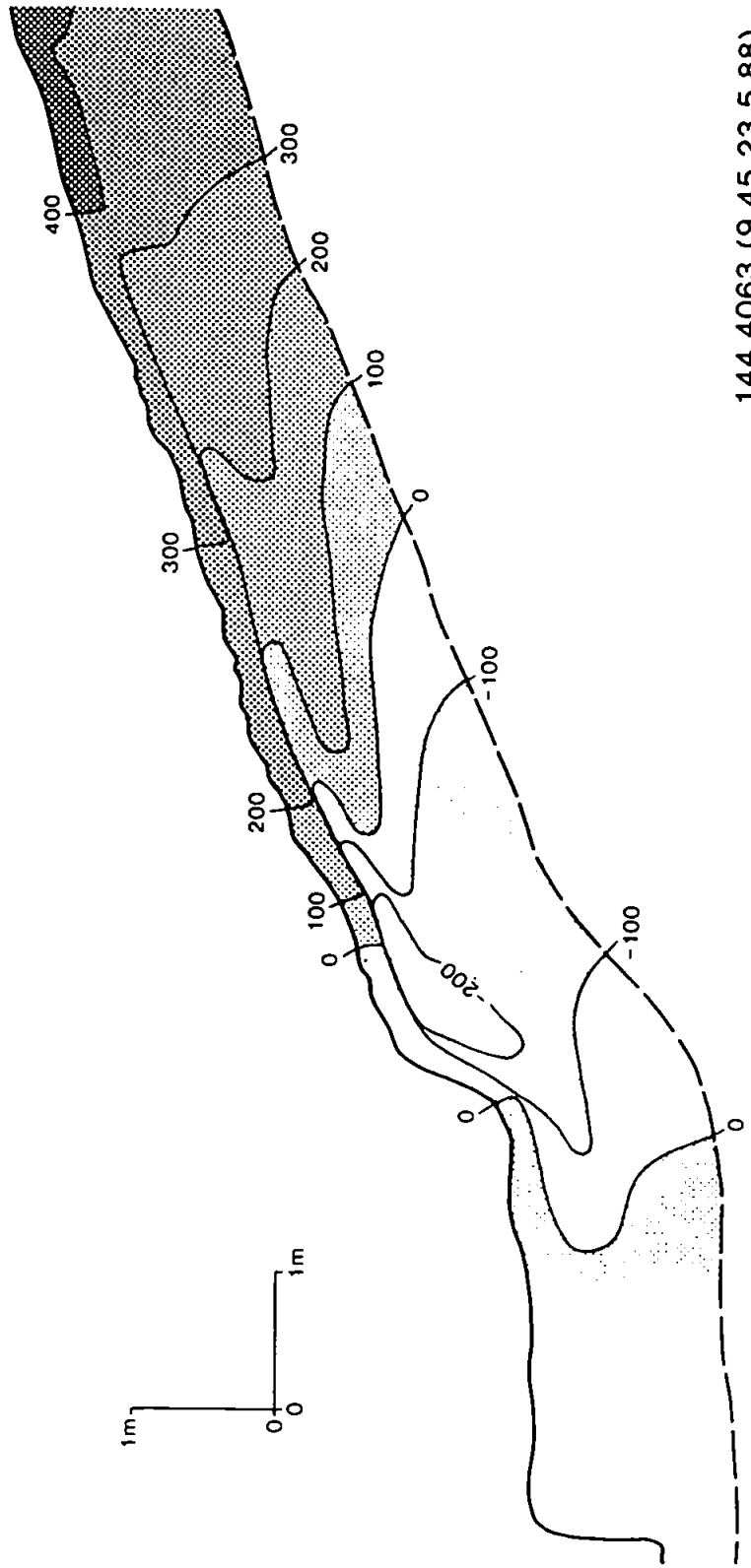

Figure 44. The distribution of total potential within the forest hillslope, during the 10 day, dry period within May 1988.

6.3.5. Near-Surface Lateral and Vertical Potential Gradients ($d\phi/dL$ or J) within the Forest and Grassland Hillslopes.

The potential gradients laterally within the forest and grassland A/E horizon (**02.5E, 2.55E, 510E, 4020A**) were almost always less than the gradients vertically from the A/E to the B horizon (0EB, 2.5EB, 5EB, 10EB, 40AB, 20AB; Tables 40, 41 and 42).

Within the forest hillslope, the vertical potential gradients from the A/E to B horizon at the 0 m, 2.5 m, and 5 m slope positions are approximately at unity (i.e. 10^0) during most of the year, only increasing to 10^1 during the dry, 10 day period within May (Julian Date 500-510; Tables 40 and 41). The steEper vertical gradients down into the forest B horizon during the dry period are also shown within Figure 44. The vertical potential gradients at 10 m up the forest hillslope (10EB) are an order of magnitude less than at the other slope positions (Tables 40 and 41). This could have resulted from the impact of the large buttress root 1 m downslope of the tensiometer array. By extending across the slope, the root may have forced water to move vertically (in addition to the across-slope deflection), and thereby remove the discontinuity between the hydraulic conductivity of the A/E and B soil horizons (Zaslavsky and Rogowski, 1969). This would in turn lead to reduced vertical potential gradients.

If the A/E horizon had a state-dependent hydraulic conductivity the same as the lower B horizon (i.e. a homogenous soil profile) or even less than the B horizon, then the dominance of the vertical potential gradients would direct most of the flow in the vertical rather than lateral plane. As the ploughed section of the grassland hillslope has lower conductivities within the A/E horizon compared with the B horizon (Section 7.4.9) then vertical flow should dominate.

Within the forest hillslope, however, the A/E horizon is always more conductive than the underlying B horizon (Section 7.4.9). In this situation the increased vertical gradients could be produced by a greater flux within the A/E horizon compared with the B horizon. This would, therefore, imply a greater *lateral* flux within the A/E horizon compared with the vertical flux from the A/E to B horizon.

In summary, this means that the potential gradients only indicate the dominant direction of flow within a homogenous soil body, which may be the whole hillslope or an individual soil horizon (Section 3.5.4).

Although the lateral potential gradients within A/E horizon of the ploughed upper section of the grassland hillslope are always relatively similar to the gradients within the forest hillslope, the vertical potential gradients from the A/E to B horizon are quite different during dry periods (Tables 40, 41 and 42). During the 10 day, dry period in May (14-24/5/88 : Julian Date 500-510) when streamflow was at its lowest (Table 29 : inter 9-10) the vertical potential gradients indicated that the vertical flow although increasing greatly within both hillslopes, continued to direct flow down into the forest B horizon (Table 41), but directed flow up

towards the surface of the grassland hillslope (Table 42). This marked difference may be the result of an increased ET_a loss from the grassland surface during the *relatively* warm (max. temp. 14-24/5/88 = 11.7 °C) dry periods, as compared to the near-surface ET_a losses from the forest soil (Section 6.3.6).

Table 40. Lateral total potential gradients within the A/E horizon and vertical total potential gradients from the A/E to B soil horizon within the forest hillslope, during 1987.

	TOTAL POTENTIAL GRADIENTS (dϕ/dL)						
JULIAN DATE	0 EB	02.5E	2.5EB	2.55E	5EB	510E	10EB
282.49	-0.533	-0.468	-0.867	-0.104	-1.467		
312.50	-0.400	-0.452	+2.133	-0.080	-2.200	-0.458	-0.200
313.58	-2.067	-0.488	-1.200	-0.096	-1.667	-0.440	-0.400
314.35	-2.533	-0.464	-1.667	-0.100	-2.000	-0.436	-0.333
314.53	-2.533	-0.476	-1.067	-0.108	-2.200	-0.434	-0.467
314.66	-2.467	-0.480	-1.067	-0.108	-2.067	-0.434	-0.467
315.47	-1.733	-0.476	-0.733	-0.108	-2.000	-0.434	-0.267
315.59	-1.467	-0.476	-0.733	-0.104	-1.267	-0.438	-0.267
316.40	-0.667	-0.476	-0.733	-0.104	-1.867	-0.440	-0.400
319.36	-0.800	-0.508	-0.800	-0.108	-3.000	-0.434	-0.067
323.50	-0.533	-0.464	-0.600	-0.116	-1.533	-0.436	-0.200
323.57	-0.533	-0.464	-0.733	-0.112	-1.400	-0.436	-0.200
323.69	-0.467	-0.464	-0.600	-0.112	-1.333	-0.438	-0.200
323.87	-0.467	-0.464	-0.667	-0.108	-1.333	-0.440	-0.267
324.43	-0.400	-0.468	-0.867	-0.112	-1.733	-0.432	-0.200
324.58	-0.533	-0.452	-1.000	-0.120	-1.867	-0.430	-0.267
326.57	-0.467	-0.472	-1.667	-0.084	-2.000	-0.246	+6.400
326.70	-1.200	-0.472	-1.667	-0.080	-1.933	-0.450	-0.333
331.63	-1.867	-0.456	-1.800	-0.084	-1.667	-0.472	-0.867

by convention: - = **downslope** and down-profile gradients and + = **upslope** and up-profile gradients.

OEB = E to B horizon at 0 m upslope, 02.5E = E horizon between 0 and 2.5 m upslope, 2.5EB = E to B horizon at 2.5 m upslope, 2.55E = E horizon between 2.5 m and 5 m upslope, 5EB = E to B horizon at 5 m upslope, 510EB = E horizon between 5 and 10 m upslope, 10EB = E to B horizon at 10 m upslope.
JULIAN DATE = Julian day + decimal time (for 1987) + 365 (for 1988)

Table 41. Lateral total potential gradients within the E horizon and vertical total potential gradients from the E to B soil horizon within the forest hillslope, during 1988.

	TOTAL POTENTIAL GRADIENTS (dϕ/dL)						
JULIAN DATE	0EB	02.5E	2.5EB	2.55E	5EB	510E	10EB
377.58	-1.733	-0.444	-0.867	-0.104	-1.533	-0.446	-0.267
396.57	-2.467	-0.460	-0.667	-0.108	-1.667		
397.43	-2.133	-0.460	-0.600	-0.108	-1.867	-0.428	-0.000
398.54	-1.067	-0.460	-0.533	-0.108	-1.667	-0.432	-0.067
417.56	-2.333	-0.448	-1.600				-0.467
426.68	-2.267	-0.440	-1.400	-0.116	-2.133	-0.474	-0.400
438.64	-3.467	-0.384	-0.733				-0.200
439.44	-2.000	-0.380	-0.667	-0.160	-2.467	-0.412	-0.333
440.46	-2.067	-0.356	-0.267				-0.400
473.58	-5.533	-0.352	-1.267	-0.044	-2.933	-0.444	-0.267
474.40			-1.467	-0.060	-3.200	-0.444	-0.467
482.68	-6.267	-0.292	-3.533	-0.140	-3.400	-0.448	-0.867
485.48	-5.800	-0.296	-2.933	-0.160	-3.400	-0.450	-0.733
487.50	-6.333	-0.300	-3.000	-0.156	-3.400	-0.452	-0.600
488.63	-7.533	-0.376	-1.200	-0.132	-4.133	-0.372	-0.667
490.38	-5.267	-0.368	-0.733	-0.160	-2.733	-0.392	-1.000
497.62	-7.467	-0.248	-3.200	-0.176	-3.933	-0.460	-1.400
508.53	-9.333	+0.020	-19.000	-0.380	-9.067	-0.554	-2.867
509.41	-10.267	+0.396	-17.400	-0.748	-11.267	-0.580	-3.867
509.69	-3.667	+0.436	-17.667	-0.800	-12.133	-0.560	-3.400
510.40		-0.384	-31.800	+0.200	-3.867	-0.548	-4.000
510.77		-0.392	-20.800	+0.008	-1.333	-0.440	-4.067
511.58	-2.600	-0.376	-7.067	-0.108	-5.000	-0.408	-3.533
512.35	-1.600	-0.396	-4.933	+0.080	-2.533	-0.524	-3.933
512.46	-5.667	-0.372	-4.867	+0.100	-0.200	-0.550	-4.133
517.76	-1.867	-0.388	-0.867	-0.048	-1.000	-0.476	-0.333
519.53	-2.800	-0.376	-1.267	-0.080	-1.867	-0.454	-0.400
520.49	-2.867	-0.368	-1.400	-0.100	-2.067	-0.450	-0.267
529.46	-3.333	-0.372	-2.267	-0.088	-3.800	-0.442	-0.533
539.32	-2.867	+0.048	-2.267	-0.712	-11.867	-0.354	-1.933
618.42	-4.133	-0.328	-1.600	-0.104	-2.333	-0.446	-0.467

see Table 40 for key.

Table 42. Lateral total potential gradients within the A/E horizon and vertical total potential gradients from the A to B soil horizon within the ploughed section of the grassland hillslope (1987-1988).

	TOTAL POTENTIAL GRADIENTS (dϕ/dL)		
JULIAN DATE	40AB	4020A	20AB
282.4931	+3.867	-0.412	+1.800
312.4583	-0.800	-0.426	-0.933
313.6375	-1.333	-0.428	-1.467
314.3153	-1.067	-0.427	-0.800
314.5014	-0.933	-0.426	-1.267
314.5420	-0.800	-0.427	-1.133
314.6563	-0.933	-0.426	-1.067
315.4375	-1.133	-0.426	-1.733
315.5417	+0.333	-0.425	-0.467
315.6563	-0.533	-0.427	-0.467
316.3750	-1.067	-0.428	-1.267
319.3403	-0.733	-0.426	-0.800
323.4938	-0.267	-0.423	-0.867
323.5194	-0.933	-0.427	-0.933
323.5847	-0.733	-0.427	-1.000
323.6715	-1.733	-0.428	-0.933
323.8764	-1.200	-0.428	-0.867
323.4361	-1.200	-0.429	-1.333
324.5917	-1.200	-0.429	-1.400
326.5806	-1.667	-0.426	-2.533
326.7160	-1.467	-0.427	-2.200
332.6910	+0.400	-0.428	-0.933
485.5410	+4.067	-0.425	+1.933
487.4931	+0.267	-0.405	-4.733
488.5757	+0.533	-0.420	-2.133
490.5139	-2.800	-0.424	-1.733
497.6042	+4.733	-0.444	+4.800
508.5556	+9.200	-0.630	+32.933
509.3959	+9.467	-0.648	+35.600
509.6715	+10.333	-0.653	+37.200
510.4319	+0.533	-0.448	+0.800
510.7861	-0.533	-0.421	-2.667
511.6181		-0.430	-1.133
512.3729	-0.933	-0.423	-3.200
517.7431	+1.400	-0.420	-1.000
519.5674	+1.267	-0.424	-1.733
530.4306	+3.733	-0.433	+2.267
531.5000	+5.733	-0.464	+8.267
539.5764	+11.200	-0.612	+32.067

40AB = A to B horizon at 40 m upslope; 4020A = A horizon 40 to 20 m upslope; 20AB = A to B horizon at 20 m upslope. See also key for Table 40.

6.3.6. The Impact of Individual Trees upon the Capillary Potential (ϕ_c) and Potential Gradients ($d\phi/dL$ or J) within the Forest Hillslope.

As tree roots have been shown to localize both the abstraction and infiltration of water (Section 1.5.2), then the impact of trees upon soil water potentials during dry periods, may be distinct from the impacts during wet or storm-periods.

Dry Period Impacts: As the forest soil dries out, the soil directly beneath individual conifers develops much greater negative capillary potentials (or suctions) when compared with the soil 1 to 2 m away from individual trees. Figure 45 shows that the B/C soil horizon almost directly beneath a large conifer (47 cm DBH) dried out to -550 cm on 23 May 1987 (Sections 6.3.4. and 6.3.5), while the B/C soil close to a buttress root of a small conifer (29 cm DBH) attained -150 cm, and at 1.5 m downslope of the same small tree attained only -67 cm. This implies that the localization of moisture abstraction by tree roots, particularly beneath large conifers, can be significant.

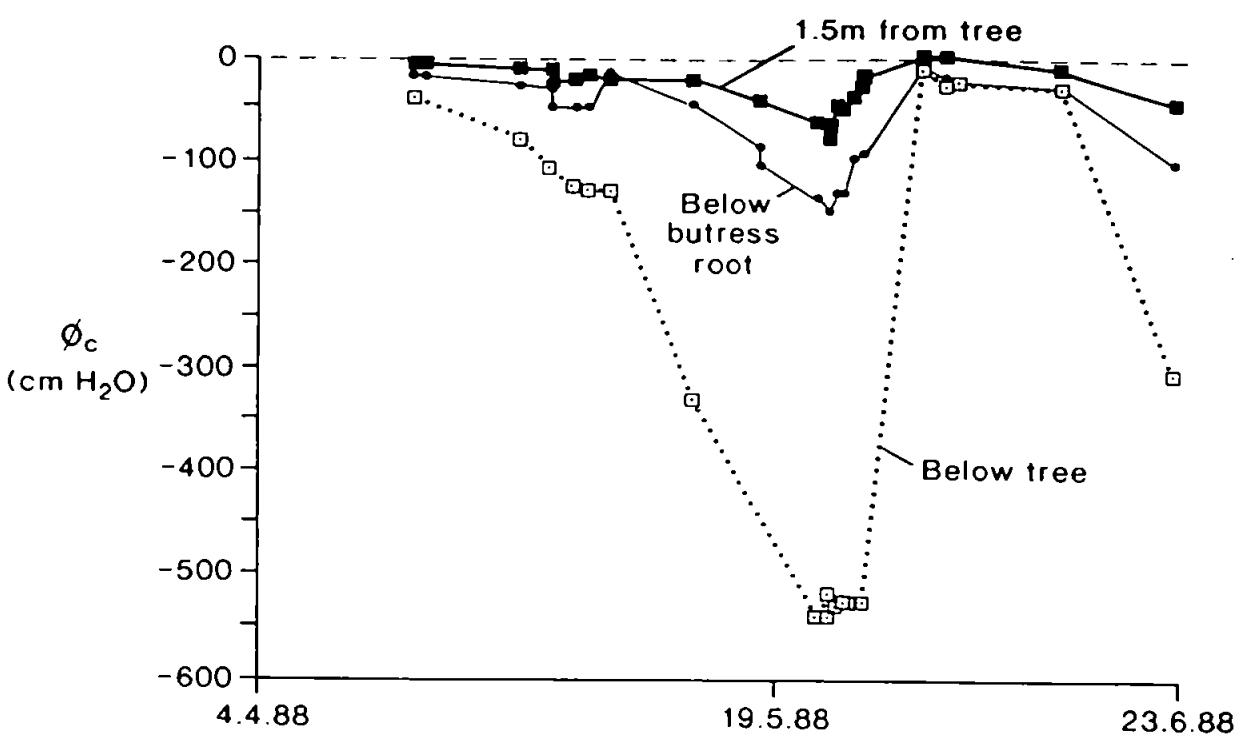

Figure 45. Capillary potential within the B/C horizon (45 cm depth) beneath a large tree (47 cm DBH), beneath the buttress root of a small conifer (29 cm DBH), and 1.5 m downslope of the same small conifer.

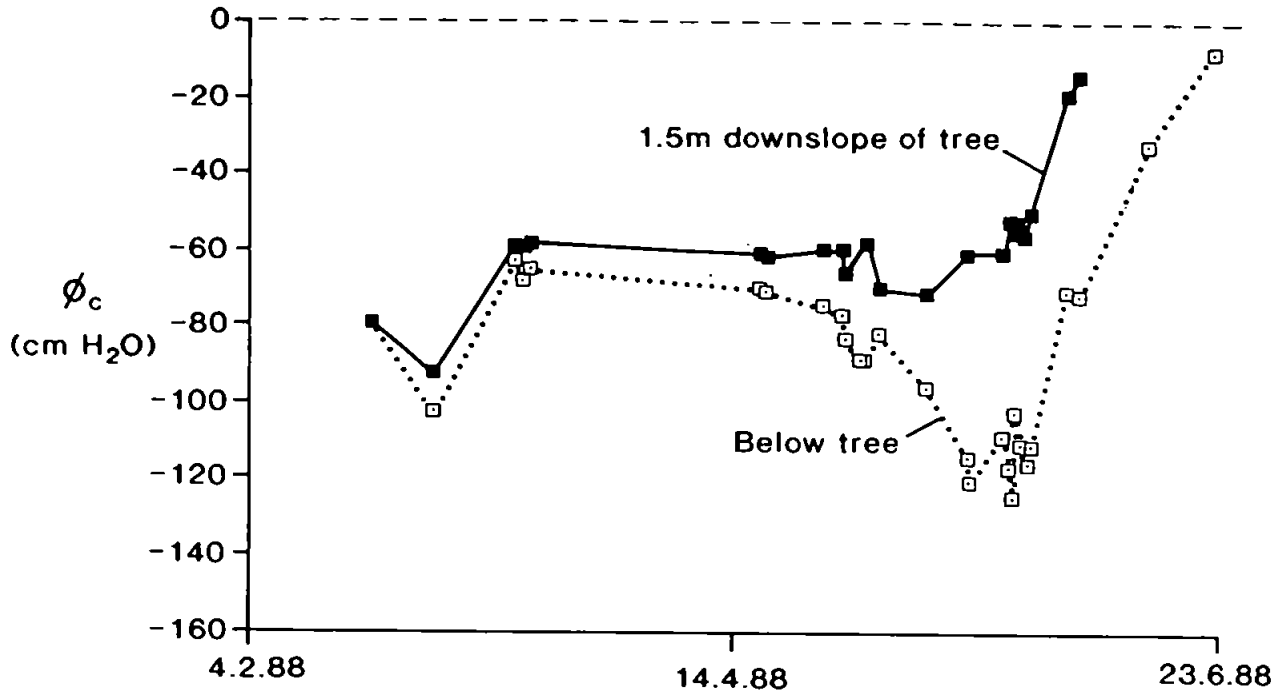

Figure 46. Capillary potential at a depth of 1 m beneath a small conifer (29 cm DBH), and at the same depth, but 1.5 m downslope of the small conifer.

During the same dry period, the regolith at a depth of 1 m immediately beneath a small conifer experienced significant drying, and yet seemed almost unaffected only 1.5 m downslope of the same tree (Figure 46). This implies that either:

1. water is being preferentially abstracted from the soil well below the platy root system of the Sitka spruce (*Picea Sitchensis*, Bong. Carr.) tree (Section 1.5.2). The sinker roots of Norway spruce (*Picea abies*) trees have been shown to abstract considerable volumes of water from a depth of 1 m in similar silt loam soils (Messenger, 1980).
2. the regolith beneath the tree is draining faster than that within inter-tree areas, as a result of an increased hydraulic conductivity beneath the individual tree (Section 7.4.4).

During the 4 month period 21 February to 22 June 1988, the vertical potential gradients (A/E to B/C soil horizon) were always greater directly beneath a single conifer compared with those between conifers (Figure 47). Moreover, the potential gradients always directed flow downwards. The difference was most pronounced when the hillslope soil was at its driest, and during rapid wetting at the end of this dry period (Figure 48).

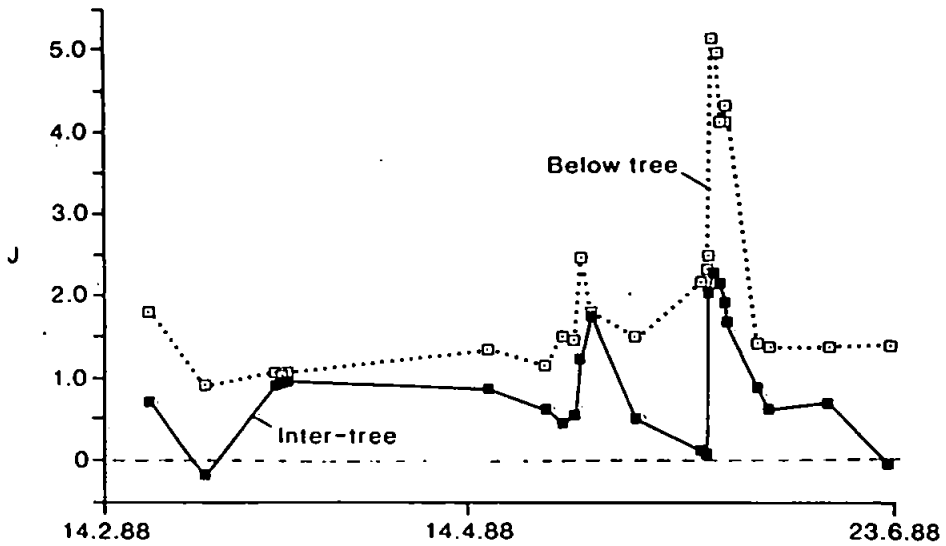

Figure 47. Vertical potential gradients between the A/E and B/C horizons of the forest hillslope, beneath two small conifers (29 and 30 cm DBH), and within the area in between the two conifers (1.5 m away from both conifers). Each line represents the average gradient between three pairs of tensiometers.

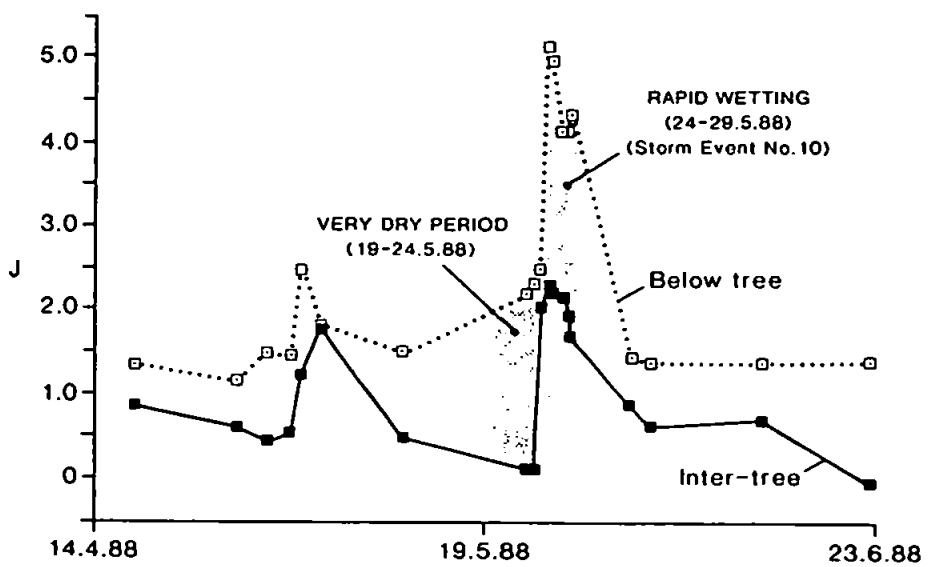

Figure 48. Periods in which the largest differences in vertical potential gradients beneath conifers and those within inter-tree areas (see Figure 46) were monitored.

During dry periods, this would imply that either:

1. the trees are abstracting more water from the B/C horizon relative to the A/E horizon,
2. drainage from the profile beneath the tree is greater than the rate of abstraction by tree roots. This would imply an increase in conductivity (see Sections 7.4.4. and 8.2.3).
3. there is an increase in lateral flow beneath individual conifers during dry periods (see Figure 44; Section 8.2.2.)

Storm Period Impacts: During the two storm-periods shown within Figure 49, the A/E horizon beneath the two small conifers (29 and 30 cm DBH) became saturated ($\phi_c = 0$), while the A/E horizon within the inter-tree area remained slightly under-saturated. This preferential wetting beneath the tree was probably caused by the large volumes of stemflow, observed running down these small conifers. As the deeper B/C horizon beneath the same tree failed to saturate, remaining drier than the B/C horizon within the inter-tree area (Figure 50), the preferential wetting of the sub-tree A/E horizon may have increased lateral flow rather than vertical flow. This would support Molchanov (1960), who suggested that lateral flow above the B horizon rather than vertical flow into the B horizon, was promoted beneath spruce trees, as a result of their *flat* root systems. A further study described by Hillman (1972) indicated that beneath a single white spruce (*Picea glauca*) growing within a gently sloping, homogenous sandy loam, lateral potential gradients were larger than the vertical potential gradients. This study is emphasised as vertical flow might have been expected given the homogeneity of the soil (Section 6.3.5).

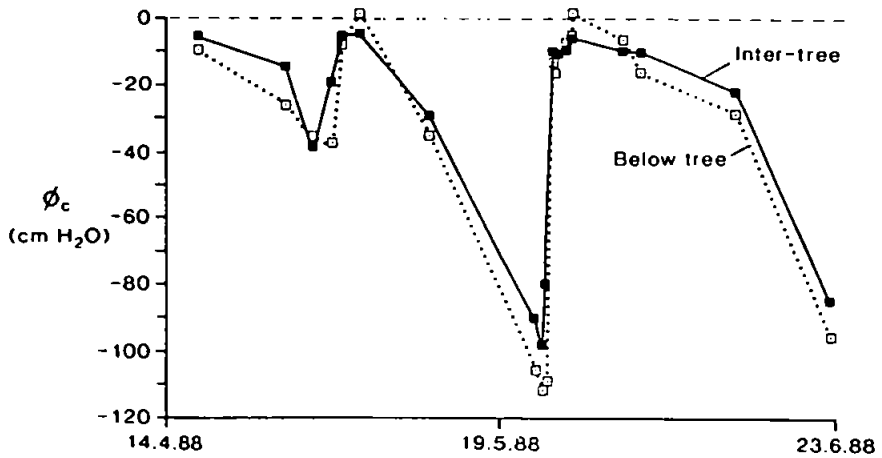

Figure 49. Capillary potentials of the below-tree and inter-tree A/E horizon, during two storm events (Storm 9 (part 2) and 10). Each line represents an average capillary potential monitored by three tensiometers.

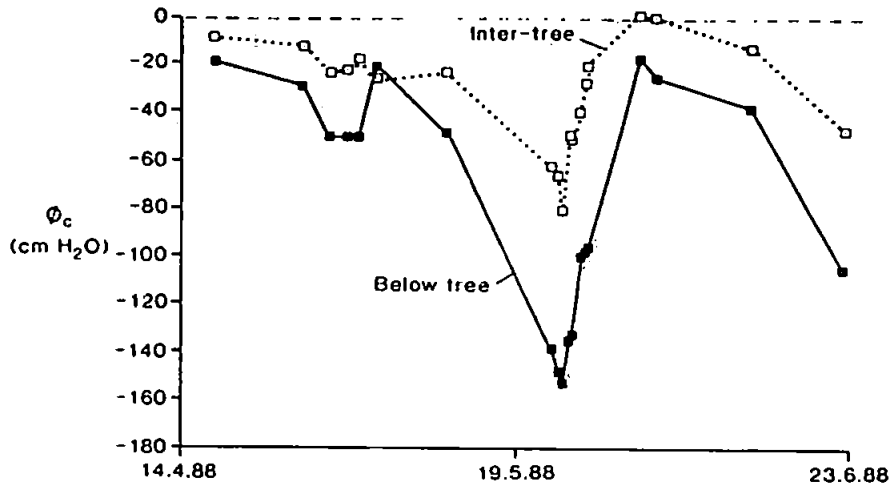

Figure 50. Capillary potentials of the below-tree and inter-tree B/C horizon, during two storm events (Storm 9 (part 2) and 10). Each line represents an average capillary potential monitored by three tensiometers.

The impact of individual trees upon the average moisture regime of the forest hillslope is examined in Section 6.2.6., and the impact upon the saturated hydraulic conductivity (K_s) and intrinsic permeability (k) is examined in Section 7.4.4.

CHAPTER 7.

Hillslope Hydrological Parameters.

7.1. Introduction.

Those physical properties which must be *parameterized* (i.e. made a unique function of the hydrological variables presented in Chapter 6) to calculate water flux by Richards' Approximation include the soil bulk density, porosity (Section 7.2), specific moisture capacity (Section 7.3), hydraulic conductivity (saturated, relative and state-dependent), fluid viscosity, and intrinsic permeability (Section 7.4). The spatial and temporal response of each these individual parameters within hillslopes, may be important controls on the pathways of soil water.

7.2. Soil Bulk Density (ρ_b) and Porosity (η).

A soil's porosity (η) will affect the quantity of water a soil volume can hold (i.e. the soil moisture content: Section 6.2), and, therefore, the relationship between the moisture content and the capillary potential (Section 7.3). A soil volume's resistance to the conduction of fluids (i.e. the inverse of the soil's intrinsic permeability) is also dependent upon the volume of pores (Bear, 1972; Childs, 1969; Kozeny, 1927; Section 7.4). The dry bulk density (or specific mass: ρ_b) of a soil volume is a function of the particle density (ρ_p) and the porosity (η), i.e.

$$\rho_b = \rho_p - (\eta \cdot \rho_p)$$

When the particle density is known, measurements of bulk density can, therefore, be used to predict the porosity. Bulk density measurements are more commonly used to calculate the volumetric moisture content (θ_v) from direct measurements of the mass wetness (θ_m) determined by gravimetric techniques (Section 4.4.2., 6.2). Where:

$$\theta_v = \theta_m \cdot \rho_b$$

The bulk density of both the forest and the grassland hillslope soils increases quite markedly with depth (Figure 51). The organic horizon on the surface of the forest soil (i.e. 0-8 cm) is much less dense (0.10-0.24 g cm^{-3}) than the surface organic horizon in the grassland (0.69 g cm^{-3}). This probably relates to the forest O/A horizon's lower particle density resulting from a greater proportion of organic matter relative to mineral soil, rather than the slightly increased porosity (Figure 52).

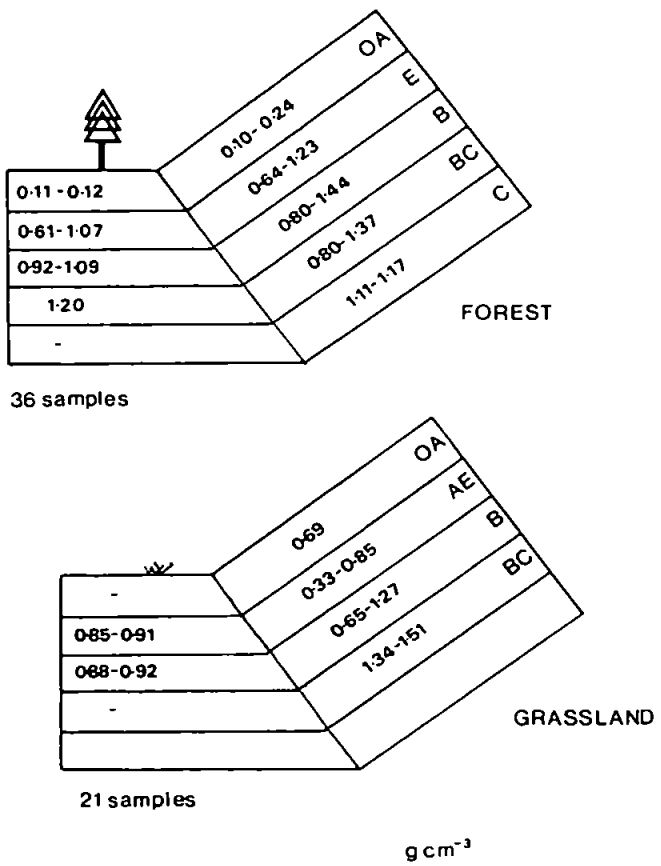

Figure 51. Range in bulk density within each soil horizon of the podzolic slopes and riparian zones, of the forest and grassland hillslopes.

The porosity values for each soil horizon within the two research hillslopes range from 0.41 to 0.78 cm^3 cm^{-3} (Figure 52); both hillslopes are generally very porous. Porosity values at both sites are very high in the organic horizons (0.71-0.78 cm^3 cm^{-3}), high within the A/E horizon (0.63-0.72 cm^3 cm^{-3}) and slightly less within the B horizon (0.44-0.66 cm^3 cm^{-3}: B horizon).

Three soil samples taken from a 1 m^2 plot beneath the ploughed section of the grassland showed a greater variability in the B horizon porosity (0.442, 0.530, 0.623S cm^3 cm^{-3}) relative to the A/E horizon (0.633, 0.662, 0.652 cm^3 cm^{-3}) probably as a result of the ploughing operation (Section 2.10.2).

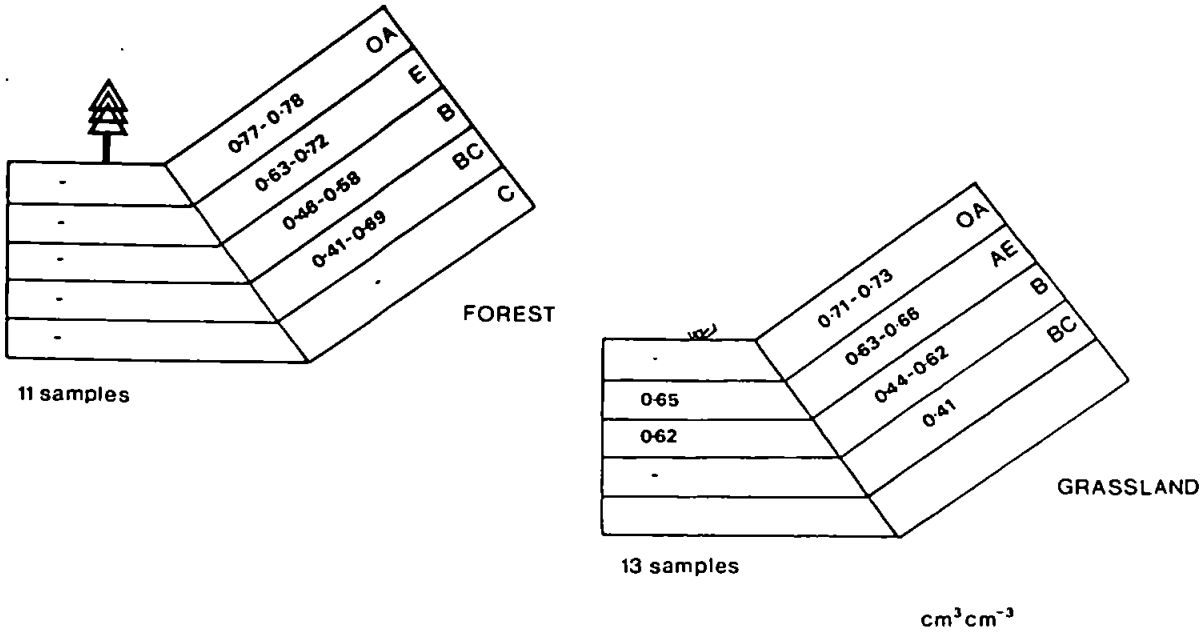

Figure 52. Range in porosity within each soil horizon of the podzolic slopes and riparian zones, of the forest and grassland hillslopes.

Similar low bulk densities and high porosities as those within the Tir Gwyn hillslopes were noted by Molchanov (1960) within a *brown forest soil* beneath a spruce stand in Bulgaria (Table 43)

Table 43. Bulk densities and porosities of brown forest soil, beneath a spruce stand in the Begliki district of Bulgaria (Molchanov, 1960).

Depth of sample (cm^3)	Soil Bulk Density (g cm^{-3})	Porosity (cm^3 cm^{-3})
0-14.6	0.588	0.770
10-14.6	0.844	0.680
25-29.6	0.862	0.660
40-44.6	0.934	0.660
70-74.6	1.081	0.620

7.3. Specific Moisture Capacity (θ/ϕ_c) and Secondary-Porosity ($\eta_{\phi 50}$).

The flow of water is equal to the specific moisture capacity (θ/ϕ_c, or C) multiplied by the change in capillary potential with time ($d\phi_c/dt$), given that the relationship between the moisture content and capillary potential is constant (Buckingham, 1907; Fuchsman, 1986; Richards, 1931).

A soil's ability to retain or release water at a given capillary potential affects soil-water-movement, as it determines the rate at which the hydraulic conductivity declines as the level of water-saturation reduces (Brooks and Corey, 1966; Campbell, 1974; Millington and Quirk, 1959; Sections 7.4.6. and 7.4.7). A rapid release of moisture, means that conductivity is soon lost as the level of water-saturation reduces.

The impact these moisture-release-curve *slopes* upon moisture-flux within each soil horizon is discussed within Section 7.4.6.

7.3.1. Laboratory versus *In Situ* Determination of θ/ϕ_c.

A total of 26 moisture capacity curves were determined in the laboratory, and a further 36 were determined in the field (Section 4.4.4). All of the field (or *in situ*) determined specific moisture capacities are similar to those capacities determined using tension table and pressure-plate apparatus within the laboratory (e.g. Figures 53, 54, 55 and 56).

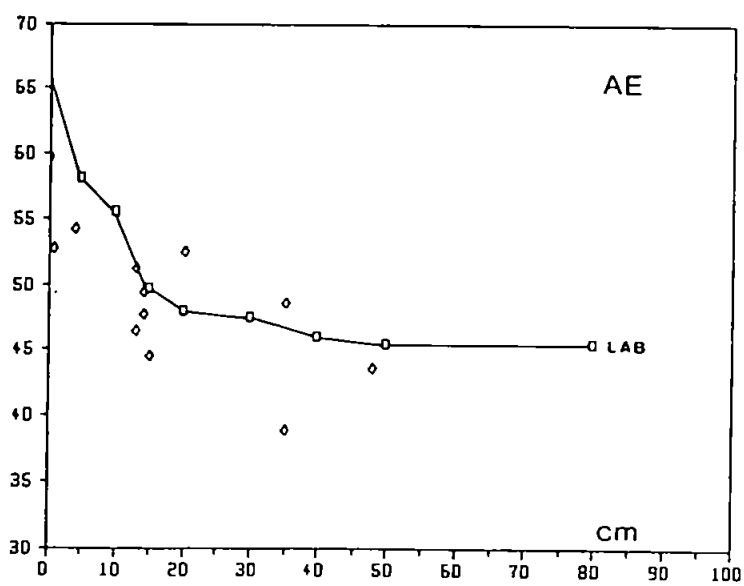

Figure 53. Moisture capacity within the A/E horizon of the forest hillslope (5 m position), determined by both *in situ* (5F15) and laboratory (C5F12-15E) based techniques.

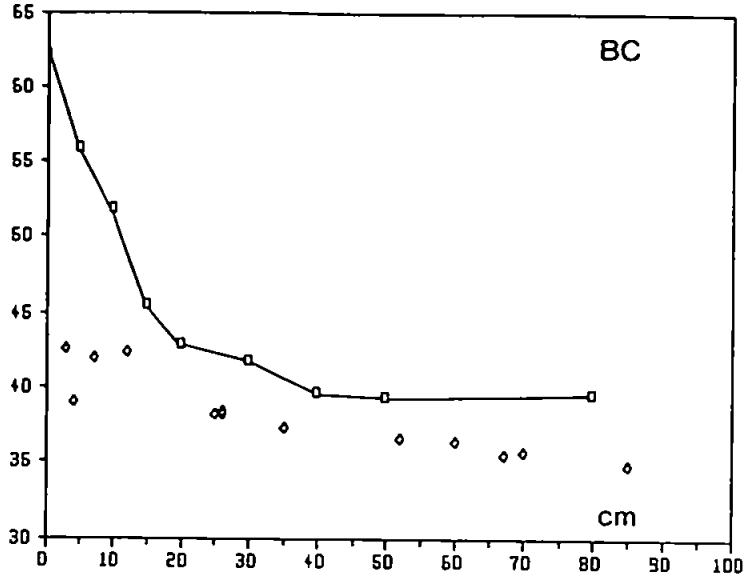

Figure 54. Moisture capacity within the B/C horizon of the forest hillslope (5 m position), determined by both *in situ* (5F45) and laboratory (C5F29-32BC) based techniques.

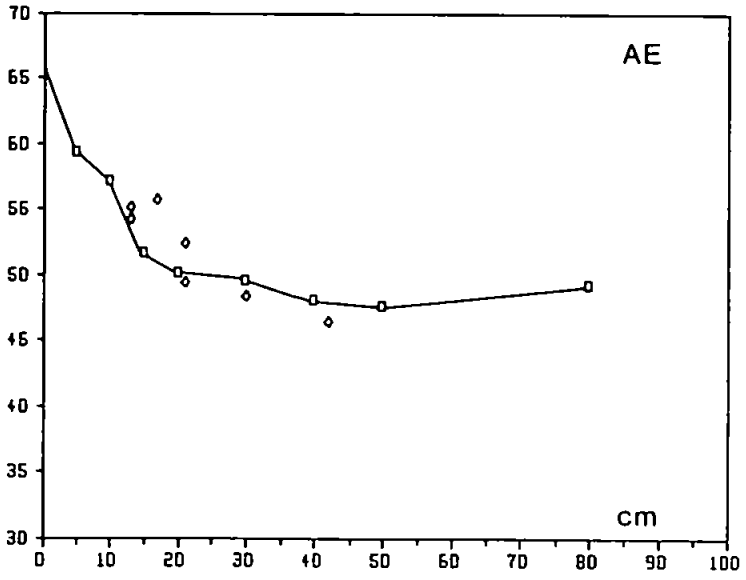

Figure 55. Moisture capacity within the A/E horizon of the grassland hillslope (40 m position), determined by both *in situ* (40G15) and laboratory (C40G14-17A3) based techniques.

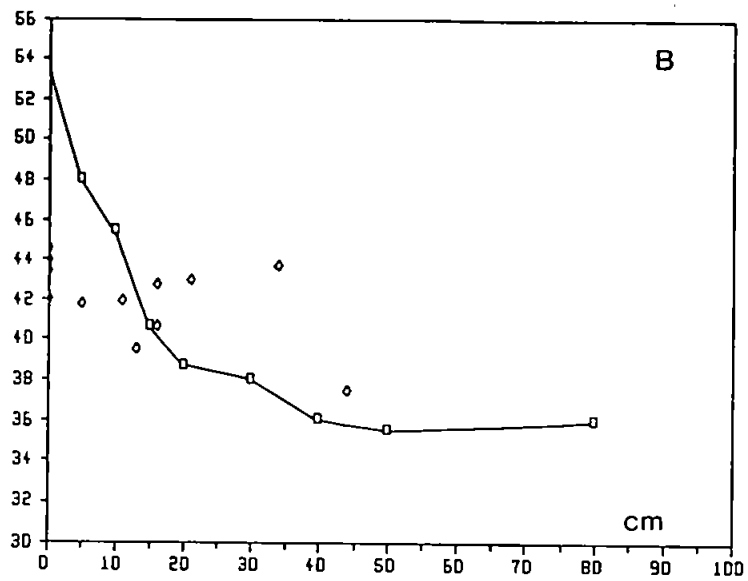

Figure 56. Moisture capacity within the B horizon of the grassland hillslope (40 m position), determined by both *in situ* (40G30) and laboratory (C40G30-33B2) based techniques.

The moisture capacities determined *in situ* at each slope position on the forest hillslope were more *noisy* or showed a less consistent trend within the A/E horizon (e.g. Figure 53) in comparison with the forest B/C horizon (e.g. Figure 54). This may be due to either:

1. the increased variability within the *apparent* moisture contents of the A/E horizon relative to the B horizon, caused by the errors associated with the use of a neutron probe close to the soil surface (Lawless *et al*, 1963; Ziemer *et al*, 1967), or
2. the non-uniform wetting of the A/E horizon relative to the B horizon, caused by a highly structured nature of the eluvial horizon of a ferric podzol soil (Sections 7.3.4. and 7.4.1).

Although the *in situ* determination of the moisture capacity within the grassland A/E horizon is subject to the same neutron gauging errors, it is the B horizon which shows the least consistent trend (Figures 55 and 56). Perhaps the action of drawing a single plough tine across the grassland field (Section 2.10.2), has either:

1. greatly increased the secondary-structure within the B horizon so that the soil horizon wets unevenly, or
2. over-turned or tilted the natural soil horizons, allowing the 30 cm tensiometer to be installed within a different soil to that surrounding the neutron probe access-tube.

An increase in spatial variablity in the B horizon of the ploughed, grassland hillslope was also noted with the porosity measurements (Section 7.2).

A *hysteretic* difference (Section 4.4.4) between the *in situ* moisture capacities during soil wetting and those during soil drying was not observed. Moreover, marked *threshold potentials* (or *air entries*) were not observed within either the laboratory- or field-determined moisture capacity curves (Section 4.4.4.; e.g. Figure 57).

7.3.2. Variability in Laboratory-determined Moisture Capacities.

Moisture was released at a similar rate from all of the cores of soil taken from the B and B/C horizons of the grassland hillslope (Figure 57). The actual moisture contents retained by each soil core at a given capillary potential were, however, very different in relation to the variation of the moisture retention of the samples taken from the A/E horizon (Figure 57).

The same pattern of a greater variability within the B/C horizon relative to the A/E horizon was noticed within the samples taken from the forest hillslope.

Given that the variability is present only within θ/ϕ_c-curve *intercepts* or *offsets*, and not within the *slopes* of the θ/ϕ_c-curves, the difference is likely to have resulted from the B and B/C horizon's increased sensitivity to disturbance during sampling (Nieber and Walter, 1981). The increased sensitivity to the disturbance of the shalely B/C horizon is a possible explanation for some of the errors within the gravimetric calibrations of the neutron probe (Section 6.2.1) and the small-core permeametry (Section 7.4.1).

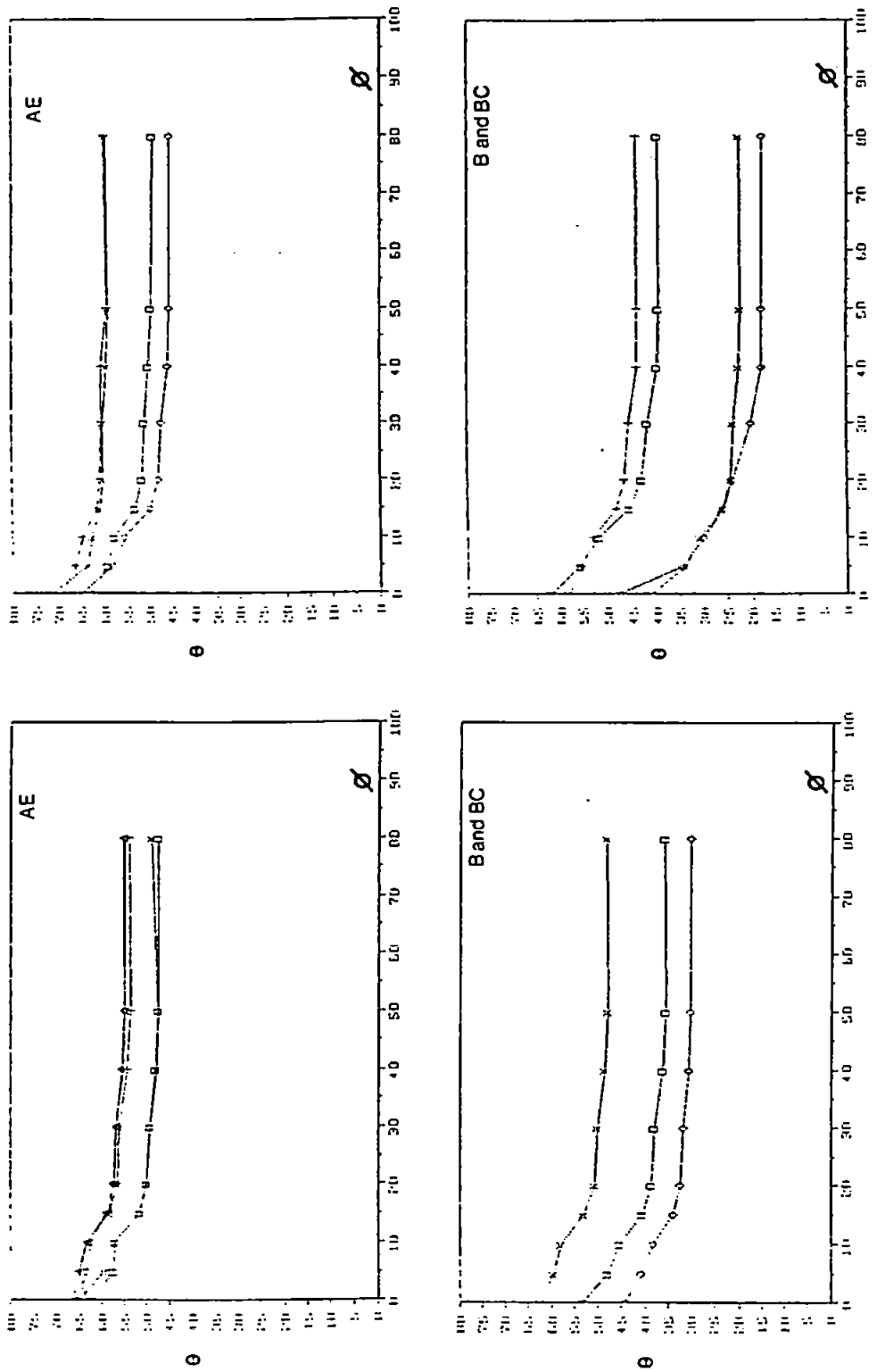

Figure 57. Variability of laboratory-determined moisture capacities within the A/E, B and B/C horizons of the forest (top) and grassland (bottom) hillslopes (θ $cm^3 cm^{-3}$ x 100; ϕ_e cm)

7.3.3. Moisture Capacity of Each Soil Horizon within the Forest and Grassland Hillslopes.

When the soil within both the forest and grassland hillslopes is near saturation, i.e. maintaining capillary potentials of between 0 and -20 cm, the moisture retention is highest within the O/A horizon, and decreases down through the profile (i.e. the rank from highest to lowest is (1) O/A, (2) A/E, (3) B, and (4) B/C; Figure 58). This order is maintained within all soil horizons (with the exception of the O/A horizon within the forest hillslope) up to capillary potentials of approximately -1500 to -2000 cm, well in excess of those potentials observed during the monitoring period. The organic or O/A horizon within forest hillslope loses water very rapidly (per unit change in small capillary potentials), so that it retains less water than the forest and grassland A/E horizons after -20 to -30 cm, and less water than the forest B horizon after -220 cm (Figures 58 and 59).

Such a decrease in the moisture retention down through the profile is due partly to the increase in the stone content and partly to the decrease in the number of large and medium sized pores.

Over the range of approximately 0 to -500 cm ϕ_c, the grassland A/E horizon retains as much water as the A/E horizon within the forest. As the potential increases, however, the grassland A/E horizon is not able to retain as much water as the forest E horizon. At capillary potentials greater than -1500 to -2000 cm the A/E horizon within the grassland retains less water than the forest B horizon, and less than the grassland B horizon after -3500 to -4000 cm (Figure 59). Ploughing may, therefore, have improved the drainage characteristics of the soil which comprises the A/E horizon.

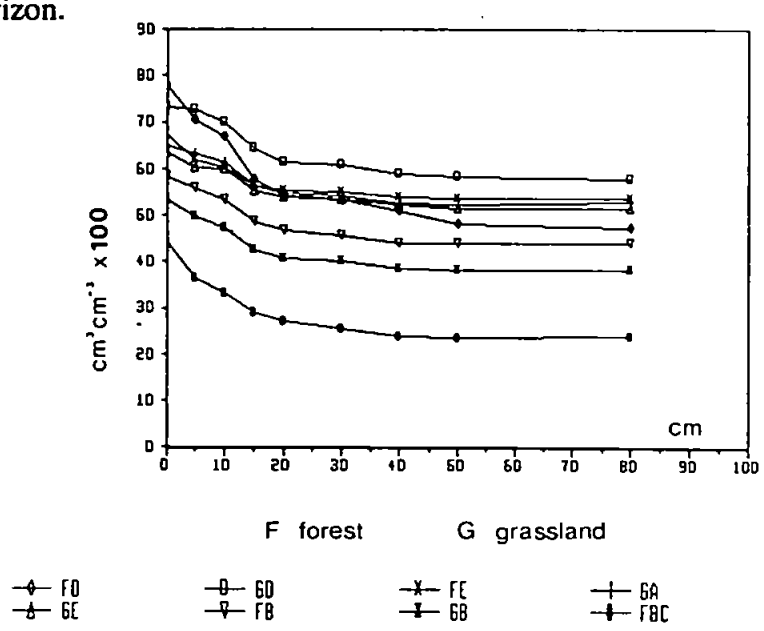

Figure 58. Mean moisture capacities within each horizon of the forest and grassland hillslopes, over a range of 0 to -100 cm capillary potential.

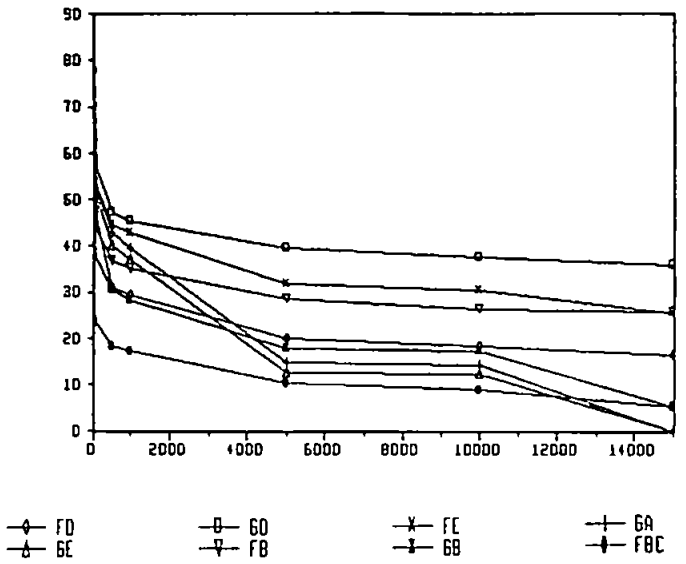

Figure 59. Mean moisture capacities within each horizon of the forest and grassland hillslopes, over a range of 0 to -15,000 cm capillary potential.

Although the A/E horizon within the forest loses water more quickly than the B horizon at these relatively high potentials, it always retains more water over the determined range of 0 to -15,000 cm (Figure 59). This high moisture retention within the A/E horizon of an un-improved ferric podzol relative to the B horizon may be the result of enhanced chlorite-breakdown and rock de-cementation within the A/E horizon, coincident with podzolization on Silurian shales (Adams *et al*, 1971; Adams and Raza, 1978).

A capillary potential of -15,000 cm is usually defined as the *permanent wilting-point* (Marshall and Holmes, 1979). At this value, the rank of moisture retention within each soil horizon, from highest to lowest is: (1) grassland O, (2) forest A/E, (3) forest B, (4) forest O, (5) grassland B, (6) grassland A /E, and (7) forest B/C (Figure 59).

7.3.4. Parameterization of the Moisture Capacity Curves.

The mean moisture capacity curve for the A/E and B soil horizons within the forest and grassland hillslopes were parameterized by:

1. compound log-log functions,
2. cubic splines,
3. Mualem's (1976) equation.

1. Log-Log Parameterization: The simplest means of describing the moisture capacity curves can be achieved by fitting compound log-log functions. The mean moisture capacity curve for the forest and grassland A/E horizon can be represented by the three log-log functions over the range 0 to -1000 cm:

$$\theta_{\text{forest E}} = 63\phi_c^{-0.015}_{(0\text{-}5\text{ cm})} \; ; \; 69\phi_c^{-0.07}_{(5\text{-}50\text{ cm})} \; ; \; 75\phi_c^{-0.085}_{(50\text{-}1000\text{ cm})}$$

$$\theta_{\text{grassland A}} = 63\phi_c^{-0.045}_{(0\text{-}5\text{ cm})} \; ; \; 69\phi_c^{-0.07}_{(5\text{-}50\text{ cm})} \; ; \; 74\phi_c^{-0.085}_{(50\text{-}1000\text{ cm})}$$

The parameters representing these two curves are very similar. The mean moisture capacity curves for the B horizon beneath the grassland can be represented by a further three log-log functions over the range 0 to -1000 cm:

$$\theta_{\text{grassland B}} = 50\phi_c^{-0.012}_{(0\text{-}5\text{ cm})} \; ; \; 59\phi_c^{-0.12}_{(5\text{-}50\text{ cm})} \; ; \; 59\phi_c^{-0.11}_{(50\text{-}1000\text{ cm})}$$

The moisture release of the B horizon within the forest is less non-linear, in comparison with the other soil horizons within both hillslopes. It is represented by a single log-log function over the range 5-15,000 cm. This may imply that the forest B horizon is less structured or *cracked* in comparison with the other horizons (Section 7.3.1.; Demond and Roberts, 1987). The moisture capacity of the forest B horizon varies from this simple relationship only close to saturation (i.e. 0-5 cm):

$$\theta_{\text{forest B}} = 56\phi_c^{-0.0069}_{(0\text{-}5\text{ cm})} \; ; \; 65\phi_c^{-0.1}_{(5\text{-}15{,}000\text{ cm})}$$

Compound logarithmic functions have also been used by Talsma (1974) to fit a $K\text{-}\phi_c$ curve (Section 7.4.7) over a range 0 to -1,500 cm.

2. Cubic Spline Parameterization: The moisture capacity curves used to calculate the relative hydraulic conductivity using the Millington-Quirk technique were parameterized using a *cubic spline* (Erh, 1972; Bruce and Luxmoore, 1986; Section 7.4.6). The relative hydraulic conductivities based upon these parameters are presented within Figure 66 .

3. Mualem Parameterization: The alternative Van Genuchten procedure for the determination of relative hydraulic conductivity is based upon Mualem's (1976) parameterization of the moisture capacity curve: i.e.

$$AWS = \frac{\theta_v - \theta_{vr}}{\theta_{vs} - \theta_{vr}} = \left\{ \frac{1}{1 + (a\phi_c)^n} \right\}^m \qquad [22]$$

given: $m = 1 - 1/n \; ; \; 0 < m < 1$ (Van Genuchten, 1980)

where AWS is available water saturation (dim. $L^3\ L^{-3}$), θ_v is volumetric moisture content at ϕ_c (dim. $L^3\ L^{-3}$), θ_{vr} is residual volumetric moisture content (dim. $L^3\ L^{-3}$), θ_{vs} is volumetric moisture content at saturation (dim. $L^3\ L^{-3}$), ϕ_c is capillary potential (dim. L), and a,m,n are shape parameters.

The parameters fitted to the mean moisture capacity curves of the A/E and B horizons are:

Forest B : a = 0.17, n = 1.25, m = 1.250
Grassland A : a = 0.20, n = 1.11, m = 0.100
Grassland B : a = 0.25, n = 1.20, m = 0.167

The relative hydraulic conductivities based upon these parameters are presented within Figure 68.

7.3.6. Secondary-Porosity ($\eta_{\phi s0}$).

A simplified form of the the Kelvin Equation can be used to estimate the size of pores which will have drained at a given capillary potential (Hanks and Ashcroft, 1980; Scheidegger, 1957):

$$r = - \frac{2 \cdot Y \cdot \cos \zeta}{\phi_c}$$

where r is equivalent radius of largest pore (dim L), Y is surface tension of water (dim. ML^{-1}), ζ is water-soil contact angle (dim. degrees), and ϕ_c is capillary potential (dim. ML^{-1}).

Pores which lose water at capillary potentials between 0 cm and -10 to -1000 cm (Beven and Germann, 1982), have been defined as the *secondary-porosity* (Bouma and Anderson, 1973; Demond and Roberts, 1987; Freeze and Cherry, 1979). Secondary-porosity is analogous to the *aerated porosity* (Bear, 1972), *macro-porosity* (Beven and Germann, 1982; Watson and Luxmoore, 1986), *field capacity* (Bear *et al*, 1968), and *air capacity* (when at -50 cm: Hall *et al*, 1977).

A capillary potential of -50 cm was chosen the separate the total porosity (Section 7.2) into the component *primary-* and *secondary- porosities*, because this appeared to be the inflection point on the moisture capacity curve between rapid drainage at high saturations, and slow drainage at low saturations (Figure 59; Bear, 1972; Childs, 1969). Furthermore, -50 cm represents an effective pore size of approximately 60 vm (0.06 mm), the standard separation of secondary- and primary- porosity used by the Soil Survey of England and Wales (SSEW; Bullock and Thomasson, 1979; Hall *et al*, 1977; Murphy *et al*, 1977a,b).

Numerous authors (e.g. Beven and Germann, 1981; Bouma, 1982; Bouma and Anderson, 1973; Burger, 1922; Childs, 1969; Douglas, 1986; Germann and Beven, 1981a,b; Smettem and Collis-George, 1985a,b,c; Watson and Luxmoore, 1986) have suggested that the hydraulic conductivity (K) of a soil at or close to saturation, is controlled by the absolute volume, geometry and continuity of these *secondary-pores*.

Table 44 shows that difference in the volume of secondary pores within individual soil horizons within the research hillslopes are almost as large as the variability between different soil horizons.

Table 44. Secondary-porosity of 22 samples extracted from the Tir Gwyn, research hillslopes

	SECONDARY POROSITY $cm^3\ cm^{-3}$	
Horizon	Forest Hillslope	Grassland Hillslope
O	0.27 0.32	0.15
A/E	0.10 0.20 0.13 0.13	0.10 0.14 0.11 0.18
B	0.14 0.14 0.18 0.14	0.17 0.14
B/C	0.19 0.30 0.23	0.13 0.16

Either the *total volume* of secondary pores is not the major determinant of saturated hydraulic conductivity, or disturbance of the 59 cm^3 cores during sampling, has significantly affected the secondary porosity.

7.4. Hydraulic Conductivity (K, K_s, K_r) and Intrinsic Permeability (k).

The average flow of water within a volume of soil is equal to the hydraulic conductivity multiplied by the potential (or energy) gradient. Flow passing between soil volumes will change its direction (and hence act over a different soil area) according to the difference between the hydraulic conductivities of the two volumes of soil (Hubbert, 1940; Jacob, 1940; Section 1.4.3).

The hydraulic conductivity (K) of a soil is a compound property dependent upon the soil's intrinsic permeability (k), the density (ρ_f) and viscosity (v) of the fluid (i.e. water), and the relative hydraulic conductivity (K_r) at the given soil moisture content and capillary potential:

$$K = K_s \cdot K_r \qquad [5]$$

$$K_s = \frac{k \cdot \rho_f \cdot g}{v} \qquad [11]$$

where K is hydraulic conductivity (dim LT^{-1}), K_s is saturated hydraulic conductivity (dim. LT^{-1}), K_r is relative hydraulic conductivity of the wetting (i.e. water) phase (dimensionless), k is intrinsic permeability (dim. L^2), ρ_f is fluid density (dim. ML^{-3}), g is gravitational acceleration (dim. LT^{-2}), and v is dynamic fluid viscosity (dim. $ML^{-1}T^{-1}$; $v/\rho_f = v$ kinematic fluid viscosity dim. L^2T^{-1}).

The hydraulic conductivity of each control-volume of soil (Sections 1.4.3. and 3.5.1) must be parameterized (i.e. a *constant* function developed) to solve the Richards Equation for a change in either potential or moisture content (Section 1.4.3.1). However, the spatial variability across the grid of control-volumes can be maintained. Authors have suggested that the variability of hydraulic conductivity between control-volumes within different soil horizons (e.g. Bonell *et al*, 1983a; Section 3.5.4) and at different catenal positions (e.g. Rogowski *et al*, 1974; Section 3.5.3) is a major determinant of hillslope flux. The saturated hydraulic conductivity and intrinsic permeability are, therefore, defined for each soil horizon (Section 7.4.2), and each catenal zone, as defined within Sections 3.5.3. and 4.2 (Section 7.4.2., 7.4.3).

Before any hydraulic conductivity functions can be compared or parameterized for flux calculations, however, the impact of changing fluid viscosities upon the saturated hydraulic conductivity must be standardized. These hydraulic conductivity functions are then calibrated to the field-temperature at each flux calculation.

7.4.1. Fluid Viscosity (v, v) Standardization.

The viscosity of water is dependent upon the temperature. The relationship can be approximated by the function:

$$\mathrm{Log}_{10} \cdot (v_{20}/v_t) = \frac{1.37023 \cdot \{(t\,^\circ C)-20\} + 8.36\times10^{-4} \cdot \{(t\,^\circ C)-20\}^2}{109 + (t\,^\circ C)}$$

(after Atkins, 1978) [23]

where ν is dynamic fluid viscosity (dim. $ML^{-1}T^{-1}$), and ν/ρ_f equals ν or kinematic fluid viscosity (dim. L^2T^{-1}).

The variation in water temperature and subsequent variation in the water viscosity is removed from hydraulic conductivity parameters by standardizing the saturated hydraulic conductivity measurements at 20 °C (Bonell *et al*, 1983a; Iwata *et al*, 1988; Marsily, 1986; Terzaghi and Peck, 1948):

$$K_{s20} = K_{st} \cdot \frac{\nu_t}{\nu_{20}} \qquad [24]$$

NOTE: The ratio of the kinematic viscosities within Equation 24, can be replaced with the ratio of the dynamic viscosities calculated by Equation 23. For field-temperatures ranging between 5 and 20°C, the water density (where $\nu = \nu/\rho_f$) changes by only 0.18 percent (Table A.2.4., in Marsily, 1986).

where K_{s20} is saturated hydraulic conductivity at 20 °C (dim. LT^{-1}), K_{st} is saturated hydraulic conductivity at the field temperature of t °C (dim. LT^{-1}), ν_t is kinematic water viscosity at the field temperature of t °C (dim. L^2T^{-1}), and ν_{20} is kinematic water viscosity at 20 °C (dim. L^2T^{-1}; equiv. dynamic viscosity / fluid density).

The variation in soil water temperature during the *in situ* permeametry experiments (Sections 7.4.2. and 7.4.3) ranged from 3.3 to 20.3 °C, sufficient to the modify the hydraulic conductivity by some 38 percent, solely through changes in the water viscosity (Figure 60).

The effect of temperature upon the hydraulic conductivity at low saturations may be further exacerbated, by its influence upon tensiometer readings (Section 6.3.2) and the *actual* soil capillary potential (Constantz, 1982; Haridasan and Jensen, 1972).

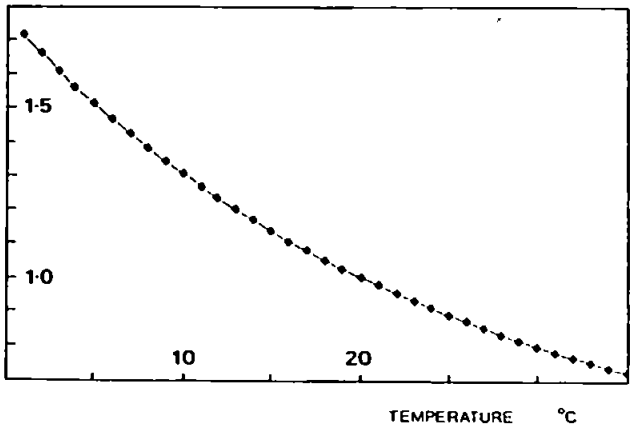

Figure 60. The relationship between water temperature and water viscosity correction factor (V_t/V_{20}).

7.4.1. Effect of Core-Size on the Measurement of Saturated Hydraulic Conductivity (K_s).

The variability of *in situ* measurements of saturated hydraulic conductivity determined from 192 cm^3 soil cores is far greater than from 7069 cm^3 soil cores (Table 45; Section 4.4.5). Within the conductive soils the mean values of conductivity measured by the small cores are similar to the large core, but this was not the case for slowly-conductive soils (Table 45).

Table 45. Saturated hydraulic conductivities measured by 7069 cm^3 ring permeameter cores versus 192cm^3 small-core permeameter cores.

SITE	HORIZON (cm)	DEPTH	Saturated Hydraulic Conductivity (cm hr^{-1}) ring permeameter (7069 cm^3 cores)	small-core permeameter (192 cm^3 cores)
grassland	O/A	0-10	**3.7**	8.2 1.8 11.9 (5.6)
grassland	O/A	0-10	**39**	9.2 31* (46)
grassland	O/A	0-10	**29**	26 1.4 (17)
grassland	A	10-20	**12**	13 206 36 (60)
forest	A/E	5-16	**221**	177 888 (396)
grassland	Egley	14-24	**0.21**	265 56 20* (67)
forest	B	19-29	**0.13**	34 14 480* (61)

The two or three small-core permeameter samples were extracted from within the larger ring permeameter cores.
* cores extracted horizontally within the ring.
() geometric mean (Marsily, 1986; Nielsen *et al*, 1973) of the small-core K_s values.

Saturated hydraulic conductivity (K_s) values are standardized to 20 °C

The silty A/E horizon within the forest, and the silty A/E and B within the ploughed grassland have saturated hydraulic conductivities larger than *representative* values of saturated hydraulic conductivity for un-clodded (i.e. un-structured) porous media (Table 46).

Water-flow within these horizons is, therefore, predominantly localized to the secondary-structure (i.e. cracks) (Section 7.3.6.; Demond and Roberts, 1987). If structural cracks associated with clodding, occur at a *scale* larger than the small (192 cm^3) core, then the increase in variability in saturated hydraulic conductivity about the geometric mean, would be expected (Table 45; Towner and Youngs, 1986).

Table 46. The range in saturated hydraulic conductivity of pimary-structures ranging from gravel to clay.

Primary-Structure (particle-size)	Saturated Hydraulic Conductivity (cm hr^{-1})	
	Marsily (1986)	Bear *et al* (1968)
sand and gravel	1E+0 to 1E-1	>1E+3 (gravel) to 1E+0
silt	1E-1 to 1E-5	1E+0 to 1E-2
clay	1E-5 to 1E-13	<1E-3

The slowly-conductive B horizon within the forest does, however, have large-core-determined saturated hydraulic conductivity values similar to the representative values for un-clodded soil, but much greater than the small-core values (Tables 45 and 46). The difference between the measurements of the two sizes of core may, therefore, relate to the relative increase in the volume of soil disturbed at the edge of the small (192 cm^3), relative to large (7069 cm^3) core (Hill and King, 1982; Rogers and Carter, 1987). Futhermore the contact between a soil-core and the wall of the permeamter ring can be more easily sealed in the large ring relative to the small ring. Field observation of the operation of the large-core, ring permeameter would suggest that even a small gap between a core of a slowly permeable soil and the ring, if left un-sealed, would dramatically increase the *recorded* conductivity.

All permeameter-based measurements of saturated hydraulic conductivity and intrinsic permeability presented within Sections 7.4.2. and 7.4.3. were determined by the large-core, ring permeameter.

7.4.2. Podzolic Slope: Saturated Hydraulic Conductivity (K_s) and Intrinsic Permeability (k).

Temperature-corrected ring permeametry (Section 4.4.5) was used to determine the saturated hydraulic conductivity (K_s) and intrinsic permeability (k) within the *podzolic slope* zones of the hillslope catenas. The K_s and k values for the *riparian* zones of the hillslope zones are presented within Section 7.4.3.

Within both the forest and the grassland podzolic slopes, the variation in K_s and k is far greater between different soil horizons, than within individual soil horizons (Figures 61 and 62; Section 3.5.4).

Slope horizon	Arithmetic mean	Geometric mean
O/A	1000	1000
E	101	71
B	0.18	0.16
B/C	28.7	28.2
C	1000	1000

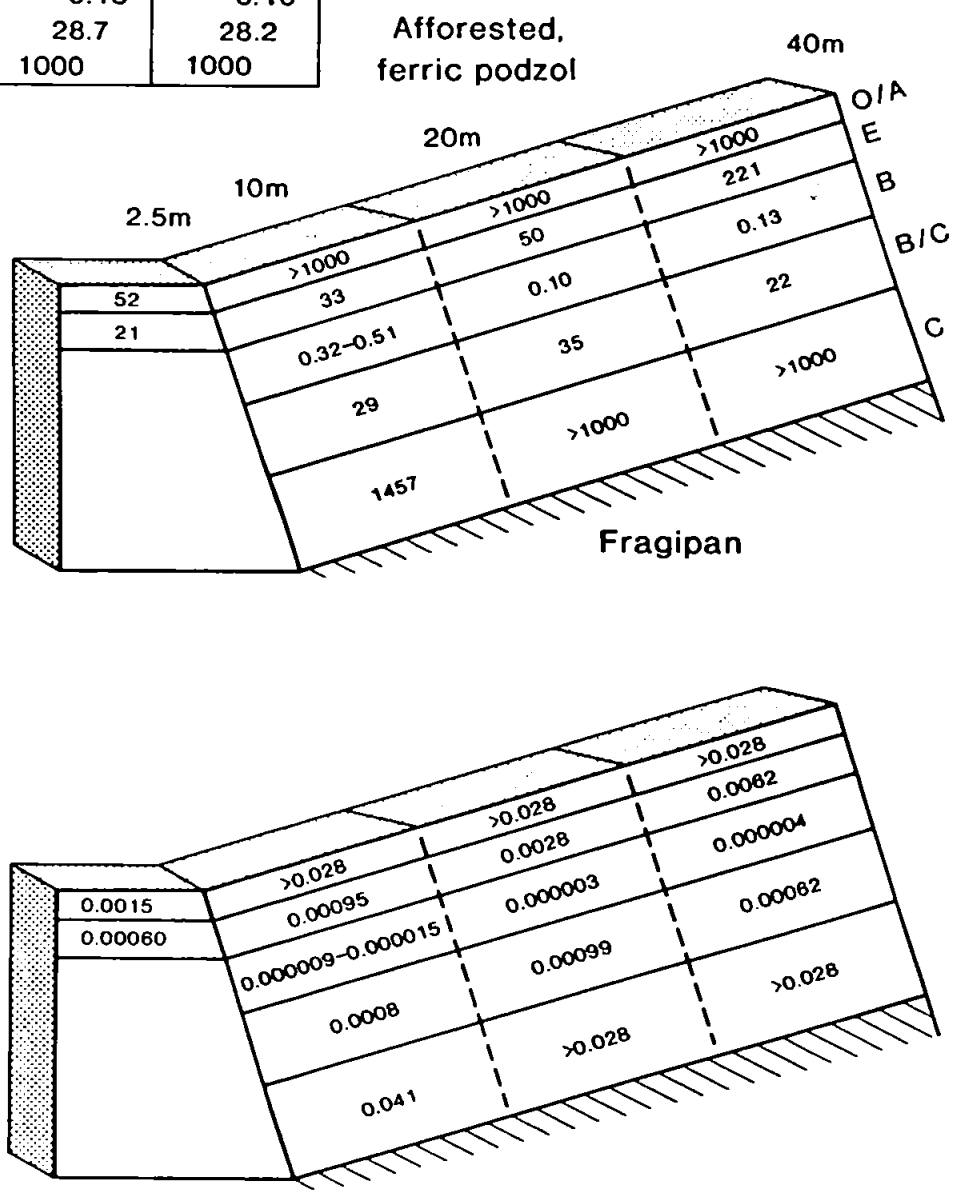

Figure 61. Distribution of saturated hydraulic conductivity at 20 °C (cm hr^{-1} : top) and intrinsic permeability (cm ^{2}: bottom), within the forest hillslope.

Forest versus Grassland Mineral Soil : The A/E horizon of the ferric-podzol hillslope within the forest (10-20 cm) is more permeable than the ferric-podzol A/E horizon within the grassland (10-20 cm) (Figures 61 and 62). The gleyed A/E horizon of the ironpan stagnopodzol soil within the riparian zone of the grassland hillslope, is particularly impermeable (Figure 62).

The B horizon within the relatively undisturbed forest hillslope (Sections 2.10.2, 7.2, and 7.3.1) is much less permeable than the ferric-podzol B horizon beneath the grassland (Figures 61 and 62).

The increased permeability within the grassland B horizon and reduced permeability within the grassland A/E horizon, may have resulted from a combination of the ploughing operation and trampling by sheep (Sections 2.10.2., 6.2. and 7.3.1).

The B/C horizons within the two hillslopes are not comparable, because the soil profile beneath the grassland rapidly grades into cobble-sized regolith and bedrock, while the soil profile beneath the forest hillslope gradually grades into gravel-sized regolith.

Vertical Variation within Each Profile : There would appear to be a major *relative hydraulic discontinuity* (Carson and Sutton, 1971; Hubbert, 1940) between the intrinsic permeability of the A/E and B horizons within the forest hillslope (Figure 61). The A/E horizon of the ferric-podzolic hillslope beneath the forest has saturated hydraulic conductivities (K_s : 33-221 cm hr^{-1}) and permeabilities (k : 9.5E-4 to 6.2E-3 cm^2) two orders of magnitude greater than those of the B horizon (K_s : 0.13-0.32 cm hr^{-1}; k : 4.0E-6 to 9.0E-6 cm^2). When the soil profile is saturated, this discontinuity will lead to the lateral deflection of water within the A/E horizons according to the Tangent Law (Section 1.4.3).

Below the forest B, or *illuvial* horizon (i.e. the zone of maximum accumulation of translocated clays, Brady, 1974), ring permeameter measurements indicate that the saturated hydraulic conductivity and permeability are two orders of magnitude greater than those within the overlying B horizon.

As the B horizon has saturated hydraulic conductivities and permeabilities two orders of magnitude less than the surrounding horizons, water will under saturated conditions, move directly across the B horizon (i.e normal to the horizon breaks) rather then laterally within the B horizon (Section 8.2.2).

No major discontinuity in intrinsic permeability is present between the A/E and B horizons within the ferric-podzol soil beneath the grassland (Figure 62). Ploughing may, therefore, lead to the reduction of the lateral deflection of flow within the A/E horizon (under saturated conditions), which results from the hydrologically-different soil horizons (Section 8.2.2).

Slope horizon	Arithmetic mean	Geometric mean
O/A	12.6	6.6
A	30.8	20.6
A/B	21.3	18.7
B/C	549	381.4

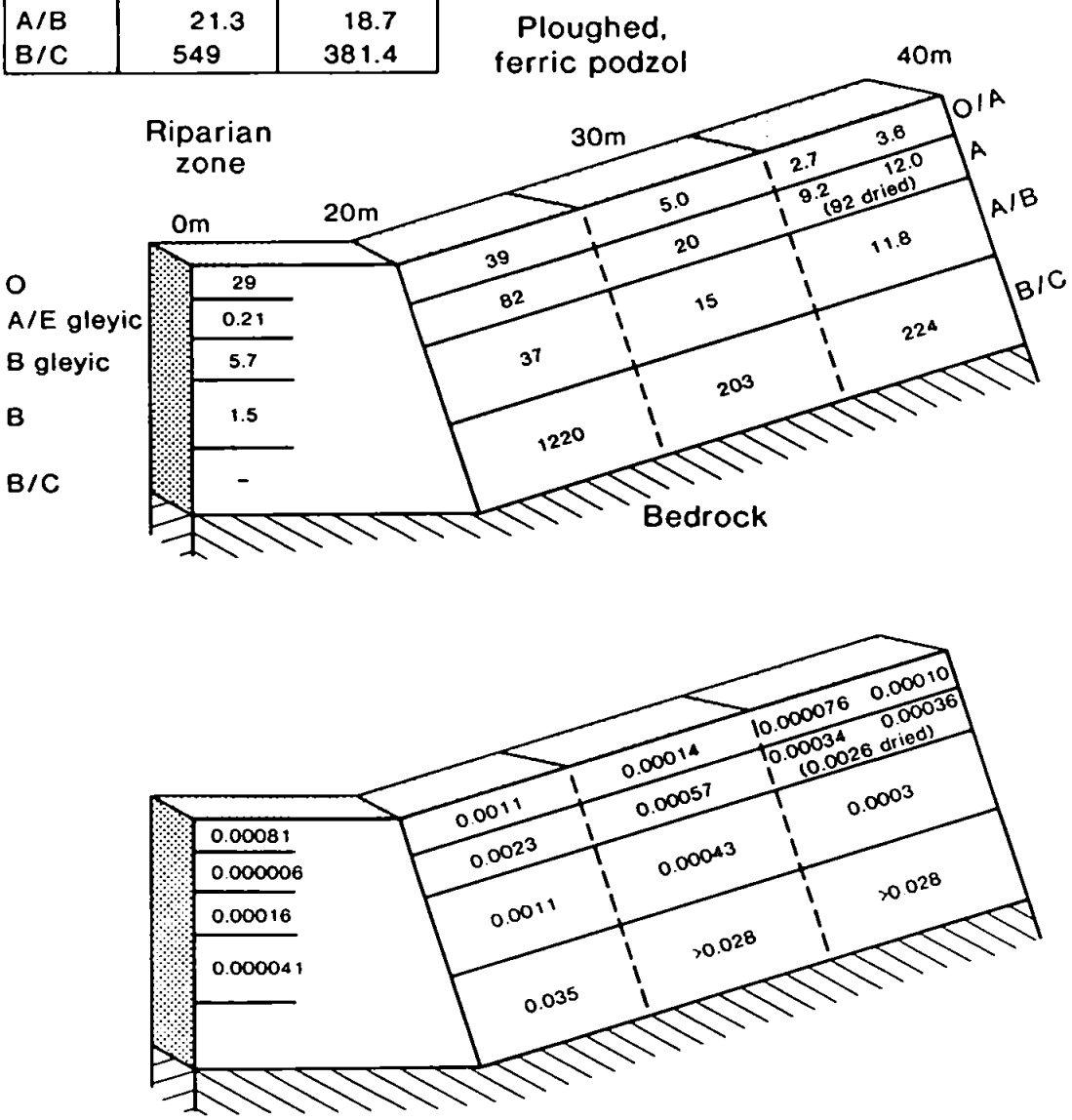

Figure 62. Distribution of saturated hydraulic conductivity at 20 °C (cm hr^{-1} : top) and intrinsic permeability (cm ^{2}: bottom), within the grassland hillslope.

Organic Horizon (Throughflow-Scaling Method) : The saturated hydraulic conductivity and permeability of the organic horizon or *forest floor* (0-5 cm, O/A; Section 1.5.2) within the forest hillslope was higher than can be measured by ring permeametry (i.e. a constant-head cannot be maintained within the permeameter for soil cores with a mean K_s : >1000-1500 cm hr^{-1}). The saturated hydraulic conductivity of the organic horizon was, therefore, estimated by a *throughflow-scaling method.*

By measuring the discharge from two or more soil horizons (under controlled boundary conditions, Sections 4.4.6 and 8.2.2) and the depth of the phreatic zone within each horizon, an unknown saturated hydraulic conductivity (K_{s1}) within one horizon can be estimated by scaling against a known saturated hydraulic conductivity (K_{s2}) within a second horizon. Thus:

$$K_{s1} = \alpha_k \cdot K_{s2}$$

where:

$$\alpha_k = \frac{q'}{b'} \qquad q' = \frac{q_1}{q_2} \qquad b' = \frac{b_1}{b_2}$$

where K_{s1} is the unknown saturated hydraulic conductivity (dim. LT^{-1}), K_{s1} is the known saturated hydraulic conductivity (dim. LT^{-1}), α_k is the conductivity scaling parameter, q' is the ratio of q_1 to q_2, q_1 is the discharge from the horizon with the unknown K_s (dim. L^2T^{-1}), q_2 is the discharge from the horizon with the known K_s (dim. L^2T^{-1}), b' is the ratio of b_1 to b_2, b_1 is the mean depth of the phreatic zone upslope of the throughflow trough within the horizon with the unknown K_s (dim. L), and b_2 is the mean depth of the phreatic zone upslope of the throughflow trough within the horizon with the known K_s (dim. L),

The technique assumes that the boundary-condition at the throughflow pit-face (Sections 4.4.6 and 8.2.2) has the same effect upon the across-slope equipotential-lines within both horizons. Within this form of the equation, the mean slope of the phreatic surfaces upslope of the pit are approximated by the sine of the slope angle (Dupuit, 1863).

During the monitoring period 6/11/1987 to 4/6/1988, the mean ratio of the discharge from the organic (O/A) horizon on the forest hillslope to the discharge from E horizon was 10.3 (i.e. 537 cm^3 hr^{-1}/52 cm^3 hr^{-1} : during periods when both the O/A and E throughflow troughs were flowing). As the depths of the phreatic surfaces recorded by the nested-piezometers within the two horizons were very similar, the conductivity scaling parameter (α_k) is equal to ratio of the two trough discharges, i.e. q'.

The mean saturated hydraulic conductivity measured within the forest A/E horizon range was 71 cm hr^{-1} (at 20 °C; Figure 61). The saturated hydraulic conductivity within the organic horizon is, therefore, estimated to be approximatly 730 cm hr^{-1}, and the intrinsic permeability is therefore 0.021 cm^2, i.e.

$$K_{sO/A} = 10.3 * 71 \text{ cm hr}^{-1}$$
$$= 730 \text{ cm hr}^{-1}$$

$$k_{O/A} = 730 \text{ cm hr}^{-1} (20\,^{\circ}\text{C}) * 2.83\text{E-}5$$
$$= 0.021 \text{ cm}^2$$

If more of soil-water was abstracted from the A/E horizon relative to the O/A horizon, then the lag in the response of the A/E horizon would be greater (Section 8.2.2). This would mean that the outflow from the A/E horizon would be under-estimated relative to that from the O/A horizon. This would lead to a smaller conductivity scaling parameter (α_k). The value of the conductivity for the basal zone of the O/A horizon (730 cm hr^{-1}) would, therefore, be an *over-estimate.*

Given that the scaling parameter is correct, the predicted hydraulic conductivity of the saturated basal zones of the O/A horizon (i.e. 730 cm hr^{-1}) is less than the saturated hydraulic conductivity of the complete O/A horizon calculated by ring permeametry (i.e. >1000 cm hr^{-1}; Figure 61). The difference may be explained by a vertical reduction in the conductivity of the O/A horizon (Zaslavsky and Sinai, 1981e). This is plausible, given that the basal zone of the O/A horizon appears to have a greater mineral content and density, in comparison with the upper layers.

Again, assuming that the technique is reasonably accurate, there is a 1.5 order of magnitude difference in saturated hydraulic conductivity and permeability between the *forest floor* (O/A horizon) and the A/E horizon within the ferric-podzol hillslope beneath the forest.

The *organic horizon* (0-10 cm, O/A) of the grassland hillslope has permeability values less than the underlying A/E horizon (10-20 cm; Figure 62). This would suggest that either trampling by sheep (Section 2.10.2; Fletcher, 1952) or the development of a root-mat, has reduced the permeability of the organic horizon (Molchanov, 1960).

7.4.3. Riparian Area : Saturated Hydraulic Conductivity (K_s) and Intrinsic Permeability (k).

The saturated hydraulic conductivity and intrinsic permeability of the riparian areas of the research hillslope-catenas were determined from a combination of piezometer recovery tests, and ring permeametry (Figure 63).

Recovery Tests : The saturated hydraulic conductivity of the soil surrounding the intake-point of piezometers within the riparian zones, was calculated from measurements of the recovery of piezometer water-level following an instantaneous draw-down. Two analytical solutions were applied to the recovery data. These were the:

1. Kirkham Equation:

$$K_s = \frac{\pi \cdot r^2 \cdot \{ \ln (H - y_1) / (H - y_2) \}}{A \cdot (t_2 - t_1)}$$

(Bouwer, 1962; Luthin and Kirkham, 1949; Reeve and Kirkham, 1951)

2. Ernst Equation:

$$K_s = \frac{4000}{\{(H/r) + 20\} \cdot \{2 - (y^*/H)\}} \cdot \frac{r}{y^*} \cdot \frac{dy^*}{dt} \cdot \frac{100}{24}$$

when S >= 1/2 H

(Ernst, 1950; Van Beers, 1958)

where K_s is saturated hydraulic conductivity (cm hr^{-1}), r is radius of piezometer (cm), H is depth from phreatic surface to piezometer base (cm), y_1 is distance between the phreatic surface and mean depth of water in piezometer at time t_1 (cm), y_2 is distance between the phreatic surface and mean depth of water in piezometer at time t_2 (cm), y^* is distance between the phreatic surface and mean depth of water in piezometer during the time interval dt (cm), t is time (s), A is a shape function, dependent upon the intake geometry, and S is depth to an impermeable layer (i.e. K_s less than 1/10 of the overlying layer) beneath the piezometer (cm).

A shape factor (A) of 34 was estimated for the 15 cm (l) x 2 cm (o.d) piezometer intakes, by extrapolating data given in Youngs (1968). All of the recovery tests were conducted between 13-20 June 1988, when the local water-tables (or phreatic surfaces) were relatively stationary. The ground-temperature during the initial stage of the recovery tests ranged from 14.0 to 15.5 °C. The temperature-standardized results of the two techniques are presented in Table 47 and Figure 63.

Table 47. Saturated hydraulic conductivity and intrinsic permeability within the forest and grassland riparian soils, determined using the Kirkham and Ernst equations.

Piezometer	Saturated Hydraulic Conductivity (cm hr^{-1} at 20 °C) (Intrinsic Permeability, cm^2)	
	KIRKHAM (A=34)	ERNST (S >=1/2H)
forest FDP81	0.071 (2.0E-6)	0.017 (4.9E-7)
forest F0P111	0.415 (1.2E-5)	1.042 (2.9E-5)
grassland G10P78	0.072 (2.0E-6)	0.108 (3.1E-6)
grassland G0P95	0.035 (9.9E-7)	0.015 (4.3E-7)

The two techniques indicated that the saturated hydraulic conductivity of the gleyed soil (Section 2.8.2) at a depth of some 70-120 cm within the riparian zone of the forest hillslope, is approximately 0.02-0.07 cm hr^{-1} (FDP81) directly beneath the drainage channel, and 0.42-1.04 cm hr^{-1} (F0P111) 1.5 m upslope of the channel (Figure 63).

Within the grassland riparian zone, the saturated hydraulic conductivity of the stagno-humic gley at a depth of 70-90 cm is approximately 0.07-0.11 cm hr^{-1}. Ten metres further downslope at a depth of 80-110 cm (Figure 63), the gleyed horizon of the ironpan stagnopodzol has a 0.02-0.04 cm hr^{-1} saturated hydraulic conductivity.

Ring Permeametry : At the edge of the stream within the grassland the soil is a stagno-humic gley. At a distance of only 2-5 m away from the stream the soil is an ironpan stagno-podzol (Figure 9). The saturated hydraulic conductivity of the surface (0-10 cm) layer of these two soils are 11 cm hr^{-1} (k : 3.1E-4 cm^2) and 29 cm hr^{-1} (k : 8.2E-4 cm^2) respectively, which is similar to that of the surface horizon of the ploughed slope (Figure 62; Section 7.4.2).

The gleyed E horizon (10-20 cm) of the ironpan stagno-podzol is much less conductive (K_s : 0.2 cm hr^{-1}) than the E horizon of the ferric podzol within the forest hillslope ($<K_s>$: 71 cm hr^{-1}). Furthermore, the B horizon (20-30 cm) of the ironpan stagno-podzol is more conductive (K_s : 5.7 cm hr^{-1}) than the corresponding horizon of the ferric podzol within the forest hillslope ($<K_s>$: 0.16 cm hr^{-1}). This shift in the least conductive zone of a soil profile as the intensity of podzolization increases was noted by Adams and Raza (1978), Crampton (1967) and Rudeforth (1967), and is idealized within Figure 6.

The saturated hydraulic conductivity of the surface layer (0-10 cm) of the stagno-gley soil within the riparian zone of the forest hillslope (K_s : 52 cm hr^{-1}; k : 1.5E-3 cm^2) is similar to that within the surface layers of the grassland riparian zone (see above). This high saturated hydraulic conductivity is, however, maintained within the underlying soil horizon

(10-20 cm, K_s : 21 cm hr^{-1}; k 6.0E-4 cm^2), unlike in the grassland riparian soil. By using this conductivity (i.e. 21 cm hr^{-1}) within the Darcy equation, an accurate prediction (R^2 83 percent) of the streamflow generation could be made, from the hydrological properties and geometry of the riparian zone alone (Section 8.2.1). This may provide some verification for the measurements from the ring permeameter, and corroborate the field observation, that the riparian soil is relatively homogenous between a depth of approximately 10 and 80 cm below the surface (Sections 6.2.3.; 8.2.1). During storm-periods, much of the sub-surface flow within the riparian zone should be perched above the 80 cm depth, because the saturated hydraulic conductivity reduces to approximately 0.4-1 cm hr^{-1} at 70-120 cm below the surface (Figure 63).

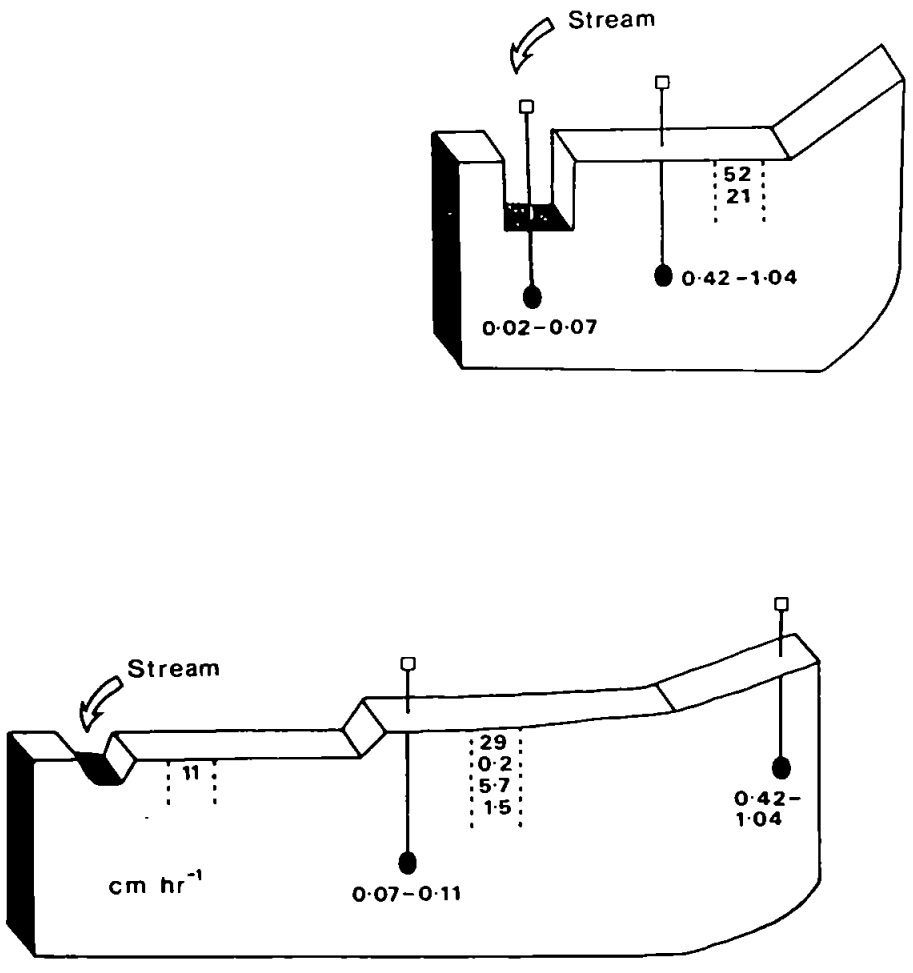

Figure 63. Distribution of saturated hydraulic conductivity (at 20 °C) within the forest riparian zone (top) and grassland riparian zone (bottom).

7.4.4. The Impact of Individual Trees upon the Saturated Hydraulic Conductivity of the Soil Horizons within the Forest Hillslope.

An attempt was made to assess the impact of individual trees upon the saturated hydraulic conductivity of the podzolic B, B/C and C horizons within the forest hillslope (Section 7.4.2).

Measurements were taken with a well permeameter (Talsma and Hallam, 1980, Bonell *et al*, 1983a; Section 4.4.6) as close to tree boles as possible, and at a distance of 1 m away from individual trees. Three separate analytical solutions were used to calculate the saturated hydraulic conductivities:

1. Jones solution (Bonell *et al*, 1983; Jones, 1951),
2. Zanger solution (Zanger, 1953), and
3. Reynolds solution (Reynolds and Elrick, 1985; Reynolds *et al*, 1983, 1985).

The particular form of the Reynolds Solution used, was the *Laplace solution* with a shape function (C) derived from the full *Glover solution* (Reynolds *et al*, 1983, 1986; Table 48).

The saturated hydraulic conductivities predicted by well permeametry were compared with those calculated from ring permeametry measurements (Table 48).

Well Permeametry versus Ring Permeametry : The saturated hydraulic conductivity values predicted by the Jones solution appeared to be far more sensitive to the S-parameter (i.e. depth to an impermeable layer), compared with the well-permeameter discharge and geometry (Table 48), and, therefore, warranted little confidence.

Both the Zanger and Reynolds solutions predicted similar saturated hydraulic conductivities. These values were, however, similar to the values predicted by the ring permeametry, for the B horizon only (Table 48). The values predicted for the B/C horizon were 2 to 3 orders of magnitude less than those predicted by the ring permeameter, and the values for the C horizon were perhaps 3 to 4 orders of magnitude lower (Table 48).

Table 48. Saturated hydraulic conductivity values calculated by both well and ring permeametry.

Auger No.	horizon	depth (cm)	head (h,cm)	Q:rate of head-loss (cm s^{-1}) T°C	predicted K_s (cm hr^{-1}, 20°C) JONES (S)	ZANGER	REYNOLDS
9WT1	tree B	20-35	15	0.022 13	73(40)	**0.08**	**0.10**
8WT1	inter B	20-35	15	0.029 13	8(40)	**0.11**	**0.12**
1WT2	tree B/C	45-55	10	0.011 8	8(20)	**0.07**	**0.10**
2WT3	tree Cu	60-70	10	0.040 8	13(0)	**0.28**	**0.35**
3WI3	inter Cu	60-70	10	0.051 8	18(0)	**0.35**	**0.43**
4WT3	tree Cu+	40-60	20	0.062 8	173(10)	**0.19**	**0.21**
5WI3	inter Cu+	40-60	20	0.175 9	491(10)	**0.51**	**0.55**
7WT4	tree C	60-80	20	1.000 11	2728(30)	**2.77**	**2.99**
6WI4	inter C	60-80	20	0.650 10	5466(30)	**1.86**	**1.99**

JONES EQ: $$K_s = \frac{3Q\ln(h / r)}{\pi h(3h + 2S)}$$

S = depth to an impermeable layer (cm) r = permeameter radius (= 3.2 cm)

ZANGER EQ: $$K_s = \frac{Q}{2\pi h^2}\left\{ \ln\left[\frac{h}{r} + \mathrm{SQRT}\left(\frac{h^2}{r^2} + 1\right)\right] - 1 \right\}$$

REYNOLDS EQ: $$K_s = \frac{QC}{2\pi h^2\{1+(C/2)(r/h)^2\}}$$ (Laplace Solution)

where: $$C = \sinh^{-1}\left\{\frac{h}{r}\right\} - 1$$ (full Glover Solution)

RING PERMEAMETER (7069 cm^3 cores)

(sampled within 3 m of the well permeameter measurements)

B horizon	(16-24 cm)	K_s 0.20 cm hr^{-1} (20°C)
B/C horizon	(30-40 cm)	K_s 28 cm hr^{-1} (20°C)
Cu horizon	(40-50 cm)	K_s >1500 cm hr^{-1} (20°C)

A constant-head appeared to be maintained within all of the auger holes, and the predicted values (using the Zanger and Reynolds solutions) lie within the instrument's capability (i.e. 0.036 - 360 cm hr^{-1} : Reynolds and Elrick, 1985). Moreover, the discrepancy between the two techniques cannot be attributed solely to *smearing* of clay on the walls of the auger-hole as others (e.g. Bonell *et al*, 1983; Reynolds *et al*, 1983) have suggested, as the largest discrepancy occurred when the auger-hole extended into the gravel-sized regolith (C horizon). Either there is an error within the analytical solution for flow into an auger-hole (Boersma, 1965; Bouwer, 1962), or the insertion of the ring into the gravelly regolith has greatly enhanced the conductivity *recorded* by the ring permeameter. There is some suggestion that the gravelly regolith within the C horizon and possibly B/C horizon may also have been disturbed during the porosity (Section 7.2) and gravimetric moisture content determinations (Section 7.3.2).

Below versus Inter-Tree K_s : Despite the uncertainty surrounding the well permeametry technique, consistent differences between the below-tree and inter-tree measurements of saturated hydraulic conductivity can be compared. If the small sample of measurements taken from only 4 different below-tree soils, and 3 inter-tree soils is representative, then it might be concluded that the B, B/C and C horizons directly beneath individual conifers are infact *less permeable* than the inter-tree soils (Table 48). This may be the result of the compaction of the soil due to both the weight of tree and the movement of such shallow-rooted (Section 2.9.2) trees during windy conditions (Hornung, 1984; Romans, 1959; Savill, 1976).

The impact of individual trees upon the moisture regime of the forest hillslope ia examined in Section 6.2.6, and the impact of the capillary potential (ϕ_c) and potential gradient ($d\phi/dL$) of the forest hillslope as a whole is examined in Section 6.4.6.

7.4.5. Stationarity and Wettability (W_{10}).

As soils dry, cracking or secondary-structure (Section 7.3.6) can develop which may change the soil's intrinsic permeability (k) and hence its saturated hydraulic conductivity (K_s) (Wilcock and Essery, 1984). In addition, as some soils dry, the contact angle between the soil-water and the soil-particles may exceed 90°, and make the soil non-wettable with respect to the water (Bear, 1972). Such variable wettability will affect the soil's intrinsic permeability (Burch *et al*, 1989), storativity (Hemond and Goldman, 1985; Equation 9), and moisture capacity (Adams and Raza, 1978; Fuchsman, 1986). These changes are obviously modifications of those hillslope hydrological properties usually assumed to be constant or *stationary* (i.e. parameters) and, therefore, their significance must be addressed.

A 7069 cm^3 core of the A/E horizon (10-20 cm) was excavated from the grassland hillslope (at the 40 m slope position), and the saturated hydraulic conductivity measured by ring permeametry. The core was then covered, and left to drain for a 28 day period (16/5/88-

13/6/88 : mean mid-day ground-temp. 7.5 °C). The saturated hydraulic conductivity was measured again after this period. The temperature-corrected, saturated hydraulic conductivity of this A horizon increased by exactly one order of magnitude, from 9.2 cm hr^{-1} (at 20 °C; k : 2.6E-4 cm^2) to 92.0 cm hr^{-1} (at 20 °C; k : 2.6E-4 cm^2) (Figure 62). The permeability of the surface soils within the grassland hillslope may, therefore, increase during warm summer months (Adams and Raza, 1978). The effects of freeze/thaw activity and trampling by sheep may subsequntly reduce the localized-cracking during the winter months. Such an annual cycle would be similar to the annual development and destruction of *ephemeral pipes* (Section 1.4.2) within the soils of Tir Gwyn and Plynlimon massif as a whole (Gilman and Newson, 1980; Hudson, pers. comm. 1987). The ephemeral pipes within the peaty soils of the Tir Gwyn grassland catchment may develop following a combination of summer drying and large seepage forces (Irmay, 1964 in Bear, 1972) within the winter storms.

A similar experiment was conducted on a 7069 cm^3 core of the B horizon (16-26 cm) within the forest hillslope. During the 115 day period 19/1/88 to 16/5/88, the temperature-corrected, saturated hydraulic conductivity of this sample of podzolic B horizon only changed from 0.32 cm hr^{-1} (at 20 °C; k 9E-6 cm^2) to 0.51 cm hr^{-1} (at 20 °C; k 1.5E-5 cm^2). The B horizon within the forest hillslope would, therefore, appear to have a much more *stationary* intrinsic permeability and saturated hydraulic conductivity in comparison to the surface layers within the grassland catchment.

The impact of drying upon the *wettability* of each soil horizon within the forest and grassland hillslopes were compared by placing a droplet of water onto a number of oven-dried soil aggregates (105 °C for 48 hours) and noting whether the water was absorbed within 10 seconds (Krammes and Debano, 1965).

The soil aggregates collected from within the B and B/C horizons of both hillslopes remained wettable after oven-drying (Table 49). Those aggregates collected from the organic (O and O/A) horizons of each hillslope did, however, become non-wettable, as did the A/E horizon within the grassland profile. The A/E horizon beneath the forest in contrast to the grassland A/E horizon, remained wettable in all cases, with the exception of the E/B intergrade soil.

A reduction in soil wettability within the A/E horizon of the grassland hillslope during periods of intense drying, will probably not affect the hydrological properties as much as cracking, but may direct even more of the water-flow to the developing secondary-structure (Section 1.5.2).

Direct field-observation would suggest that the impact of reduced wettabilities upon the infiltration of rainfall into dry conifer litter (Table 8) and the grassland root-mat is more important. Although the organic soils have high saturated hydraulic conductivities (forest O/A : >1000 cm hr^{-1}; grassland O/A : 3-39 cm hr^{-1}), localized, Hortonian overland flow (Section 1.4.2) has occasionally been observed during the initial stages of storms occurring

during dry periods. A similar association between reduced wettability and percolation within dry, organic soils has been recorded during the laboratory experiments of Grelewicz and Plichta (1983, 1985) and Sozykin (1939, in Molchanov, 1960).

Table 49. Wettability of soils after being dried at 105 °C for 48 hours.

	slope position	depth (cm)	horizon	Wettability (W_{10})
forest soils	40	2-5(1)	O	NON-WETTABLE
	40	2-5(2)	O	NON-WETTABLE
	5	12-15	A/E	wettable
	10	7-10	A/E	wettable
	40	10-13	A/E	wettable
	10	14-17	E/B	NON-WETTABLE
	40	24-27	B	wettable
	5	29-32	B/C	wettable
grassland soils	40	2-5	O	NON-WETTABLE
	40	14-17	A/E	NON-WETTABLE
	0	7-10	A/E	NON-WETTABLE
	40	29-32	B	wettable
	20	29-32	B	wettable

7.4.6. Relative Hydraulic Conductivity (K_r): Moisture Capacity Method.

The relative hydraulic conductivity (K_r) of a soil is the ratio of the hydraulic conductivity at a particular level of water-saturation to the hydraulic conductivity at complete water-saturation. This component of the hydraulic conductivity curve (Equation 5; Section 7.4.7) must, therefore, be determined (in addition, to the saturated hydraulic conductivity component) for the calculation of water-flow within soils which are less than fully-saturated with water. The K_r relationship is dependent upon upon how much moisture is released at a given capillary potential (i.e. the moisture capacity relationship; Section 7.3).

Five separate techniques which predict relative hydraulic conductivity from moisture capacity data, were applied to the Tir Gwyn soils. These techniques were developed by Campbell (1974), Brooks and Corey (1964, 1966), Millington and Quirk (1959, 1960), and Van Genuchten (1980). By fitting each technique's parameterization of the moisture capacity curve to a very small range in capillary potential (e.g. 0 to -10 cm), all five techniques produced similar relative hydraulic conductivity values (Figure 64). The techniques employed by Brooks and Corey (1964, 1966) and Campbell (1974) could, however, not be fitted to the moisture capacity curves over the complete field-monitored range (Figure 65), and, therefore, could not accurately predict the relative hydraulic conductivity function.

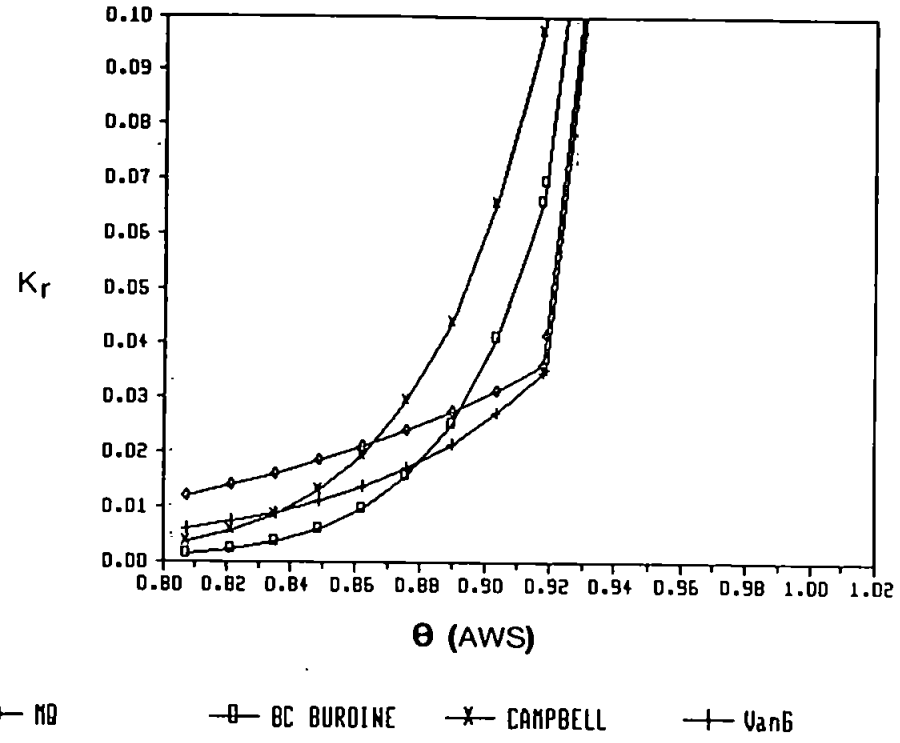

Figure 64. The relative hydraulic conductivity function at capillary potentials of between 0 and -10 cm, predicted by the techniques developed by Campbell (1974), Brookes and Corey (1964, 1966), Millington and Quirk (1959, 1960) and Van Genuchten (1980). The moisture capacity data for the forest B horizon is used for the comparisons.

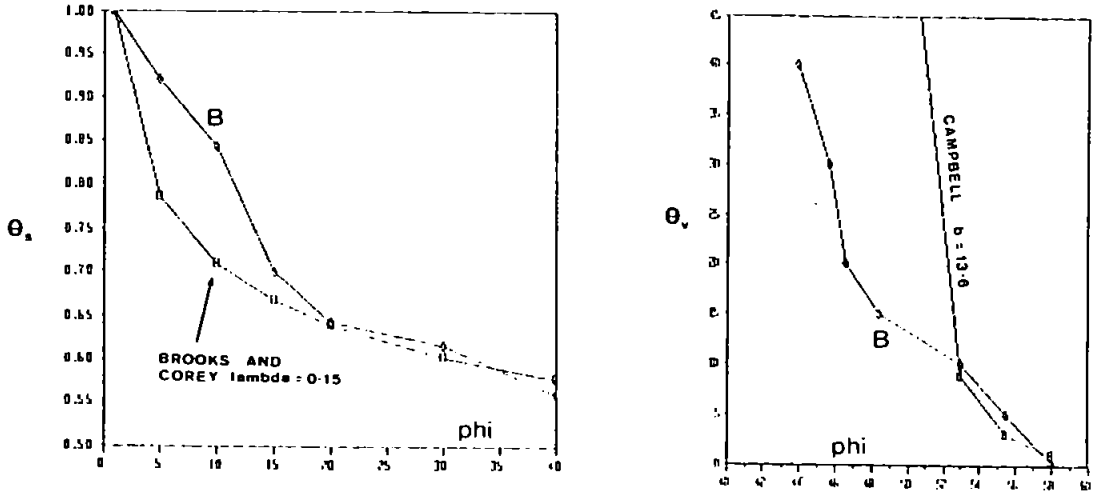

Figure65. The best fit or optimization of the parameters within Campbell's (1964) and Brooks and Corey's (1964, 1966) equations approximating the shape of the moisture capacity curve for the forest B horizon. The moisture capacity for this horizon has the least complex shape (Section 7.4.3).

Although the Tir Gwyn moisture capacity curves could be approximated by compound logarithmic curves (Section 7.3.5), the most accurate method of parameterizing each curve was achieved by fitting a *cubic spline* (Erh, 1972; Bruce and Luxmoore, 1986). A solution of the Millington-Quirk Equation (Millington and Quirk, 1959, 1960) developed by Dowd (1988a) used the spline parameterization directly. The form of the Millington-Quirk Equation used was:

$$K = MF \cdot 9.608E\text{-}5 \cdot \frac{\eta^{4/3}}{N} \{ \phi_{c1}^{-2} + 3\phi_{c2}^{-2} + .. + (aN - 1)\phi_N^{-2} \}$$

$$MF = K_{s\ measured} / K_{s\ predicted}$$

(dim. cm hr^{-1} at 20°C; Millington and Quirk, 1960; Jackson *et al*, 1965)

The Millington-Quirk technique predicts that the relative hydraulic conductivities for the wetting phase of each soil horizon within the forest and grassland hillslope decline markedly as the water-saturation reduces (Figure 66). Moreover, this decline appears relatively similar within all of the soils of the Tir Gwyn hillslopes at these high saturations (i.e. 55-85 percent θ_s at -100 cm)(Figures 66 and 73). At only -5 cm ϕ_c the relative hydraulic conductivity (K_r) has reduced by almost 1.5 orders of magnitude, by -15 cm the K_r is 3 orders of magnitude smaller, and by -100 cm the K_r is between 4.1 and 5.1 orders of magnitude smaller. By approximating this relationship with a log-log function, it can be seen that between complete-saturation and 5 cm suction (or -5 cm capillary potential) the relative hydraulic conductivity declines almost linearly ($\phi_{c-}^{-0.8}$) with the increase in suction/tension :

$$K_r = 0.15\phi_{c-}^{-0.8}$$

(K_r = dimensionless; ϕ_{c-} = cm H_2O suction)

Between 5 and 100 cm suction (or -5 and -100 cm capillary potential) the relative hydraulic conductivity declines more than *quadratically* with a unit change in potential:

$$K_r = 1.4\phi_{c-}^{-2.3}$$

(K_r = dimensionless; ϕ_{c-} = cm H_2O suction)

As capillary potential is frequently between -5 and -100 cm within storm events, this will mean that small changes in capillary potential will give rise to large changes in hydraulic conductivity (Section 7.4.9) and hence soil water flux (Section 8.2.2). The calculation of soil water movement is, therefore, sensitive to changes within capillary potential.

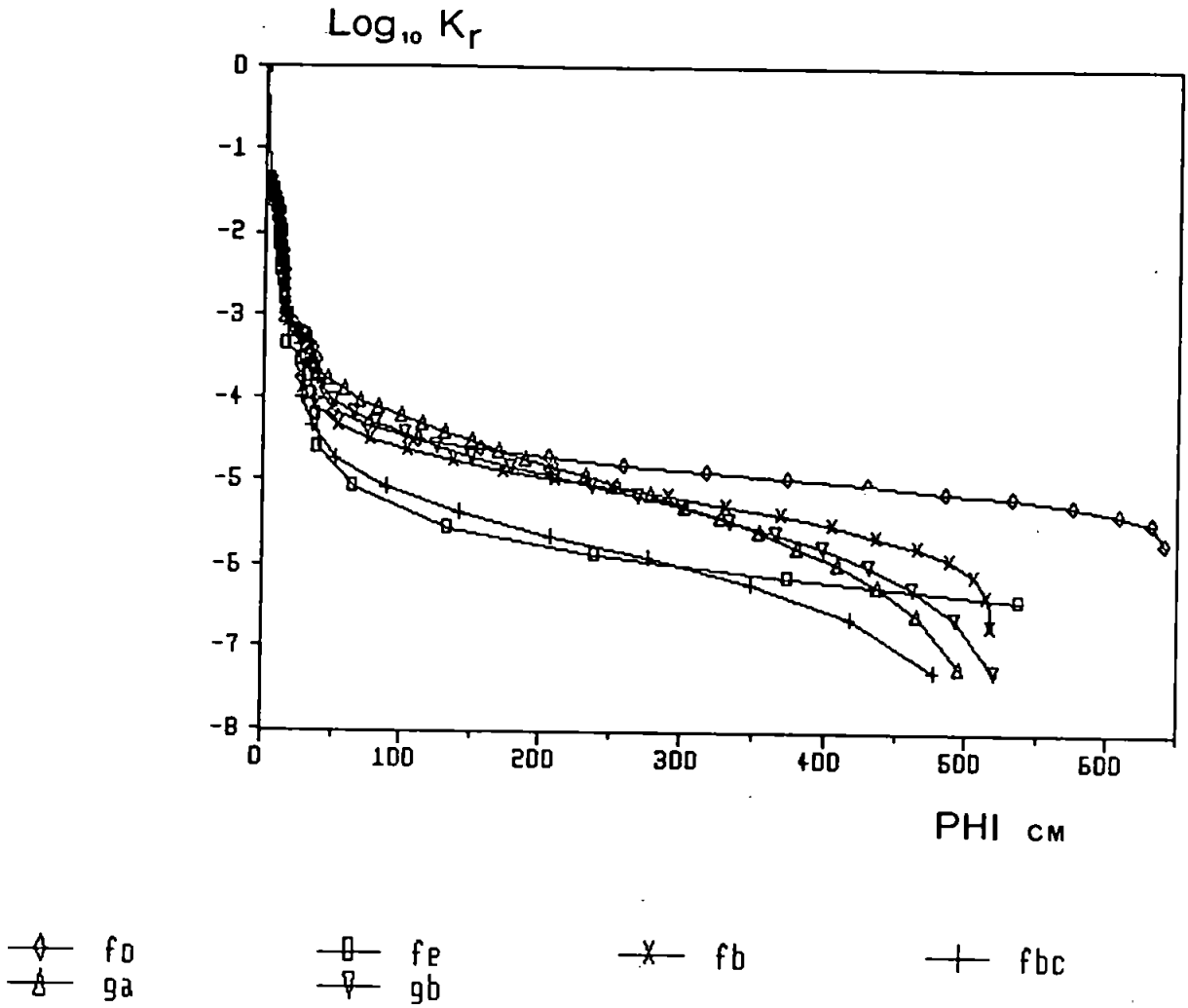

Figure 66. Mean relative hydraulic conductivity function for each soil horizon within the forest and grassland hillslopes. The functions are predicted by the Millington-Quirk equation using moisture capacity data, parameterized with a cubic spline.

The relative hydraulic conductivity curves predicted by the Millington-Quirk technique were very similar to those predicted using the alternative, Van Genuchten technique (Figure 67/68). The version of the Van Genuchten technique used was based upon Mualem's (1976) parameterization of the moisture capacity curve (Section 7.3.5; Van Genuchten, 1980), i.e.

$$K_r = AWS^{1/2} \{ 1 - (1 - AWS^{1/m})^m \}^2 \qquad [25]$$

where K_r is relative hydraulic conductivity (dimensionless ratio), AWS is available water saturation (Equation 22; dim. $L^3\ L^{-3}$), and m is a shape parameter, dependent upon the shape of the moisture capacity curve.

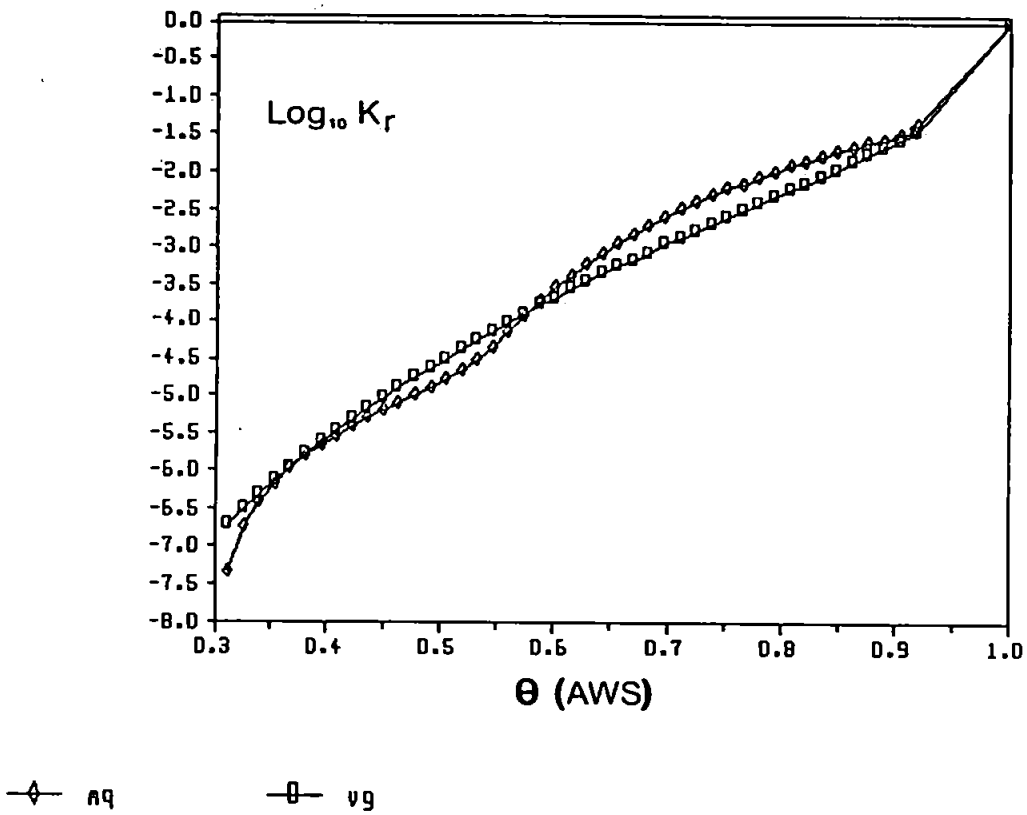

Figure 67/68. Relative hydraulic conductivity against available-water-saturation for the B horizon of the forest hillslope, predicted by both the Millington-Quirk equation (mq) and the Van Genuchten eqaution (vg).

7.4.7. Validation of the Moisture Capacity Determination of Relative Hydraulic Conductivity using a Tangent-Continuity Method.

The relative hydraulic conductivities predicted by moisture capacity data can be validated or verified by comparison with the difference in relative hydraulic conductivity between two soil horizons, predicted by a tangent-continuity method.

The ratio of the hydraulic conductivity within the forest B horizon to that within the forest E horizon for example, must be equal to the ratio of the tangent of their respective *streamline* angles (Equation 26), in order to maintain continuity (Hubbert, 1940; Jacob, 1940; Section 1.4.3.; Equations 13-18). A *streamline* is an isoline of instantaneous or steady-state, specific flux (Bear, 1972).

From Equation 18:

$$K_E = K_B \{ \frac{\tan b_E}{\tan b_B} \} \qquad [26]$$

where b_E is the streamline angle within E horizon (degrees), b_B is a streamline angle within B horizon (degrees), K_E is (isotropic) hydraulic conductivity: E horizon (dim. LT^{-1}), and K_B is (isotropic) hydraulic conductivity: B horizon (dim. LT^{-1}).

As the hydraulic conductivity of the forest B horizon is consistently several orders of magnitude less than the forest E horizon (Section 7.4.9), the angle of the streamline within the B horizon should approach the slope-normal (Section 7.4.2., 8.2.2.; Chappell *et al*, 1990). The tangent of a streamline angle of for example, 0.1 degrees from the slope-normal equals 0.0017453. As only the ratio of the hydraulic conductivity of the two horizons is required, Equation 26 can be further simplified by replacing K_B with 1. Hence:

$$\frac{K_B}{K_E} = \frac{1}{K_E} = \left(\frac{1}{\{ \frac{\tan b_E}{0.0017453} \}} \right) \qquad [27]$$

The angle of a streamline (b) within an isotropic porous media is always perpendicular to the angle of an equipotential-line (a). The relationship between the angle of the streamline from the slope-normaland the angle of the equipotential-line from the slope-angle is, therefore:

$$b_E = 90 - a_E - \text{slope angle} \qquad [28]$$

The equipotential-line angle within the forest A/E horizon (a_E) can be approximated from the (total) potential loss (per unit distance) between a tensiometer at the centre of the A/E horizon and the position on the E-B horizon boundary crossed by an equipotential-line drawn normal to the slope, from a tensiometer at the centre of the B horizon.

The K_B/K_E ratios predicted by both the moisture capacity method (Millington-Quirk technique) and tangent-continuity method, are compared at two intermediate slope positions. These slope positions correspond to the 2.5 m and 5 m tensiometer arrays within the forest hillslope (Figures 4 and 17).

Figures 69, 70, 71, and 72 show that the difference between the two techniques is generally less than one order of magnitude. The moisture capacity method is, therefore, justified, given the range in the hydraulic conductivity within each horizon (Section 7.4.6., 7.4.8., 7.4.9) and the errors associated with:

1. the assumptions used to simplify the tangent-continuity method (above),
2. the impact of spatial variability upon the tangent-continuity method (the tensiometers at the 2.5 m slope position are 8 cm appart, and 76 cm appart at the 5 m position), and
3. the relative hydraulic conductivity functions developed by the Millington-Quirk technique (Section 7.4.6) are based upon the geometric mean of the saturated hydraulic conductivities, and arithmetic mean of the moisture capacities determined from the whole podzolic hillslope (i.e. 2.5-40 m slope position).

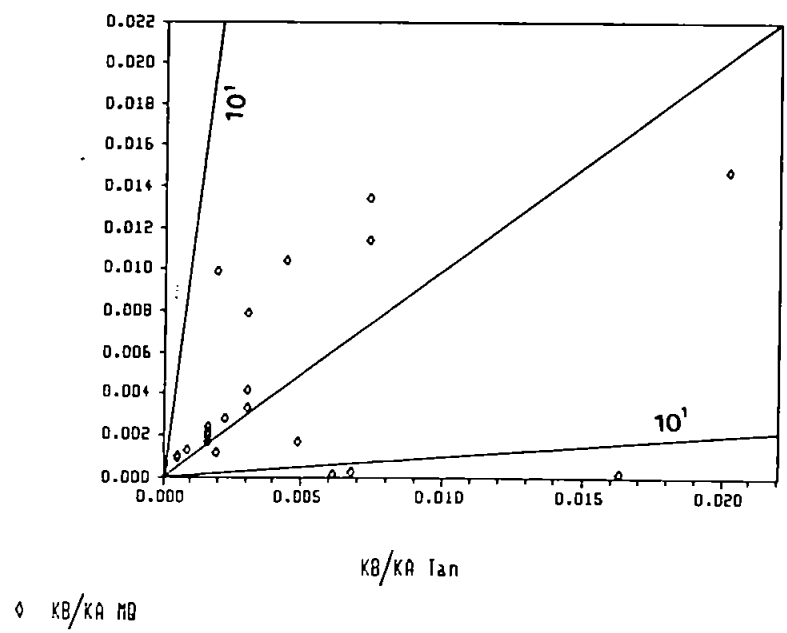

Figure 69. The K_B/K_E ratio predicted by the moisture capacity method (Millington-Quirk equation) against the K_B/K_E ratio predicted by a Tangent-Continuity method: Downward flow at the 2.5 m position on the forest hillslope.

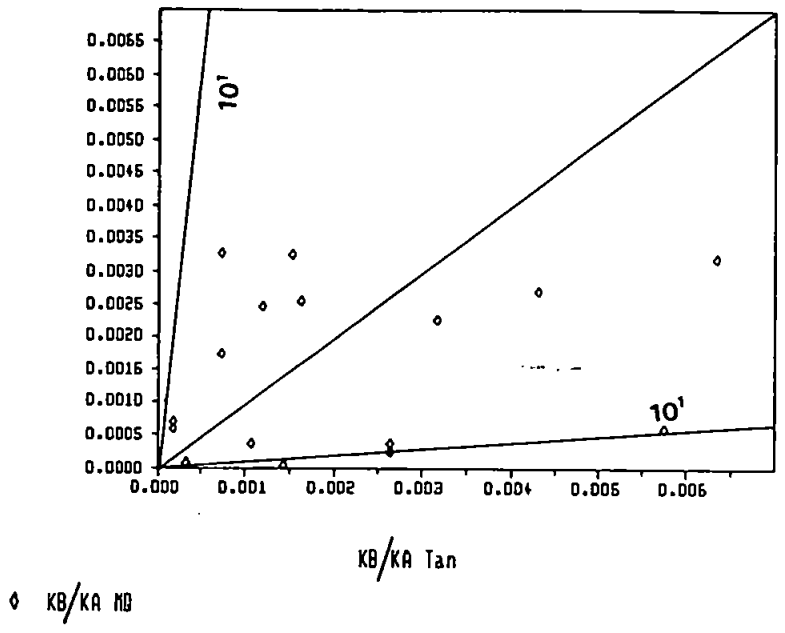

Figure 70. The K_B/K_E ratio predicted by the moisture capacity method (Millington-Quirk equation) against the K_B/K_E ratio predicted by a Tangent-Continuity method: Upward flow at the 2.5 m position on the forest hillslope.

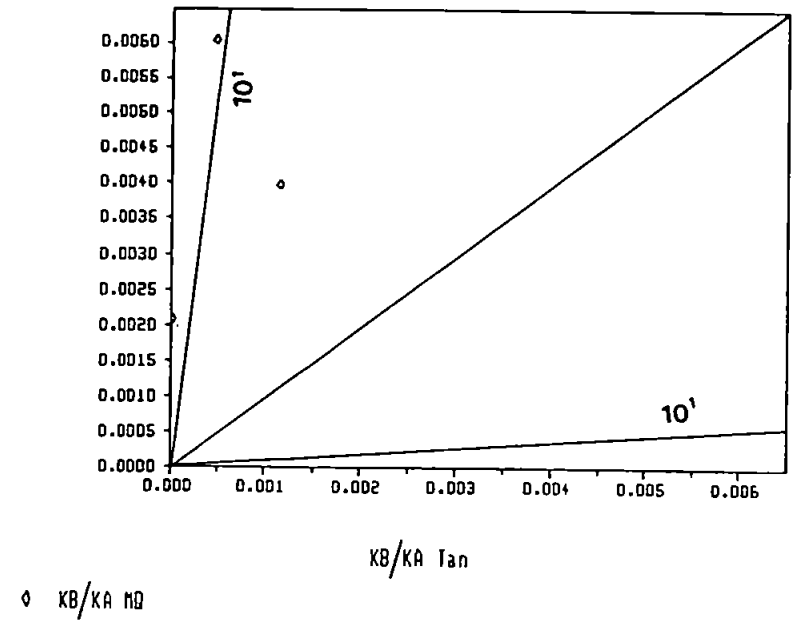

Figure 71. The K_B/K_E ratio predicted by the moisture capacity method (Millington-Quirk equation) against the K_B/K_E ratio predicted by a Tangent-Continuity method: Downward flow at the 5 m position on the forest hillslope.

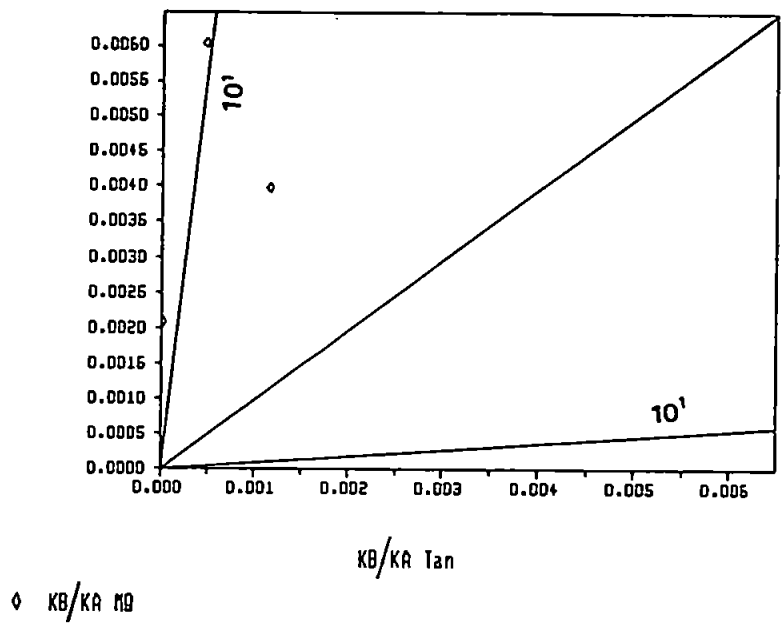

Figure 72. The K_B/K_E ratio predicted by the moisture capacity method (Millington-Quirk equation) against the K_B/K_E ratio predicted by a Tangent-Continuity method: Upward flow at the 5 m position on the forest hillslope.

7.4.8. Validation of the Moisture Capacity Determination of Relative Hydraulic Conductivity by comparison with Steady-State Permeametry.

The rapid reduction in the relative hydraulic conductivities predicted using the moisture capacity and saturated hydraulic conductivity data (Section 7.4.6), are very similar to the values determined by *steady-state permeametry* (Richards, 1931) for the O/A horizons of a podzolic soil within the nearby Gwy Catchment (Figure 73; data averaged from Tables 10.3 and 10.4, Knapp, 1970).

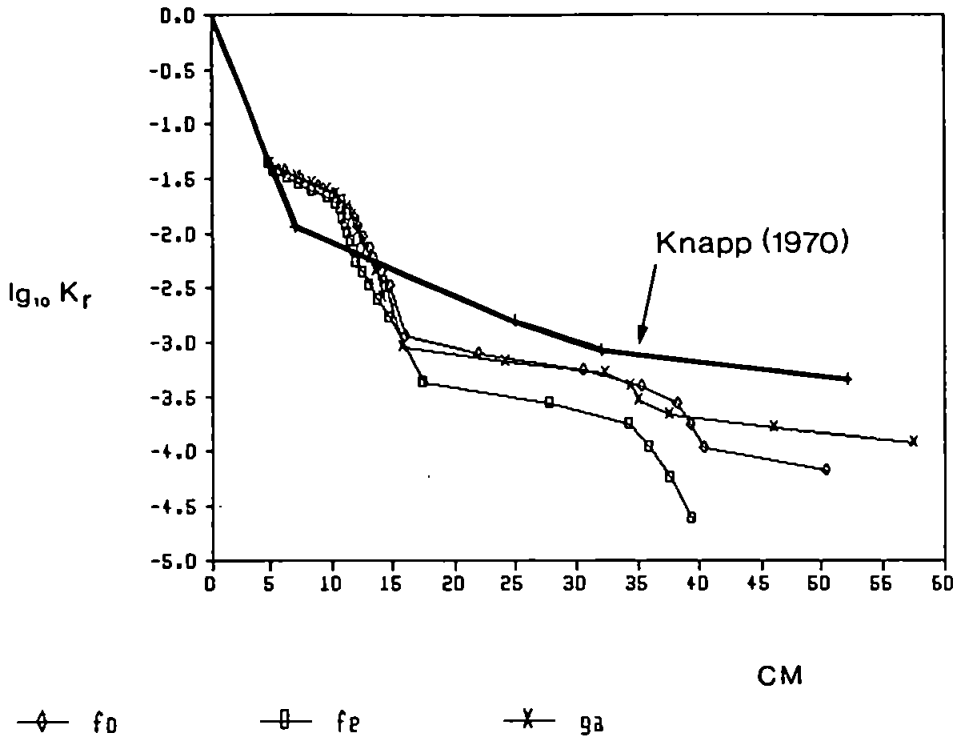

Figure 73. A mean relative hydraulic conductivity curve for the peaty O/A horizon of an ironpan stagnopodzol at Plynlimon, determined by steady-state permeametry (data from Knapp, 1970) and the mean relative hydraulic conductivity curves for the O/A and A/E horizons of the forest hillslope and that of the A/E horizon of the grassland hillslope. The curves for the forest and grassland hillslopes were derived from moisture capacity data applied to the Millington-Quirk equation.

7.4.9. Hydraulic Conductivity (K) within A/E and B Soil Horizons.

The relationship between the *state-dependent* hydraulic conductivities (K; i.e. $K_s * K_r$) and the negative capillary potential (or suction) within the A/E and B horizons within the forest and grassland hillslopes can be approximated using compound log-log functions (after Talsma, 1972):

$$K_{\text{forest E}} = 7.5\phi_c^{-0.9}{}_{(0\text{-}10\text{ cm})} \; ; \; 15000\phi_c^{-3.99}{}_{(10\text{-}30\text{ cm})} \; ; \; 23\phi_c^{-2.3}{}_{(30\text{-}1000\text{ cm})}$$

$$K_{\text{forest B}} = 0.025\phi_c^{-0.9}{}_{(0\text{-}10\text{ cm})} \; ; \; 18\phi_c^{-3.99}{}_{(10\text{-}30\text{ cm})} \; ; \; 0.0012\phi_c^{-1.25}{}_{(30\text{-}300\text{ cm})}$$

$$2000\phi_c^{-3.7}{}_{(300\text{-}500\text{ cm})}$$

$$K_{\text{grassland A}} = 3.4\phi_c^{-0.8}{}_{(0\text{-}10\text{ cm})} \; ; \; 5000\phi_c^{-3.99}{}_{(10\text{-}30\text{ cm})} \; ; \; 10\phi_c^{-2}{}_{(30\text{-}300\text{ cm})}$$

$$1E{+}15\phi_c^{-7.7}{}_{(300\text{-}500\text{ cm})}$$

$$K_{\text{grassland B}} = 3.1\phi_c^{-0.8}{}_{(0\text{-}10\text{ cm})} \; ; \; 5000\phi_c^{-3.99}{}_{(10\text{-}30\text{ cm})} \; ; \; 10\phi_c^{-2}{}_{(30\text{-}300\text{ cm})}$$

$$1E{+}15\phi_c^{-7.7}{}_{(300\text{-}500\text{ cm})}$$

(dim. K cm hr^{-1}; ϕ_c cm H_2O)

By applying the capillary potentials monitored at each slope position to the K-parameterizations (see above), and then averaging the resultant hydraulic conductivities over the whole length of the hillslope, the temporal variation of the A/E horizon conductivities can be compared with those of the B horizon (Figures 74 and 75).

Within the forested hillslope, the conductivity of the E horizon was almost always 3 orders of magnitude greater than that within the B horizon (Figure 74). In contrast, the conductivity of the A/E horizon within the grassland hillslope was, generally, an order of magnitude less conductive than the B horizon (Figure 75).

The state-dependent conductivity data, therefore, implies that the forest hillslope should develop a much greater *lateral* rather than *vertical specific flux* (Section 8.2.2) within the A/E horizon, while the specific flux from the grassland A/E horizon is predominantly vertical.

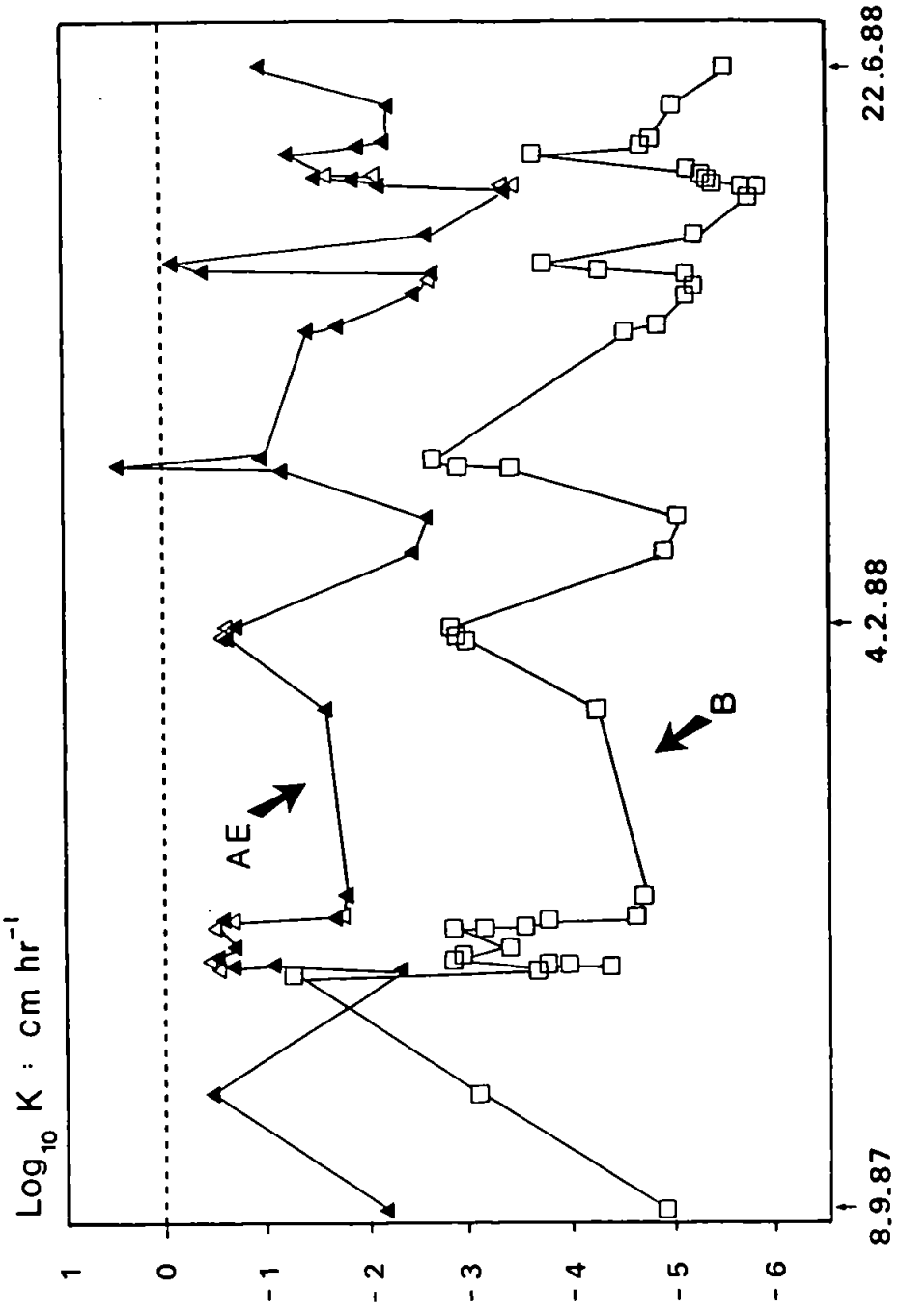

Figure 74. Mean state-dependent hydraulic conductivities of the A/E and B horizons within the forest hillslope, over time.

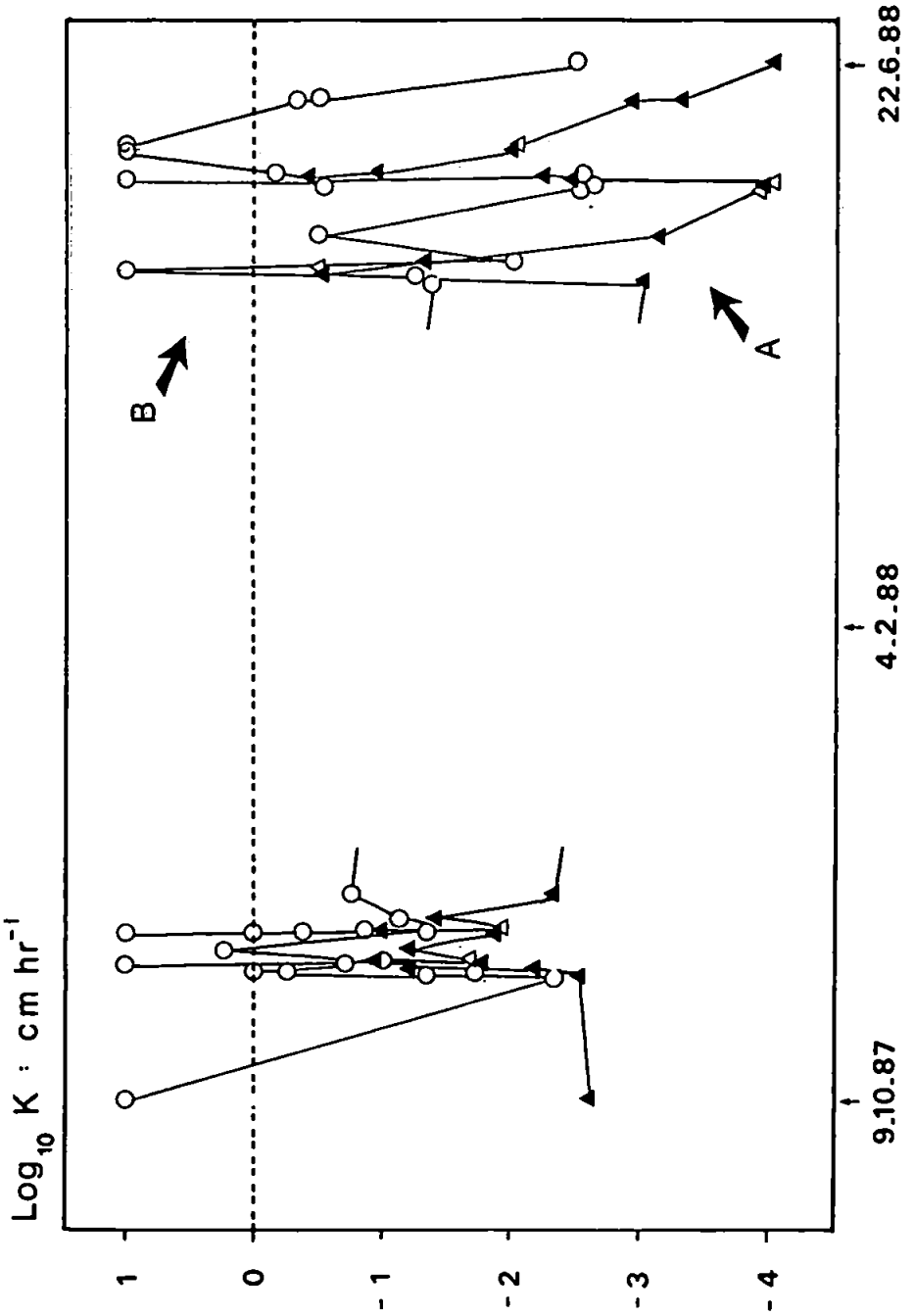

Figure 75. Mean state-dependent hydraulic conductivities of the A/E and B horizons within the grassland hillslope, over time.

7.4.10. Hillslope Hydraulic Conductivity by Inverse Solution.

The mean hydraulic conductivity of the whole forest hillslope was calculated from an *inverse solution* of the *general motion equation* (Equation 3). The inverse solution simply involves dividing the specific discharge (per unit catchment area) recorded at the upper-drain weir by a *representative* potential gradient, i.e.

$$<K_{hillslope}> = \frac{<q>}{J} \qquad [29]$$

Given that the state-dependent hydraulic conductivity within the riparian zone is within the range of conductivty within the podzolic slope, then the phreatic surface within the riparian zone will be a function of the flow rate from the podzolic slopes. The representative potential gradient for the hillslope (J) was, therefore, assumed to be approximated by the Darcian potential gradient between the riparian borehole and the stream surface (Hursh and Brater, 1941). This approximation is justified, given that the predicted values (J in Table 50) are close to the *sin of the mean slope angle* (i.e. sin 19.7° = 0.337), an approximation which has been shown to adequately represent potential gradients at both the aquifer and hillslope-scale (Dupuit, 1863; Zaslavsky and Sinai, 1981c; Tables 6-7 and 6-8). Moreover, the impact of errors within J upon the prediction of $K_{hillslope}$ are insignificant, given that the $K_{hillslope}$ is much more sensitive to variations within the specific discharge (<q> ; Table 50).

As a check on the inversion technique, the hydraulic conductivity was calculated for several *storm-periods* (defined within Section 5.3). The predicted hydraulic conductivities within each storm-period (excluding storm period 10, for which the complete hydrograph recession was not monitored) range from only 0.12 to 0.22 cm hr^{-1} (Table 50), indicating that the technique is consistent.

A mean hillslope hydraulic conductivity of 0.15 cm hr^{-1} (weighted arithmetic mean for periods 3-4, 7, 8, and 9) is 3 orders of magnitude greater than the state-dependent hydraulic conductivity within the B soil horizon (Figure 74), the horizon controlling the rate of water-flow within the whole subsoil/regolith (Section 8.2.2). Highly conductive zones within the near-surface O/A and A/E horizons must, therefore, be transmitting lateral flow to generate the storm-period streamflows reflected in the mean hillslope hydraulic conductivity.

Table 50. The calculation of the hillslope hydraulic conductivity using an inverse solution based upon the discharge recorded at the upper-drain weir.

PERIOD (D, days)	q (mm)	<q> (cm hr^{-1})	<H_1> (cm)	J	$K_{hillslope}$ (cm hr^{-1})
3-4 (22)	173	0.033	50	0.293	**0.17**
7 (10)	98	0.041	60	0.360	**0.22**
8 (13)	87	0.028	50	0.293	**0.15**
9 (44)	230	0.022	40	0.227	**0.12**
10 (>30*)	>16*	>0.002*	15	0.060	0.01*

where: $J = \frac{(<H_1> - <H_2>)}{L}$ L = 150 cm; $<H_2>$ = 6 cm

PERIOD=storm-period (Section 5.3.1)
D=duration of storm-period (Table 20)
*=incomplete hydrograph recession
q=total discharge per unit hillslope area, monitored at the upper-drain weir (Table 20)
<q>=mean discharge during each storm-period
<H_1>=mean height of phreatic surface, at the data-logged borehole (Figure 19)
<H_2>=mean depth of the phreatic surface at the seepage face
L=distance from the borehole to the seepage face at the streambed
J=Darcian potential gradient within the phreatic zone
<K_s>=saturated hydraulic conductivity within the riparian area

CHAPTER 8.

Hillslope Water-Flux Solutions.

8.1. Introduction.

Numerous methods of solving the physical representations of hillslope water movement can be found within the literature (see, e.g. Bear and Verruijt, 1987; Bear *et al*, 1968; Marsily, 1986; Pinder and Gray, 1977; Raudkivi and Callander, 1976). The two types of solution used to *calculate* water flux within the Tir Gwyn hillslopes were the approximative, and numerical types of solution. Approximative solutions are solutions based upon simplifications of:

1. the geometry of the flow-region (or domain),
2. the distribution of hydrological parameters,
3. the temporal resolution of the predictions, and
4. the motion equations themselves (Bear *et al*, 1968).

Other studies using approximative techniques to solve hillslope flow problems are presented within Table 51.

Numerical solutions by definition, are mathematical simplifications (to algebraic expressions) of the partial differential equations (pde's) describing the flow processes. Numerical solutions are assumed to be able to solve the spatial and temporal derivative of the rate of change of the hydrological properties and, hence, be solvable at successive short time steps.

Studies using numerical techniques to solve hillslope flow problems are presented within Table 52. Some of the numerical solutions presented within Table 52 (i.e. Anderson and Howes, 1986; Bernier, 1982; Beven *et al*, 1987; Troendle, 1979), use very coarse *discretizations* - or spatial resolutions of the internal-state of the flow region. Given that the accurate simulation of water-pathways over successive short time steps, requires that the derivative of the rate of change of the properties is approached, then it is not surprising that these simulations have not been validated against *measured* internal-state properties.

If the moisture content of a hillslope changes over time, then the magnitude and direction of water through the hillslope is not adequately represented by the *streamlines* (Section 1.4.3) predicted by the numerical solutions presented within Table 52. This *transient* situation requires the calculation of *pathlines* using a local coordinate system (Section 1.4.3). Selected studies using numerical techniques to predict the *pathlines* of sub-surface flow (Section 1.4.3) are presented within Table 53.

Table 51. Studies using approximative solutions to hillslope flux.

REFERENCE	TECHNIQUE	RESEARCH HILLSLOPE
Ahuja and Ross (1982, 1983)	Gram-Schmidt Orthonormalization	Hypothetical hillslope
Anderson (1982)	2D Drainage Simulation Model	Winford Catchment, Som., U.K. (Anderson and Kneale 1980)
Beven (1982)	Dupuit (kinematic)	East Twin Brook, Som., U.K.(Weyman, 1970)
Beven *et al* (1984)	TOPMODEL (Dupuit-based) Beven and Kirkby (1979)	Crimple Beck and Hodge Beck (Yorks) and Wye Catchment (Powys) U.K.
Bren (1978)	Dupuit (Boussinesq)	Clem Creek, Vict., Aust.
Engman and Rogowski (1974)	Dupuit (kinematic)	A hillslope in Pennsylvania, U.S.A
Hammermeister *et al* (1982b)	2D Resultant Flux Harr (1977)	Willamette Valley, OREG, U.S.A
Harr (1977)	2D Resultant Flux	W10,H. J. AndrewsExp. Forest, OREG, U.S.A.
Haus (1987)	Dupuit (numerical soln.)	Lange Bramke Catchment, Norway.
Hurley and Pantelis (1985)	Dupuit (kinematic)	Hypothetical hillslope
Moore *et al* (1986)	Saturated Source Area Function	Geeting Creek, NSW, Aust.
Sloan and Moore (1984)	Dupuit (kinematic + Boussinesq)	Hewlett Soil Model, Coweeta, N.C. U.S.A.
Smith and Hebbert (1983)	Dupuit (kinematic)	Batalling Creek, W. Aust.
Weyman (1973)	Dupuit for saturated flux	East Twin Brook, Som., U.K.
White and Jayawardena (1975)	Diffusive approximation	Wye Catchment, Powys, U.K.

Table 52. Hillslope hydrological studies using numerical solutions of the full Richards equation.

REFERENCE	NUMERICAL SOLUTION	RESEARCH HILLSLOPE
Anderson and Howes (1986)	1D Finite Difference (Sat/Unsaturated) modified HYMO	North Creek, TEX, U.S.A. and Sixmile Creek, ARK, U.S.A.
Bernier (1982)	2D Finite Difference (Sat/Unsaturated) VSA2	Whitehall Watershed, GA, U.S.A.
Beven (1977)	2D Finite Element (Sat/Unsaturated) Beven (1975)	Hypothetical hillslope
Beven *et al* (1987)	2D Finite Element IHDMv4	Wye Catchment, Powys, U.K. (Sat/Unstaurated)
Nieber and Walter (1981)	2D Finite Element (Sat/Unsaturated)	Laboratory Model
Reeves and Duguid (1975)	2d Finite Element (Sat/Unsaturated)	Hillslope soil model (Hewlett and Hibbert, 1963)
Sharma *et al* (1987)	3D Integrated Finite Difference (Sat/Unsaturated) HYSPAC: see Ward *et al* (1986)	A Tennessee forest hillslope (Luxmoore, 1983)
Sloan and Moore (1984)	2D Finite Element (Sat/Unsaturated) Nieber (1979)	Hewlett Soil Model, Coweeta, N.C. U.S.A.
Troendle (1979)	2D Finite Difference (Sat/Unsaturated) VSA1	W5, Fernow Exp. Watershed, GA, U.S.A.
Yeh (1981)	2D Finite Element (Sat/Unsaturated)	Reynolds Creek Exp. Watershed, IDAHO, U.S.A. (Stephenson and Freeze, 1974)
Stephenson and Freeze (1974)	2D Finite Element (Sat/Unsaturated) Freeze (1971)	Reynolds Creek Exp. Watershed, IDAHO, U.S.A.

Table 53. Selected studies using numerical solutions employing local coordinates

REFERENCE	NUMERICAL SOLUTION	HYDROLOGICAL SCALE
Barry *et al*, (1988)	2D, Dagan (1984)	Bordon landfill, CA, USA
DeSmedt and Wierenga (1979)	1D Finite Difference (Sat/Unsaturated)	Glendale silt loam soil profile
Gvirtzman *et al*, (1988)	1D Finite Difference (Sat/Unsaturated)	Loess aquifer, Omer, Be'er Seva, Isreal
Jinzhong (1988)	2D Finite Difference (Sat/Unsaturated)	Sand box (Vauclin *et al*,1975)
Kipp *et al*, (1986)	1D Finite Difference (Saturated)	Uranium-scrap recovery plant, Wood River Jnt., Rhode Island, USA
Nkedi-Kizza *et al*, (1983)	1D Finite Difference (Sat/Unsaturated)	Oxisol soil core
Osborne and Sykes (1986)	2D Finite Element (2 phase immiscible)	Hyde Park landfill, Niagara Falls, NY, USA
Pickens and Lennox (1976)	2D Finite Element (Sat/Unsaturated)	Hypothetical groundwater flow system
Russo (1988a,b)	1D Finite Difference (Sat/Unsaturated)	Hypothetical soil profiles
Voss (1984)	2D Finite Element/IFD (Sat/Unsaturated) SUTRA	(1)Panoche clay loam soil profile (Warrick *et al*, 1971). (2) Sea-Water Intrusion (Henry, 1964)
Wagenet and Hutson (1987)	1D Finite Difference (Unsaturated) LEACHM	
Warrick *et al* (1971)	1D Finite Difference (Sat/Unsaturated)	Panoche clay loam soil profile

The forest and grassland hillslope-catenas (Sections 2.8.2., 3.5.3. and 4.2) both have marked differences between the distribution of their hydrological parameters within their gently sloping, riparian zones (Section 7.4.3) compared with their podzolic slopes (Section 7.4.3). Flow within the two elements of the hillslope-catena is, therefore, calculated separately (Sections 8.2.1, 8.2.2, 8.3.2, 8.3.3),

8.2. Approximative Solutions.

Once a *link* is established between the hydrological response within the forest riparian zone, and that of the stream, the flux from that riparian zone into the stream is calculated by an approximative solution based upon the dynamics of the phreatic surface (Section 8.2.1).

Flow within the steep, podzolic slopes beneath both the forest and grassland covers (Section 8.2.2), is calculated using:

1. an approximative solution of the Richards' equation applied to capillary potentials determined by tensiometry,
2. the free-surface method applied to piezometer measurements, and
3. throughflow-trough outflows, scaled against piezometer-based fluxes.

The *unit* or *specific fluxes* (dim. LT^{-1}) laterally within the A/E horizon and vertically into the B horizon, which are predicted by the tensiometric techniques are compared. Lateral fluxes are *coupled* and integrated to give a *volumetric flux per 50 m^2 of hillslope surface*, so that they might be compared with the vertical fluxes. Flows within the forest hillslope are compared with those within the grassland hillslope, for representative dry-period and wet-period storms (Section 8.2.2).

Predictions of water-flux based upon internal-state hydrological properties are compared with the mean-areal-fluxes predicted from external-state, streamflow data (Section 8.2.3).

8.2.1. Flux within the Forest, Riparian Saturated Zone.

As water moves through a catchment or hillslope towards a stream, it must *concentrate*, because the area of the stream-seepage-face is always smaller than the area of the ground receiving precipitation. The greatest concentration of water (with respect to either the depth of the profile, hillslope length, or stream length) generally takes place close to the stream-outflow (i.e. within the riparian area) (Ahuja and Ross, 1982; Bren and Turner, 1979; Jaeger, 1956; Troendle, 1985).

This concentration or convergence of flow may be the main determinant of stream development (Bunting, 1961; Nutter, 1973).

Given that soil pores must be almost saturated with water, for water to drain from a soil and thereby generate *saturation overland flow* or a stream (Bren, 1978), this convergence of flow can lead to the development of saturated zones in otherwise partially-saturated

hillslopes (Zaslavsky and Rogowski, 1969). Response of these saturated zones within stream-side or *riparian* zones has been shown to be very dynamic, closely following the response within the adjacent stream (Hewlett, 1969; Hursh and Brater, 1941; Kudelin, 1949 in Chebotarev, 1962; Ragan, 1968). Such a similarity between the response of the stream and the that of the *riparian saturated zone*, is exhibited within the forest catchment at Tir Gwyn (Section 6.3.3).

Stream and Riparian Saturated Zone Responses.

The response of the stream, monitored at the upper-drain weir, shadows the rise and fall of the phreatic surface (or water-table) within the riparian zone at the base of the forest hillslope (Figure 78; Section 6.2.2.2). The height of the phreatic surface within the forest riparian zone was continuously monitored by a datalogged well, installed at 1.5 m upslope of the forest drain, and 1.5 m downslope of the break-in-slope between the riparian zone and the podzolic slope (Figure 19).

When the phreatic surface (at the well) is less than 10 cm below the ground-surface, and greater than 5-10 cm above the level of the stream surface, then its relationship to the streamflow generated can be expressed by a linear equation:

$$q_s = -10 + 300H \quad \text{or} \quad q_b = -0.3 + 1.8H$$

where q_s is specific stream discharge per unit area of seepage face (7.2 m^2) (dim. mm hr^{-1}), q_b is specific stream discharge per unit area of the hillslope (1480 m^2) (dim. mm hr^{-1}), and H is head or height of the phreatic surface above the stream surface (dim. m).

When the phreatic surface is less than 10 cm from the ground surface, a small increase in head produces a much greater stream discharge (Figure 76), which can be expressed by a second linear equation:

$$q_s = -5500 + 8310H \quad \text{or} \quad q_b = -34 + 50H$$

This implies, first, that the near-surface soil is more conductive (Section 7.4.3) and second, that flow moving through this conductive near-surface soil is able enter the stream without moving through less-conductive, deeper soil (Section 6.2.3; 7.4.3).

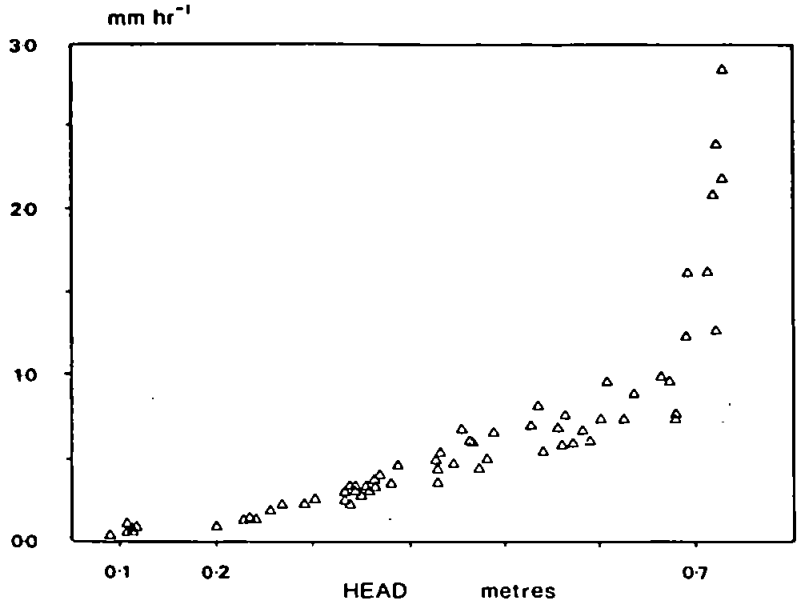

Figure 76. Specific stream discharge (per unit hillslope area) against the capillary potential or head monitored within the borehole at the base of the forest hillslope.

Riparian Outflow by the Free-Surface Method.

The empirical relationship between the height of the phreatic surface and the stream discharge given in the previous section, can be expressed physically with a knowledge of the the hydrological properties and geometry of the flow-region.

For periods when the phreatic surface is less than 10 cm from the surface, and greater than 5-10 cm above the level of the stream surface, the stream discharge can be approximated with Equation 30.

$$Q_w = \langle K_s \rangle \cdot \langle J \rangle \cdot \langle h \rangle \cdot w \qquad [30]$$

where:

$$\langle J \rangle = (H_1 - \langle H_2 \rangle) / L \qquad \text{(Darcy Gradient)} \qquad [31]$$

$$\langle h \rangle = 0.5(H_1 - \langle H_2 \rangle) + 0.625(H_1 - \langle H_2 \rangle)^2 \qquad [32]$$

(Figure 77)

$\langle K_s \rangle = 21$ cm hr^{-1} $w = 100$ cm $\langle H_2 \rangle = 6$ cm $L = 150$ cm

where Q_w is stream discharge per unit metre length stream channel (dim. $L^{-3}T^{-1}L^{-1}$), $\langle K_s \rangle$ is mean saturated hydraulic conductivity within the riparian area (dim. LT^{-1}), $\langle J \rangle$ is mean potential gradient within the phreatic zone (dim. LL^{-1}), $\langle h \rangle$ is mean depth of the phreatic surface (Figure 77) (dim. L), w is width of the hillslope segment (dim. L), H_1 is depth of phreatic surface, at the data-logged borehole, which is equivalent to ϕ_c at the base of the riparian zone, directly below the bore-hole (dim. L), $\langle H_2 \rangle$ is mean depth of the phreatic

surface at the seepage face (dim. L), and L is distance from the borehole to the seepage face at the stream-bed (dim. L)

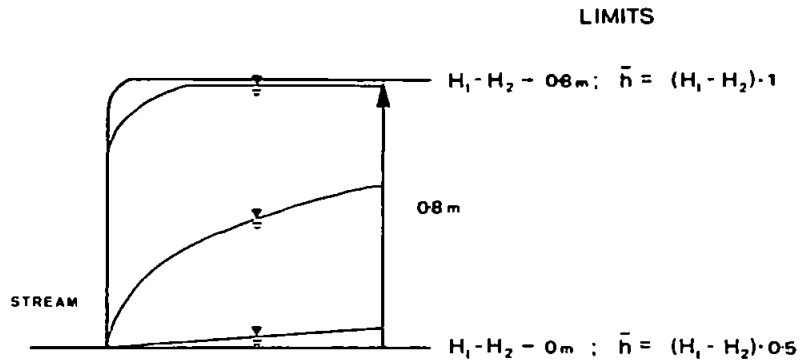

Figure 77. Calculation of the mean head within the riparian zone of the forest hillslope.

This relationship can be seen to reproduce the observed streamflow response (Figure 78), with the exception of periods of peak streamflow. The linear relationship between the *predicted* streamflow and the streamflow monitored at the upper-drain weir (Figures 3 and 13; Section 4.3.4) has an R^2 of 83.08 percent (Pearson Coef. 0.91) during all periods excepting those at the peak streamflow. The 1.13 l min^{-1} m^{-1} of streamflow predicted for storm-period 7, the 127 mm snow-event, is far less than that recorded within the weir (2.33 l min^{-1} m^{-1}, *not shown in Figure 78*) because of the likelihood of the generation of overland flow, during the snow melt (Price and Hendrie, 1983).

The statistical representation of the physical relationship between the response of the phreatic zone (at the well) and the streamflow per metre length of stream channel takes the form of an *quadratic* increase, i.e.

$$Q_w = 2.1 \langle H \rangle^{2.1} \qquad [33]$$

(dim. Q_w = l min^{-1} m^{-1}; H = m)

This relationship between the response of the phreatic surface and streamflow generated by the Tir Gwyn, forest hillslope is, therefore, *less non-linear* in comparison with the response of the brown podzolic slope monitored by Weyman (1973). The *groundwater rating curve* (Zaltsberg, 1987) developed by Weyman (*op. cit.*) approached a *quartic* increase, i.e.

$$Q_w = 8.7 \langle H \rangle^{3.73}$$

(dim. Q_w = l min^{-1} m^{-1}; H = m)

$Q = K \cdot A \cdot (dH/dL)$ where: $q = QA^{-1}$

if: $A = 200\ cm^2$ (surface area of soil at top of core)

dH = loss of head between the core top and base

L = length of the soil core within permeameter

Ring with 10 cm depth soil (L) and 5 cm of constant head upon the surface of the soil, gives dH =15 cm

$q = 300\ cm\ hr^{-1}$ (10 cm soil)

$q = 600\ cm\ hr^{-1}$ (5 cm soil in bottom half of the soil core: dH = 15 cm)

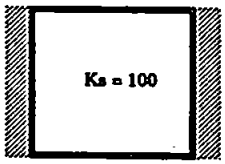

$q = 30{,}000\ cm\ hr^{-1}$ (10 cm soil)

$q = 40{,}000\ cm\ hr^{-1}$ (5 cm soil, in top half of the soil core: dH = 10 cm)

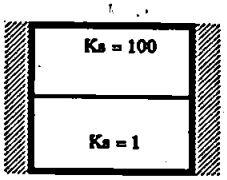

$q = 15{,}150\ cm\ hr^{-1}$ (arithmetic-mean conductivity: $\{1 + 100\}/2 = 50.5\ cm\ hr^{-1}$)

Thus the flow through the 10 cm long, layered core (15,150 cm hr-1), predicted using the mean conductivity of the two horizons would be far greater than that predicted through 5 cm of the least conductive horizon alone (600 cm hr-1) with the same head applied. This would appear to be erroneous.

Figure 79. The calculation of inter-horizon conductivity using anarithmetic mean.

Bear *et al* (1968) and Childs (1969) suggest that the mean-vertical-conductivity through two soil horizons can be accurately represented with a *harmonic mean*, i.e.

$$K_{ih} = \frac{(D_1 + D_2)}{(D_1/K_1 + D_2/K_2)} \qquad [34]$$

Adding A/E and B horizon depths (D) of 10 and 20 cm respectively (Table 8) to Equation 34, it can be shown that *when* the hydraulic conductivities of the two soil horizons are very different, Equation 34 is approximately equivalent to the conductivity (K) of the least conductive horizon, i.e.

$$\text{where: } D_1 = D_2 \qquad \text{then: } K_{ih} = K_{min}$$

The flow of water beneath the soil horizon with the least water-flow will, therefore, be controlled by the vertical flow through that overlying horizon. Such a suggestion has also been made by Bear *et al* (1968), Hillel (1987), Hursh and Hoover (1941), Molchanov (1960), Nielsen *et al* (1973), Parlange (1974) and Weyman (1973). In addition, where a fine textured soil overlies a coarse textured soil the vertical flow of water into the coarse textured soil is controlled by that flowing through the fine textured soil (Section 1.4.2.; Parlange, 1974)

As the B soil horizon within the forest hillslope has both a lower intrinsic permeability and finer texture than the underlying B/C and C horizons (Figure 61), it is, therefore, suggested that it controls the rate of vertical flow into those underlying horizons.

Within the podzolic slope of the forest hillslope-catena, the B soil horizon is generally 3 orders of magnitude less conductive than the A/E horizon (Figure 74). Within the grassland slope the B horizon was generally one order of magnitude greater than the A/E horizon (Figure 75). The use of the arithmetic-mean conductivity would, therefore, have produced highly inaccurate *inter-horizon conductivities*, particularly in the forest hillslope

The state-dependent vertical-conductivities within both the forest and grassland hillslopes are, therefore, determined from the value for the least conductive soil horizon. Vertical water-fluxes predicted using these mean-vertical-conductivities or *profile conductivities* are presented within the following section and within Section 8.2.3.

Vertical Flux from A/E to B Soil Horizons.

The *specific* vertical flow of water from the A/E to B soil horizon within the ploughed, grassland slope is generally 1.8 orders of magnitude greater than that within the forest (e.g. storm 3-4, Figures 80 and 81). Fifteen to 38 percent of difference can be accounted for by a 15 percent (Hudson, 1988) to 38 percent (Section 5.2.4) greater evapo-transpirational loss from the forest hillslope. The remainder of the difference must result from a greater lateral flux of water within the O/A or A/E horizons of the forest slope.

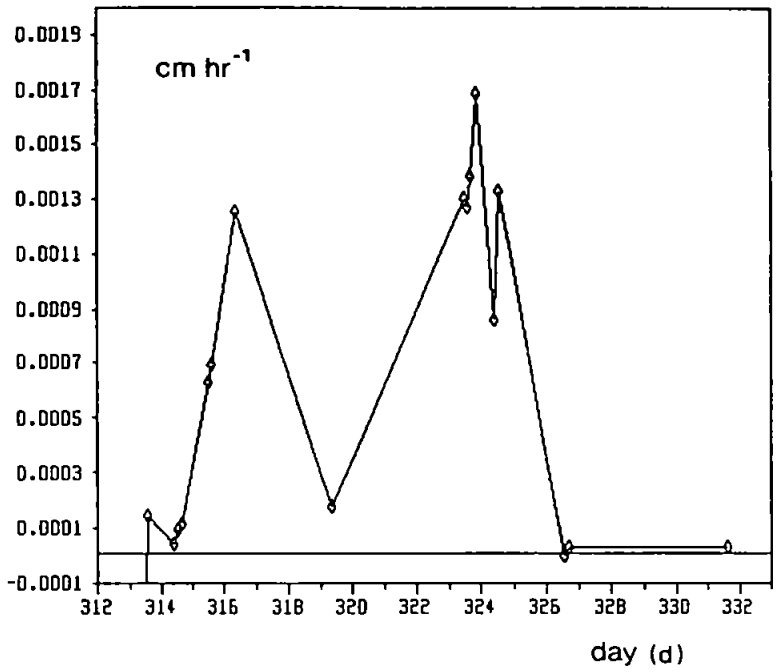

Figure 80 Specific flux through the B horizon of the forest hillslope, during storm-period 3-4.

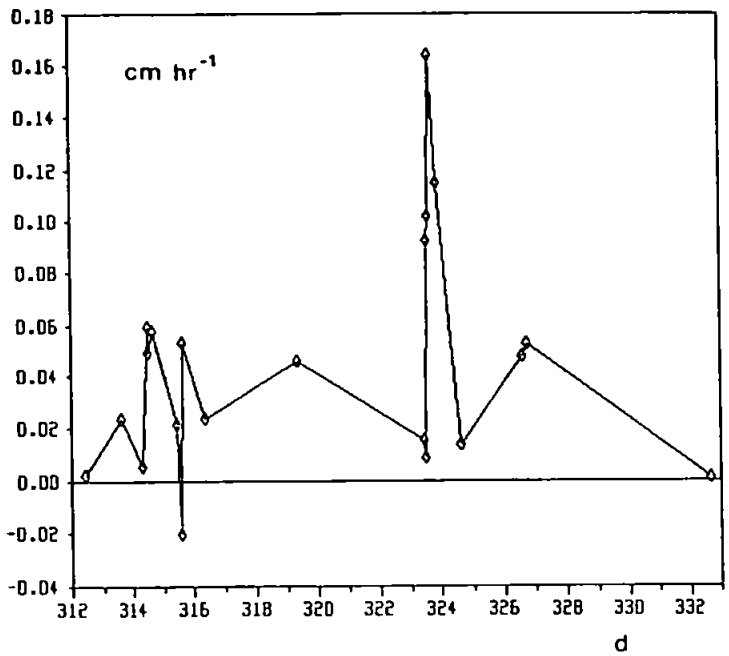

Figure 81. Specific flux through the B horizon of the grassland hillslope, during storm-period 3-4.

Lateral Flux within Un-Saturated Zones of A/E Soil Horizons.

The *specific* lateral flux of water within the un-saturated zone (10-18 cm deep) of the forest A/E horizon is generally 0.7 orders of magnitude greater than that within the ploughed, grassland A/E horizon (e.g. Figures 82, 83, 84 and 85).

This increase in lateral flux within the forest A/E soil horizon compared with that of the grassland slope can be attributed to either:

1. the 4.7° increase in mean slope-angle (Ahuja and Ross, 1982; Sharma *et al*, 1987; Section 2.11), or
2. the much greater (relative) discontinuity between the hydraulic conductivities of the forest A/E and B soil horizons, when compared with that between the corresponding horizons within the grassland slope (Figures 74 and 75; Section 8.3.1).

Gaskin (1987) and Plamonden *et al* (1972) suggested that an increase in the slope angle may emphasize the impact of the lateral deflection of flow resulting from hydraulic discontinuities

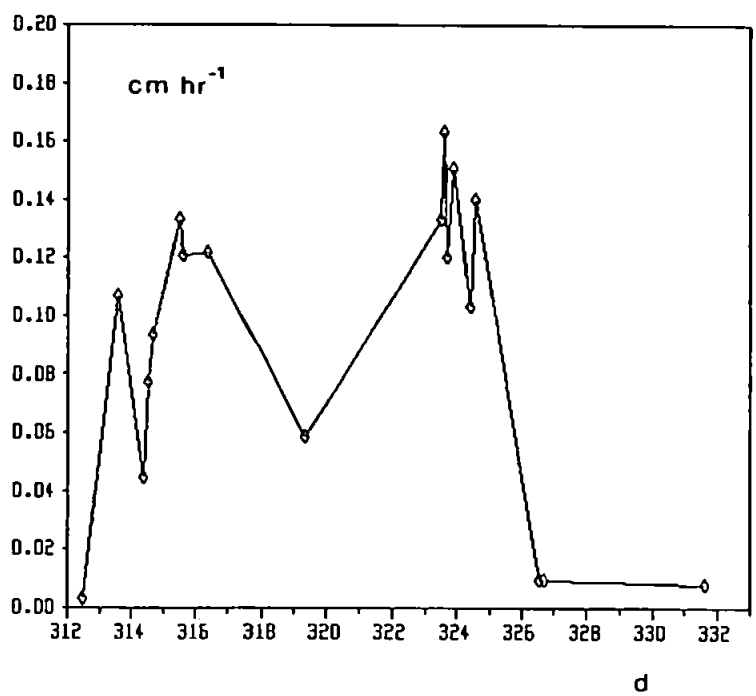

Figure 82. Specific lateral flux within the un-saturated upper zone of the forest A/E horizon, during storm 3-4.

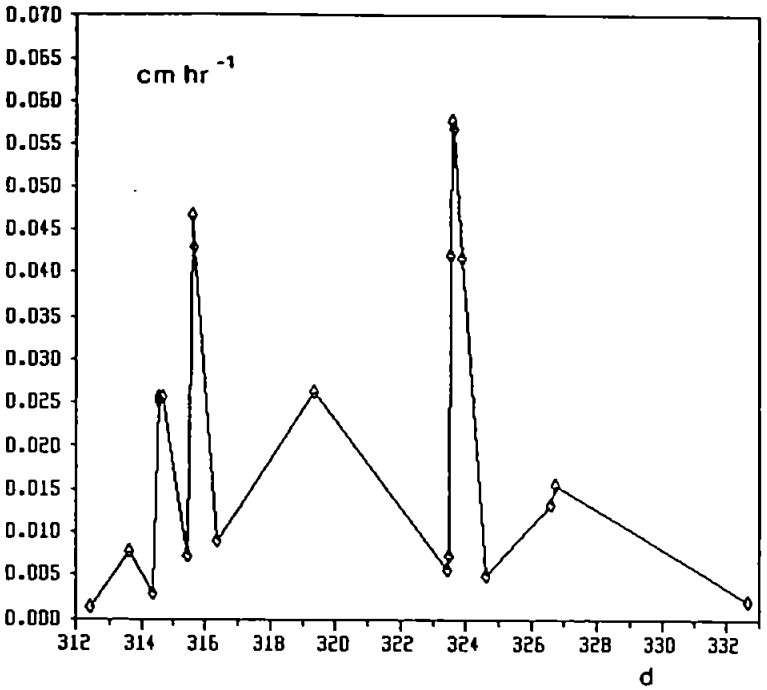

Figure 83. Specific lateral flux within the un-saturated upper zone of the grassland A/E horizon, during storm 3-4.

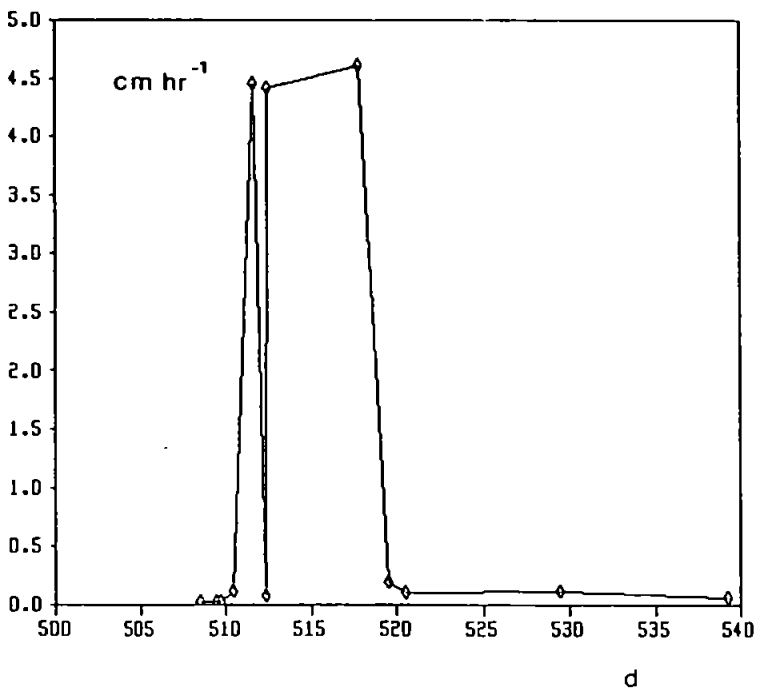

Figure 84. Specific lateral flux within the un-saturated upper zone of the forest A/E horizon, during storm 10.

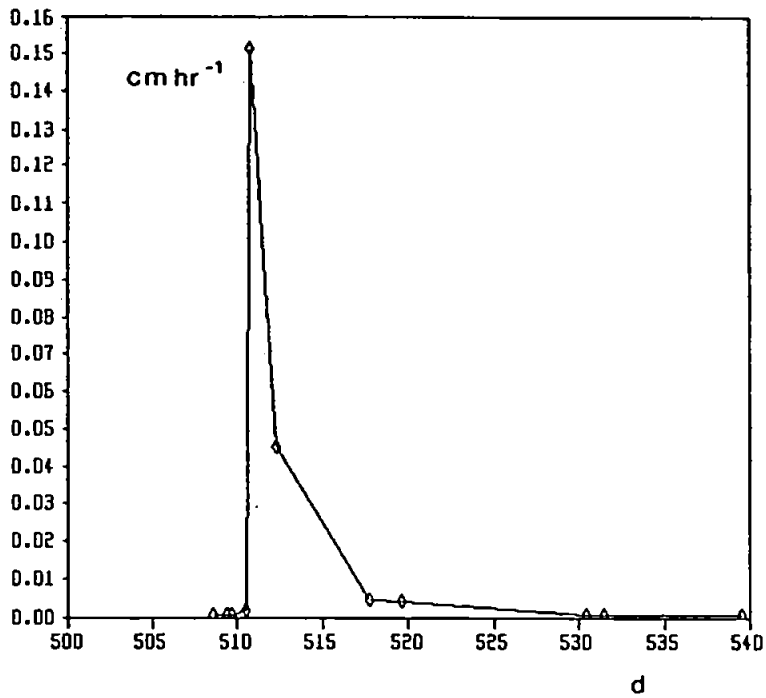

Figure 85. Specific lateral flux within the un-saturated upper zone of the grassland A/E horizon, during storm 10.

Vertical A/E to B Flux in relation to Lateral Un-Saturated A/E Flux.

Within the forest hillslope, lateral flow within the un-saturated zones of the A/E horizon always dominates over vertical flow into the underlying B horizon. Unsaturated lateral flow is generally some 2.2 orders of magnitude greater than the vertical flow (e.g. Figures 80 and 82).

The dominance of lateral flow within the forest A/E horizon results from higher *lateral to vertical* hydraulic conductivities (Sections 7.4.9) dominating over higher *vertical to lateral* potential gradients (Section 6.3.5). The rate of lateral flow is only similar to the vertical flow towards the end of the very dry, 10 day period within May (Section 6.3.2., 6.3.4., 6.3.5), when the lateral flow reduced by some 4 orders of magnitude from that during the previous storm (Figure 86).

In contrast, the specific lateral flow within the A/E horizon of the ploughed, grassland hillslope is slightly less than the specific vertical flow into the B horizon. The specific lateral flow within the A/E horizon is approximately half (or 0.3 orders of magnitude) of that moving into the B horizon (e.g. Figures 81 and 83).

The smallest lateral flux within the grassland A/E horizon (0.00006 cm hr^{-1}) occurred within the very dry, 10 day period within May (14-24/5/88: Sections 6.3.2., 6.3.3. and 6.3.4; Figure 87) and at the end of the monitoring period (23 June 1988).

Relatively small precipitation events within the summer appeared to generate as much or more specific lateral flux *at particular points in time* within the grassland A/E horizon, as the large events within the winter. A relatively small precipitation event of 28 mm within the dry period between 30 April and 4 May 1988 (mean intensity: 6 mm day^{-1}) generated as much lateral flux within the grassland A/E horizon (Figures 87) as within wet-periods related to storms 3 and 4 (9-27 November 1987: mean intensity 14 mm day^{-1}) (Figure 83). During this small dry-period event, the lateral flow was slightly greater than the vertical flow into the B horizon (Figure 87).

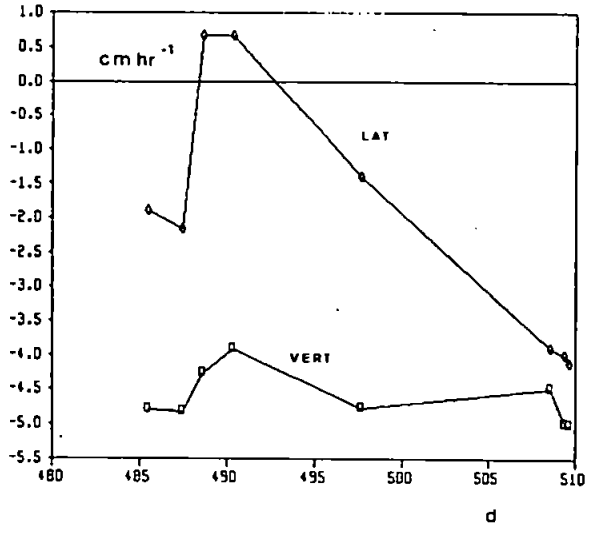

Figure 86. Specific lateral flux within the un-saturated upper zone of the forest A/E horizon, during the 10 day, dry period 14 - 24/5/88.

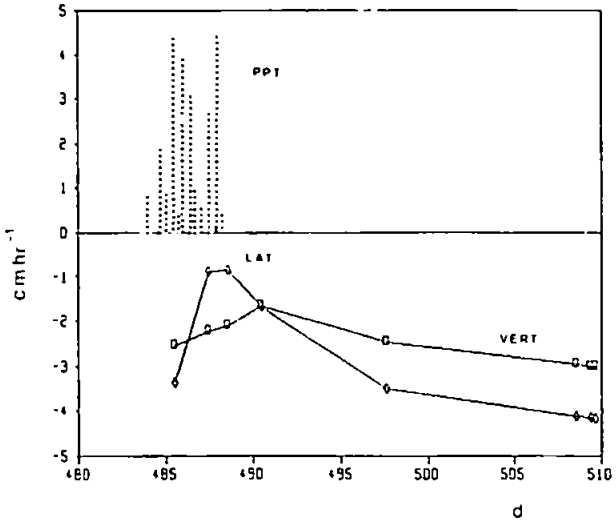

Figure 87. Specific lateral flux within the un-saturated upper zone of the grassland A/E horizon, during the 10 day, dry period 14 - 24/5/88.

The forest hillslope exhibited the same large response to this small precipitation event, after an initial lag of several hours (Figure 86). Gaskin (1987) monitoring flow within a hillslope section in the Coweeta catchment (NC, USA) also noted larger lateral A horizon fluxes during the dry summer months compared to the winter months.

Lateral Flux within Un-Saturated Zones of O/A Soil Horizons.

Capillary potential was not monitored within the O/A horizon (0-10 cm) of the ploughed, grassland hillslope. As the saturated hydraulic conductivity (Section 7.4.2.; Figure 62), bulk density and porosity (Section 7.2.; Figures 51 and 52) of this horizon are only slightly larger than those of the underlying A horizon, the specific flux within O/A horizon is taken to be the same as that within the A horizon.

The under-estimation of flux resulting from this approximation is, however, small. This is because almost all of the flux from the grassland slope into the riparian zones passes vertically through the B horizon (Table 56).

Capillary potential within the O/A horizon of the forest hillslope was determined by 13 tensiometers, 9 of which were located around the 2 trees (Section 4.4.3). The remaining 4 tensiometers were located at 0, 2.5, 5, and 10 m along the instrumented transect, and monitored using a *Scanivalve* system (Section 4.4.3). The *Scanivalve* system produced a very fragmentary record. The capillary potential of the O/A horizon was, however, similar to that of the A/E horizon monitored by those tensiometers located around the two trees, and those linked to the *Scanivalve*. Lateral flow within the unsaturated zone of the O/A horizon is discussed further within Sections 8.2.3.

Lateral Flux within Saturated Zones of O/A and A/E Soil Horizons.

The lateral flux within the saturated, basal zones of both the O/A and A/E horizons of the forest hillslope were calculated from :

1. point-measurements of piezometer water-level, and
2. *continuous* monitoring of throughflow troughs.

To remove the effects of the artificial seepage face created by the presence of the throughflow troughs, the predicted flows were scaled against those determined by the piezometer technique.

1. Piezometer-based Flux: Point-measurements of lateral flux within the saturated, basal zones of the O/A and A/E horizons of the forest hillslope were calculated from piezometer water-level data (Sections 4.4.3. and 6.3.3) using Equation 35, i.e.

$$Q_{piez} = \langle K_s \rangle \cdot \langle J \rangle \cdot \langle h \rangle \cdot w \cdot L_s \qquad [35]$$

$$\langle K_s \rangle = 730 \text{ cm hr}^{-1} \qquad w = 100 \text{ cm} \qquad L_s = 50 \text{ m}$$

where Q_{piez} is lateral water-flux within the perched water-table (dim. $LT^{-1}L^2$), $\langle K_s \rangle$ is mean saturated hydraulic conductivity along the length of the perched water-table (dim. LT^{-1}), $\langle J \rangle$ is mean potential gradient (Darcian) between all piezometers (dim. LL^{-1}), $\langle h \rangle$ is mean depth of the phreatic surface at all piezometers (dim. L), w is width of the hillslope segment (dim. L), and L_s is length of the hillslope segment (dim. L).

The resultant fluxes within the saturated basal zones of the A/E horizon presented within Figure 88, were calculated for specific *points in time* during the period 8 November 1987 and 23 June 1988. The response of the shallow phreatic zones at the base of the O/A horizon are shown for an individual storm-period with the response of the forest stream (Figure 89). Perched water-tables did not develop within the O/A or A/E horizons on the ploughed, grassland slope (Section 6.3.3).

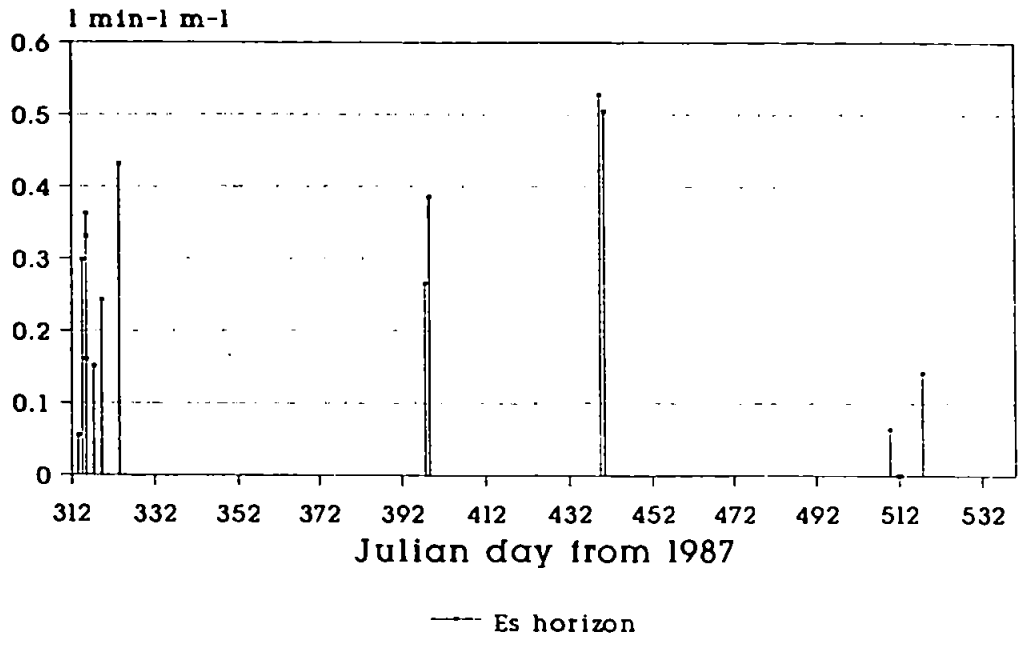

Figure 88. Instantaneous lateral flux within the saturated basal zones of the A/E horizon of the forest hillslope.

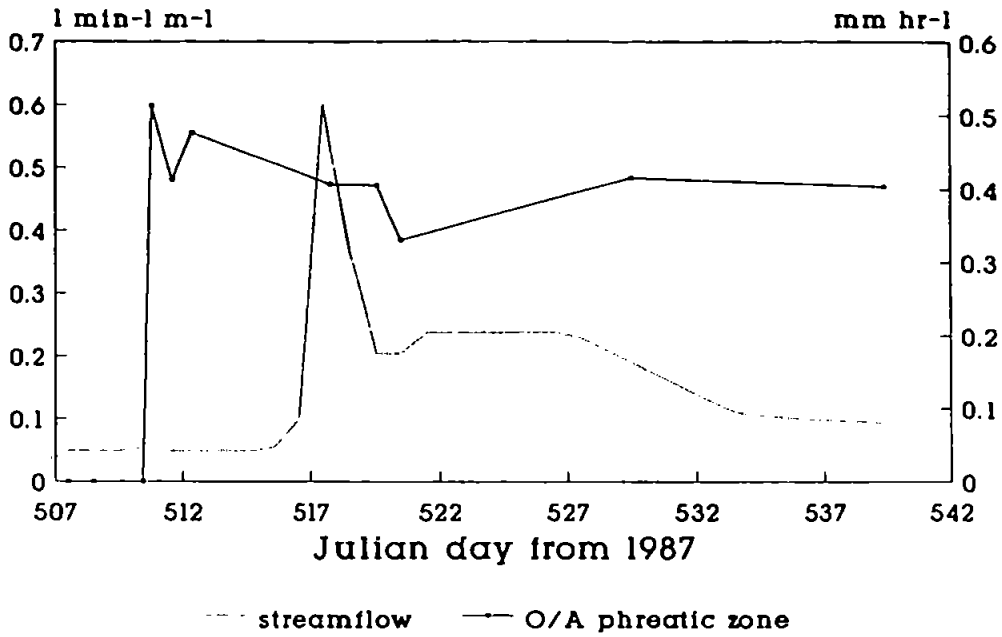

Figure 89. Lateral flux within the saturated basal zone of the O/A horizon of the forest hillslope, during storm-period 10. The flux is an average value calculated from 7 litter-layer piezometers located at the 0, 2.5, 5, 10, 20, 30 and 40 m slope positions.

2. Trough-based Flux: A *throughflow pit* was excavated at the mid-point of the hillslope-catena, some 20 m upslope of the forest drainage channel (Figure 3). A 1 m wide throughflow trough was installed within the pit at a depth of 10 cm, and the outflows from the O/A horizon continuously monitored using a tipping-bucket mechanism (Section 4.4.6).

The use of this technique for the determination of lateral flux within saturated soil zones, is complicated by the vertical (Ahuja and Ross, 1982) and across-slope (Knapp, 1971, 1974) convergence of water-flow towards the artificial seepage-face which is necessary to collect the water.

The temporal distribution of discharge from the throughflow trough was very different to response of the piezometers within the O/A horizon (Figures 89 and 91). The differences between the 2 techniques may be the result of either:

1. the impact of an artificial seepage face, or
2. the impact of an individual tree upon the trough outflows

1. Impact of an Artificial Seepage Face. During storm-periods the water-level within each O/A piezometer remained relatively constant in comparison with the throughflow trough outflows. At times when piezometer water-levels were high and the throughflow troughs were not flowing (Figures 89 and 91), the difference between the two instruments can be attributed to a lag in trough response resulting from enhanced soil-drying and stream-line divergence (in

under-saturated soil) close to an artificial seepage-face (Atkinson, 1978). Clearly, this would lead to the under-estimation of the total water-flux during storm periods. Of greater significance is the great variability in flow during periods when the throughflow troughs were flowing.

As the flow of water within a porous media increases, the *boundary conditions* of a flow region (Section 8.3.1) exert a greater and greater influence upon the flow, relative to that of the *internal conditions* (i.e. hydrological parameters: Chapter 7) (Anderson, 1982; Anderson and Howes, 1986; Binley *et al*, 1989). Given this, the largest relative amount of draw-down of any phreatic surface upslope of the pit is likely to occur when the phreatic surface is at its highest. To fit the trough outflows to the piezometer-based flux would, therefore, require the application of a *non-linear correction factor*. By applying an exponential function with a shape function of 0.7, the throughflow trough outflows could be fitted to the 54 piezometer-based fluxes during storm-period No.10 (Figure 92), i.e.

$$Q_w = 3000 (0.7^{Qtrough}) \qquad [36]$$

where Q_w is the lateral flux within the saturated basal zone of the O/A horizon (dim. l min^{-1} 50 m^2) and Qtrough is the measured outflow from the 1 m wide, O/A throughflow trough (dim. cm^3 hr^{-1}). The shape function of 0.7 determines the extent of the non-linearity within relationship between trough outflow and the true lateral flux; a value of 1 would indicate a linear relationship.

The lateral flux within the saturated basal zone of the O/A horizon based upon scaling trough outflows against piezometer measurements are presented within Table 54.

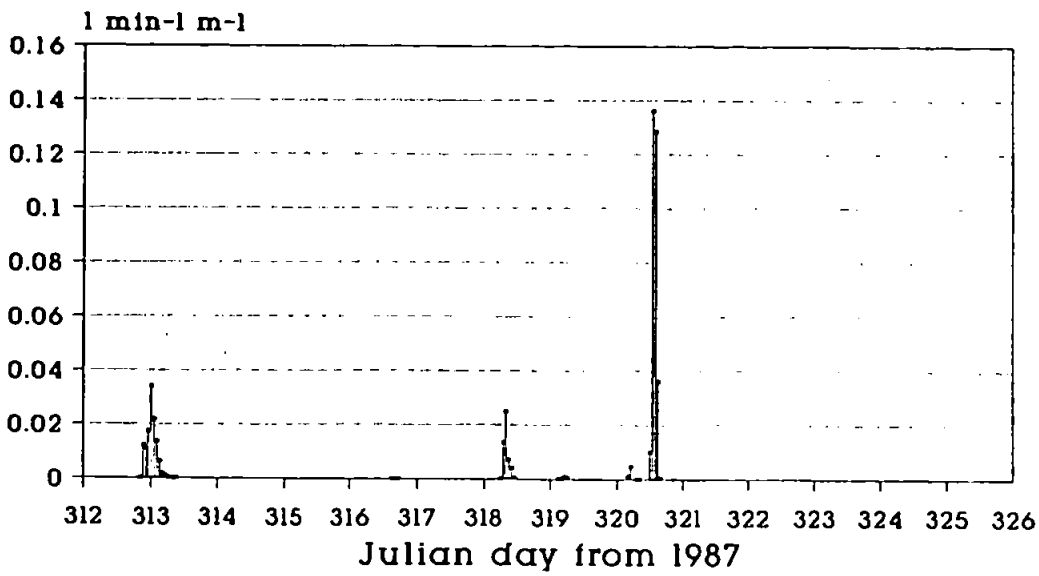

Figure 90. Predicted lateral flow within the saturated basal zone of the forest O/A horizon, based upon linear-scaling of the average storm-flux calulated from piezometer measurements against the outflow from the O/A horizon throughflow trough (non-linear convergence is not taken in to account). Data for storm-period 3-4.

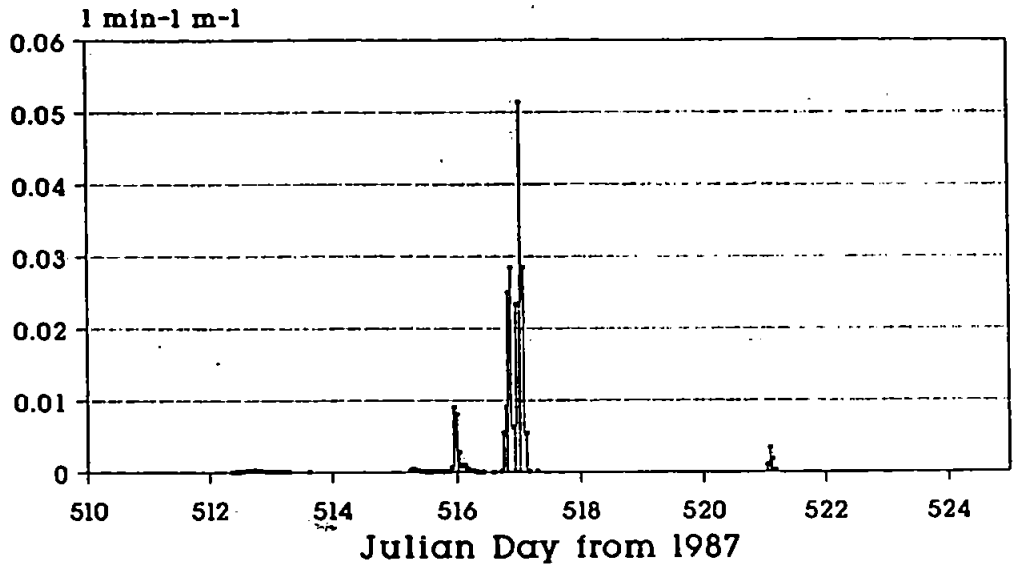

Figure 91. Predicted lateral flow within the saturated basal zone of the forest O/A horizon, based upon linear-scaling of the average storm-flux calulated from piezometer measurements against the outflow from the O/A horizon throughflow trough (non-linear convergence is not taken in to account). Data for storm-period 10.

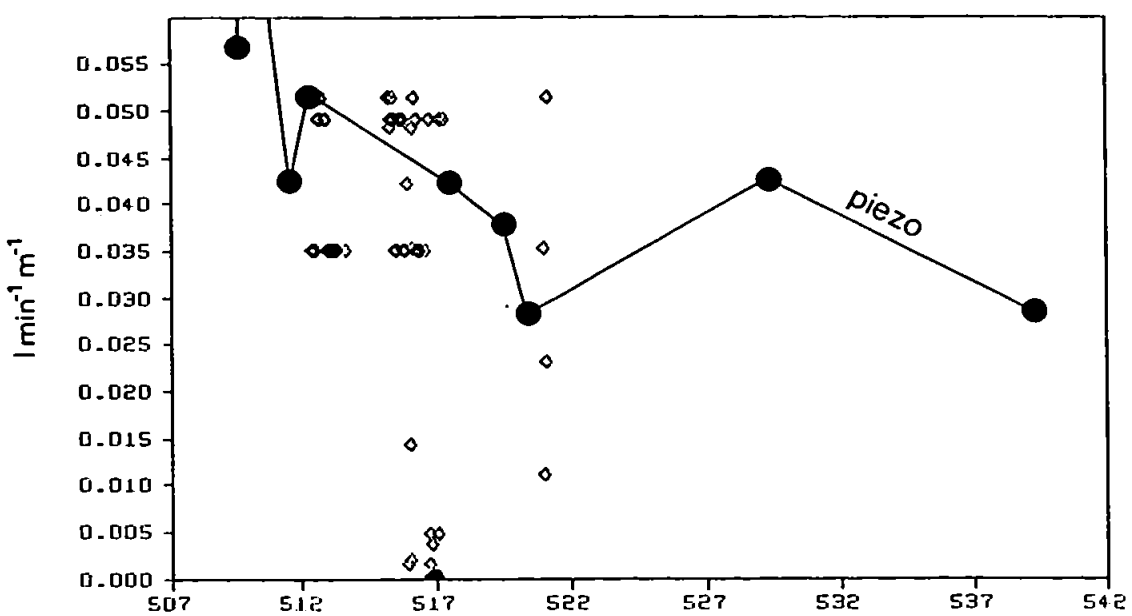

Figure 92. Predicted lateral flow within the saturated basal zone of the forest O/A horizon, based upon scaling of the outflow from the O/A horizon throughflow troughs against a non-linear function of the average storm-flux calulated from piezometer measurements. A non-linear function is used to remove the non-linearity in the convergence towards the thoughflow troughs. Data for storm-period 3-4.

2. *Impact of an Individual Tree.* The alternative explanation for the different responses measured by the two techniques results from the throughflow trough being 1 m downslope of a large tree. The temporal variability in the trough outflows might, therefore, be caused by localized stemflow inputs (Sections 5.2.1., 6.2.5. and 6.3.6) in to a soil experiencing enhanced root abstractions of water (Sections 6.2.5. and 6.3.6). A *possible reduction* of the intrinsic permeability of the B/C and C horizons (Section 7.4.4), as a result the tree's weight or it's movement during windy conditions, might enhance the impact of the stemflow inputs upon the temporal variability of the generation of lateral flow. Given the possible impact of the tree upon the trough response, the difference between the total volumes OF water monitored by the throughflow troughs during individual storm-periods is presented in Table 54, together with the piezometer-scaled fluxes.

Podzolic Slope Flux.

To calculate the total flux water into the riparian zone from the podzolic slope, as well as the relative contribution of purely topsoil flux (lateral flow within O/A and A/E horizons) and flux which has passed through the B horizon, the specific fluxes were *coupled* in both parallel and series.

Parallel Coupling of Lateral Flow: The specific fluxes (dim. LT^{-1}) within the unsaturated and saturated zones of the O/A and A/E horizons are multiplied by the respective horizon depths and then summed, to calculate the total flux (dim. L^2T^{-1}) moving laterally above the B soil horizon. This procedure is known as *parallel coupling* (Bear *et al*, 1968). The lateral flow from the 50 m long hillslope lengths is integrated over a 1 m wide hillslope segment, to give a volumetric flow per the 50 m^2 area of hillslope surface (dim. $L^3T^{-1}L^{-2}$) (Figure 93). These lateral flows are presented within Tables 54, 55, and 56.

Serial Coupling of Vertical Flow: The vertical flux through the B soil horizon of both hillslopes is integrated over same 1 m wide and 50 m long hillslope segment as the lateral flux (dim. $L^3T^{-1}L^{-2}$) (Figure 93). These vertical flows are presented within Tables 54, 55, and 56.

Both the parallel and serially coupled flows are calculated for two representative, major storm-periods:

1. storm No. 3-4 (Table 19), which occurred during the winter months when the antecedent moisture status was high (i.e. a pre-storm streamflow generation of 0.17 mm per unit area of forest catchment: Table 26).
2. storm No. 10 (Table 19), which occurred during the summer months when the antecedent moisture status was low (i.e. a pre-storm streamflow generation of 0.01 mm per unit area of forest catchment: Table 26).

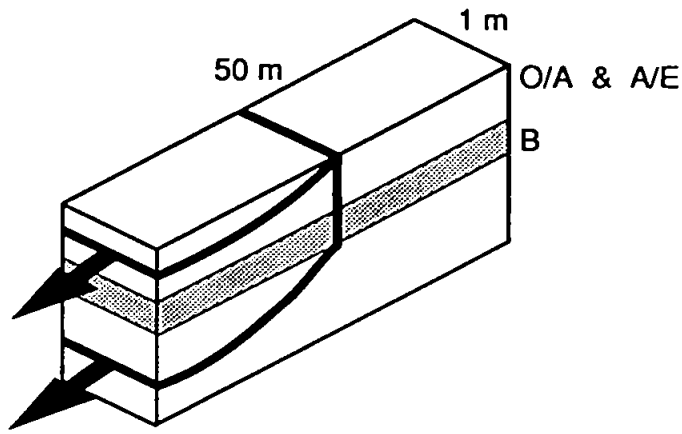

Figure 93. Parallel and serial coupling within the forest and grassland hillslopes.

Total Slope Flux during a Winter-Storm: The average flow within the forest hillslope during the winter storm-event is 39 percent smaller than that within the grassland hillslope (i.e. (0.00492/0.00801)*100); Tables 54 and 55). The smaller flow within the forest hillslope will partly have resulted from the 15 percent (Hudson, 1988) to 29 percent (Section 5.2.4) greater evapo-transpiration loss from the forest relative to that from the grassland.

Water-Pathways during a Winter-Storm: The water-pathways generating the larger flux within the grassland are very different to those generating the flux within the afforested slope. Within the grassland slope, 99.8 percent of the winter storm-period flow recharges the riparian zone only after moving vertically through the B horizon (i.e. (0.4/0.4006)*100; Table 55).

In sharp contrast, only 24 percent of the water-flow within forest slope moved through the B horizon before reaching the riparian zone (i.e. (0.06/0.246)*100; Table 54). The riparian zone within the forest slope catena was, therefore, recharged by primarily by lateral flow within O/A and A/E horizons (i.e. 76 percent of the flow). This lateral deflection of flow results from the marked profile differentiation concomitant with ferric-podzol soils (Crampton, 1967; Grieve, 1978; Table 8). Marked discontinuities are present between the hydraulic conductivity of the O/A and A/E horizons, and between the A/E and B horizons (Figure 74; Section 7.4.9). These discontinuities lead to the development of shallow, saturated zones just above the horizon boundaries (Section 6.3.3), which in the case of the A/E horizon transmit most of the horizon's lateral flow.

Such a dramatic increase in lateral flux just above the horizon-breaks, corroborates Zaslavsky's theoretical model of an *exponential* increase in capillary potential and lateral flux down towards horizon boundaries (Zaslavsky, 1964; Zaslavsky and Rogowski, 1969; Zaslavsky and Sinai, 1981c,d; Section 8.3.1). This might mean that lateral flux within the grassland A/E horizon is slightly under-estimated. This is because a small non-linearity in the

distribution of capillary potential would produce a large non-linearity in state-dependent hydraulic conductivity (Section 7.4.6.; Figure 66) and hence flux. This non-linearity *cannot* be observed from the tensiometer network in the grassland because the tensiometers were installed to average the capillary potential over the whole depth of each horizon are (Sections 4.2., and 4.4.3.). Non-linearities in potential have been sufficiently parameterized within the forest hillslope, because phreatic conditions developed and could, therefore, be monitored in detail with the piezometer nests.

These possible errors within the calculation capillary potential within the grassland O/A and A/E horizons could not, however, account for their 2.5 orders of magnitude reduction in lateral flow relative to the sub-forest horizons. This reduction in lateral flow is most likely produced by the single ploughing operation 11 years prior to the hydrological monitoring.

Table 54. Lateral flow within the O/A and A/E horizons, and vertical flow through the B horizon of the forest hillslope.

Mean storm-period flux for a 1 x 50 m hillslope segment (horizon flux: l min^{-1} 50 m^{-2}; total slope flux : l min^{-1} m^{-2}).		
Flux direction and horizon	Storm No. 3-4 wet, winter period 9/11/87-27/11/87	Storm No. 10 dry, summer period 28/5/88-26/6/88
lateral O/A	nd	nd
lateral O/A (sat)	0.035*	0.040
lateral A/E	0.0010	<0.020 (large range)
lateral A/E (sat)	0.15	<0.020
vertical B	0.06	0.04 (large range)
Total (/50 m)	0.00492	0.00240 (large range)

E flux is integrated over a soil depth 10 cm.
B flux is integrated over a hillslope length of 50 m.
Flux within individual soil horizons is l min^{-1} 50 m^{-2} (area: 1 x 50 m).
Total flux from the podzolic slope is the sum of the fluxes for each horizon divided by the 50 m slope length (l min^{-1} m^{-2}).
* is the flux calculated from throughflow trough outflows scaled against piezometer-based fluxes.
The total volume of outflow from the O/A throughflow trough was 17 percent less during storm 10 in comparison with storm 3-4.

Table 55. Lateral flow within the O/A and A/E horizons, and vertical flow through the B horizon of the ploughed section of the grassland hillslope.

Mean storm-period flux for a 1 x 50 m hillslope segment (horizon flux: l min^{-1} 50 m^{-2}; total slope flux : l min^{-1} m^2).		
Flux direction and horizon	Storm No. 3-4 wet, winter period 9/11/87-27/11/87	Storm No. 10 dry, summer period 28/5/88-26/6/88
lateral O/A and A/E	0.0006	0.00025 (large range)
vertical B	0.4	0.06 (large range)
Total (/50m)	0.00801	0.00121

O/A flux is assumed to be the same as that within the A/E horizon.
(The flux within the 2 horizons is integrated over a soil depth 20 cm).
B flux is integrated over a hillslope length of 50 m.
Flux within individual soil horizons is l min^{-1} 50 m^{-2} (area: 1 x 50 m).
Total flux from the podzolic slope is the sum of the fluxes for each horizon divided by the 50 m slopelength (l min^{-1} m^{-2}).

Total Slope Flux during a Summer-Storm: The flux within all soil horizons of both the research hillslopes was very much more variable through the summer-storm event in comparison with the winter-storm event. This relates to the rapid wetting of dry soils (i.e. the grassland A/E horizon attained -126 cm ϕ_c (mean 20-40 m slope position) prior to storm 10). This variability in response, added to a smaller number of measurements during the storm-peak makes the calculations for the summer storm rather less certain in comparison with the winter-storm.

During the summer-storm the forest slope generated 51 percent *less* flux in comparison with the winter-storm, and the grassland slope generated 85 percent of the average winter-storm flux (Tables 54 and 55). This resulted in the grassland slope generating 50 percent less flow than the forest slope. Given that the grassland slope generated half (49 percent) and the forest slope generated twice (195 percent) the average flow calculated for the respective catchment areas (Table 56), errors in the integration of flow over the whole storm-period (as a result of the extreme temporal variability of flux) is, therefore, assumed for both hillslopes.

Water-Pathways during a Summer-Storm: Despite the noticeable errors within the values of total slope flow for the summer-storm, the dominance of vertical flow within the grassland (i.e. 99.6 percent of total flow) and lateral flow within the forest (i.e. 67 percent of total flow) is maintained (Tables 54 and 55).

8.2.3. Internal-State versus External-State Flux Predictions.

For the winter-storm event, the predictions of water-flow based upon internal-state properties are very similar to those based upon the external (i.e. streamflow) response of the hillslope and catchment areas (Table 56). The predicted flow within the grassland hillslope is 100 percent of the average flow over the whole catchment, and that within the forest hillslope is 83 percent of the average catchment flow and 90 percent of the average hillslope flow. Given that the two hillslopes generate their streamflow by very different water-pathways, this similarity between external- and internal-state predictions *verifies* the accuracy of the techniques based upon the response of internal-state hydrological variables and parameters.

The slight under-prediction of the flow within the forest hillslope relative to the streamflow-based predictions, may result from the un-determined flux within:

1. the unsaturated upper part of the O/A horizon,
2. upslope inflow along the fragipan,
3. vertical flow down tree roots.

1. If the flow within this horizon were the same as that within the unsaturated part of the A/E horizon, then the predicted flow would only increase by 0.4 percent. If, however, the flow was 10 times that of the unsaturated A/E horizon, then the flow prediction would increase by 29 percent. Given such an uncertainty, a *rough estimate* of the flow within the unsaturated O/A horizon was not included within the value for total hillslope flux.

2. The angle of the slope-section above the 19.7° instrumented slope is much less steep, being approximately 10°. Moreover, a *forest ride* in use during the thinning operation in 1978 (Section 2.11) crosses the slope only 10 m above the transect. These two factors may allow vertical flow to traverse the B horizon at a greater rate and, therefore, generate the un-determined component of flow into the riparian zone.

3. During storm-periods, the *slightly* elevated moisture contents and capillary potential at a depth of 45 to 60 cm, beneath individual trees (Sections 6.2.6 and 6.3.6) may suggest that there is a greater vertical flow of water beneath individual trees in comparison with that in inter-tree areas. This could generate the un-determined component of flow into the riparian zone.

In comparison with the winter-storm period, predictions based upon the internal response of the two hillslopes are much less certain during the storm occurring during a dry, summer period. This partly relates to the smaller number of measurements taken at the beginning of the storm-period, but also to the uncertainties surrounding the calculation of a mean flow given the greatly increased temporal variability of flux (e.g. Figures 84 and 85). This greater variability in response probably results from the rapid wetting of dry soils (Dowd and Williams, 1989).

Table 56. Water-flux based upon internal-state response against those based upon the external-state response.

	MEAN AREAL FLUX per 1 m^2 surface area of the flow region ($l\ min^{-1}\ m^{-2}$).	
	Storm No. 3-4 wet, winter period 9/11/87-27/11/87	Storm No. 10 dry, summer period 28/5/88-26/6/88
Gross Precipitation	0.00967	0.00278
Grassland Catchment	0.00800	0.00248
Grassland Hillslope	0.00801	0.00121
Forest Catchment	0.00660	0.00123
Forest Hillslope (external-state)	0.00547	0.00037
Forest Hillslope (internal-state)	0.00492	0.00240-0.01160

Gross Precipitation is from 14 mm d^{-1} (0.58 mm hr^{-1}) during event No.3-4, and 4 mm d^{-1} (0.167 mm d^{-1}) during event No. 10 (Table 21). The storm-period durations for the grassland catchment, forest catchment and forest hillslope catchment within event No. 3-4 were 19 d, 21 d, and 22 d, respectively, and within event No. 28 were 26 d, and 30 d, respectively (Table 20). Storm-period streamflows generated within the same 3 areas were 219 mm (0.48 mm hr^{-1}), 200 mm (0.397 mm hr^{-1}), and 173 mm hr^{-1}) respectively (Table 25 and 29). Internal-state predictions of hillslope water-flux are from Tables 54 and 55. Catchment areas are 122,941 m^2, 109,464 m^2, and 1480 m^2 respectively. Gross precipitation is integrated over the area of the grassland catchment.

8.3. Numerical Solutions using Mathematical Models.

8.3.1. Boundary-Value Problems.

Hydrological models which are designed to solve the derivative of the rate of change (d/dx) within partial differential equations (e.g. Equations 6 to 10, and 19), are all *boundary-value problems*. All of the models presented within Tables 52 and 53, generate solutions to boundary-value problems. This means that for a model to predict the distribution of an internal-state variable (e.g. soil moisture content, or capillary potential; Chapter 6) within a chosen flow-region, both the internal-state parameters (Chapter 7) and *boundary conditions* must be characterized.

In the case of a *hillslope flow problem*, the boundary conditions are the specified potentials and fluxes at the edges of the specified flow region (e.g. a 2D flow-strip : Section 3.5.2). These include, the precipitation inputs, any inflow from upslope regions, losses to deep seepage, and flows at the interface of the stream bed and stream bank. These boundary-conditions can have as much effect upon the flow of water within a hillslope, as the internal-state parameters (Ahuja and Ross, 1982, 1983; Bear, 1972).

Models which require the input of these boundary conditions in addition to internal conditions, are both difficult to *parameterize* (i.e. specify the correct internal and boundary values for the simulation; Sections 1.1 and 1.3) and mathematically very complex. The mathematical complexity of such models means that they must in general, be solved by *numerical techniques* (Section 8.1; Freeze and Harlan, 1969).

Although such models are innately difficult to parameterize and solve, they do provide the means by which approximative solutions can be tested or verified (Sections 3.5.5. and 3.5.6; Dunne, 1983). Furthermore, they enable the prediction of more detailed spatial and temporal distributions of variables, than can be achieved by the approximative solutions.

8.3.2. The Impact of Podzolic Soil Horizons upon the Equipotential-Net.

Within the forest hillslope, the development of shallow phreatic zones within the basal zones of the O/A and A/E soil horizons (Section 6.3.3), together the large volumes of lateral flow within these horizons (Section 8.2.2), would suggest that there are large differences in the hydrological parameters between different soil horizons. The impact of observed vertical changes in the hydrological parameter of hydraulic conductivity was, therefore, examined using *boundary-constrained* mathematical simulations. A 2 dimensional *finite element* model called TRIANGLE (Dowd, 1989b) was used for the simulations. The results of one of the TRIANGLE simulations is presented within Figure 94.

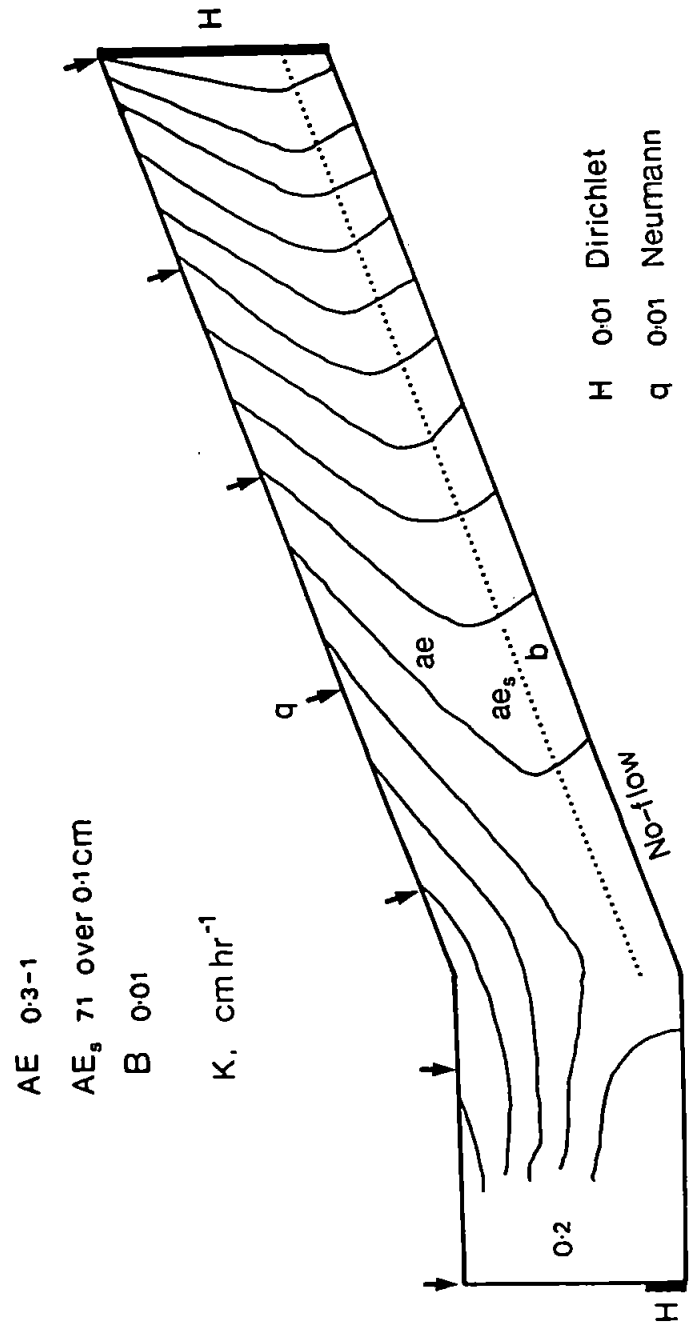

Figure 94. A segment of the equipotential net within the A/E horizon of the forest hillslope predicted by a boundary-constrained numerical simulation applied to internal and boundary conditions at the peak of storm 3-4.

A flow-region comprising of 128 triangular elements was used to simulate the impact of the state-dependent hydraulic conductivities within the saturated and un-saturated zones of A/E horizon, and the upper layer of the B horizon, upon the direction of flow.

The internal-condition of hydraulic conductivity, and the boundary-conditions of: inflow rates vertically into the A/E horizon and laterally into the profile were averages of those monitored during storm 3-4 . The vertical inflow into the A/E horizon was defined as a *specified flux* or *Neumann boundary*, with a rate equivalent to the 0.14 mm hr^{-1} mean net-precipitation beneath the forest canopy (i.e. 24 percent of 0.58 mm hr^{-1} mean gross-precipitation, Tables 21 and 23). The lateral inflow into the horizons at the upslope boundary was controlled by a *constant head (Dirichlet boundary)* of 0.01 cm H_2O. The lower boundary of the flow-region was specified as a *no-flow boundary*, purely for numerical stability. The mean state-dependent hydraulic conductivity of upper unsaturated zone of the A/E horizon was 0.3 cm hr^{-1}, that of the basal saturated zone of the A/E horizon was 71 cm hr^{-1}, and that of the upper zone of the B horizon was 0.01 cm hr^{-1}(Figures 61 and 74). The hydraulic conductivity of the un-saturated A/E at the boundary with the saturated zone was estimated to be 1 cm hr^{-1}. A *downslope* area of riparian soil with a conductivity of 0.2 cm hr^{-1} was included.

The simulation predicts that the *equipotential line* within the A/E horizon, is deflected in a downslope direction. This implies that lateral flow increases as flow approaches the boundary between the A/E and B soil horizons. Such a deflection of flow near the base of those soil horizons overlying less conductive horizons was similarly predicted by Zaslavsky and Sinai,1981d,e). The numerical simulation, therefore, verifies the observed association between hydraulic discontinuities and the development of perched water-tables (Sections 6.3.3. and 7.4.9).

8.3.3. The Interaction of Slope-Flux with Riparian-Flux.

The second numerical simulation presented arose from an *apparent* contradiction of flow-pathways. The calculations of the distribution of both flow and hydraulic conductivity within the podzolic slope (Sections 7.4.9. and 8.2.2) suggested that the O/A and A/E horizons (i.e. 0-20 cm layer) provided a large proportion of the inflow to the riparian zone. In contrast, differences between the moisture content at the mid-point and upslope-boundary within the riparian zone suggested that flow from the podzolic slope was entering the riparian zone at a depth of 25 to 30 cm, equivalent to the depth of the B horizon within the podzolic slope. Numerical simulations were, therefore, conducted to examine the depth at which the podzolic slope flux would enter the riparian zone. These simulations were performed using a *modified* version of the *Saturated-Unsaturated-TRAnsport* or SUTRA model. The original source-code for SUTRA was developed by the US Geological Survey (Voss, 1984). Only simulation No. SA36 is presented.

The simulated flow-region was divided into 80 rectangular elements, 30 of which represented the downslope riparian zone, 25 represented the *topsoil* (i.e. O/A and A/E horizons: 0-20 cm), and the remaining 25 represented the *subsoil* (i.e. B and B/C horizons: 20-50 cm; Figure 95). A state-dependent hydraulic conductivity representing 0.01 cm hr^{-1} within the subsoil was applied (Sections 8.2.2 and 8.3.2). The average lateral conductivity of the topsoil was represented by a value of 1 cm hr^{-1}, and the vertical conductivity was represented by the value for the underlying B horizon (see 2. *Mean-Conductivity* in Section 8.2.2). All of the boundaries were considered to be impermeable (i.e. no-flow boundaries) with the exception of the upper topsoil boundary and the lower segment of the downslope boundary of the riparian zone (Figure 95). The upper topsoil boundary was defined as a *Neumann boundary* to represent infiltration, and the lower segment of the downslope boundary of the riparian zone was defined as a *Dirichlet boundary* to represent the seepage-face at the soil-stream interface.

To achieve the most accurate prediction of the soil-depth contributing the most flux to the riparian zone, the numerical errors (or model-related errors) associated with the specification of the boundary conditions within small *discretizations* (i.e. only 80 elements), were reduced by:

1. increasing the number of elements per area of flow-region near the Neumann boundary, and
2. reducing the hydraulic conductivity representing that of the riparian area to that of the subsoil (i.e. 0.01 cm hr^{-1}).

The predicted distribution of specific flux at the centroid of each of the 80 elements is presented within Figure 95.

Figure 95 shows that although the subsoil as a whole, has a much smaller flux in comparison with the topsoil horizon, its flow dramatically increases at the point where the topsoil flux enters the riparian soil.

Given that that there is a marked increase in slope-angle between the riparian zone and the podzolic slope at the 2.5 m slope position (Figure 3) the lateral flow within the O/A and A/E horizon will develop a larger vertical component of flow at the 2.5 m position and enter the riparian zone lower within the profile. The reduced vertical potential gradient at the 2.5 m slope position relative to those at the 5 m slope position (Tables 40 and 41) may also indicate that the hydraulic discontinuity at this position is reduced and flow is moving vertically.

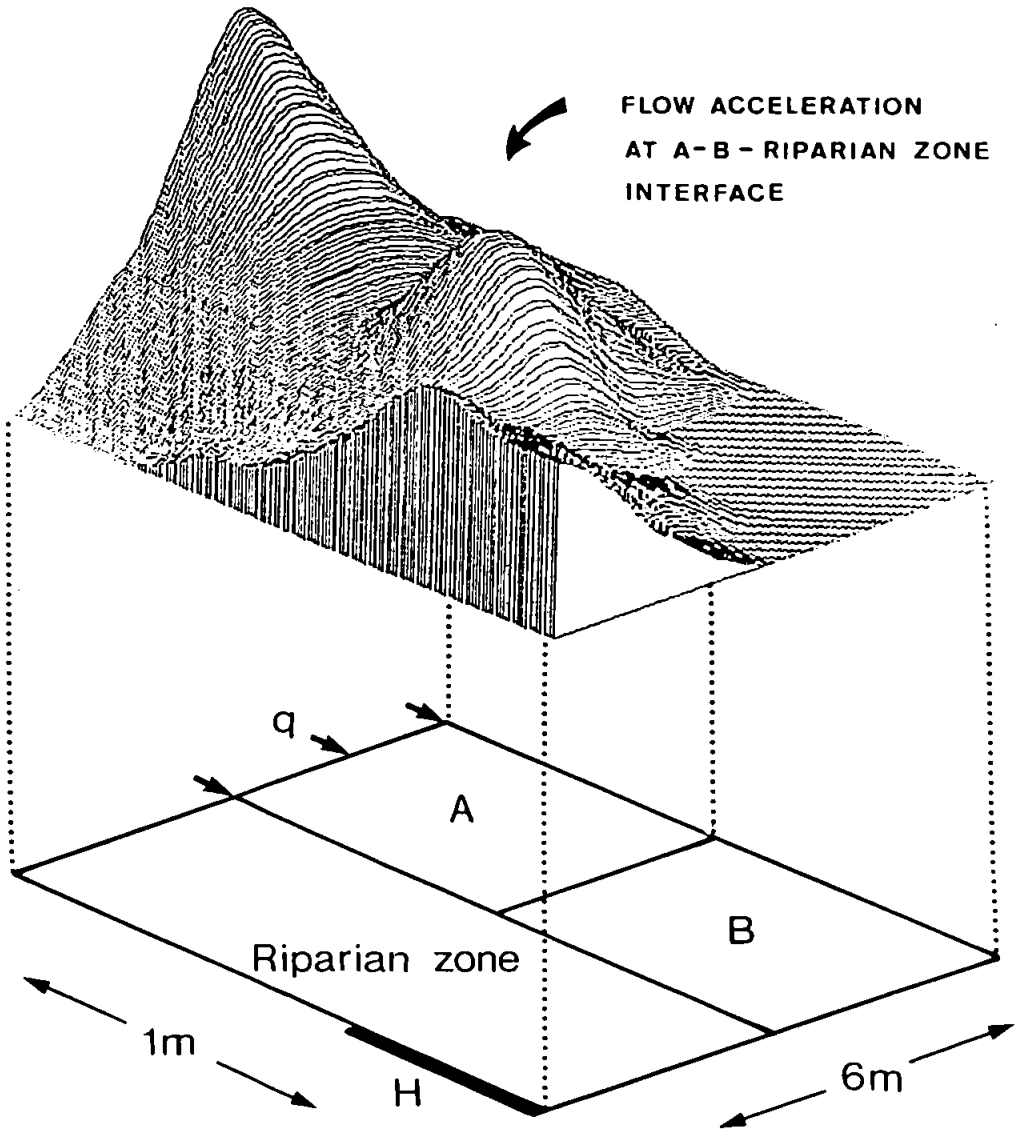

Figure 95. The specific flux predicted at the centroid of each element at the interface between a podzolic slope with a marked hydraulic discontinuity (between the topsoil and subsoil) and the riparian zone.

CHAPTER 9.

Synthesis and Conclusions.

9.1. External-State Rainfall-Runoff.

Rainfall-Runoff Volumes.

The forest catchment generated 29 percent less runoff than the grassland catchment (Section 5.2.4). Streamflows prior to major *storm-periods* (Section 5.3.1) were similarly smaller (Section 5.3.4). Forty seven percent of the gross-precipitation received by the forest and 25 percent of that received by grassland failed to generate runoff (Section 5.2.2). These rainfall-runoff responses are 18 and 9 percent less than those within the larger afforested and grassland, Institute of Hydrology, Plynlimon catchments (Sections 5.2.2. and 5.3.3). Differences in the volume of flow lost to deep seepage may, therefore, account for part of the difference between the two Tir Gwyn catchments. The very high evaporation rates from wetted conifer canopies, which reduce the effective precipitation reaching the forest floor by 39 percent (Section 5.2.1) may, however, account for a significant proportion of the difference in the rainfall-runoff response of the forested and grassland catchments at Tir Gwyn.

Rainfall-Runoff Timing.

Storm-period streamflows within the forest catchment were generally maintained for some 7 to 10 percent longer than that within the grassland catchment (Section 5.3.4), which is less of a difference than that expressed in the runoff volumes. Moreover, the time between the initial hydrograph response and the peak streamflow were generally synchronous (Section 5.3.4), and the runoff response of both catchments conforms very closely (R^2 86-91 percent) to a linear relationship with the storm-period gross-precipitation (Section 5.3.5). This may imply that the physical controls which are similar within the two catchments (Sections 1.4.4. and 2.11), namely, the temporal distribution of gross-precipitation input and catchment geometry (i.e. topography, depth to porous media, and stream morphometry), exert as much or more of a control upon the form of the rainfall-runoff response, than does the vegetation cover/land-use. A similar conclusion was educed by Bren (1978).

Relationship between Hillslope and Catchment Response.

The instrumented forest hillslope failed to maintain flows during prolonged dry periods (Section 5.3.4) and generated less runoff in response to storms occurring within such periods (Section 5.3.5). In addition, storm-period streamflows (or streamflows larger than the pre-storm level) generated by the forest hillslope were maintained for longer than those generated by the forest catchment as a whole (Section 5.3.4). These differences between the individual hillslope and whole catchment probably result from the hillslope being steeper, shallower, and shorter in comparison with the average slopes for the whole catchment (Sections 5.3.4., 5.3.5). This would lead to a larger proportion of the hillslope's streamflow generation occurring soon after precipitation input.

9.2. Riparian Saturated Zones and Streamflow Generation.

The instrumented forest hillslope (and the whole forest catchment) generated streamflow by subsurface flow. Infiltration-excess or saturation-excess overland flow may have generated part of the stream hydrograph only during the snow-melt on the 23 February 1988 (Section 8.2.1). Occasionally, saturation-excess overland flow was observed on the peaty riparian zones of the grassland catchment (Figure 2). This may account for the 41 percent difference between the peak streamflow within the grassland catchment and that within the forest catchment (Section 5.3.4), being a larger than the difference in rainfall-runoff response and antecedent streamflow (Section 9.1).

During all storm-periods, the rise and recession of the stream hydrograph at the base of the instrumented forest slope was paralleled by the growth and diminution of saturated zones within the riparian area (Section 6.3.3). These zones extended some 10 m up the 19.7 ° podzolic slope (Section 6.3.3). The streamflow generated by the forest hillslope was calculated by a characterization of the internal-state hydrological properties and geometry of the riparian area. This internal-state calculation could accurately predict (R^2 83 percent) the streamflows observed within the slope-base-weir, without any recourse to parameter optimization or fitting (Section 8.2.1).

9.3. Verification of Macroscopic Flow Predictions.

Although the relationship between the response of the riparian saturated zone and that of the adjacent stream has been shown by many studies, the understanding of how such zones are recharged by flow from upslope soils remains uncertain (Sections 1.2. and 1.4.2). This uncertainty stems from an inability to predict flow within heterogenous hillslopes, from an accurate characterization of hydrological properties averaged across control-volumes of soil (Sections 1.2., 1.4.3. and 3.5.1). The inability to accurately characterize these properties results partly from the complexity of the processes, and partly from the misconceptions arising from the inadequate characterization of the artificial conditions created by the use of most groundwater instruments (Section 1.2., 1.4.3. and 3.5.6). This research aimed to overcome some of the problems, by comparison of the results of several field and mathematical techniques applied to same two hillslopes.

By using this integrated approach, water-flow within layered podzolic hillslopes could be accurately predicted by macroscopic-averaging of hydrological properties, for periods when the soil moisture status was high (Sections 8.2.2. and 8.2.3).

The concordant predictions of water-flow based upon these different techniques, are outlined in the following section (9.4). The accuracy of these predictions are *verified* or *proven* by the results of tests to examine the accuracy of both the measurement and representational techniques : (1) the ability to predict subsurface flows within two hillslopes, maintaining very different water-pathways (Sections 3.2.2., 8.2.2. and 8.2.3), (2) comparison of standard and *in situ* calibrations of the neutron attenuation technique (Section 6.2.1), (3) comparison of the measurements of capillary potential recorded by tensiometers, piezometers and unconfined-boreholes (Section 6.3.2), (4) comparison of laboratory and *in situ* determined moisture capacities (Section 7.3.1), (5) examining the impact of core-size upon the measurement of saturated hydraulic conductivity (Section 7.4.1), (6) comparing saturated hydraulic conductivities determined by ring permeametry with those determined by well permeametry (Section 7.4.4), throughflow-trough outflows (Section 7.4.2), piezometer recovery tests (Section 7.4.3) and observed riparian zone outflows (Section 8.2.1), (7) the use of several analytical equations to calculate saturated hydraulic conductivity by recovery tests (Section 7.4.3) and well permeametry (Section 7.4.4), (8) conducting experiments to determine any variation in the wettability and stationarity of the hydrological parameters (Section 7.4.5), (9) comparing several analytical techniques of determining the relative hydraulic conductivity from moisture capacity data (Section 7.4.6), (10) comparing relative hydraulic conductivities determined from moisture capacity data, with both a flow-net based, tangent-continuity method (Section 7.4.7), and steady-state permeametry (Section 7.4.8), (11) comparing piezometer-based and trough-based lateral flux (Section 8.2.2), (12) comparing

internal-state flow predictions with external-state flow predictions based on mean aerial streamflow generation (Section 8.2.3), (13) comparison of horizon-specific equipotential-nets predicted by field techniques (Section 6.2) with those predicted by numerical solutions, and (14) comparison of the chemistry of water within each soil horizon with that within the riparian zone and stream (Section 9.5; Chappell et al, 1990).

The ability to calculate flows within layered hillslopes during the rapid wetting of dry soils in summer-periods remains less certain.

9.4. Water-Pathways within Afforested and Grassland Hillslopes.

The pathways of soil water verified within Section 9.3, are very different within the two instrumented hillslopes. Within the forest hillslope the marked horizon development, in particular the presence of an indurated B horizon, deflects percolation laterally within the O/A and A/E horizons. This conclusion is based upon (1) the approximative (Section 8.2.2) and numerical (Sections 8.3.2. and 8.3.3) predictions of flow based upon the measured hydrological properties, (2) the development of perched water-tables at the base of the O/A and A/E horizons (Section 6.3.3), (3) the greater change of moisture content within surface soil horizons (Section 6.2.3) and within the downslope area of the forest hillslope (Section 6.2.4), (4) the potential gradients which are steeper vertically between hydrologically-different soil horizons than they are laterally within individual horizons (Section 6.3.5), (5) higher porosities and lower bulk densities within the surface horizons (Section 7.2), and (6) the marked hydraulic discontinuity in saturated and state-dependent hydraulic conductivities between each of the soil horizons (Sections 7.4.2. and 7.4.9).

In sharp contrast, the pathways of water within the grassland hillslope are dominated by vertical flow (Section 8.2.2). A ploughing operation, some 11 years prior to the monitoring (Section 2.10.2), has dramatically increased the intrinsic permeability of the B horizon (Section 7.4.2). This has (1) lead the development of a more vertically-homogenous profile, with respect to the saturated and state-dependent hydraulic conductivity (Section 7.4.2), and (2) prevented the development of perched water-tables (Section 6.3.3), a critical pathway of flow within the forest hillslope.

The total flow from the ploughed section of the grassland hillslope into the riparian zone is 39 percent larger than that from the podzolic slope into riparian zone within the forest (Section 8.2.3). Given the degree of averaging within the flow predictions, such a difference could be accounted for by the 29 percent difference in the rainfall-runoff behaviour of the two land covers (Section 9.1).

9.5. Corroboration of the Water-Pathways by Analysis of Water-Chemistry.

Within Chappell et al (1990) the ionic concentrations of waters collected from A/E, B and B/C horizons of the podzolic slope were compared with those collected from the riparian soil and stream draining the instrumented forest hillslope. Emphasis was given to the collection of water samples during storm-periods. The concentration of hydrogen ion within the B horizon were always much smaller (16-17 $\mu M\ l^{-1}$) than those within the overlying A/E horizon (32-50 $\mu M\ l^{-1}$), riparian soil (21-28 $\mu M\ l^{-1}$), and stream (10-45 $\mu M\ l^{-1}$). Equally, the concentration of total monomeric aluminium was always far higher within the B horizon (1.5-2.1 $mg\ l^{-1}$) than that within overlying A/E horizon (0.95-1.5 $mg\ l^{-1}$), riparian soil (1.1-1.4 $mg\ l^{-1}$), and stream (0.2-1.6 $mg\ l^{-1}$). This may suggest that little of the flow during storm-periods moves vertically through the B horizon on its passage to the riparian zone. Although any number of biogeochemical equilibria and exchange reactions could affect this very simplistic portrayal of the water chemistry, the dissimilarity between B horizon and riparian/stream chemistry concords with the pathways predicted by the hydrometric techniques (Section 9.4).

9.6. Impact of Individual Conifers upon Hillslope Water Pathways.

The spatial variability of precipitation beneath the forest canopy is far greater than that in the open (Section 5.2.1). Although the total volumes are small, the rate of flow down individual conifer stems may be almost twice those of the throughfall (Section 5.2.1). During intense storm-events, this can lead to the saturation of the A/E horizon beneath those conifers with the higher stemflow volumes - often the smaller (30 cm DBH) conifers (Section 6.3.6). An increase in vertical flow into the underlying horizons might be expected, as a result of preferential flow of water down those roots which penetrate the slowly permeable B horizon. This pathways could not be observed beneath these small conifers. A very large increase in lateral flow downslope of individual conifers is, however, indicated by (1) the large increase in the vertical potential gradients between the sub-tree A/E and B/C horizon, which indicate a discontinuity in flow within soil horizons maintaining different levels of hydraulic conductivity (Sections 6.3.5. and 6.3.6), (2) the observation that the B/C horizon beneath the small conifers remained drier than that within inter-tree areas (Section 6.3.6), (3) a possible reduction in the permeability of the B, B/C, and Cu horizons beneath individual conifers, as a result of compaction caused by the weight of the tree, or the movement of tree roots during

windy conditions (Section 7.4.4), and (4) the possible increase in the temporal dynamics of the perched water-table 1 m downslope of a tree, evidenced in the very dynamic response of the O/A horizon throughflow trough (Section 8.2.2).

Such a conclusion of the dominance of lateral flow downslope of those conifers growing on steep layered hillslopes would accord with the results of tracing experiments conducted by Reynolds (1966), who observed large lateral deflections of flow beneath individual spruce trees. The flat, platy nature of spruce root-systems was suggested to be the principal cause of this preferential movement in the lateral or slope-ward direction. Extensive evidence from throughflow trough outflows and direct observation within eastern bloc countries, lead Molchanov (1960) to similarly concluded that the platy root systems of spruce trees give rise to the lateral deflection of flow.

There is some evidence to suggest that large conifers (i.e. 40-50 cm DBH) may increase the vertical flow of water on the podzolic hillslope (Section 6.2.6). Beneath a large conifer growing within the riparian zone of the forest hillslope, larger changes in moisture content at depth and smaller changes within the surface soil in comparison with those within inter-tree soils were monitored (Section 6.2.6). The increase in vertical flow implied by this observation is expected, given that the riparian zone is only gently sloping and is relatively homogenous in comparison with the podzolic slopes.

9.7. Implications for Hillslope and Catchment Modelling.

Although a verified and accurate mathematical simulation of the pathway of water through a natural, layered hillslope has yet been presented, the approximate, internally-verified prediction of soil-water-pathways within the two hillslopes at Tir Gwyn, would suggest that subsurface flow can be calculated by averaging hydrological properties over volumes of soil (Sections 7.4.7., 7.4.8., 8.2.2 and 8.2.3). Given a knowledge of the extent to which hillslope profiles exhibit horizonation and catenal differences within their hydrological properties, then distributed catchment-scale models may be able to produce accurate predictions of the subsurface water-pathways (rather than just streamflow) using relatively simple discretizations (i.e. large grid squares over which to average the hydrological properties).

To date, most of the catchment-scale hydrological models simplify subsurface flow calculations by assuming that all of the subsurface flow upslope of the saturated zones within the riparian areas, is vertical. The marked horizonation observed within podzolic soils (Crampton, 1967; Gieve, 1978; Rudeforth, 1967) has been shown by this research, to generate large volumes of lateral flow within steep hillslopes with un-ploughed, ferric-podzol soils.

The simplification inevitably associated with mathematical simulation of hydrological pathways at the catchment scale, therefore, must not extend to the simplification of the anisotropic internal-behaviour of layered hillslopes, if accurate predictions of soil-water-pathways are to be produced. Without an accurate characterization of the soil-water-pathways, mathematical models cannot predict the pathways of solute transport (Bache, 1984; Bear and Verruijt, 1987).

9.8. Implications for Stream Acidification.

Conifers have been shown to enhance the concentration of solutes within those precipitation waters entering the soil, particularly those flowing down stems (Chappell et al, 1990). This research has shown the dominant role of lateral flow within those soil horizons above the least conductive horizon of a typical podzolic hillslope (Section 9.4; In the case of a ferric podzol, the B horizon is the least conductive : see Figure 6). Furthermore, individual plantation conifers have been shown to enhance this lateral deflection of flow (Section 9.6). A combination of these three factors could lead to both the lateral transport of elevated loadings of hydrogen ion within the O/A and A/E horizons and the release of aluminium complexes from the A/E and top of the illuvial B horizon and, therefore, generate the observed concentrations of these ions within riparian soils and streams. Further analysis linking the horizon-specific ionic concentrations with intra-control-volume mixing of *old* and *new* waters (Section 1.4.3. p16) is, however, required to provide an accurate prediction of the path of particular ions through the Tir Gwyn forest hillslope.

9.9. Implications for Future Afforestation.

The root systems of conifers do not appear to allow a significant increase in the vertical component of flow in steeply sloping podzolic soils (Section 9.6). As a consequence, the transport of *acidic solutes* down into the lower profile, which often has a higher buffering capacity (Bache, 1984) will not be increased. Ploughing of podzolic slopes is, however, shown to increase dramatically the vertical component of flow (Section 9.4). If future afforestation were to include podzolic slopes, then ploughing prior to planting may allow *acidic waters* to percolate to depth and thereby be more greatly buffered before reaching a stream.

References.

Abbott, M.B., Bathurst, J.C., Cunge, J.A., O'Connell, P.E. and Rasmussen, J.(1986) An introduction to the European Hydrological System - System Hydrologique Europeen, "SHE" 2. Structure of a physically-based, distrubted modelling system. *J. Hydrol. 87: 61-77.*

Abdul, A.S., and Gillham, R.W.(1984) Laboratory studies of the effects of the capillary fringe on streamflow generation. *Water Resources Res. 20: 691-698.*

Adams, W.A., and Evans, L.J., and Abdulla, H.H.(1971) Quantitative pedological studies on soils derived from Silurian mudstones. III Laboratory and *in situ* weathering of chlorite. *J. Soil Sci. 22: 158-165.*

Adams, W.A., and Raza, M.A.(1978) The significance of truncation in the evolution of slope soils in mid-Wales. *J. Soil Sci. 29(2): 243-257.*

Ahuja, L.R., and Ross, J.D.(1982) Interflow of water through a sloping soil with seepage face. *Soil Sci. Soc. Am. J. 46: 245-250.*

Ahuja, L.R., and Ross, J.D.(1983) Effect of subsoil conductivity and thickness on interflow pathways, rates and source areas for chemicals in a sloping layered soil with seepage face. *J. Hydrol. 64: 189-204.*

Alharthi, A., and Lange, J.(1987) Soil water saturation : dielectic determination. *Water Resources Res. 23,4: 591-595*

Anderson, M.G.(1982) Modelling hillslope soil water status during drainage. *Trans. Inst. Br. Geogr .7: 337-353.*

Anderson, M.G., and Burt, T.P.(1978) Toward more detailed field monitoring of variable source areas. *Water Resources Res. 14,6: 1123-1131.*

Anderson, M.G., and Burt, T.P.(1985) Modelling strategies. In *Hydrological Forecasting* (eds) M.G. Anderson and T.P. Burt (Wiley, Chichester) 1-13.

Anderson, M.G., and Howes, S.(1986) Hillslope hydrology models for forecasting in ungauged watersheds. In *Hillslope Processes* (ed) A.D. Abrahams (Allen and Unwin, Boston) 161-186.

Anderson, M.G., and Kneale, P.E.(1980) Topography and hillslope soil water relationships in a catchment of low relief. *J. Hydrol. 47: 115-128.*

Anderson, M.G., and Rogers, C.C.M.(1987) Catchment scale distributed hydrological models: A discussion of research directions *Prog. in Phys. Geography 11,1: 29-51.*

Archer, J.R., and Marks, M.J.(1982) Techniques for measuring soil physical properties. *ADAS Ref. Book 441.* (MAFF)

Armstrong, W., Booth, T.C., Priestley, P., and Read, D.J.(1976) The relationship between soil aeration, stability and growth of Sitka spruce (*Picea sitchensis*, Bong. Carr.) an upland peaty gleys. *Applied Ecology 585-591.*

Arnett, R.R.(1974) Environmental factors affecting the speed and volume of topsoil interflow. *Inst. Brit. Geographers Special Publication 6 :7-22.*

Arnett, R.R.(1976) Some pedological features affecting the permeability of hillslope soils in Caydale, Yorkshire. *Earth Surface Processes 1: 3-16.*

Atkins, T.C.(1978) *Physical Chemistry.* (Oxford University Press, Oxford, UK.)

Atkinson, T.C.(1978) Techniques for measuring subsurface flow on hillslopes. In *Hillslope Hydrology* (ed) M.J. Kirkby (Wiley) 73-120.

Aubertin, G.M.(1971) Nature and extent of macropores in forest soils and their influence on subsurface water movement. *USDA Forest Service Res. Paper NE-192 : pp. 33.*

Avery, B.W.(173) Soil Classification in the Soil Survey of England and Wales. *J. Soil Sci. 24: 324-338.*

Bache, B.W.(1984) Soil-water interactions. *Phil. Trans. R. Soc. Lond. B. 30S : 393-407.*

Bachmat, Y., and Bear, J.(1986) Macroscopic modelling of transport phenomena in porous media. 1: The continuum approach. *Transport in Porous Media. 1: 213-240.*

Baloutsos, G.(1985) *Hillslope flow processes in an upland catchment in SE Scotland.* Unpubl. PhD Thesis. Dept. Forestry and Natural Resources Univ. Edingburgh :.

Barry, D.A.I., Coves, J., and Sposito, G.(1988) On the Dagan Model of solute transport in groundwater: application to the Borden Site. *Water Resources Res. 24,10: 1805-1817.*

Bear, J. (1961) On the tensor form of dispersion. *J. Geophys. Res. 66,4: 1185-1197.*

Bear, J.(1972) *Dynamics of Fluids in Porous Media.* (Elsevier, New York).

Bear, J., and Verruijt, A.(1987) *Modelling Groundwater Flow and Pollution.* (D. Reid Publ. Co.,) 414.

Bear, J., Zaslavsky, D., and Irmay, S.(1968) *Physical Principles of Water Percolation and Seepage.* (UNESCO, France).

Beasley, R.S.(1976) Contribution of subsurface flow from the upper stages of forested watersheds to channel flow. *Soil Sci. Soc. of America J. 40: 955-957.*

Bell, J.P.(1973) Neutron Probe Practice. *Inst. Hydrology Report 19 :.*

Berglund, E.R., Ahycud, A., and Tayaa, M.(1981) Comparison of soil and infiltration properties of range and afforested sites in Northern Morocco. *Forest Ecology and Management 3: 295-306.*

Berndt, H.W.(1971) Early effects of forest fire on streamflow characteristics. *Res. Note U.S. Dep. Agric. For. Serv., PNW-148, pp9.*

Bernier, P.Y.(1982) *VSAS2: A revised source area simulator for small forested basins.* Unpubl. PhD thesis. University of Georgia, USA

Berryman, C.(1974) Infiltration rates and hydraulic conductivity. *Tech. Bull. 74/4 FDEU (MAFF) pp. 17.*

Berryman, C., Thorburn, A.A., and Trafford, B.D.(1976) Soil water tensiometers. *FDEU Tech. Bull 76-7 pp 22.*

Betson, R.P.(1964) What is watershed runoff?. *J. Geophys. Res. 69(8): 1541-1552.*

Betson, R.P., and Marius, J.B.(1969) Source areas of storm runoff. *Water Resources Res., 5 (3): 574-582.*

Beven, K.(1975) *A deterministic, spatially distributed model of catchment hydrology.* Unpubl. Phd thesis, School of Environmental Sci., University of East Anglia, Norwich.

Beven, K.(1977) Hillslope hydrographs by the finite element method. *Earth Surface Processes 2: 13-28.*

Beven, K.(1982) On subsurface stormflow: Predictions with single kinematic theory for saturated on unsaturated flows. *Water Resources Res. 18,6: 1627-1633.*

Beven, K.(1987) Towards a New Paradigm in Hydrology. In *Water of the Future: Hydrology in Perspective (Proc. of the Rame Symposium. April 1987) IAHS Publ. 164*

Beven, K.(1988) Scale Considerations. In *Recent Advances in the Modeling of Hydrologic Systems.* NATO Advanced Study Institute, Sintra, Portugal, 10-23 July 1988.

Beven, K., Calver, A., and Morris, E.M.(1987) The Institute of Hydrolgy Distributed Model. *Inst. Hydrology Report No. 98*

Beven, K., and germann, P.(1981b) Water flow in soil macropores II A combined flow model.*J. Soil Sci. 81,32: 15-29.*

Beven, K., and Germann, P.(1982) Macropores and water flow in soils. *Water Resource Res. 18,5: 1311-1325.*

Beven, K., and Kirkby, M.J.(1979) A physically based, variable contributing area model of basin hydrology. *Hydrol. Sci. Bull. 24,1*

Beven, K., Kirkby., M.J., Schofield, N., and Tagg., A.F.(1984) Testing a physically-based flood forecasting model (Topmodel) for three U.K. catchments. *J. Hydrol. 69: 119-143.*

Beven, K.J., and O'Connell, P.E.(1982) On the role of physically-based distributed modelling in hydrology. *Inst. Hydrology Report 81*

Binley, A., Elgy, J. and Beven, K.(1989) A physically based model of heterogeneous hillslopes. 1. Runoff production. *Water Resources Res. 25,6: 1219-1226.*

Blake and Hartage (1986) Bulk density. In *Methods of Soil Analysis: Part 1: Physical and Mineralogical Methods.* (ed) Klute, A. (Am. Soc. Agron., Madison, U.S.A.)

Blevins, R.L., Holowaychuk, N., and Wilding, L.P.(1970) Micromorphology of soil fabric at tree root-soil interface. *Soil Sci. Soc. Am. Proc. 34: 460-465.*

Bo, M.W., Tae, H.K., and Kyong, H.K.(in press) Rainfall interception loss from canopy in forest catchment. In *Regional seminar on Tropical Forest Hydrology,* 4-9 Sept. 1989, Kuala Lumpur, Malaysia.

Boersma, L.(1965) Field measurement of hydraulic conductivity above a water table. In *Methods of Soil Analysis Part 1* (eds) C.A. Black, D.D. Clark, J.L Evans, D.D. White, and Ensiminge, L.E. 234-252.

Boggie, R., and Knight, A.M.(1980) Tracing water movement using tritium a peaty gley soil under Sitka spruce. *Forestry 53,2: 179-185.*

Bonell, M., Gilmour, D.A., and Cassells, D.S.(1983a) A preliminary survey of the hydraulic properties of rainforest soils in tropical north-east Queensland and the implications for the runoff processes. In *Rainfall simulation, runoff, and soil erosion Catena Suppl. 4* (ed) J. De Ploey. 3-24.

Bonell, M., Gilmour, D.A., and Cassells, D.S.(1983b) Runoff generation in tropical rainforests of northeast Queensland, Aust. and the implications for land use management Proc. Hamburg Symp. August, IAHS Publication 14. *Hyd. of Humid Tropical Regions with Partic. Ref. to the hydro. effects of agriculture and forestry practice : 287-297.*

Bonell, M., Gilmour, D.A., and Sinclair, D.F.(1981) Soil hydraulic properties and their effect on surface and subsurface water transfer in a tropical rainforest catchment. *Hydrol. Sci. Bull. 26,1,3: 1-18.*

Bonell, M., Hendriks, M.R., and Imeson, A.Z.(1984) The generation of storm runoff in a forested clayey drainage basin in Luxemburg*J. Hydrol. 71: 53-77.*

Bonneau, M., Brethes, A., Lelong, F., Nys, C. and Souchier, B. (1979) Effets de boisements resineux purs sur l'evolution de la fertilit du sol. *Rev. for. fr., 31: 198-207.*

Bouma, J.(1982) Measuring the hydraulic conductivity of soil horizons with continuous macropores. *Soil Sci. Soc. Am. J. 46: 438-441.*

Bouma, J., and Anderson, J.L.(1973) Relationship between soil structure characteristics and hydraulic conductivity. In *Field Soil Moisture Regime. Soil Sci. Soc. Am. Spec. Publ.* (ed) R.R. Broze. 77-105.

Bouma, J., and Dekker, L.W.(1978) A case study on infiltration into dry clay soil. 1. Morphological observations. *Geoderma 20: 27-40.*

Bouwer, H.(1962) Measuring saturated hydraulic conductivity of soils. *Am. Soc. Agric. Eng. Spec. Publ., SP-SW-0262 : pp. 19.*

Bouyoucos, G.(1972) A new electrical soil moisture measuring unit: note. *Soil Sci. 114,6: 493.*

Box, G.E.P., and Jenkins, G.M.(1971) *Time Series Analysis, Forcasting and Control.* Holden-Day, San Francisco.

Brady, N.C.(1974) *The Nature and Properties of Soils.* (MacMillan, New York).

Brater, E.F.(1939) The Unit Hydrograph principle applied to small water-sheds. *Am. Soc. Civ. Engineer.*

Bren, L.J.(1978) *The numeric prediction of some hydrological processes on a small, forested catchment.* Phd thesis, University of Melbourne.

Bren, L.J., Funn, D.W., Hopman, S.P., and Leitch, C.J.(1979) The hydrology of small forested catchment in North-eastern Victoria. 1. Establishment of the Copper Creek Project. *Forests Commission Bull. (Victoria) 27*

Bren, L.J., and Turner, A.K.(1979) Hydrologic behaviour of a small forested catchment. *J. Hydrol. 76: 333-350.*

Brenner, R.P.(1973) A hydrological model study of a forested and a cutover slope. *Hydrol. Sci. Bull. VIII 26: 125-144.*

Brewer, R.(1960) Cutans: Their definition, recognition and interpretation. *J. Soil Sci. 11,2: 280-292.*

Brewer, R., and Sleeman, J.R.(1963) Pedotubules: their definition, clarification, and interpretation. *J. Soil Sci. 14,1: 156-166.*

Bricker, O.P.(1987) Catchment flow paths. *Proc. Int. Symp. on Acidification and Water Pathways.* Norway 2-5 May NNCH/UNESCO/WMO/IHP

British Standards Institution (1965a) *Methods of measurement of liquid flow in open channels Part 4 Weirs and Flumes. 4A Thin Plate wells and venturi flumes.* BS3680

British Standards Institution (1965b) *Methods of measurement of liquid flow in open channels Part 2. Dilution methods* BS3680

British Standards Institution (1975) *Methods of testing soils for engineering purposes,* BS1377.

Brooks, R.H., and Corey, A.T.(1964) Hydraulic properties of porous media. *Hydrology papers No. 3, Colorado State University, Fort Collins, Colo.*

Brooks, R.H., and Corey, A.T.(1966) Properties of porous media affecting fluid flow. *J. Irrig. Drain. DW. Proc. ASCE 4855 (IR2) : 61-88.*

Brown, J.C.(1877) *Forests and Moisture: Effects of forests on humidity of climate.* (Oliver and Boyd, Edinburgh, Scotland).

Bruce and Luxmoore (1986) Soil Moisture Capacity. In *Methods of Soil Analysis: Part 1 Physical and Mineralogical Methods.* (ed) Klute, A. (Am. Soc. Agron., Madison, U.S.A.)

Brunsden, A.P.(1981) The stable isotope analysis of rainfall and runoff at Plynlimon. *Stable Isotope Technical Report 11 Inst. Hydrology 25/01*

Brutsaert, W.(1982) *Evaporation into the Atmosphere : Theory, History and Applications.* (Reidel, Dortrecht)

Buckingham, E.(1907) Studies on the movement of soil moisture. *USDA Bureau of Soils 38.*

Bucknell, A.J., Hill, P.J., and Newson, A.J.(1977) Two research rain gauge installation procedures from the Plynlimon catchments.In *Selected measurement techniques in use at Plynlimon experimental catchments. Inst. Hydrology* 1-10.

Bullock, P., and Thomasson, A.J.(1979) Rothamsted studies of soil structure II measurement and characteristics of macroporosity by image analysis and comparison with data from water retention measurement. *J. Soil Sci. 30: 341-413.*

Bunting, B.T.(1961) The role of seepage moisture in soil formation, slope development, and stream initiation. *Am. J. Sci. 259: 503-518.*

Burch, G.J., Bath, I.D., Moore, and O'Loughlin, E.M.(1987) Comparative hydrological behaviour of forested and cleared catchments in Southeastern Australia. *J. Hydrol. 90: 19-42.*

Burger, V.H.(1922) Physilealische Eigenschaften der Wald-und Freilandboden. *Mitt. Schweiz. Anst. Forest Versuchswes 13(1): 1-221.*

Burt, T.P.(1978) An automatic fluid-scanning switch tensiometer system. *Brit. Geomorph. Res. GpTechnical Bull. 21: pp. 30.*

Burt, T.P.(1985) Slopes and slope processes: runoff processes on hillslopes. *Prog. in Phys. Geography 9,4: 582-599.*

Burt, T.P.(1987) Slopes and slope processes: Storm runoff mechanisms. *Prog. Phys. Geography : 598-611.*

Burt, T.P., and Butcher, D.P.(1985) On the generation of delayed peaks in stream discharge. *J. Hydrol. 78: 361-378.*

Burt, T.P., Butcher, D.P., Coles, N., and Thomas, A.D.(1983) The natural history of Slapton Ley nature reserve: hydrological processes in the Slapton wood catchment. *Field Studies 5: 731-752.*

Butcher, T.B.(1977) Impact of moisture relationships on the management of *Pinus pinaster* plantations in western Australia. *Forest Ecology and Management 1: 97-107.*

Calder, I.R.(1976) The measurement of water losses from a forested area using a 'natural' lysimeter. *J. Hydrol. 30: 311-325.*

Calder, I.R.(1978) Transpiration observations from a spruce forest and comparisons with predictions from an evaporation model *J. Hydrol. 38: 33-47.*

Calder, I.R., Hall, R.L., Harding, R.J., Wright, L.R., and Rosier, P.T.W.(1980) Report on collaborative project with the British waterways board on the effects of alteration on the runoff from the catchments supplying the Cinnan Canal Reservoirs.

Calder, I.R., and Newson, M.D.(1979) Landuse and upland water resources in Britain - a strategic look. *Water Res. Bull. 15,6: 1628-1639.*

Calder, I.R., Newson, M.D., and Walsh, P.D.(1982) The application of catchment, lysimeter and hydrometeorological studies of coniferous afforestation in Britain to land-use planning and water management. *Proc. Symp. Hydrol. Res. Basins Sonderh. Landeshydrologie Bern : 853-863.*

Campbell, G.S.(1974) A simple method for determining unsaturated conductivity from moisture retention data. *Soil Sci. 117: 311-314.*

Carlson, C.A., Reinhart, K.G., and Horton, J.S.(1956) Predicting soil moisture in the surface foot of soil. *Soil Sci. Am. Proc. 20,3: 412-415.*

Carson, M.A., and Sutton, E.A.(1971) The hydrologic response of the Eaton River Basin, Quebec. *Canad. J. Earth Sci. 8: 102-115.*

Carter, A.(1983) *Solute pathways in a forested catchment.* Unpubl. PhD thesis, Coventry Polytechnic, Dept. of Geography.

Centre for Agricultural Strategy (1980) *Strategy for the UK Forestry Industry.* CAS Report, Reading.

Chappell, N.A., Ternan, J.L., Williams, A.G., Reynolds, B.(1990) Preliminary analysis of water and solute movement beneath a coniferous hillslope in mid-Wales, U.K. *J. Hydrol. 116: 201-215.*

Chaney, W.R.(1981) Sources of water. In *Water Deficits and Plant Growth: Vol. VI Woody Plant Communities* (ed) T.T. Kozlowski (Academic Press) 1-47.

Chebotrarev, N.P. (1962) *Theory of Stream Runoff.* Transl. from Russian. (IPST, Jerusalem) 464

Childs, E.C.(1969) *An Introduction to the Physical Basis of Soil Water Phenomenon.* (Wiley, London).

Chow, V.T., Maidment, D.R., and Mays, L.W. (1988) *Applied Hydrology.* (McGraw-Hill)

Christophersen, N. and Neal, C.(1987) Some results important for further development of hydrochemical models describing fresh water acidification. In *Int. Workshop on Geochem and Monitoring in Rep. Basins. (ed) Molden, B. and Paces, T. (Geol. Surv., Prague).*

Clarke, R.T., Leese, M.N., and Newson, A.J.(1973) Analysis of data from Plynlimon raingauge networks April 1971-March 1973. *Inst.Hydrology Report 27.*

Constantz, J.(1982) Temperature dependence of unsaturated hydraulic conductivity of two soils. *Soil. Sci. Soc. Am. J. 46: 466-470.*

Cook, H.L.(1943) Report of committee on runoff 1942-1943. *Trans. Am. Geophys. Union 24: 422.*

Cook, H.L.(1946) The infiltration approach to the calculation of surface runoff. *Trans. Am. Geophys. Union 27: 726-743.*

Cooper, H.H. Jr.(1966) The equation of groundwater flow in fixed and deforming coordinates *J. Geophys. Res. 71,20: 4785-4790.*

Costalles, E.F.(1979) Infiltration rates of soils as influenced by some land-use types in the Benguet pine watershed. *Sylvatrop Philipp Forest Res. J. 4(4): 255-260.*

Courtney, F.M.(1978) Unpublished data, Department of Geographical and Environmental Sci., Manchester Polytechnic, UK.

Crabtree, R.W., and Trudgill, S.T.(1985) Hillslope hydrochemistry and stream response on wooded permeable bedrock: The role of stemflow. *J. Hydrol. 80: 161-178.*

Crampton, C.B.(1963) The development and morphology of ironpon podzols in Mid and South Wales. *J. Soil Sci. 14: 282-302.*

Crampton, C.B.(1967) The evolution of soils on the hills of south Wales and factors affecting their distribution, and their past, present and potential use. In *Upland Soils: Welsh Soils Disc. Group Report 8* (ed) D. Jenkins.

Crawford, N.H., and Linsley, R.K.(1966) Digital simulation in hydrology: Stanford Watershed Model IV. *Dept. Civil Eng. Stanford University Technical Report 39.*

Cresser, M., and Edwards, A.(1988) *Acidification of Freshwaters.* Cambridge Environmental Chemistry Series: Cambridge University Press, Cambridge, UK.

Croney, D., and Coleman, J.D.(1954) Soil structure in relation to soil suction (pF). *J. Soil Sci. 5,1: 75-84.*

Curtis, L.F., and Trudgill, S.(1975) The measurement of soil moisture. *BGRG Tech. Monogr. 13 13:.*

Cvetkovic, V.D.(1986) A continuum approach to high velocity flow in a porous medium. *Transport in Porous Media. 1,1: 63-97.*

Dagan, G.(1979) The generalization of Darcy's Law for Nonuniform flows. *Water Resources Res. 15,1: 1-7.*

Dagan, G.(1984) Solute transport in heterogeneous porous formations. *J. Fluid. Mech. 145: 151-177.*

Darcy, H.(1856) *Les fontaines publiques de la ville de Dijon.* (Victor Dalmont, Paris).

Demond, A.H., and Roberts, P.V.(1987) An examination of relative permeability relations for two-phase flow in porous media. *Water Res. Bull. 23,4: 617-628.*

De Smedt, F., and Wierenga, P.J.(1979) Simulation of water and solute transport in unsaturated soils. In *Surface and Subsurface Hydrology* (eds) H.J. Morel-Seytoux, J.D. Salas, T.G. Saunders, and R.E. Smith 430-446.

DeVries, J., and Chow, T.L.(1978) Hydrologic behaviour of a forested mountain soil in coastal British Columbia. *Water Resources Res. 14, 5: 935-942.*

Dixon, J.C.(1986) Solute movement on hillslopes in the alpine environment of the Colorado Front Range. In *Hillslope Processes* (ed) A.D. Abrahams (Allen & Unwin, Boston) 139-159.

Dixon, R.M., and Simanton, J.R.(1979) Water infiltration processes and air-earth interface conditions. In *Surface and Subsurface Hydrology* (eds) H.J. Morel-Seytoux, J.D. Salas, T.G. Saunders, and R.E. Smith 314-330.

Dooge, J.C.(1986) Looking for hydrologic laws. *Water Resource Res. 22,9: 465-585.*

Douglas, I.(1977) *Humid Landforms.* (Australian National University Press, Canberra).

Douglas, J.T.(1986) Macroporosity and permeability of some soil cores from England and France. *Geoderma 37: 221-231.*

Douglass, J.E. and Fletcher, P.W.(1947) Effect of removal of stream-bank vegetation upon water yield. *Trans. Am. Gephys. Union. 28: 105-110.*

Dowd, J.F.(1979) A modified version of GM8: A boundary-integral-equation-method (BIEM) solution. (unpubl.).

Dowd, J.F.(1988a) A PC-based program for the calculation of relative hydraulic conductivity using the Millington-Quirk Equation (v1.01). (unpubl.)

Dowd, J.F.(1988b) TRIANGLE: A two-dimensional, triangular finite-element model for groundwater flow. (unpubl.)

Dowd, J.F., and Williams, A.G.(1988) Calibration and use of pressure transducers in soil hydrology. *Hydrological Processes.*

Driscoll, C.T.(1984) A procedure for the fractionation of aqueous aluminium in dilute acidic waters. *Int. J. Environ. Anal. Chem. 16: 267-284.*

Dubreuil, P.L.(1985) Review of field observations of runoff generation in the tropics. *J. Hydrol. 80: 237-264.*

Dunne, T.(1978) Field studies of hillslope flow processes. In *Hillslope Hydrology* (ed) M.J. Kirkby (Wiley).

Dunne, T.(1983) Relation of field studies and modelling in the prediction of storm runoff. *J. Hydrol. 65: 25-48*

Dunne, T., Black, R.D., and (1970a) An experimental investigation of runoff production in permeable soils. *Water Resources Res. 6 (2): 478-490.*

Dunne, T., Black, R.D., and (1970b) Partial area contributions to storm runoff in a small New England watershed. *Water Resources Res. 6 (5): 1296-1311.*

Dupuit, J.(1863) *Etudes Theoriques et Practiques sur le Mouvement des Eaux dans les Canaux Decouverts at a Travers les Terrains Permeables.* 2nd. Ed., (Dunod, France).

Duysings, J.J.H.M., Verstraten, J.M., and Bruijnzeel, L.(1983) The identification of runoff sources of a forested lowland catchment: a chemical and statistical approach. *J. Hydrol. 64: 357-375.*

Eden, M.L., and Green, C.P.(1971) Some aspects of granite weathering and tor formation on Dartmoor, England. *Geografiska Annaler 53: 92-99.*

Eeles, C.W.O.(1969) Installation of access tubes and calibration of neutron moisture meters. *Intsitute of Hydrology Res. Rpt. 7.*

Englund, F.(1953) On the laminar and turbulent flow of groundwater through homogenous sand. *Trans. Danish Acad. Tech. Sci. No. 1.*

Engman, E.T., and Rogowski, A.S.(1974) A partial area model for storm flow synthesis. *Water Resources Res. 10,3: 464-472.*

Erh, K.T.(1972) Application of a spline function to soil science. *Soil Sci. 114,5: 333-338.*

Erichsen, B., and Nordseth, K.(1984) Runoff models--Do they tell what actually happens!. *Nordic Hydrol. 15: 273-282.*

Ernst, L.F.(1950) *A new formula for the calculation of the permeability factor with the auger hole method.* T.N.O. Groningen.

Euler,.(1755) Principes generaux du mouvement des fluides. *Hist. de L'Acad. de Berlin.*

Evans, L.J., and Adams, W.A.(1975) Chlorite and illite in some lower Palaeozoic mudstones of mid-Wales. *Clay Minerals 10: 387-397.*

Fellner-Feldegg, J. (1969) The measurement of dielectics in the time domain. *J. Phys. Chem. 73: 616-623*

Finlayson, B.(1977) Runoff contributing areas and erosion. *Res. Paper 18, School of Geography, Uni. Oxford.*

Fitzpatrick, E.A.(1956) An indurated soil horizon formed by permafost. *J. Soil Sci. 7: 248-254.*

Fletcher, P.W.(1952) The hydrologic function of forest soils in watershed management. *J. Forestry 50: 359-362.*

Forchheimer, P.(1901) Wasserbewegung durch Boden. *Z. Ver. Deutsch. Ing. 45: 1782-1788.*

Ford, E.d., and Deans, J.D.(1977) Growth of a Sitka spruce plantation, spatial distribution and seasonal fluctuations of lengths, weights, and carbohydrate concentrations of pine nuts. *Plant and Soil 47: 463-485.*

Ford, E.D., and Deans, J.D.(1978) The effects of canopy structure on stemflow, throughfall and interception loss in young Sitka spruce plantations. *J. Applied Ecology 15: 905-917.*

Freeze, R.A.(1971) Three-dimensional, transient, saturated-unsaturated flow in a groundwater basin. *Water Resources Res. 7,2: 347-366.*

Freeze, R.A.(1972) Role of subsurface flow in generating surface runoff 2. Upstream Source Areas. *Water Resource Res. 8, 5: 1272-1283.*

Freeze, R.A.(1974) Streamflow generation. *Reviews of Geophysics and Space Physics (November) 12 (4): 627-647.*

Freeze, R.A.(1978) Mathematical models of hillslope hydrology. In *Hillslope Hydrology* (ed) M.J. Kirkby (Wiley).

Freeze, R.A.(1980) A stochastic-conceptual analysis of rainfall-runoff processes on a hillslope. *Water Resources Res. 16,2: 391-408.*

Freeze, R.A., and Cherry, J.A.(1979) *Groundwater.* (Prentice-Hall, New Jersey) pp. 604.

Freeze, R.A., and Harlan, R.L.(1969) Blueprint for a physically-based, digitally-simulated hydrologic response model. *J. Hydrol. 9: 237-258.*

Fuchsman, C.H.(1986) The unresolved problems of peat-water relationships. In *Peat and Water* (ed) C.H. Fuchsman (Elsevier) 1-7.

Gaiser, R.N.(1952a) Root channels and roots in forest soils. *Soil Sci. Soc. Am. Proc. 16: 62-65.*

Gaiser, R.N.(1952b) Readily available water in forest soils. *Soil Sci. Soc. Am. Proc. 16: 334-338.*

Gardner, W. (1986) Soil Moisture Content. In *Methods of Soil Analysis: Part 1. Physical and Mineralogical Methods.* (ed) Klute, A. (Am. Soc. Agron., Madison, U.S.A.)

Gardner, W., Isrealsen, O.W., Edlefsen, N.E., and Clyde, D.(1922) The capillary potential function and its relation to irrigation practice. *Phys. Rev. 20: 196.*

Gardner, W.R., and Kirkham, D.(1952) Determination of soil moisture by neutron scattering. *Soil Sci. 73: 391-401.*

Gash, J.H.C., and Stewart, J.B.(1977) The evaporation from Thetford Forest in 1975. *J. Hydrol. 35: 385-396.*

Gash, J.H.C., Wright, I.R., and Lloyd, C.R.(1980) Comparative estimates of interception loss from three coniferous forests in Great Britian. *J. Hydrol. 48: 89-105.*

Gaskin, J.W.(1987) *Water and solute movement in the soil of a pinus strobus plantation during storm events.* unpubl. MSc Thesis, University of Georgia, Athens, Georgia : pp. 42.

Gebhardt, H., and Coleman, N.T.(1974) Anion adsorption by allophanic tropical soils: I Chloride Adsorption. *Soil Sci. Soc. Am. Proc. 38: 255-461.*

Gee, A.S., and Stoner, J.H.(1984) The effects of seasonal and episodic variations in water quality on the ecology of upland waters in Wales. *IWPC/IWES Joint meeting on Acid Rain*, 28 March, Birmingham

Germann, P., and Beven, K.(1981a) Water flow in soil macropores I An experimental approach. *J. Soil Sci. 32: 1-13.*

Germann, P., and Beven, K.(1981b) Water flow in soil macropores III A statistical approach. *J. Soil Sci. 32: 31-39.*

Gillham, R.W.(1984) The capillary fringe and its effect on water-table response. *J. Hydrol. 67: 307-324.*

Gilman, K.(1980) Estimating the soil heat flux in an upland drainage basin. *Hydrol. Sci. Bull. 25, 4: 435-451.*

Gilman, K., and Newson, M.D.(1980) Soil pipes and pipeflow: A hydrological study in upland Wales. *BGRG Res. Monogr. (Norwich: Geobooks) 1: pp. 110.*

Gilmour, D.A., and Bonell, M.(1979) Runoff Processes in tropical rainforests with special reference to a study in North-east Australia. In *Geographical Approaches to Fluvial Processes* (ed) A.F. Pitty. 73-92.

Gilmour, D.A., Bonell, M., and Sinclair, D.F.(1980) An investigation of storm drainage processes in a tropical catchment. *Aust. Water Res. Council Tech. Paper No. 56 Dept. Nat. Dev. and Energy.*

Graham, B.F.(1960) Transfer of dye through natural soil grafts of *Pinus strobus. L. Ecology 41: 56-64.*

Grant, D.R.(1975) Measurement of soil moisture near the surface using a neutron moisture meter. *J. Soil Sci. 26,2: 124-129.*

Gray, W.G., and O'Neill, K.(1976) On the general equations for flow in porous media and their reduction to Darcy's Law. *12,2: 148-154.*

Gregory, K. and Walling, D.(1973) *Drainage Basin Form and Process: A Geomorphological Approach.* (Edward Arnold, London).

Grelewicz, A., and Plichta, W.(1983) Water absorption of xeromor forest floor samples. *Forest Ecology and Management 6: 1-12.*

Grelewicz, A., and Plichta, W.(1985) Water absorption in samples of different types of forest humus. *Forest Ecology and Management 10: 1-11.*

Greminger, P.J., Sud, Y.K., and Nielsen, D.R.(1985) Spatial variability of field-measured soil-water characteristics. *Soil Sci. Soc. Am. J. 49, 5:.1075-1083*

Grieve, I.C.(1978) Some effects of the plantation of conifers on a freely drained lowland soil, Forest of Dean, UK. *Forestry 51,1: 21-28.*

Gupta, V.K., and Bhattacharya, R.N.(1986) Solute dispersion in multidimensional periodic saturated porous media. *Water Resources Res. 22,2: 156-164.*

Gvirtzman, H., Paldor, N., Magaritz, M., and Bachmat, Y.(1988) Mass exchange between mobile freshwater and immobile saline water in the unsaturated zone. *Water Resources Res. 24,10: 1638-1644.*

Hall, D.G.M., Reeve, M.J., Thomasson, A.J., and Wright, J.F.(1977) Water retention, porosity and density of field soils. *Soil Survey Tech. Monogr 9: pp. 75.*

Hammermeister, D.P., Kling, G.F., and Vomocil, J.A.(1982a) Perched water tables on hillsides in western Oregon: I Some factors affecting their development and longevity. *Soil Sci. Soc. Am. J. 46: 811-818.*

Hammermeister, D.P., Kling, G.F., and Vomocil, J.A.(1982b) Perched water tables on hillsides in western Oregon: II Preferential downslope movement of water and anions. *Soil Sci. Soc. Am. J. 46: 819-826.*

Hanks, R.J., and Ashcroft, G.L.(1980) *Applied Soil Physics.* Adv. Series in Agric. Sci. (Springer-Verlag,) pp.73.

Hannoura, A.F., and Barends, F.(1981) Non-darcy flow; state of the art. In *Flow and Transport in Porous Media* Proc Euromech 13, Delft, 2-4 Sept. 1981, (ed) Verruijt, A. and Barends, F.B.J. 37-51

Harding, R.J.(1979) Radiation in the British Uplands. *J. Applied Ecology 16: 161-170.*

Haridasan, M., and Jensen, R.D.(1972) Effect of temperature on pressure head-water content relationship and conductivity of two soils. *Soil Sci. Soc. Am. J. 36: 703-708.*

Harr, R.D.(1977) Water flux in soil and subsoil on a steep forested slope. *J. Hydrol. 33: 37-58.*

Harr, R.D.(1986) Effects of clearcutting on rain-on-snow runoff in Western Oregon: A new look at old studies. *Water Resources Res. 22, 7: 1095-1100.*

Harris, C.(1987) Solifluction and related periglacial deposits in England and Wales. In *Periglacial Processes and Land Forms in Britain and Ireland* (ed) J. Boardman (Cambridge Univ. Press, Cambridge).

Harrison, J.G., and Newson, M.D.(1978) Raingauge design and siting in the uplands: A simple comparison from Plynlimon. *Cambria 5, 2: 117-132.*

Hart, G.E., and Lomas, D.A.(1979) Effects of clearcutting on soil water depletion in an Engelmann spruce stand. *Water Resources Res. 15,6: 1598-1602.*

Hauhs, M.(1987) A model of ion transport through a forested catchment at Lange Bramke, West Germany. *Geoderma 38: 97-113.*

Haverkamp, R., Vauclin, M., and Vachaud, G.(1984) Error analysis in estimating soil water content from neutron probe measurements: 1 Local Standpoint. *Soil Sci. 137, 2: 78-90.*

Heald, W.R., and Rogowski, A.S.(1977) Soil water and chemical movement in a sloping fragipan system. In *Watershed Res. in Eastern North America: A workshop to compare results* (ed) D.L. Correll (Smithsonian Institute, Maryland).

Helvey, J.D.(1971) A summary of rainfall interception by certain conifers of North America. In *Proc. Int. Symp. Forest Hydrolgy Professors: Biological Effects in the Hydrological Cycle* (Purdue Univ, Lafayette, Ind, USA) 103-113.

Hemond, H.F., and Goldman, J.C.(1985) On non-darcian water flow in peat. *J. Ecology 73: 579-584.*

Henderson, R., Ford E.D., Renshaw, E., and Deans, J.D.(1983) Morphology of the structural root system of Sitka spruce I. Analysis and Quantitative Description. *Forestry 56, 2: 121-135.*

Henry, H.R.(1964) Effects of dispersion on salt encroachment in coastal aquifers: in sea water in coastal aquifers. *USGS Water Supply Paper 1613-c.*

Herrmann, A., and Stichler, W.(1980) Groundwater--runoff relationships. *Catena 7: 251-263.*

Herwitz, S.R.(1986) Infiltration excess caused by stemflow in a cyclone prone tropical rainforest. *Earth Surface Processes and Landforms 11: 401-412.*

Hewlett, J.D.(1961) Soil moisture as a source of base flow from steep mountain watersheds. *USDA Forest Service Southeastern Forest Exp. Stn. Ashville, NC Stn. Paper No. 132.*

Hewlett, J.D.(1969) Tracing storm and base flow to variable source areas on forested headwaters. *Tech. Rpt. No.2 School of Forest Res., University of Georgia, Athens, Georgia. pp21.*

Hewlett, J.D.(1974) Comments on letters relating to 'Role of subsurface flow in generating surface runoff, 2, Upstream Source Areas by R. Allen Freeze. *Water Resources Res. 10 (3): 605-607.*

Hewlett, J.D.(1982) *Principles of Forest Hydrology.* University of Georgia Press, Athens, GA, USA.

Hewlett, J.D., Cunningham, G.B., and Troendle, C.A.(1977) Predicting stormflow and peakflow from small basins in humid areas by the R-Index method. *Water Resources Bull. 13,2: 231-253.*

Hewlett, J.D., and Hibbert, A.R.(1963) Moisture and energy conditions within a sloping soil mass during drainage. *J. Geophys Res. 68: 1081-1087.*

Hewlett, J.D., and Hibbert, A.R.(1967) Factors affecting the response of small watersheds to precipitation in humid areas. In *Forest Hydrology* (eds) W.E. Sopper and H.W. Lull (Pergamon Press, New York) 275-290.

Hewlett, J.D., and Nutter, W.L.(1970) The varying source area of streamflow from upland basins. Proc. of Symp. *Interdisciplinary Aspects of Watershed Management,* Aug.3-6, 1970, Montana State University, USA.

Hewlett, J.D., Post, H.E., and Doss, R.(1984) Effect of clear-cut silviculture on dissolved ion transport and water yield in the Piedmont. *Water Resources Res. 20,7: 1030-1038.*

Hibbert, A.R.(1967) Forest treatment effects on water yield. In *Proc. Int. Symp. on Forest Hydrology (1965) Pennsylvania State University* (Pergammon Press, New York) 527-543.

Hill, R.L., and King, L.D.(1982) A permeameter which eliminates boundary flow errors in saturated hydraulic conductivity measurements. *Soil Sci. Soc. Am. J. 46:877-880.*

Hillel, D.(1977) Computer simulation of soil-water dynamics: A compendium of recent work. *Int. Dev. Res. Centre 082e*

Hillel, D.(1982) *Introduction to Soil Physics.* (Academic Press, New York) pp.364.

Hillel, D., Krentos, V.D., and Stylianovy(1972) Procedure and test of an internal drainage method for measuring soil hydraulic characteristics. *Soil Sci. 114, 5: 395-400.*

Hillman, G.R.(1972) Using potential flow theory to determine soil moisture distribution about an isolated tree. In *Fundamentals of Transport Phenomena in Porous Media,* Proc. 2nd Symp. IAHR-ISSS, Univ. Guelph, Aug. 7-11, 1972.

Hino, M., Fujita, K., and Shutto, H.(1987) A laboratory experiment on the role of grass for infiltration and runoff processes. *J. Hydrol. 90: 303-325.*

Hodgson, J.M. (1978) *Soil Sampling and Soil Description.* (Clarendon Press, Oxford) 241

Holtan, H.N.(1971) A formulation for quantifying the influence of soil porosity and vegetation on infiltration. *Proc. 3rd Int. Sem. for forest hydrology professors.* Perdue University, Indiana, USA.

Hoover, M.D.(1943)

Hoover, M.D.(1949) Hydrologic characteristics of South Carolina Piedmont forest soils. *Soil Sci. Soc. Am. Proc. 14: 353-358.*

Hoover, M.D.(1953) Interception of rainfall in a young loblolly pine plantation. *USDA Forest Serv. Southeastern Forest Exp. Stn. Pap. 21, pp13.*

Hoover, M.D.(1956)

Hoover, M.D.(1962) Water action and water movement in the forest. In *Forest Influences--FAO Forestry and Forest Product Studies*, Rome 31-80.

Hoover, M.D., Olson, D.F., and Greene, G.E.(1953) Soil moisture under a young loblolly pine plantation. *Soil Sci. Proc. 17,2: 147-150.*

Hornung, M.(1984) Precipitation-canopy and soil-water interactions. *IWPC/IWES Joint meeting on Acid Rain.* Birmingham, 28 March.

Hornung, M., and Newson, M.D.(1986) Upland afforestation: influences on stream hydrology and chemistry. *Soil Use and Management 2,2: 61-64.*

Hornung, M., Reynolds, B., Stevens, P.A., and Neal, C.(1987a) Increased acidity and aluminium concentrations in streams followig afforestation: Causative mechanisms and processes. *Proc. Int. Symp. on Acidification and Water Pathways,* Norway 2-5 May.

Hornung, M., Reynolds, B., Stevens, P.A., and Neal, C.(1987b) Stream acidification resulting from afforestation in the UK: evaluation of causes and possible amdicavative measures. In *Forest Hydrology and Watershed Management.* Proc. Vancouver Symp. Aug. IAHS-AISH Publ. No. 167, 1987

Hornung, M., Adamson, J.K., Reynolds, B., and Stevens, P.A.(1986a) Influence of mineral weathering and catchment hydrology on drainage water chemistry in three upland sites in England and Wales. *J. Geol. Soc. Lond. 143: 627-634.*

Hornung, M., Stevens, P.A., and Reynolds, B.(1986b) The effects of forestry on soils, soil water and surface water chemistry. In *Env. Aspects of Plantation Forestry in Wales ITE Symp. No. 22.*

Horton, J.H., and Hawkins, R.H.(1965) Flow path of rain from the soil surface to the water table. *Soil Sci. 100, 6: 377-383.*

Horton, R.E.(1933) The role of infiltration in the hydrological cycle. *Trans. Am. Geophysics Union : 446-460.*

Horton, R.E.(1945) Erosional development of streams and their drainage basins: hydrophisical approach to quantitative morphology. *Bull. Geol. Soc. Amer. 56: 275-370.*

Hubbert, M.K.(1940) The theory of ground-water flow. *J. Geol. 48: 785-944.*

Hubbert, M.K.(1956) Darcy law and the field equations of the flow of underground fluids. *Trans. Am. Inst. Min. Metal. Eng. 207: 222-239.*

Huck, M.G., Klepper, B., and Taylor, H.M.(1970) Diurnal variations in root diameter. *Pl. Physiol. 45: 529-530.*

Hudson, J.A.(1988) The contribution of soil moisture storage to the water balances of upland forested and grassland catchments *Hydrol. Sci. J. 33,3,6: 289-309.*

Hudson, J.A., and Leeks, G.(1989) Catchment experiments in Wales. Paper presented at the *British Hydrolgical Society national meeting on Forest Hydrology, 9 May 1989, Wallingford, UK.*

Hurley, D.G., and Pantelis, G.(1985) Unsaturated and saturated flow through a thin porous layer on a hillslope. *Water Resources Res. 21,6: 821-824.*

Hursh, C.R.(1936) Storm water and absorption *Eos Trans. AGU. 17: 301-302.*

Hursh, C.R.(1944) Appendix B--Report of sub-committee on subsurface flow. *Trans. Am. Geophys. Union. 5: 743-746.*

Hursh, C.R., and Brater, E.F.(1941) Separating storm-hydrographs from small drainage-areas into surface-and subsurface flow. *Trans. Am. Geophysics Union : 863-871.*

Hursh, C.R., and Hoover, M.D.(1941) Soil profile characteristics pertinent to hydrologic studies in the southern Appalachians *Soil Sci. Soc. Am. Proc. 6: 414-422.*

Hutchinson, I., and Roberts, M.C.(1981) Vertical Variation in Stemflow Variation. *J. of Appl. Ecology 18: 521-527.*

Imeson, A.C., and Jungerius, P.D.(1976) Aggregate stability and colluration in the Luxenbourg Ardennes; an experimental and micromorphological study. *Earth Surface Processes 1: 259-271.*

Institute of Hydrology (1976) Water balance of the headwater catchments of the Wye and Seven 1970-1975. *Inst. Hydrology Report Rpt. 33: pp. 62.*

Institute of Hydrology (1981) User's handbook for the Institute of Hydrology neutron probe system. *Inst. Hydrology Report Rpt. 79.*

Institute of Hydrology (1987) Sediment storage, bed fabric and particles features of two mountain streams at Phynlimon (mid-Wales) *Inst. Hydrology Report Rpt. 97.*

Institute of Hydrology (1988) Research on Forestry and Water Resources. WRC CS 4139 RX Rpt. *Institute of Hydrology.* (unpublished).

Institute of Hydrology (1989) *Hydrological Data UK: 1988 Yearbook.* (Institute of Hydrology, NERC).

Institute of Hydrology (in press) 'The Plynlimon Report'. *Institute of Hydrology.*(in press).
Iwata, S., Tabuchi, T., and Warkentin, B.P.(1988) *Soil Water Interactions.* (Marcel Dekker. Inc. New York).
Jacob, C.E.(1940) The flow of water in an elastic artesian aquifer. *Trans. Am. Geophys. Union. 2: 574-586.*
Jackson, R.D., Reginato, R.J., and Van Bavel, C.H.M.(1965) Comparison of measured and calculated hydraulic conductivities of unsaturated soils. *Water Resources Res. 1,3: 375-380.*
Jackson, R.J.(1973) Catchment hydrology and some of its problems. *Proc. Soil and Plant Water Symp.* (Palmeston North New Zealand Apr. Information Series New Zealand Dept. Sci Ind. Res. 9: 73-80.
Jaeger, C.(1956) *Engineering Fluid Mechanics.* Blackie, London.
Jayawardane, N.S., Meyer, W.S., and Barrs, H.D.(1983) Moisture measurement in a swelling clay soil using neutron moisture meters *Aust. J. Soil Res. 22: 109-117.*
Jeffreys, H.(1917) On the vegetation of four Durham coal-measure fells. III on water-supply as an ecological factor. *J. Ecology 5: 129-154.*
Jenkins, D.A.(1967) The parentage of upland soils. In *Upland Soils: Welsh Soil Size Group Report 8* (ed) D. Jenkins.
Jinzhong, Y.(1988) Experimental and numerical studies of solute transport in two-dimensional saturated-unsaturated soil. *J. Hydrol.97: 303-322.*
Jones, O.T.(1929) The geology of central Wales. *Geol. Surv. Memoirs, HMSO.*
Jones, C.W.(1951) Comparison of seepage based on well-permeameter and ponding tests. *Earth Materials Lab. Rpt. EM-264, Bureau of Reclamation, Denver, Colorado.*
Jones, J.A.A.(1981) The nature of soil piping--a review of research. In *BGRG Res. Monogr.* (Geobooks, Norwich) pp. 301.
Jones, J.A.A., and Crane, F.G.(1981) Pipeflow and pipe erosion in the Maesnant experimental catchment. In *Catchment Experiments in Fluvial Geomorphology* (eds) T.P. Burt and D.E. Walling (Geobooks, Norwich) 55-72.
Kasran, B. (in press) Rainfall interception in dipterocarp forest of Peninsular Malaysia. In *Regional seminar on Tropical Forest Hydrology.* 4-9 Sept. 1989, Kuala Lumpur, Malaysia (FRIM/IHP/UNESCO).
Kennedy, J.C., Kendall, C., Zellweger, G.W., Wyermanta, and Aranzino, R.J.(1986) Determination of the components of stormflow using water chemistry and environmental isotopes, Mattole River Baisn, California. *J. Hydrol. 84: 107-140.*
King, E.H.(1899) Principles and conditions of the movements of ground water. *USGS 19th An. Rpt., part 2*
King, J.A., Smith, K.A., and Pyatt, D.G.(1986) Water and oxygen regimes under conifer plantations and native vegetation on upland peaty gley soil and deep peat soils. *J. Soil Sci. 37: 485-497.*
Kirkby, M.J.(1971) Hillslope process-response models based on the continuity equation. *Inst. Brit. Geographers Special Publication 3: 15-29.*
Kirkby, M.J.(1978) *Hillslope Hydrology.* (Wiley, Chichester).
Kirkby, M.J.(1985) Hillslope hydrology. In *Hydrological Forecasting* (eds) M.G. Anderson and T.P. Burt (Wiley, Chichester).
Kirkby, M.J.(1988) Hillslope runoff processes and models. *J. Hydrol. 100: 315-339.*
Kirkby, M.J., and Chorley, R.J.(1967) Throughflow, overland flow and erosion. *Bull. Int. Assoc. Sci. Hydrol. 5-21.*
Kitteredge, J., Loughead, H.J., and Mazubau, A.(1941) Interception and stemflow in a pine plantation. *J. Forestry : 505-520.*
Klein, M.(1984) Effect of catchment size on runoff relationships--a comment. *J. Hydrol. 71: 191-195.*
Klemes, V.(1978) Physically based stochastic hydrologic analysis. *Adv. in Hydroscience : 285-356.*
Klemes, V.(1983) Conceptualization and scale in hydrology. *J. Hydrol. 65: 1-23.*
Klemes, V.(1986) Dilettautism in Hydrology: Transition or Destiny?. *Water Resources Res. 22 (9): 1775-1885.*
Klute, A.(1952) A numerical method for solving the flow equation for water in unsaturated materials. *Soil Sci. 73: 105-116.*
Klute, A.(1965) Water Capacity. In *Methods of Soil Analysis, Part 1* (eds) C.A. Black, F.E. Clark, L.E. Ensiminger, and D.D. W.h.i.t.e. J.L. Evans (Am. Soc. Agron., Inc., 273-314.
Klute, A.(1973) Soil water flow theory and its application in field situations. In *Field Soil Water Regime* (eds) R.R. Bruce, K.W. Flack, and H.M. Taylor. 9-35
Knapp, B.J.(1970) *Patterns of water movement on a steep upland hillslide, Plynlimon, Central Wales.* Unpubl. PhD Thesis, Univ. Reading, Sept. 1970.
Knapp, B.J.(1973) A system for the field measurement of soil water movement. *BGRG Tech. Bull. 9: pp. 26.*
Knudsen, M.(1909) *Ann. Phys. 28,75.* (in Scheidegger, 1974)
Kornev (1921)

Kozeny, J.(1927) Uber kapillare Leitung des Wassers im Boden. *Sitzungsber. Akad. Wiss. Wein. 136: 271-306.* (in Bear, 1972).

Krammes, J.S., and Debano, L.F.(1965) Soil wettability: A neglected factor in watershed management. *Water Resources Res. 1,2: 283-286.*

Krug, E.C., and Frink, C.R.(1983) Acid rain on acid soil: a new perspective. *Sci. 221: 520-525.*

Lai, F.S., and Osman, S.(in press) Rainfall interception, throughfall and stemflow in two *Acacia mangium* stands, in Kemasul, Penang, Peninsular Malaysia. In *Regional seminar on Tropical Forest Hydrology.* 4-9 Sept. 1989, Kuala Lumpur, Malaysia (FRIM/IHP/UNESCO).

Lamb, Sir H.(1932) *Hydrodynamics.* 6th Edition.

Langan, S.J., Wheater, H.S., Miller, J.D., and Ferrier, R.C.(1987) The use of representative field plots for the determination of hydrological flowpaths and associated hydrochemistry in studies of surface water acidification. *Proc. Int. Symp. on Acidification and Water Pathways.* Norway 2-5 May.

Laroussi, C.H., Touzit, and DeBacker, L.W.D.E.(1981) Hydraulic conductivity of saturated porous media in relation to their geometrical characteristics. *Soil Sci. 132, 6: 387-393.*

Lascano, R.J., and Van Bauel, C.H.M.(1982) Spatial variability of soil hydraulics and remotely sensed soil parameters. *Soil Sci. Soc. Am. J. 46, 2: 223-228.*

Law, F.(1956) The effect of afforestation upon the yield of water catchment areas. *J. Brit. Waterworks Assn. 38: 484-494.*

Law, F.(1957) Measurement of rainfall, interception and evaporation losses in a plantation of Sitka spruce trees. *IUGG/IASH: Gen. Assembly, Toronto. 397-411.*

Lawless, G.P., MacGillivray, and Nixon, P.R.(1963) Soil moisture interface effects upon readings of neutron moisture probes. *Soil Sci. Soc. Am. J. : 502-161.*

Lawrence, A.R, and Foster, S.S.D.(1987) The pollution threat from agricultural pesticides and industrial solvents. *BGS Hydrogeological Rpt. 87/2.*

Lawrence G.B., Fuller, R.D., and Driscoll, C.T.(1986) Aqueous aluminum chemistry in the streams of two upper elevation watersheds in the White Mountains of New Hampshire. *Biogeochemistry 2: 115-135.*

Lea, J.W.(1974) The morphology of soils from lower Palaeozoic rocks in Wales. *Welsh Soils Discussion Group 15: 47-60.*

Leeks, G.J.L., and Roberts, G.(1987) The effects of forestry on upland streams with special reference to water quality and sediment transport. In *Environmental aspects of Planation forestry in Wales ITE Symposium No. 22* (ed) J.E.G. Good.

Lelong, F., Durand, P., Didon, J.F., and Dupraz, C.(1987) Comparative hydrological and hydrochemical budgets in three little watersheds with contrasted vegetations (Mart Lozene, France. In *Int. Workshop on Geochemistry and Monitoring in Rep. Basins.* (eds) B. Molden and T. Paces (Geol. Survey, Prague, Czech) 6-9.

Leuning, R., and Talsma, T.(1979) Water movement and retention in a forest soil. *Aust. Forest Resources 9: 233-240.*

Leyton, L., Reynolds, E.R.C., and Thompson, F.B.(1967) Rainfall interception in forest and moorland. In. *Int. Symp. on Forest Hydrology.*(ed) Sopper, W.E., and Lull, H.W. Pergamon, Oxford. 163-178.

Liakopoulos, A.C.(1965) Retention and distribution of moisture in soils after infiltration has ceased. *Bull. Int. Assoc.Sci. Hydrol. 10 2: 58-69*

Linsley, R.K. Jr., Kohler, M.A., and Paulhus, J.L.H.(1988) *Hydrology For Engineers.* (McGraw-Hill, London).

Littlewood, I.G.(1986) Research and development of a streamflow dilution gauging technique for the Llyn Brianne Acid Waters Study, Wales. *University College of Swansea, Acid Waters Series 2: pp. 36.*

Loague, K.M., and Freeze, R.A.(1985) A comparison of rainfall-runoff modelling techniques on small upland catchments. *Water Resource Res. 21, 2: 229-248.*

Lowdermilk, W.C.(1934) The role of vegetation in erosion control and water conservation. *J. Forestry 32: 529-536.*

Luthin, V.N., and Kirkham, D.(1949) A piezometer method for mesuring permeability of soil *in situ* below a water table. *Soil Sci. 68: 349-358.*

Luxmoore, R.J.(1983) Water budget of an eastern deciduous forest stand. *Soil Sci. Soc. Am. J. 47: 785-791.*

Luxmoore, R.J., and Abner, C.H.(1987) *Field Facilities for Subsurface Transport Res. ONRL-6352* (Oak Ridge National Laboratory, Tenn., USA).

Manley, G.(1952) *Climate and the British Scene.* Collins pp382.

Marshall, T.J., and Holmes, J.W.(1979) *Soil Physics.* (Cambridge Univ. Press,).

Marsily, G. de.(1986) *Quantitative Hydrogeology.: Groundwater Hydrology for Engineers.* Transl. by G. de Marsily from *Hydrology Quantitative*, Masson, 1981. (Academic, Orlando)

Martinec, J.(1975) Subsurface flow from snowmelt traced by tritium. *Water Resources Res. 11, 3: 496-498.*
Mathur, R.N., Singh, R.P., and Gupta, M.U.(1982) Comparative study of infiltration in soils under forest cover and agriculture in temperate climate. *Indian Forester 108(10): 648-652.*
McColl, J.G.(1972) Dynamics of ion transport during moisture flow from a Douglas fir forest floor. *Soil Sci. Soc. Am. Proc. 36: 668-676.*
McCord, J.T., and Stephens, D.B.(1987) Lateral moisture flow beneath a sandy hillslope without an apparent impeding layer *Hydrological Proc. 1: 225-238.*
McGowan, M.(1974) Depths of water extraction by roots. In *Isotope and Radiation Techniques in Soil Physics and Irrigation Studies.* IAEA-SM-176/17, Vienna, Austria, 1973.
McMillan, W.D., and Burgy, R.H.(1960) Interception loss from grass. *J. Geophys. Res. 65: 2389-2394.*
Messenger, A.S.(1980) Spruce plantation effects on soil moisture and chemical element distribution. *Forest Ecology and Management 3: 113-125.*
MEXE(1963) a multi-cell field tensiometer unit. *MEXE Report 835.*
MEXE(1969) A plaster of paris adsorbtion block for measuring soil moisture under field conditions. *MEXE Report 838 838: pp. 8.*
Meyboom, P.(1966) Groundwater studies in the Assiniboine river drainage basin Part 1: The evaluation of a flow system in South-Central Saskatchewan. *Geol. Surv. Canada (DMTS) Bull. 139*
Millington, R.J., and Quirk, J.P.(1959) Permeability of porous media. *Nature. 183: 387-388.*
Millington, R.J., and Quirk, J.P.(1960) Permeability of porous solids. *Trans. Faraday Soc. 57: 1200-1206.*
Milne, G.(1936) *J. Ecology 35: 192-265.*
Milne, R., Ford, E.D., and Deans, J.D.(1983) Time lags in the water relations of Sitka spruce. *Forest Ecology and Management 5: 1-25.*
Miyazaki, T.(1988) Water flow in unsaturated soil in layered slopes. *J. Hydrol. 102: 201-214.*
Molchanov, A.A.(1963) *The Hydrological Role of Forests.* Translated by: Isreal Prog. For. Sci. Trans. (Acad. Sci. USSR Inst. For., Jerusalem).
Moore, I.D., Burch, G.J., and Wallbrink, P.J.(1986) Preferential flow and hydraulic conductivity of forest soils. *Soil Sci. Soc. Am. J. 50: 878-881.*
Morel-Seytoux, H.J.(1983) Infiltration affected by air, seal, crust ice and various sources of heterogeneity (special problems). In *Adv. in Infiltration Proc. Nat. Conf. on Adv. in Infiltration Chicago, Illinois, Dec. 12-13.*
Morton, F.I.(1984) What are the limits on forest evapotranspiration?. *J. Hydrol. 74: 373-398.*
Mosley, M.P.(1979) Streamflow generation in a forested watershed New Zealand. *Water Resources Res. 15, 4: 795-806.*
Mosley, M.P.(1982) Subsurface flow velocities through selected forest soils, South Island, New Zealand. *J. Hydrol. 55: 65-92.*
Mualem, Y.(1976) A new model for predicting the hydraulic conductivity of unsaturated porous media. *Water Resources Res. 12: 512-522.*
Mulvany, T.J.(1851) On the use of self-registering rain and flood gauges. *Inst. Civ. Eng. (Ireland) Trans. 4,2: 1-8.*
Murphy, C.P., Bullock, P., and Biswell, K.J.(1977) The measurement and characterization of voids in soil thin sections by image analysis. Part II Application. *J. Soil Sci. 28: 509-518.*
Murphy, C.P., Bullock, P., and Turner, R.H.(1977) The measurement and characterisation of voids in soil thin sections by image analysis. Part 1. Principles and techniques. *J. Soil Sci. 28: 498-508.*
Musiake, K., Oka, Y., and Koike, M.(1988) Unsaturated zone soil moisture behaviour under temperate humid climatic conditions - tensiometric observations and numerical simulations. *J. Hydrol. 102: 179-200.*
Muskat, M., and Meres, M.W.(1936) The flow of heterogenous fluids through porous media. *Physics. 7: 246-363.*
Navier, B.L.M.H.(1822) Memoire sur les equation generales de l' equilibre et du mouvement des fluids. *Mem. de l'Acad. des Sciences, VI. 389.*
Natural Environment Research Council (1975) *Flood Studies Report.* (NERC).
Neal, C., Reynolds, B., Stevens, P., and Hornung, M.(1989) Inorganic aluminium hydrogeochemical controls for acidic stream and soil water in two upland catchments in Wales.
Neal, C., Smith, C.J., Walls, J., and Dunn, C.S.(1985) Hydrochemical budgets of coniferous forest: A progress report. *Inst. Hydrology Report 95: pp. 26.*
Neal, C., Smith, C.J., Walls, J., and Dunn, C.S.(1986) Major, minor and trace element mobility in the acidic upland forested catchment of the upper River Severn, mid-Wales. *J. Geol. soc. Lond. 143: 635-648.*
Neal, C., and Thomas, A.G.(1985) Field and laboratory measurement of pH in low-conductivity natural waters. *J. Hydrol. 79: 319-322.*

Neary, D.G., Bush, P.B., Douglass, J.E., and Todd, R.L.(1985) Picloram movement in an Appalachian hardwood forest watershed. *J. Env. Quality 14,4: 585-591.*

Newson, A.J.(1976a) Some aspects of the rainfall of Plynlimon, mid-Wales. *Inst. Hydrol. 34: pp. 36.*

Newson, M.D.(1975) The Plynlimon floods of August 5th/6th 1973. *Inst. Hydrology Report 26: pp. 34.*

Newson, M.D.(1976b) The physiography, deposits and vegetation of the Plynlimon catchments. *Inst. Hydrology 30*

Newson, M.D.(1978) Channel studies in the Plynlimon experimental catchments. *Inst. Hydrology 47.*

Newson, M.D.(1984) Slope and channel runoff processes in upland catchments: interfaces between precipitation and streamflow acidity. *IWPC/IWES Joint Meeting on Acid Rain.* Birmingham, March 28 : pp. 20.

Newson, M.D., and Harrison, J.G.(1978) Channel studies in the Plynlimon experimental catchments. *Institute of Hydrology Rpt. 47.*

Nieber, J.L.(1979) *Hillslope Runoff Characteristics.* unpublished Phd dissertation, Cornell University, Ithaca, N.Y., USA.

Nieber, J.L., and Walter, M.F.(1981) Two-dimensional soil moisture flow in a sloping rectangular region: experimental and numerical studies. *Water Resources Res. 17,6: 1722-1730.*

Nielsen, D.R., Jackson, R.D., Cary, J.W., and Evans, D.D.(1972) *Soil Water.* (Am. Soc. Agron, SSSA, Madison, Wisconsin).

Nielsen, D.R., and Biggar, J.W.(1961) Miscible Displacement in Soils: 1. Experimental information. *Soil Sci. Soc. Am. Proc 25, 1: 1-5.*

Nielsen, D.R., Biggar, J.W., and Erh, K.T.(1973) Spatial variability of field-measured soil water properties. *Hilgardia 42, 7: 215-259.*

Nielsen, D.R., Van Genuchten, M.T.h., and Biggar, J.W.(1986) Water flow and solute transport processes in the unsaturated zone. *Water Resources Res. 22, 9: 895-1085.*

Nikolaevskii, V.N.(1959) Convective diffusion in porous media. *J. Appl. Math. Mech. (PMM) 23,6: 1042-1050.*

Nikolaevskii, V.N., and Somov, B.E.(1978) Heterogeneous flows of multi-component mixtures in porous media-review. *Int. J. Multiphase Flow 4: 203-217.*

Nkedi-Kizza, P., Biggar, J.W., Van Genuchten, M.Th., Wierenga, P.J., Selim, H.M., Davidson, J.M., and Nielsen, D.R.(1983) Modeling tritium and chloride 36 transport through an aggregated soil. *Water Resources Res. 19,3: 691-700.*

Nnyamah, J.V., and Black, T.A.(1977) Rates and patterns of water upstate in a Douglas-fir forest. *Soil Sci. Soc. Am. Proc. 41: 972-979.*

Nutter, W.L.(1973) The role of soil water in the hydrologic behavior of upland basins. In *Field Soil Water Regime* (eds) R.R. Bruce, K.W. Flack, and H.M. Taylor. 181-193.

Nutting, P.G.(1930) Physical analysis of oil sands. *Bull. Am. Ass. Petr. Geol. 14: 1337-1349.*

Nys, C.(1981) Modifications des characteristiques physico-chemiques d'un sol brun acide des Ardennes primaires par la monoculture d'Epicea commun. *Ann. Sci. For. 38: 237-258.*

Nys, C., and Ranger, J.(1985) Influence de l'espece sur le fonctionnement de lecosysteme forestier. Le cas de la substitution d'une essence resineuse a une essence feuillue. *Sci. Sol. 203-216.*

Oliver, J.(1967) Upland Climates and Soil Formation. In *Upland Soils: Welsh Soil Disc. Grp. Report 8* (ed) D. Jenkins.

Osborne, M., and Sykes, J.(1986) Numerical modelling of immiscible organic transport at the Hyde Park landfill. *Water Resources Res. 22,1: 25-33.*

Oxley, N.C.(1974) Suspended sediment delivery rates and the solute concentration of stream discharge in two Welsh catchments. In *Fluvial Processes in Instrumented Watersheds.* (eds) K. Gregory and D.E. Walling IBG Special Publ. No. 6. 141-154 (1973)

Parlange, J.-.Y.(1974) Water movement in soils. *Geophys. Surveys 1: 357-387.*

Pathak, P.C., Pandey, A.N., and Singh, J.S.(1985) Apportionment of rainfall in central Himalayan Forests (India). *J. Hydrol. 76: 319-332.*

Patric, J.H.(1966) Rainfall interception by mature coniferous forests of southeast Alaska. *J. Soil and Water Conserv. 21,6: 229-231.*

Patric, J.H., Douglass, J.E., and Hewlett, J.D.(1965) Soil water absorption by mountain and piedmont forests. *Soil Sci. Soc. Am. Proc. 29(3): 303-308.*

Pearce, A.J., Stewart, M.N., and Sklash, M.G.(1986) Storm runoff generation in humid headwater catchments 1. where does the water come from. *Water Resources Res. 22, 8: 1263-1272.*

Petrov, E.G.(1980) Formation and role of capillary water in forest soils. *Lesovendnie.* (translated by J. Sallnow).

Pickens, J.F., and Lennox, W.C.(1976) Numerical simulation of water movement in steady groundwater flow systems. *Water Resources Res. 12,2: 171-180.*

Pierce, R.S.(1967) Evidence of overland flow on forest watersheds. In *Forest Hdrology* (ed) Sopper, W.E., and Lull, H.W., Pergamon, New York.

Pierce, R.S., Hornbeck, J.W., Likens, G.E., and Bormann, F.H.(1970) Effect of elimination of vegetation on stream water quality and quantity. *Int. Assoc.Sci. Hydrol. 96: 311-328.*

Pierson, T.C.(1983) Soil pipes and slope stability. *Q. J. Eng. Geol. Lond. 16: 1-11.*

Pilgrim, D.H., Huff, D.D., and Steele, T.D.(1978) A field evaluation of subsurface and surface runoff. *J. Hydrol. 38: 319-341.*

Pinder, G.F., and Gray, W.G.(1977) *Finite element simulation in surface and subsurface hydrology.* (Academic Press, New York).

Plamondon, P.A., Black, T.A., and Goodell, B.C.(1972) The role of hydrologic properties of the forest floor in watershed hydrology. *Nat. Symp. on Watersheds in Transition.* June 1972, Am. Water Res. Assoc. Colorado State Univ. Colorado : 341-348.

Plinston, D.T., and Hill, A.(1974) A system for the quality control and processing of streamflow, rainfall and evapotranspiration. *Inst. Hydrol. 15.*

Poiseuille, J.L.M.(1846) Recherches experimentales sur le mouvement des liquides dans les tubes de tres petits diametres (Comptes Rendus XI.XII 1840-1). *Mem. des Sav. Etrangers IX.* (in Lamb, 1932).

Pond, S.F.(1971) Qualitative investigation into the nature and distribution of flow processes in Nant Geng. *Inst. Hydrology Subs. Hydrology Report No. 28 28:.*

Potter, F.I., Lynch, J.A., and Corbett, E.S.(1988) Source areas contributing to the episodic acidification of a forested headwater stream. *J. Contam. Hydrol. 3,2-4: 293-305.*

Price, A.G., and Hendrie, L.K.(1983) Water motion in a deciduous forest during snowmelt. *J. Hydrol. 64: 339-356.*

Pritchett, W.L.(1979) *Properties and Management of Forest Soils.* (Wiley)

Pyatt, D.G.(1967) Soil survey for forestry purposes in upland Wales. *Upland Soils: Welsh Soils Disc. Group Report 8.*

Pyatt, D.G., Anderson, A.R., Stannard, J.P., and I.M.S., White.(1985) A drainage experiment on a peaty gley soil at Kershape Forest, Cumbria. *Soil Use and Management 1, 3: 89-94.*

Quinn, P., Beven, K., Morris, D., and Moore, R.(1989) The use of digital terrain data in modelling the response of hillslopes and headwaters. Paper presented at the *Second National Hydrology Symposium*, 4-6 Sept. 1989, Sheffield, UK.

Raats, P.A.C.(1971) The role of inertia in the hydrodynamics of porous media. *Arch. Rat. Mech. Anal. 44: 267-283.*

Ragan, R.M.(1968) An experimental investigation of partial area contributions. *Int. Assoc. Sci. Hydrol. Symp. of Bern, Publ. No. 76: 241-251.*

Raudkivi and Callander (1976)

Reeve, R.C., and Kirkham, D.(1951) Soil anisotropy and some field methods for measuring permeability. *Trans. Am. Geophys. Union 32, 4: 582-590.*

Reeves, M. and Duguid, J.O.(1975) *Water movement through saturated-unsaturated porous media: A finite-element Galerkin model. ONRL-4927* Oak Ridge National Lab., Tenn. USA.

Reid, I., and Parkinson, R.J.(1984) The nature of the tile-drain outfall hydrograph in heavy clay soils. *J. Hydrol. 72: 289-205.*

Reiners, W.A.(1972) Nutrient content of canopy throughfall in three Minnesota forests. *Oikos 23: 14-22.*

Remezov, N.P., and Pogrebnyall, P.S.(1969) *Forest Soil Science.* Transl.: Isreal Prog. Sci. Transl. Jerusalem.

Reynolds, B.(1981) Methods for the collection and analysis of water samples for a geochemical cycling study. *Bangor Occ. Paper No.5* (Institute of Terrestrial Ecology, Bangor, UK).

Reynolds, B.(1984) An assessment of the spatial variation in the chemical composition of bulk precipitation within an upland catchment. *Water Resources Res. 20,6: 733-735.*

Reynolds, B., and Stevens, P.A.(1987) A simple stemflow collection and tipping-bucket gauge for chemical flux measurements in forests. *Shorter Tech. Methods (VI) BGRG Tech Bull. 36 Geobooks, Norwich.*

Reynolds, E.R.C.(1966) The percolation of rainwater through soil demonstated by fluorescent dyes. *J. Soil Sci. 17,1.*

Reynolds, E.R.C., and Leyton, L.(1961) Measurement and significance of throughfall in forest stands. In *The Water Relations of Plants* (eds) A.J. Rutter and E.H. Whitehead (Blackwell, London) 127-141.

Reynolds, W.D., and Elrick, D.E.(1985) In situ measurement of field-saturated hydraulic conductivity, sorptivity, and the a-parameter using the Guelph permeameter. *Soil Sci. 140, 4: 292-302.*

Reynolds, W.D., Elrick, D.E., and Clothier, B.D.(1985) The constant head well permeameter: effect of unsaturated flow. *Soil Sci. 139, 2: 172-180.*

Reynolds, W.D., Elrick, D.E., and Topp, G.C.(1983) A re-examination of the constant head well permeameter method for measuring saturated hydraulic conductivity above the water table. *Soil Sci. 136, 4: 250-268.*

Reynolds, W.D. *et al* (1986) *Groundwater Monitoring Review 6,1: 84-95.*

Richards, L.A.(1931) Capillary conduction of liquids through porous medium. In *Physics 1: 318-333.*

Richards, L.A.(1949) Methods of measuring soil moisture tension. *Soil Sci. 68: 95-112.*

Richards, L.A.(1959)

Richards, L.A., Russell, M.B., and Neal, O.R.(1937) Further developments on apparatus for field moisture studies. *Soil Sci. Soc. Am Proc. 1: 55-63.*

Robinson, A.C., and Rodda, J.C.(1969) Rain, wind and the aerodynamic characteristics of raingauges. *Met. Mag. 98: 113-120.*

Robinson, M.(1980) The effect of pre-afforestation drainage on the streamflow and water quality of a small upland catchment. *Inst. Hydrology Report 73.*

Robinson, M.(1985) The hydrological effects of moorland gripping: a re-appraisal of the Moor House Res.. *J. Environ. Management 21: 205-211.*

Robinson, M., and Newson, M.D.(1986) Comparison of forest and moorland hydrology in an upland area with peat soils.

Rodda, J.C.(1971) Report on precipitation. *Inst. Hydrology Report No. 11 11: pp. 29.*

Rodhe, A.(1981) Spring flood: meltwater or groundwater. *Nordic Hydrol. 12: 21-30.*

Rogers, C.C.M., Beven, K.J., Morris, E.M., and Anderson, M.G.(1985) Sensitivity analysis calibration and predictive uncertainity of the Institute of Hydrology Distributed Model. *J. Hydrol. 81: 179-191.*

Rogers, J.S., and Carter, C.E.(1987) Soil core sampling for hydraulic conductivity and bulk density. *Soil Sci. Soc. Am. J. 51: 1393-1394.*

Rogowski, A.S., Engman, E.T., and Jacoby, E.L.(1974) Transient response of a layered, sloping soil to natural rainfall in the presence of a shallow water table: experimental results. *ARS-NE-30 : pp. 27.*

Romans, J.C.C.(1959) Some measurements of air space in Scottish Soils. *J. Soil Sci. 10: 201-214.*

Rudeforth, G.C.(1967) Upland soils from lower Palaeozoic sedimentary rockis in mid-Wales. In *UplandSoils: Welsh Soil Disc. Group Rept. No. 8* (ed) D. Jenkins. 42-51

Rudeforth, G.C.(1984) Soils and their use in Wales. *SSEW Bull. No. 11.*

Russo, D.(1988a) Numerical analysis of the nonsteady transport of interacting solutes through unsaturated soil 1. Homogeneous systems. *Water Resources Res. 24, 2: 271-284.*

Russo, D.(1988b) Numerical analysis of the nonsteady transport of interacting solutes through unsaturated soil 2. Layered systems. *Water Resources Res. 24, 2: 285-290.*

Rutter, A.J.(1963) Studies in the water relations of *Pinus sylvestris* in plantation conditions, I measurements of rainfall and interception. *J. Ecology 51, 1: 191-203.*

Savill, P.S.(1976) The effects of drainage and ploughing of surface water gleys on rooting and windthrow of Sitka spruce in Northern Ireland. *Forestry 49, 2: 133-141.*

Scheidegger, A.E.(1961) General theory of dispersion in porous media. *J. Geophys. Res. 66: 3273-3278.*

Scheidegger, A.E.(1974) *The Physics of Flow Through Porous Media.* (Univ. of Toronto Press, Toronto).

Selby, M.J.(1973) An investigation into causes of runoff from a catchment of pumice lithology in New Zealand. *Hydrol. Sci. Bull. 18,39: 255-280.*

Sharma, M.L., and Luxmoore, R.J.(1979) Soil spatial variability and its consequences on simulated water balance. *Water Resources Res. 15,6: 1567-1573.*

Sharma, M.L., Luxmoore, R.J., De Angezis, R., Ward, R.C., and Yeh, G.T.(1987) Subsurface water flow simulated for hillslopes with spatially dependent soil hydraulic characteristics. *Water Resources Res. 23, 8: 1523-1530.*

Sherman, L.K.(1932) Streamflow from runoff by the unit-graph method. *Eng. News-Record. 108: 501-505.*

Sklash, M.G., and Farjolden, R.N.(1982) The use of environmental isotopes in the study of high-runoff episodes in streams. In *Isotope Studies of Hydrologic Processes* (eds) E.C. Perry and C.W. Montgomery (N. Illinois University, N. Illinois).

Sklash, M.G., and Farvolden, R.N.(1979) The role of groundwater in strom runoff. *J. Hydrol. 43: 45-65.*

Sklash, M.G., Stewart, M.K., and Pearce, A.J.(1986) Storm runoff generation in humid headwater catchments 2. A case study of hillslope and low-order stream response. *Water Resources Res. 22, 8: 1273-1283.*

Sloan, P.G., and Moore, I.D.(1984) Modelling subsurface stormflow on steeply sloping forested watersheds. *Water Resources Res. 20, 12: 1815-1822.*

Smart, P.L., and Wilson, C.M.(1984) Two methods for the tracing of pipeflow on hillslopes. *Catena 11: 159-168.*

Smettem, K.R.J., and Collis-George, N.(1985a) Statistical characterization of soil biopores using a soil peel method. *Geoderma 36: 27-36.*

Smettem, K.R.J., and Collis-George, N.(1985b) The influence of cylindrical macropores on steady-state infiltration in a soil under pasture. *J. Hydrol. 79: 107-114.*

Smettem, K.R.J., and Collis-George, N.(1985c) Prediction of steady-state ponded infiltration distributions in a soil with vertical macropores. *J. Hydrol. 79: 115-122.*

Smith, R.E., and Hebbert, R.H.B.(1983) Mathematical simulation of interdependent surface and subsurface hydrologic processes. *Water Resources Res. 19,4: 987-1001.*

Snow, D.T.(1968) Rock fracture spacings, openings and porosities. *J. Soil Mech. Found. Div., Am. Soc Civ. Eng. 94: 73-91.*

Snyder, F.F.(1932) Synthetic unitgraphs. *Trans. Am. Geophys. Union 19th Ann. Meeting 1938, Part 2. pp447.*

Sorooshian, S.(1988) Parameter estimation, parameter identifiability and model verification. Paper presented at the NATO Advanced Study Institute, *Recent Advances in the Modeling of Hydrologic Systems*. Sintra, Portugal, 10-23 July 1988.

Sozykin, N.F.(1939) Hydrological significance of forest litter and physical properties of forest soils: The moisture regime in forests. *Trudy VNIILKh, Moskva, No. 18* (in Molchanov, 1960).

Sposito, G.(1986) The "physics" of soil water physics. *Water Resources Res. 22: 835-885.*

Stalfelt, M.G.(1961) On the distribution of the precipitation in a spruce stand. In *The water relations of plants* (eds) A.J. Rutter and F.H. Whitehead (Blackwell, London) 115-126.

Stauffer, F., and Dracos, T.(1986) Experimental and numerical study of water and solute infiltration in layered porous media. *J. Hydrol. 84: 9-34.*

Stein, J. and Kane, D.L. (1983) Monitoring the unfrozon water content of soil and snow using time-domain reflectrometry. *Water Resources Res. 19,6: 1573-1584*

Stephenson, G.R., and Freeze, R.A.(1974) Mathematical simulation of subsurface flow conditions to snowmelt runoff, Reynolds Creek Watershed, Idaho. *Water Resources Res. 10, 2: 284-294.*

Stevens, P.A.(1981) Modification and operation of ceramic cup soil solution sampler for use in geochemical cycling study. *Bangor Occ. Paper. No. 8.* Institute of Terrestrial Ecology, Bangor, UK.

Stewart, J.B.(1977) Evaporation from the wet canopy of a pine forest. *Water Resources Res. 13,6: 915-920.*

Stokes, Sir G.G.(1845) On the theories of the internal friction of fluids in motions. *Camb. Trans. VIII 287 (papers, I.75)*

Stoner, J.H., and Gee, A.S.(1985) Effects of forestry on water quality and fish in Welsh rivers and lakes. *J. Inst. Water Eng. Scient. 39: 27-45.*

Strangeways, I.C.(1985) Automatic Weather Stations. In *Facets of Hydrology* (ed) J.C. Rodda (Wiley) 25-68.

Strickland, T.C., Fitzgerald, J.W., and Swank, W.T.(1986) In situ mobilization of sulphur-35 labelled organic sulphur in litter and soil from a hardwood forest. *Soil Biol. Biochem. 18,5: 463-468.*

Strong, W.L., and LaRoi, G.H.(1985) Root density-soil relationships in selected boreal forests of central Alberta, Canada. *Forest Ecology and Management 12: 233-251.*

Sullivan and Koppi (1987)

Talsma, T.(1969) *In Situ* measurement of sorptivity. *Aust. J. Soil Res. 7: 269-276.*

Talsma, T.(1974) The effect of initial moisture content and infiltration quality on redistribution of soil water. *Aust. J. Soil Res. 12: 15-26.*

Talsma, T., and Hallam, P.M.(1980) Hydraulic conductivity measurement of forest conductivity. *Aust. J. Soil Res. 30: 139-148.*

Talsma, T., Hallam, P.M., and Mansell, R.S.(1979) Evaluation of porous cup soil-water extractors: Physical factors. *Aust. J. Soil Res. 17: 417-422.*

Tani, M., and Abe, T.(1987) Analysis of stormflow and its source area expansion through a simple kinematic wave equation. In *Forest Hydrology and Watershed Management.* Proc. Vancouver Symp. Aug 1987. IAHS-AISH.

Taylor, C.M.(1982) The effect of storm runoff response of seasonal variations in contributing zones in small watersheds. *Nordic Hydrol. 13: 165-182.*

Templeman, R.F.(1978) The translation of Microdata style automatic weather station data. *Inst. Hydrology Report 48: pp. 18.*

Terman, J.L., and Williams, A.G.(1979) Hydrological pathways and granite weathering on Dartmoor. In *Geographical Approaches to Fluvial Processes* (ed) A.F. Pitty (Geobooks, Norwich) 5-30.

Ternan, J.L., Williams, A.G., and Solman, H.(1987) A preliminary assessment of soil hydraulic properties, and their implications for Agric forestry management in Grenada, W. Indies. *Forest Hydrology and Watershed Management* IAHS Publ No. 167 : 409-422.

Terzaghi, K., and Peck, R.B.(1948) *Soil Mechanics in Engineering Practice.* (Wiley, New York).

Ting, J.C., and Chang, M.(1985) Soil-moisture depletion under three southern pine plantations in east Texas. *Forest Ecology and Management 12: 179-193.*

Tinker, P.B.(1976) Roots and water: Transport of water to plant roots in soil. *Phil Trans R. Soc. Cond. B 273: 445-461.*

Tischendorf, W.G.(1969) *Tracing stormflow to varying source areas in a small forested watershed in the southeastern Piedmont.* unpublished Phd thesis, University of Georgia, pp113.

Topp, G.C.(1969) Soil water hysteresis measured in a sandy loam and compared with the hysteresis domain model. *Soil Sci. Soc. Am. J. 33: 645-651.*

Topp, G.C., Davis, J.L., and Annan, A.P.(1980) Electromagnetic determination of soil water content: measurements in coaxial transmission lines. *Water Resources Res. 16, 3: 574-582.*

Topp, G.C., Davis, J.L., Bailey, W.G., and Zebchuk, W.D.(1984) The measurement of soil water content using a portable TDR hand probe. *Can. J. Soil Sci. 64: 313-321.*

Topp, G.C., Davis, J.L., and Chinnick, J.M.(1983) Using TDR water content measurements for infiltration studies. In *Adv. In Infiltration.* Proc. nat. Conf. on Adv. in Infilt. Chicago, Illinois December 12-13

Towner, G.C.(1986) A thermistor hygrometer. *Unpubl. BSWPG Conf. September 1986, Rothamstead.*

Towner, G.C., and Youngs, E.G.(1986) Application of drainage theory in the field. *Soil Use and Management 2,2.*

Troendle, C.A.(1979) *A variable source area model for stormflow prediction on first order forested watershed.* Unpubl. PhD thesis, University of Georgia.

Troendle, C.A.(1985) Variable Source Area Models. In *Hydrological Processing* (eds) M.C. Anderson and Burt. T.P. (Wiley).

Trudgill, S.T., Crabtree, R.W., Pickles, A.M., Smettem, U.R.J., and Burt, T.P.(1984) Hydrology and solute uptake in hillslope soils on Magnesian limestone: the Whitwell root project. In *Catchment Exp. in Fluvial Geomorph.* (eds) T.P. Burt and D.E. Walling (Geobooks, Norwich) 183-215.

Truesdale, V.W., and Howe, J.M.(1977) Measurement of small flows: Water level records and weir tank. In *Selected measurement techniques in use at Plynlimon experimental catchments* (Inst. Hydrology Report 43) 33-37.

Tsukamuto, Y., and Ohta, T.(1988) Runoff process on a steep forested slope. *J. Hydrol. 102: 165-178.*

Turner, J.V., and Stokes, R.A.(1987) The mechanisms of catchment flow processes using natural variations in deuterium and oxygen-18. *J. Hydrol. 94: 143-162.*

Valentin, C.(1981) *Organisations pelliculaires superficielles de quelques sols de region subdesertiques.* These 3eme cycle, Univ. Paris VII, Paris.

Van Beers, W.F.J.(1958) The auger-hole method: A field method of the hydraulic conductivity of soil below the water table. *Int. Inst. Land Reclaim. and Improvements Bull. No. 1 (H. Veenman and Zonen, Wageningen) : pp. 32.*

Van Genuchten, M.T.h.(1980) A closed-form equation for predicting the hydraulic conductivity of unsaturated soils. *Soil Sci. Soc. Am. J. 44: 892-898.*

Van Vliet-Lanoe, B.(1985) Frost effects in soils. In *Soils and Quaternary Landscape Evolution* (ed) J. Boardman.

Vauclin, M., Vachaud, G., and Khanji, J.(1975) Two dimensional numerical analysis of transient water transfer in saturated-unsaturated soils. In *Modeling and Simulation of Water Resources Systems.* (ed) Vansteenkiste, G.C.: 299-321.

Voigt, G.K.(1960) Distribution of rainfall under forest stands. *Forest Sci. 6, 1: 2-9.*

Voss, C.I.(1984) *SUTRA - A finite-element simulation model for saturated-unsaturated, fluid-density-dependent ground-water flow with energy transport or chemically reactive single-species solute transport.* USGS, Reston, Virginia, USA.

Wagenet, R.J., and Hutson, J.L.(1987) *LEACHM - Leaching Estimation and Chemistry Model.* Continuum, Water Resources Institute, Cornell University, Ithaca, NY, USA.

Walsh, R.P.D.(1980) Runoff processes and models in the humid tropics. *Zeit. Für Geomorph. 36: 176-202*

Walsh, R.P.D.(1987) Interception and stemflow in tropical rainforest environments. *Swansea Geogr. 24: 44-60.*

Walsh, R.P.D., and Voigt, P.J.(1977) Vegetation litter: an underestimated variable in hydrology and geomorphology. *J. Biogeog. 4: 253-274.*

Ward, R.C., Luxmoore, R.J., and Yeh, G.T.(1986) HYSPAC-simulating hydraulic flow in spatially correlated soils. *Oakridge National Labortory Report ONRL-5849.*

Waring, R.H., Rogers, J.J., and Swank, W.T.(1981) Water relations and hydrologic cycles. In *Dynamic Properties of Forest Ecosystems.* (ed) Reiche, D.E.

Warrick, A.W., Biggar, J.W., and Nielsen, D.R.(1971) Simultaneous solute and water transfer for an unsaturated soil. *Water Resources Res. 7,5: 1216-1225.*

Warrick, A.W., and Nielsen, D.R.(1980) Spatial Variability of Soil Physical Properties in the Field. In *Applications of Soil Physics* (ed) D. Hillel (Academic Press, London).

Watson, E.(1967) The geomorphological factor in upland soil formation. In *Upland Soils: Welsh Soils Disc. Group Report 8* (ed) D. Jenkins.

Watson, E.(1968) The periglacial landscape of the Aberystwyth region. In *Geography at Aberystwyth. Essays written on the occassion of the Departmental Jubilee 1917-18 - 1967-68.* (ed) Bowen, E.G., Carter, H., and Taylor, J.A..

Watson, K.K., and Jackson, R.D.(1967) Temperature effects in a tensiometer-pressure transducer system. *Soil Sci. Soc. Am. Proc. 31: 156-160.*

Watson, K.W., and Luxmoore, R.J.(1986) Estimating macroporosity in a forest watershed by use of a tension infiltrometer. *Soil Sci. Soc. Am. J. 50: 578-582.*

Webster, R.(1966) The measurement of soil water tension in the field. *New Phytologist 65: 249-258.*

Wellings, S.R., Bell, J.P., and Raynor, R.J.(1985) The use of gypsum resistance blocks for measuring soil water potential in the field. *Inst. Hydrology Report 92: pp.32.*

Werling, J.A., and Tajchman, S.J.(1983/4) Soil thermal and moisture regimes on forested slopes of an appalachian watershed. *Forest Ecology and Management 7: 297-310.*

Weyman, D.R.(1970) Throughflow on hillslopes and its relation to the stream hydrograph. *Bull. Int. Assoc. Sci. Hydrol. 15,36: 25-33.*

Weyman, D.R.(1973) Measurements of the downslope flow of water in soil. *J. Hydrol. 70: 267-288.*

Weyman, D.R.(1975) *Runoff Processes and Streamflow Modelling.* Theory and Practice in Geography. (Oxford University Press).

Wheater, H.S., Langan, S.J., Miller, J.D. and Ferrier, R.C.(1987) The determination of hydrological flow paths and associated hydrochemistry in forested catchments in central Scotland. *Forest Hydrology and Watershed Management.* Proc. Vancouver Symp. Aug. IAHS Publ. 167.

Whipkey, R.Z.(1965) Subsurface stormflow on forested slopes. *Bull. Int. Assoc. Sci. Hydrol. 10 (2): 74-85.*

Whipkey, R.Z.(1967) Theory and mechanics of subsurface stormflow. In *Proc. Int. Symp. on Forest Hydrology Pennsylvania State University* (eds) W.E. Sopper and H.W. Lull (Pergamon,) 255-260.

Whipkey, R.Z.(1967b) Storm runoff from forested catchments by subsurface routes. Proc. Leningrad Symp. *Floods and Their Computation* .Gentbrugge, Belgium : 773-779.

Whipkey, R.Z., and Kirkby, M.J.(1978) Flow within the soil. In *Hillslope Hydrology* (ed) M.J. Kirkby (Wiley) 121-144.

White, J.K. and Jayawardena, A.W.(1975) A distributed and deterministic catchment model using finite elements. *Internal Report, King's College, London Dept. Civil Engineering : pp. 21.*

Wilcock, D.N., and Essery, C.T.(1984) Infiltration measurements in a small lowland catchment. *J. Hydrol. 74: 191-204.*

Will, G.M.(1977) A field lysimeter to study water movement and nutrient content in a pumice soil under pinus radiation forest. 1. Site and construction details. *New Zealand Forest Sci. 7 (2): 144-150.*

Williams, A.G., Kent, M., and Ternan, J.L.(1987) Quantity and quality of bracken throughfall, stemflow and litter flow in a dartmoor catchment. *J. Ecology 24: 217-230.*

Williams, A.G., Ternan, J.L., and Kent, M.(1984) Hydrochemical characteristics of a Dartmoor hillslope. In *Catchment Experiments in Fluvial Geomorphology* (eds) T.P. Burt and D.E. Walling 374-398.

Williams, A.G., Ternan, J.L., and Kent, M.(1986) Some observations on the chemical weathering of the Dartmoor granite. *Earth Surface Processes and Landforms, 11: 557-574.*

Wood, H.B.(1977) Hydrologic differences between selected forested and agricultural soils in Hawaii. *Soil Sci. Soc. Am. J. 41 (1): 132-136.*

Wyckoff, R.D., and Botset, H.G.(1936) The flow of gas-liquid mixtures through unconsolidated sands. *Physics 7: 325-345.*

Yair, A., and Lavee, H.(1985) Runoff generation in arid and semi-arid zones. In *Hydrological Forecasting* (eds) M.G. Anderson and T.P. Burt (Wiley, Chichester) 183-220.

Yeh, G.T.(1981) Numerical solutions of Navier-Stokes equations with an integrated compartment method (ICM). *Int. J. for Numerical Meth. in Fluids 1: 207-223.*

Yeh, W.G.(1986) Review of parameter identification procedures in Groundwater Hydrology: The Inverse Problem. *Water Resources Res. 22, 2: 95-108.*

Youngs, E.G.(1968) Shape factors for Kirkham's piezometer method for determining the hydraulic conductivity of soil in silty soils overlying on impermeable stratum. *Soil Sci. 106, 3: 235-237.*

Zahner, R.(1958) Controlled soil moisture experiments in forest tree water relations. In *North American Forest Soils Conference,* Michigan State University, East Lansing, Michigan, Sept. 8-11, 1958.

Zaltsberg, E.(1987) Evaluation and forecasting of groundwater runoff in a small watershed in Manitoba. *Hydrol. Sci. J. 32: 69-84.*

Zanger, C.N.(1953) Theory and problems of water percolation. *Eng. Monogr. No. 8.* Bureau of Reclaimation, Denver, Colorado, USA. 48-71.

Zaslavsky, D.(1964) Theory of unsaturated flow into a non-uniform soil profile. *Soil Sci. 6,97: 400-410.*

Zaslavsky, D., and Rogowski, A.S.(1969) Hydrologic and morphologic implications of anisotropy and infiltration in soil profile development. *Soil Sci. Soc. Am. Proc. 33: 594-599.*

Zaslavsky, D., and Sinai, G.(1981a) Surface hydrology: I Explanation of phenomena. *J. Hydraul. Div. (HYI) : 1-16.*

Zaslavsky, D., and Sinai, G.(1981b) Surface hydrology: II Distribution of raindrops. *J. Hydraul. Div. : 17-34.*

Zaslavsky, D., and Sinai, G.(1981d) Surface hydrology: IV flow in sloping, layered soil. *J. Hydraul Div. : 53-64.*

Zaslavsky, D., and Sinai, G.(1981e) Surface hydrology: V In-surface transient flow. *J. Hydraul. Div. : 65-93.*

Zegelin, S.J., White T., and Jenkins, D.R. (1989) Improved field probes for soil water content and electrical conductivity measurement using time domain reflectrometry. *Water Resources Res.*

Ziemer, R.R.(1968) Soil moisture depletion patterns around scattered trees. In *Pacific Southwest Forest and Range Experimental Station. USDA For. Ser. Res. Note PSW-166.*

Ziemer, R.R., Goldberg, I., and MacGillivry, N.A.(1967) Measuring moisture near soil surface: minor differences due to neutron source type. In *Southwest FDorest and Range Experimental Station. USDA For. Serv. Stn. Paper 158.*